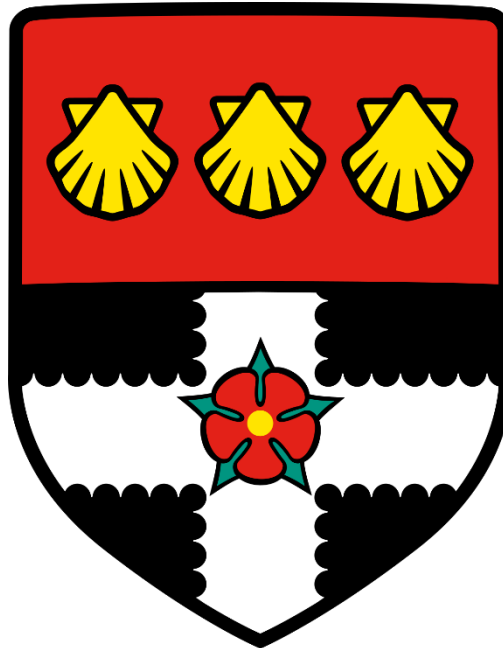


University of Reading



Investigation into the Therapeutic Potential of a Clinically Compliant Amniotic Fluid-Derived Stem Cell Conditioned Media

Ben Mellows

Thesis submitted for the degree of Doctor of Philosophy

School of Biological Sciences

July 2018

Declaration

I confirm that this is my own work and the use of all material from other sources has been properly and fully acknowledged.

Acknowledgments

The completion of this work over 4 years could not have been carried out without the contribution and support of a number of people, some of which may not be enumerated. Firstly I would like express my gratitude to my supervisor Professor Ketan Patel for providing the opportunity to carry out this project along with his support and guidance throughout. I would also like to thank my co-supervisor Dr Paolo De Coppi and Dr Steve Ray for providing the opportunity to work on this project and their guidance. I also appreciate the assistance of Dr Robert Mitchell, Dr Darius Widera, Dr Marie Zeuner and Dr Jonathan Sheard with work carried out. In addition, I would like to say thank you to the members of Professor Ketan Patel's lab as well as those in the labs of those discussed for their support throughout.

Finally, I would like to say a special thank you to my parents and family, who I dedicate this work to because you have supported me tirelessly, not just throughout the PhD but always.

Professional Acknowledgements:

Professor Ketan Patel of the School Biological Sciences at The University of Reading – Project supervisor

Manuela Antoniollo of the Department of Epidemiology and Preclinical Research at the National Institute for Infectious Diseases IRCCS – mass spectrometry and protein GOMF term analysis

Oliver Kretz of the Department of Medicine, Faculty of Medicine, University of Freiburg, Germany – TEM imaging

David Chambers of the Wolfson Centre for Age-related Diseases at King's College London – RNA characterisation

Darius Widera of The School of Pharmacy at The University of Reading - miRNA characterisation and analysis

Bernd Denecke of the Interdisciplinary Centre for Clinical Research Aachen at Aachen University, Germany – miRNA characterisation and analysis

Abstract

Necrotising enterocolitis (NEC) is a devastating disease that can affect pre-term infants and if survived can lead to long term intestinal damage. Currently a variety of antibiotics and in extreme cases surgery is required to manage the disease. However, no treatment exists that attenuates the widespread cell death and suppresses the innate pro-inflammatory response whilst promoting regeneration in the intestine thus reducing long term damage and the need for surgery. The discovery of stem cells, in particular multipotent stem cells (MSCs) has shown them to have potent regenerative therapeutic properties. In particular, C-kit⁺ foetal derived MSCs from amniotic fluid (amniotic fluid stem cells - AFSCs) when introduced into a rat model of NEC increased the survival of animals affected whilst also promoting the repair of damaged epithelial layers. Nevertheless, the ability of stem cells to promote regeneration was independent of transplanted cell engraftment. This led to a paradigm shift in which it was proposed that regeneration was via the secretion of factors acting in a paracrine manner with target cells. This was proven by the introduction of stem cell conditioned media (CM), which mimicked the beneficial effect seen when whole MSCs were introduced. However, much of the MSC CM is produced from non-stressed MSCs. Stressing MSCs has been shown to increase the secretion of paracrine factors and the extracellular vesicles that contain them. Creation of an AFSC CM (AF-CM) under conditions of stress using a protocol created by industrial partners was therefore hypothesised to produce a more potent AF-CM beneficial for regeneration and in particular for the treatment of NEC. Here we characterise the AF-CM under conditions of stress but also in a clinically compliant manner. The AF-CM was characterised for protein and RNA content, which elucidated to a multitude of proteins present but interestingly showed that the majority of RNA present was miRNA. *In vitro* investigation into AF-CM treatment also showed significant improvements in cellular proliferation and migration capacity whilst protecting from senescence. Furthermore, I showed that AF-CM treatment accelerated the regeneration of skeletal muscle fibres following an established mouse model of acute cardiotoxin damage *in vivo*, of which could be partly attributed to increased blood vasculature.

Abbreviations

µg	-	Micrograms
µL	-	Microliters
µm	-	Micrometers
AdDMEM	-	Advanced DMEM
AF-CM	-	AFSC conditioned media
AFSC	-	Amniotic fluid derived stem cells
BSA	-	Bovine serum albumin
CM	-	Conditioned media
CO ₂	-	Carbon Dioxide
CSA	-	Cross sectional area
CTX	-	<i>Naja pallida</i> cardiotoxin
DAPI	-	4, 6-diamidino-2-phenylindole
DEG	-	Differentially expressed genes
DMEM	-	Dulbecco's modified eagle medium
DMSO	-	Dimethyl sulfoxide
EV	-	Extracellular vesicle
FBS	-	Foetal bovine serum
g	-	Force of gravity
H ₂ O ₂	-	Hydrogen peroxide
hADMSC	-	Human adipose derived mesenchymal stem cells
IM	-	Intra muscular
ISC	-	Intestinal stem cell
IV	-	Intra-venous
MyoD	-	Myoblast determination protein
ng	-	Nanograms

O ₂	-	Oxygen
Pax7	-	Paired box protein 7
PBS	-	Phosphate buffered saline
Penstrep	-	Penicillin Streptomycin
PFA	-	Paraformaldehyde
RT-qPCR	-	Reverse transcriptase quantitative polymerase chain reaction
T24	-	Time plus 24 hours
T48	-	Time plus 48 hours
T72	-	Time plus 72 hours
TA	-	Tibialis anterior
TGF-β	-	Transforming growth factor-β
TNF-α	-	Tumour necrosis factor-α
VEGF	-	Vascular endothelial factor

Contents

Declaration	2
Acknowledgments	3
Abstract	4
Abbreviations	5
Contents	7
1. General Introduction	16
Necrotising Enterocolitis	17
Cellular Homeostasis and Regeneration of the Intestine	18
<i>In Vivo</i> rodent models of NEC	21
Current Medical Management.....	22
Stem Cells.....	22
Potency.....	23
Morphology.....	25
Use of Stem Cells for Therapy	27
Advantages and Disadvantages of Stem Cells for Therapy	27
Amniotic Fluid	29
Amniotic Fluid Stem Cells.....	30
Advantages of Amniotic Fluid Stem Cells for the Use of Therapy	31
Conditioned Media.....	32
Microvesicle and Exosome Biogenesis and Release	33
Microvesicle and Exosome Isolation and Analysis	36
Shuttle RNA	37
Microvesicle Proteins.....	39
Cell Targeting	41

The role of inflammation in tissue regeneration	42
Macrophages.....	42
M1 and M2 macrophages	43
Alteration of Inflammatory state with Stem cells and conditioned media.....	44
Treatment of NEC with AFSC CM	47
Aims, Objectives and Hypotheses.....	48
Background:	48
Novelties of Project:.....	49
Overall Project Hypothesis:.....	50
Overall Project aims:	50
Results Chapter 1: Characterisation of Amniotic Fluid Stem Cell Conditioned Media	51
Aims and objectives:	51
Outcome:.....	51
Results Chapter 2: Investigation into the Regenerative Potential of AFSC CM <i>in Vitro</i>	52
Aims and objectives:	52
Outcome:.....	52
Results Chapter 3: Investigation into the Regenerative Potential of AFSC CM in an Acute CTX Damage Mouse Muscle Model <i>in Vivo</i>	53
Aims and objectives:	53
Outcome:.....	53
Results Chapter 4: Establishment of an NEC Intestinal Organoid Model to Test the Regenerative Capability of AFSC CM.....	54
Aims and objectives:	54
Outcome:.....	54
2. Methods	56
Ethical Approval	57
Animal maintenance	57
Euthanasia procedure	57
Cell culture and In-vitro experimentation.....	57
Cell culture conditions	57
AFSCs	57
U251 NF- κ B reporter cells	58
IMR-90 Lung Fibroblast cells	59
Adipose Derived Stem Cells	59
THP-1 Monocytes and Macrophages	59
Differentiation to M0 THP-1 macrophages:.....	59

Differentiation of M0 to M1 THP-1 macrophages:	59
Differentiation of M0 to M2 THP-1 macrophages:	59
Thawing of cells for culture	59
Passaging cells	60
Freezing of cells for storage	60
Conditioned media (CM) generation	60
Extracellular vesicle (EV) isolation	61
Fixation of cells.....	61
Flow Cytometry	61
Adipogenic Differentiation.....	62
Osteogenic Differentiation.....	62
Chondrogenic Differentiation	63
Cellular Proliferation Assay	63
Migration Assay.....	64
Cellular Senescence Assay	64
NF- κ B p65 Nuclear Translocation Assay.....	64
NF- κ B luciferase gene reporter assays	65
Uptake of PKH26-stained EVs by IMR-90 cells.....	65
Intestinal organoid Culture and Isolation	66
Passage of Matrigel containing Crypts.....	67
Fixing of organoids	67
Molecular analysis:.....	68
SDS-PAGE:	68
Silver staining	68
Western Blotting	69
Western Blot Staining and visualisation.....	69
Real Time- Quantitative Polymerase Chain Reaction	69
Sample preparation for Mass Spectrometry (MS)	70
Mass Spectrometry Analysis	70
miRNA Array and analysis	71
Transmission Electron Microscopy	71
<i>In-Vivo</i> experimentation:	72
In Vivo Cardiotoxin induced Mouse TA Injury and AFSC CM/EV Treatment	72
Dissection of Tibialis anterior (TA):	72
Preparation of Muscles for Cryo-sectioning:	72

Histology:	73
Paraffin embedding and processing:	73
De-paraffinisation and rehydration:	74
Antigen retrieval	74
Haematoxylin and Eosin staining	74
Acid phosphatase staining	75
Immuno-histochemical staining.....	75
Pearson’s co-localisation statistical test	76
Statistics	76
3. Chapter 3: Characterisation of Amniotic Fluid Stem Cell Conditioned Media	77
Introduction	78
Results.....	81
Flow Cytometric Analysis of AFSCs Before and After AF-CM Collection.....	81
Differentiation of AFSCs Post AF-CM Collection	84
AF-EV Size Distribution.....	84
Basic Protein and Nucleic Acid Analysis of AF-CM	87
Mass Spectrometry Analysis of AF-CM Protein Content	89
AF-CM RNA Content.....	95
Discussion.....	97
Ensuring MSC Characteristics of AFSCs.....	97
AFSCs Retain Stem Cell Characteristics Following CM Collection	98
Extracellular Vesicles within the AFSC CM	99
Basic Nucleic acid and Protein Content of AF-CM Fractions.....	99
Extensive Characterisation of AF-CM Protein Content.....	100
Extensive Characterisation of AF-CM RNA Content.....	102
4. Chapter 4: Investigation into the Regenerative Potential of AFSC CM in Vitro	105
Introduction	106
Results.....	111
Proliferation Assays.....	111
Migration Assays	113
Senescence Assays	115
NF- κ B Nuclear Translocation and Transcription	119
AF-CM Treatment of Polarised THP-1 Macrophages	127
Cellular Uptake of AF-EVs.....	129
Discussion.....	132

AF-CM Increases Allogeneic Stem Cell Proliferation Capacity	132
AF-CM Improves the Ability of ADMSCs to Close an Artificial Wound	133
Protection from Senescence Following AF-CM or AF-EV Treatment.....	134
AF-CM and AF-EV Treatment Reduces NF- κ B Activity	135
AF-EV Uptake by Target Cells is at Least Partly Dependent on Active Processes	137
5. Chapter 5: Investigation into the Regenerative Potential of AFSC CM in an Acute CTX Damage Mouse Muscle Model in Vivo	139
Introduction:	140
Regeneration in Muscle	140
Cardiotoxin Induced Muscle Damage	144
Results.....	147
AF-CM Treatment in an Acute Damage Model.....	147
Haematoxylin/ Eosin and Acid Phosphatase Staining of Damaged Muscle.....	147
Cross-Sectional Area of Newly Regenerated Fibres.....	149
Satellite Cell Activity within the Regenerating Tissue.....	151
Blood Supply to the Regenerating Tissue	153
Macrophage Infiltration	154
AF-EV Treatment in an Acute Damage Model	156
Comparison of AF-CM, AF-EV and Soluble Fraction in an Acute Damage Model	159
Discussion.....	163
Widespread Inflammation and Tissue Damage Following Cardiotoxin Injection	163
AF-CM Treatment Accelerated Newly Regenerating Fibre Growth.....	164
Increased Numbers of Macrophages in AF-CM Treated Muscles.....	165
AF-CM Treatment Increased the Number of Committed Muscle Progenitor Cells	166
AF-CM Increased the Number of blood Vessels within the Regenerating Tissue.....	167
Both AF-EV and the Soluble Fraction are Important for Improved Regeneration.....	168
6. Chapter 6: Establishment of an NEC Intestinal Organoid Model to Test the Regenerative Capability of AFSC CM	170
Introduction	171
NEC Background.....	171
Cell Types of the Intestine and Their Role in NEC.....	172
Disadvantages of In Vivo NEC Models	173
Intestinal Organoids.....	174
Intestinal Organoids for Models of NEC.....	174
Results.....	176
LPS and TNF- α Stimulation of Organoids	176

Gene Expression after Acute Stimulation and AF-CM Treatment	185
Comparison of AF-CM to AF-EV and AD-CM	187
Protein Expression after Acute LPS Stimulation and AF-CM Treatment.....	189
Protein Synthesis Signalling after Acute LPS Stimulation	192
Autophagy Signalling after Acute LPS Stimulation.....	196
Gene Expression after 24 hour Long Stimulation and AF-CM Treatment	198
AF-CM Treatment of 48 hour LPS or TNF- α Stimulated Organoids	202
Protein Synthesis and Autophagy in 48 hour Stimulated Organoids.....	205
Immuno-histological Analysis of 72 hour Stimulated Organoids.....	210
Protein Translation of 72 hour Long Stimulated Organoids	216
Autophagy Signalling in 72 hour Long Stimulated Organoids.....	219
Discussion.....	223
LPS and TNF- α Induced Cell Death and Inflammation in Organoids.....	223
AF-CM and AF-EV Organoids Treatment Acts Post-Transcriptionally.....	226
AF-CM Modulates Lysozyme Levels via NF- κ B Signalling Pathways	226
Longer Exposures to LPS or TNF- α in Organoids Mimic NEC	227
AF-CM did not Conclusively Alter Autophagy Signalling.....	229
AF-CM Decreased the Levels of Lysozyme per Paneth Cell	230
7. General Discussion	232
AF-CM Molecular Content Modulates Cellular Activity Beneficial to Regeneration <i>in Vitro</i>	234
Whole AF-CM provides a More Effective Regenerative Therapy <i>in Vivo</i> than AF-EV Alone	238
Effect of AF-CM on LPS and TNF- α Stimulated Intestinal Organoids.....	239
Main Study Limitations	243
Future Work	243
Establishing the Anti-inflammatory Properties of AF-CM Further.....	243
Establishing the Active molecules within AF-CM	244
Comparison of AF-CM to AF-CM Collected from Non-Stressed Adherent AFSCs.....	245
Increasing the Reproducibility of the Organoid NEC Model	246
Testing the Ability of AF-CM as a Therapeutic for NEC <i>in Vivo</i>	246
8. Appendix I.....	248
Primary antibodies:	248
Secondary antibodies:.....	249
Microbeads	249
Flow cytometry antibodies	249
9. Appendix II.....	250

RT-qPCR Primers	250
10. Appendix III	251
Solutions.....	251
1X PBS.....	251
Permeabilisation buffer	251
Wash Buffer.....	251
DAPI fluorescent stain.....	251
4% Paraformaldehyde (PFA) in PBS	251
Lysis Buffer	251
1x Running Buffer.....	251
Transfer Buffer	252
PBS-T	252
Blocking buffer	252
Reducing sample treatment buffer (6X RSTB)	252
Freezing Media stock	252
Alizarin Red S working solution.....	252
Oil Red O stock and working solution	252
Alcian Blue working solution.....	252
Acid phosphatase staining solution	253
Senescence Fixative (0.2% Glutaraldehyde, 2% PFA/PBS).....	253
Senescence staining solution	253
Citrate Buffer (0.01M).....	254
Chemicals	255
Materials and reagents:	256
11. References	258
12. Bibliography	281

Figures

Figure 1.1: Intestinal stem cell (ISC) populations expressing Bmi1 or Lgr5 within the crypts of the mammalian intestinal lumen.	20
Figure 1.2: Regulation of the Nanog genes transcription is tightly controlled by various transcription factors.	26
Figure 1.3: Mechanisms of exosome release.....	34
Figure 1.4: Packaging of miRNA into exosomes.....	39
Figure 1.5: Macrophage inflammatory pathways, alteration of which can cause polarisation.	46
Figure 1.6: Overview of project plan and key steps undertaken.....	53
Figure 3.1: Surface marker expression analysis of AFSCs before and after CM collection.....	83
Figure 3.2: Multipotency of post-CM generated AFSCs.....	85
Figure 3.3: Characterisation of AF-EV type and size.	86
Figure 3.4: Basic protein and nucleic acid content characterisation of AF-CM fractions.....	88
Figure 3.5: Mass spectrometry analysis of AF-CMs soluble and EV fraction.	92
Figure 3.6: RNA profiling of AF-EV.	96
Figure 4.1: ADMSC proliferation over 72 hours following AF-CM treatment.....	112
Figure 4.2: Closure of an artificial wound over 9 hours created within a confluent population of ADMSCs with AF-CM treatment.....	114
Figure 4.3: H ₂ O ₂ induced senescence within a population of IMR-90 lung fibroblasts.	117
Figure 4.4: Modulation of NF-κB activity by AF-CM.....	122
Figure 4.5: Comparison of AF-CM and AF-EV effects of NF-κB activity.	124
Figure 4.6: Potential sites of action within the NF-κB pathway that AF-CM may be acting.....	125
Figure 4.7: AF-CM treatment of pro-inflammatory polarised THP-1 macrophages.	128
Figure 4.8: Uptake of PKH26 stained AF-EVs by U251 cells.	131
Figure 5.1: Expression markers of satellite cells from the point of quiescence to activation and then differentiation into myocytes prior to myotube formation.....	142
Figure 5.2: Cardiotoxin induced muscle damage histology.	148
Figure 5.3: Newly regenerated TA muscle fibres following CTX damage.	150
Figure 5.4: Assessment of regeneration with CTX damaged muscle treated with vehicle or AF-CM.	152
Figure 5.5: Assessment of regeneration with CTX damaged muscle treated with vehicle or AF-CM.	155
Figure 5.6: Muscle regeneration following AF-EV treatment.	157
Figure 5.7: Comparison between whole AF-CM, AF-EV and soluble fraction treatment in a model of CTX damage.....	162
Figure 6.1: Organoids stimulated with E.coli LPS or TNF-α for up to 2 hours and at different concentration.....	178
Figure 6.2: Immuno-fluorescent analysis of organoids stimulated with E.coli LPS 2 hours.	181
Figure 6.3: Expression of genes commonly expressed in intestinal cells within organoids following stimulation of organoids with 10µg/ml E.coli LPS or 10ng/ml TNF-α for 48 hours.	184
Figure 6.4: Gene expression of organoids stimulated with 10ng/ml TNF-α for 0.5 hours or 1 hour with AF-CM treatment.	186
Figure 6.5: Inflammation and NF-κB signalling in organoids stimulated with 10ng/ml TNF-α for 1 hour with AF-CM, AD-CM or AF-EV treatment.....	188
Figure 6.6: Protein expression of organoids stimulated with either 50µg/ml or 100µg/ml E.coli LPS for 2 hours and treated with AF-CM.....	191

Figure 6.7: Expression of protein synthesis signalling proteins in organoids stimulated with either 50µg/ml or 100µg/ml E.coli LPS for 2 hours and treated with AF-CM.	195
Figure 6.8: Expression of autophagy signalling proteins in organoids stimulated with either 50µg/ml or 100µg/ml E.coli LPS for 2 hours and treated with AF-CM.	197
Figure 6.9: Gene expression in organoids stimulated with either 10ng/ml TNF-α or 10µg/ml E.coli LPS for 24 hours and treated with AF-CM.	201
Figure 6.10: Protein and gene expression of organoids stimulated with either 50µg/ml E.coli LPS or 10ng/ml TNF-α for 48 hours and treated with AF-CM.	204
Figure 6.11: Expression of protein synthesis signalling proteins in organoids stimulated with either 50µg/ml E.coli LPS or 10ng/ml TNF-α for 48 hours and treated with AF-CM.	207
Figure 6.12: Expression of autophagy signalling proteins in organoids stimulated with either 50µg/ml E.coli LPS or 10ng/ml TNF-α for 48 hours and treated with AF-CM.	209
Figure 6.13: Immuno-fluorescent analysis of organoids stimulated with either 50µg/ml E.coli LPS or 10ng/ml TNF-α for 72 hours and treated with AF-CM.	212
Figure 6.14: Immuno-fluorescent analysis of organoids stimulated with either 50µg/ml E.coli LPS or 10ng/ml TNF-α for 72 hours and treated with AF-CM.	215
Figure 6.15: Protein expression of organoids stimulated with either 50µg/ml E.coli LPS or 10ng/ml TNF-α for 72 hours and treated with AF-CM.	218
Figure 6.16: Expression of autophagy signalling proteins in organoids stimulated with either 50µg/ml E.coli LPS or 10ng/ml TNF-α for 72 hours and treated with AF-CM.	221

Tables

Table 3.1: Soluble and Extracellular Vesicles GOMF terms enrichment.	93
Table 3.2: Soluble only GOMF terms enrichment.	94
Table 3.3: Extracellular Vesicles only GOMF terms enrichment.	94
Table 6.1: A summary of the results seen in organoids stimulated with LPS or TNF-α for 2, 24, 48 or 72 hours with and without AF-Cm treatment.	222
Table 8.1: Primary antibodies.	248
Table 8.2: Secondary antibodies.	249
Table 8.3: Microbeads.	249
Table 8.4: Flow cytometry antibodies.	249
Table 9.1: RT-qPCR primers.	250
Table 10.1: Chemicals.	255
Table 10.2: Materials and reagents.	257

1. General Introduction

Necrotising Enterocolitis

Necrotising enterocolitis (NEC) is an intestinal disorder thought to result from extensive and substantial inflammation. Occurring in premature infants it is defined by variable stages of damage to the intestinal tract as often demarcated by the Bell staging criteria (Table 1.1.) (Zani and Pierro, 2015). NEC affects 0.5-5/ 1000 of all live births and was first described as a clinical syndrome consisting of vomiting, perforation, shock, intestinal haemorrhage and abdominal distension (Rees et al., 2008, Mizrahi et al., 1965). The prevalence of the disease is known to be directly proportional to the number of days born prematurely. Pathology ranges from mucosal injury presenting with increased gastric residuals, mild abdominal distension and occult blood in the stool to full-thickness necrosis and perforation coupled with local and systemic sepsis (Zani and Pierro, 2015). Although NEC affects around 5% of pre-term neonates its exact aetiology is still unclear (Zani and Pierro, 2015). The occurrence of NEC in preterm infants has been suggested to derive from the immaturity of a multitude of the bodies systems such as the cardiovascular, respiratory, intestinal and also the immune system (Zani et al., 2016, Zani and Pierro, 2015, Chen et al., 2016). As a general consensus it is accepted that the immaturity of these systems lead to hypoxia within the intestine, which causes cell death and inflammation. This in turn activates the innate immune system leading to extensive infiltrations of innate immune cells such as macrophages. However, the immaturity of the immune system lends to the over activation of macrophages thus producing a pro-inflammatory response which causes further cell death in the form of necrosis. Cell death via necrosis is essentially an explosion of the cell and release of its contents in an unregulated manner into the environment. Often this leads to inflammation, potential regeneration of tissue and scar formation (Zhang et al., 2014). However as in the case of NEC, inflammation proceeding necrosis can be so widespread that phagocytes cannot locate necrotic bodies efficiently enough to clear the debris. Surgery is therefore often necessary to remove necrotic tissue before further damage due to inflammation is caused (Proskuryakov et al., 2003). Although necrosis may be initially instigated by combinations of cytokines (IL-1 β , TNF- α and INF- γ) released as part of the inflammatory response, dysbiosis of the guts microbiota following inflammation can produce high levels of lipopolysaccharide (LPS), a

bacterial toxin which contributes further to necrosis (Saldeen, 2000, Emami et al., 2009). Interestingly, genes upregulated within NEC such as TLR4 and Lysozyme are also detected at high levels in inflammatory diseases of the intestine often associated with adults, for example Crohns disease (Tremblay et al., 2016, Haberman et al., 2014). In total 22% of the differentially expressed genes (DEG) and 25% of DEGs in NEC were also found to be modulated in Crohns disease and paediatric Crohns disease respectively (Tremblay et al., 2016). This suggests that similar therapies could be used to manage both conditions as long as the treatment affects similar signalling pathways.

Stage	I	IIA	IIB	IIIA	IIIB
Description	Suspected NEC	Mild NEC	Moderate NEC	Severe NEC	Severe NEC
Systemic signs	Temperature instability, apnea, bradycardia	Similar to stage I	Mild acidosis, thrombocytopenia	Respiratory and metabolic acidosis, mechanical ventilation, hypotension, oliguria, DIC	Further deterioration and shock
Intestinal signs	Increased gastric residuals, mild abdominal distension, occult blood in the stool	Marked abdominal distension \pm tenderness, absent bowel sounds, grossly bloody stools	Abdominal wall edema and tenderness \pm palpable mass	Worsening wall edema with erythema and induration	Evidence of perforation
Radiographic signs	Normal or mild ileus	Ileus, dilated bowel loops, focal pneumatosis	Extensive pneumatosis, early ascites \pm PVG	Prominent ascites, fixed bowel loop, no free air	Pneumoperitoneum
DIC, disseminated intravascular coagulopathy; NEC, necrotizing enterocolitis; PVG, portal venous gas.					

Table 1.1: Bell staging criteria of NEC as described by Zani and Pierro et al (Zani and Pierro, 2015).

Cellular Homeostasis and Regeneration of the Intestine

Derived from the endoderm, the intestine not only provides a means of nutritional digestion and absorption but also hormonal signalling, a barrier against pathogens due to immune function and also a means of symbiotically benefiting from the diverse and enormous microbiota which inhabits it.

Intestinal function is highly dependent on its tissue architecture allowing for the greatest possible surface area enabling tasks such as efficient digestion of food. The most prominent feature is the exceptionally large surface area of the lumen derived from its many projections and folds, known as villi which on an ultrastructural level is made up of a variety of cell types, the most common being epithelial cells. Epithelial cells, enterocytes, lining the intestine exhibit microvilli on the apical surface providing a greater surface area for absorption of nutrients. Due to the constant physical process of food moving through the gut, enterocytes are sloughed off and therefore replaced by new cells arising from the cells located in the crypts of Lieberkuhn. The new cells originate from stem cells near the bottom of the villi crypts, which also provide a means of cells replacement for other cells including Paneth, enteroendocrine and goblet cells. Further division and differentiation of cells as they move upwards towards the villi and in the case of enterocytes, balance the amount of lost cells with new cells. Paneth cells express and secrete a number of factors (EGF, TGF α , Wnt3 and the Notch-ligand Dll4) to maintain the stem cell niche and cellular homeostasis (Sato et al., 2011). Importantly, Wnt3 signalling initiated by binding to the 7 trans-membrane receptor Frizzled and its co-receptor LRP 5/6 and leads to inhibition of GSK3 β , Axin and APC complex which would otherwise cause β -catenin ubiquitination thus tagging it for degradation by the proteasome (MacDonald et al., 2009). Lack of β -catenin breakdown allows its levels to build in the cytoplasm so that it may translocate into the nucleus to induce β -catenin mediated gene expression providing proliferative signalling for cell progenitors (Sato et al., 2011, van de Wetering et al., 2002, MacDonald et al., 2009). Labelling of Lgr5 exposes a stem cell population (figure 1.1.), which is mitotically active under normal conditions, provides daughter cells to maintain the stem cell population but also balance normal cell loss in the stromal population (Cheng and Leblond, 1974, Yan et al., 2012, Tian et al., 2011). However, another subset also thought to exist, characterised by Bmi1 expression, activates when damage to the gut has occurred but are otherwise quiescent (Kozar et al., 2013, Yan et al., 2012, Tian et al., 2011). Functionally these two populations react differently to canonical Wnt signalling; with the Lgr5 and not the Bmi1 population proliferating to retain normal cellular homeostasis (Yan et al., 2012). Sensitivity of these two populations to damage also varies with Bmi1 positive cells showing

resistance to radiation and chemotherapy (Zhu et al., 2013, Shivdasani, 2014). On the other hand, once Bmi1 cells activate and awaken from a quiescent state their resistance diminishes (Zhu et al., 2013). Chronic disease is damaging to this Bmi1 population, which are activated after the initial damage to the tissue but are sensitised to further stress. This further stress occurs during the ongoing injury in chronic disease. Certainly this aberration of the local stem cell population within the intestine would disrupt regeneration. Chronic intestinal diseases such as coeliac disease (autoimmune) often present as long-term pro-inflammatory conditions in which cytokine production leads to cell death and diminished tissue architecture along with local stem cell reserves (Piscaglia et al., 2015). An ideal treatment for such diseases would not only protect the local stem cell population but also provide positive growth signalling for stromal cells and the stem cell population. Furthermore, acute intestinal conditions such as necrotising enterocolitis in new-borns would benefit from treatments that provide regenerative signalling such as growth signalling and modulation of the inflammatory response.

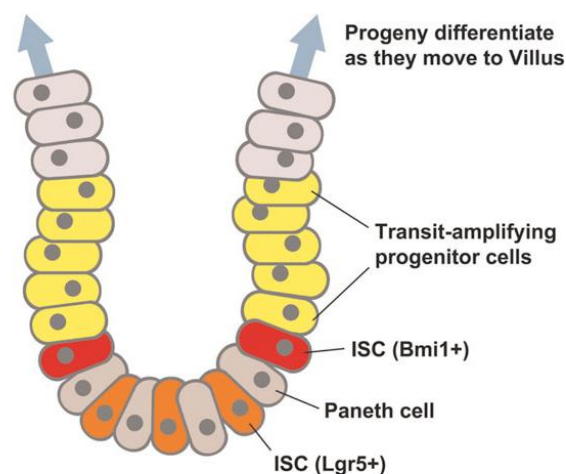


Figure 1.1: Intestinal stem cell (ISC) populations expressing Bmi1 or Lgr5 within the crypts of the mammalian intestinal lumen. The ISC progeny, the transit-amplifying cells are moved towards the tip of the villus as they differentiate. It is the Lgr5 positive ISCs that provide that maintain this constant epithelial cell homeostasis. Modified from Karpowicz and Perrimon, 2010 (Karpowicz and Perrimon, 2010).

Protection from stress is particularly important in the intestine because it serves as a barrier to infection. Stresses can originate from pathogenic bacteria infection or an imbalance in the microbiota leading to increased endotoxin levels such as LPS exposure. LPS binds to TLR4 on host cell surfaces and causes an NF- κ B signalling response and consequential inflammation (Shi et al., 2007).

***In Vivo* rodent models of NEC**

In vivo rodent models of NEC have been developed (Koike et al., 2017, Chen et al., 2016, Zani et al., 2016, Zani et al., 2014). Furthermore, a number of different methods have been used to induce the pathology and mimic that seen in humans. Such methods include hypoxia, maternal separation, gavage feeding, oral LPS administration and hyperosmolar formula feeding. Combinations of these methods have been tested to improve on the frequently used mix of gavage feeding with hyperosmolar formula and hypoxia (Zani et al., 2016). Hyperosmolar feed is thought to cause a fluid shift from the villus vessels to the bowel lumen as well as increasing gut permeability and predisposing them to bacterial toxin uptake (Zani et al., 2016, Zani and Pierro, 2015). Although not thought to be specific to maternal separation, separation is known to induce barrier dysfunction and has been proposed to contribute to endoplasmic reticulum stress and subsequent signalling responses (Li et al., 2016). Stress response proteins such as BiP and CHOP are increased along with the apoptotic marker, CC3. Moreover, maternal separation leads to decreases in Goblet cell numbers thus reducing the capability of mucus production. Arguably of most importance to the induction of NEC *in vivo* is the introduction of bacterial LPS within the neonatal intestine (Zani et al., 2016, Jilling et al., 2006). NEC has been shown not to occur within germ free rodents and does not occur in utero (widely believed to be sterile) (Jilling et al., 2006, Rozenfeld et al., 2001). The high expression of TLR4 in neonates, a receptor of LPS, may explain the high susceptibility of pre-term infants to NEC compared to full term born infants who have a lower level of TLR4 expression therefore making them more vulnerable to the inflammatory signalling instigated by LPS (Fusunyan et al., 2001, Chan et al., 2002, Jilling et al., 2006).

Current Medical Management

Managing the severity of NEC in the best way possible is highly debated, however suspected (Bell stage 1) or mild to moderate confirmed (Bell stage 2A-B) cases of NEC are often managed without surgery (Zani and Pierro, 2015). IV fluid feeding is carried out to reduce aggressive enteral feeding, which can exaggerate the hypoxic environment but also risks damaging fluid shifts in the villi described later, but also enhance bowel rest (Zani et al., 2016, Zani and Pierro, 2015, Koike et al., 2017, Chen et al., 2016). Ventilatory and inotropic support help facilitate efficient oxygenation of the intestine as well as preventing heart and respiratory failure due to under-development (Zani and Pierro, 2015). Additionally, the use of antibiotics are widely utilised clinically although their deployment varies greatly between hospital culture and individual clinicians (Zani and Pierro, 2015). It is not known whether a specific bacterial species or set of species causes NEC. Furthermore, the use of broad spectrum antibiotics may be detrimental to the neonate's health because of their tendency to destroy most if not all of the gut microflora, some of which are believed to be beneficial to the normal intestinal homeostasis (Zani and Pierro, 2015, Khailova et al., 2010, Khailova et al., 2009). Further deterioration or perforation of the gut often calls for the surgical resection of the affected region. However, if the infant survives NEC following surgical resection they will often present with long term intestinal conditions such as short bowel syndrome (Zani et al., 2014, Zani and Pierro, 2015, Rees et al., 2008). It is therefore apparent that there is a need for a treatment for NEC without significant adverse effects. However, a better understanding of stem cells and their potential as a regenerative therapeutic has led to the option of stem cells potentially being able to treat NEC.

Stem Cells

A Russian-American histologist, Alexander A. Maximow, coined the term 'Stem cell' at a special meeting of the Berlin Haematological Society on the 1st of June 1909 as he explained his Unitarian theory of haematopoiesis (Konstantinov, 2000). However, it was not until the 1960's when Ernest A.

McCulloch and James E. Till from the University of Toronto led pioneering research that opened the scientific community's eyes to stem cells (Siminovitch et al., 1963, Becker et al., 1963).

Stem cells can be defined as a cell that has the ability to self-renew and to differentiate into one or more cell types. In order to do this, it should be able to divide asymmetrical in order to produce a multipotent daughter cell and a further progeny cell which has a more specialized function (Weissman, 2000, Weissman et al., 2001). However, this classic approach to defining a stem cell has come under scrutiny since the number of studies claiming their use in the field of therapeutics has risen (Bianco and Gehron Robey, 2000, Orkin and Zon, 2002). This is particularly true due to the wide propensity of stem cells available from different tissues and developmental origins. Prior to testing cells must be isolated and purified so that the population is homogenous and then rigorously characterised to determine marker expression, which can alter during population expansion (Orkin and Zon, 2002, Bianco and Gehron Robey, 2000, Holden and Vogel, 2002). Demonstration of tissue specific functions and a significant purpose within the host tissue are other factors that have also been requested prior to the term 'Stem cell' can be applied to a prospective cell (Holden and Vogel, 2002, Anderson et al., 2001).

Potency

The potency of a stem cell describes its potential to differentiate into different cell types. Stem cells can be described mainly as being totipotent, pluripotent, multipotent, oligopotent and unipotent. Pluripotent cells are described by the National Institutes of Health Guidelines for Research Using Human Pluripotent Stem Cells as, "cells that are self-replicating, are derived from embryos or foetal tissue, and are known to develop into cells and tissues of the three primary germ layers (ectoderm, endoderm, and mesoderm). Although human pluripotent stem cells may be derived from embryos or foetal tissue, such stem cells are not considered embryos." Pluripotent cells are the descendants of blastocyst derived totipotent stem cells, that unlike pluripotent stem cells can differentiate into any cell within the body with the potential to form a complete and viable organism (Donovan and Gearhart, 2001). Multipotent stem cells can differentiate into most cell types, but do not have as

large a differentiation capacity as totipotent or pluripotent cells. Oligopotent cells, such as myeloid stem cells, only have the potential to differentiate into a few cell types. Lastly, unipotent stem cells will differentiate into a single cell type.

Embryonic stem cells are derived from the inner cell mass of the blastocyst. These pluripotent stem cells can provide limitless copies of them-selves and are extremely potent. Therefore pluripotent stem cells prove attractive for use in regenerative medicine and as a key in vitro developmental model. Foetal stem cells derive from the growing foetus following the embryonic stage. They provide the regenerative capacity to not only form new tissues, such as during organogenesis as part of normal development, but they also maintain the cellular make up of tissues. This can be part of processes such as the turnover of blood or regeneration of tissue following injury. Adult stem cells, which are often multipotent, also provide a bank of cells ready to divide in order to both replenish the stem cell niche following injury or normal cell turnover such as the cells lining intestinal villi. Lastly, induced pluripotent stem cells (iPSCs) are frequently produced by introducing various factors to the culture of a multipotent stem cell whilst in embryonic culture conditions in order to re-programme them from a multipotent cell to pluripotent, thus creating a more flexible cell for use (Takahashi and Yamanaka, 2006). Four transcription factors, known collectively as OSKM (Oct4, Sox2, Klf4 and c-Myc) were found to be the key to pluripotency induction (Takahashi and Yamanaka, 2006). All of which are involved in regulating self-renewal and differentiation of undifferentiated embryonic stem cells. Unfortunately, the altered signalling involved in creating iPSCs is poorly understood and their use for therapy is widely considered to be unsafe until more is known about these processes (Ohnuki and Takahashi, 2015).

Octamer-binding transcription factor 4 (Oct-4) is frequently used as a marker for undifferentiated cells (Niwa et al., 2000). This transcription factor must be tightly regulated (Figure 1.2.) within stem cells in order to prevent too much or too little expression which can lead to differentiation (Niwa et al., 2000). Oct-4 interacts with many other proteins such as WD repeat containing protein 5 (WDR5) (Ang et al., 2011). Furthermore, it was found via chromatin immune-precipitation that the WDR5

gene (intron 1) is a downstream target of Oct4 and Nanog 1 (another marker of undifferentiated cells) (Ang et al., 2011). Research such as this not only shows the complexity of the undifferentiated state but also the wide propensity of markers for undifferentiated cells.

Morphology

Stem cells can present morphologically as either epithelial or mesenchymal. Epithelial stem cells, including those that reside in the crypts of Lieberkühn within the intestinal villi, do not actively migrate and so their role is often to replenish the cell population at the site at which they lie (Blanpain et al.). In contrast, at the point at which cells lose all their connection to their stroma they become mesenchymal. Mesenchymal stem cells, although traditionally found in the bone marrow, can be found in many tissues and are often multipotent and thus frequently present a more valuable cell than their epithelial counterparts. Classical definitions of MSCs describe them as being both adherent and non-haematopoietic whilst expressing CD90, CD73 and CD105 but do not express CD45, CD34 and CD14 (Madrigal et al., 2014).

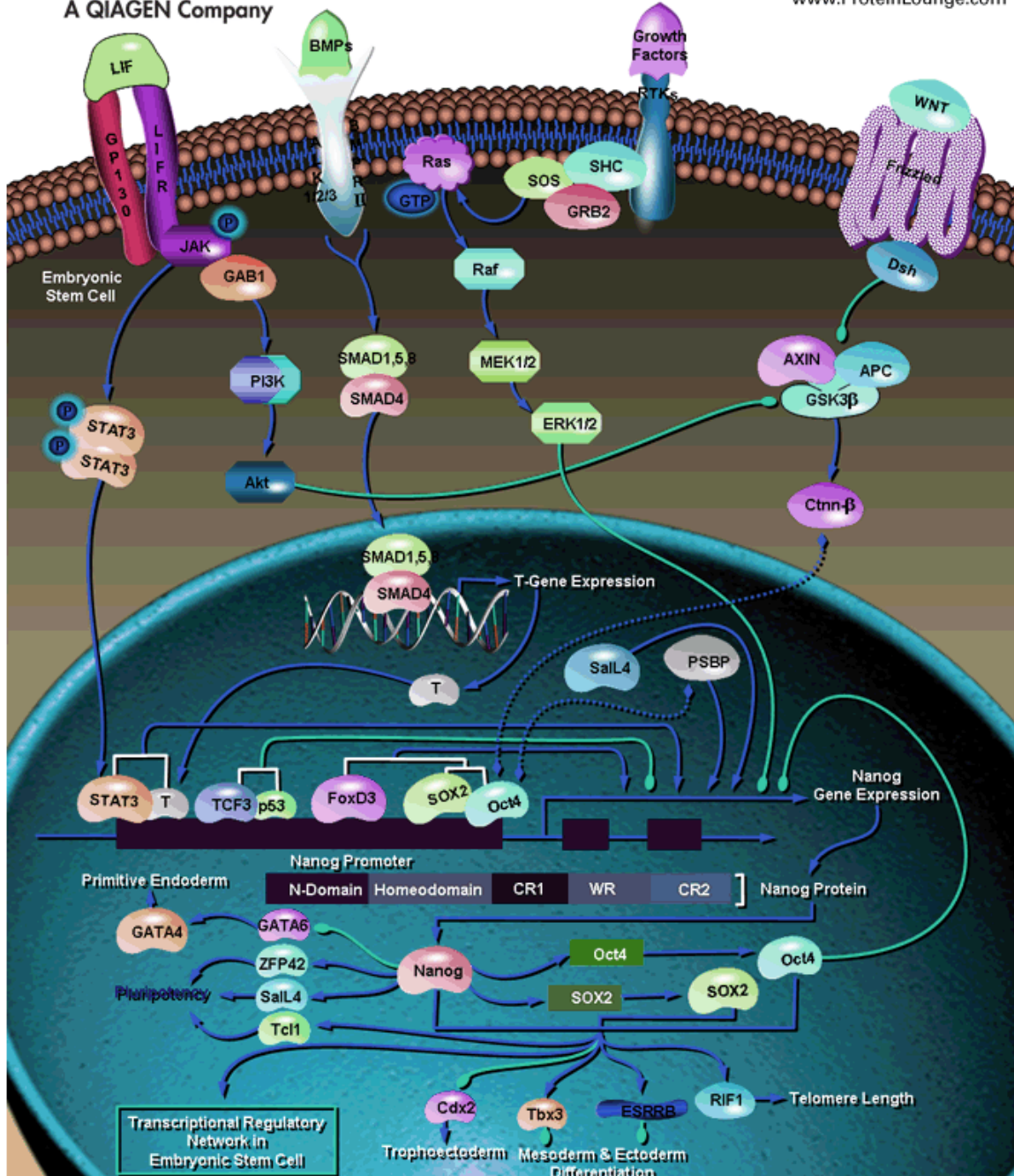


Figure 1.2: Regulation of the Nanog genes transcription is tightly controlled by various transcription factors. SOX2 and Oct 4 bind to the Nanog gene aiding its expression to promote self-renewal in the embryonic stem cell. However, too much Oct-4 expression can lead to an autogenic inhibition of Nanog and therefore differentiation of the cell. From Qiagen.

Use of Stem Cells for Therapy

Although not fully understood at the time, the use of stem cells for therapy arose with the development of bone marrow transplants established through the 1950's to 1970's by E. Donnall Thomas and his team (Thomas et al., 1957). This work showed that the intravenously injected blood cells could repopulate the bone marrow niche in order to restore bone marrow reserves and function. In 2011 the stem cell therapeutics market, although mostly made up by the bone marrow transplant sector, was estimated to be worth \$2.7 billion. Additionally, auxiliary stem cell products and stem cell bio-banking sectors were estimated to be worth \$2.6 billion. The overall market was worth \$8.8 billion by 2016 (Visiongain, 2012). This data shows how the promise of stem cell based therapeutics entering our health care system in the future has attracted massive funding in a race to not only find the best stem cell source for use but also the optimum way to apply them.

Advantages and Disadvantages of Stem Cells for Therapy

Ethical concerns over the use of embryonic stem cells make their use an issue, especially in the USA due to federal funding restrictions. This comes mainly from the fact that they originate from the inner cell mass of a blastocyst, and in order to isolate them the potential future foetus is terminated. Much of the time, blastocysts used for this isolation are retrieved from in vitro fertilisation procedures where some blastocysts are simply discarded. However, due to the high regenerative potential of the ESCs, cell lines can be produced, thus reducing the requirement of freshly isolated ESCs. Many stem cell lines were isolated in the 1990's and are still in use today for research. Therefore, the ability to create these cell lines in this way has an advantage over many adult stem cells, which must be harvested frequently to provide a primary supply suitable for research. Unfortunately there is a risk of teratoma formation due to the high regeneration potential involved when using pluripotent cells and they must be rigorously tested before being used clinically (Ohnuki and Takahashi, 2015). Furthermore, the 'stem cellness' can decline over time with continued passaging. Additionally, the current techniques involved in differentiating these cells must be refined so that they become more specific as to not form unwanted cell types in vivo. As an example, in the

case of a search for stem cell use in creating an unrestricted supply of red blood cells for blood banks, much of the research is presently untranslatable from small scale lab work to large scale industrial production. The wide use of animal products, such as foetal bovine serum (FBS), creates the issue of infection and immune related risks when adapting a lab created product to a clinically used product. The Food and Drugs Agency (FDA) set up guidelines to prevent such issues (Halme and Kessler, 2006). Efforts have been made to culture cells in serum free medium or autologous derived serum based medium (Bhasin et al., 2011, Honmou et al., 2011). Furthermore a huge tissue bank would most probably be required in order to receive cells for tissue matching. This is not so much the case for iPSCs, although they do require more processing in order to attain the pluripotency.

An important factor to consider when using stem cells is the heterogeneity of the body's cellular population. The programming of cells in the body varies greatly depending on where they reside and thus collate stromal signals into a resulting pattern of gene expression. As stem cells are found throughout the body and from various sources, gene expression can be highly heterogenic and may result in stem cells acting in different ways, something that should be considered prior to their clinical use (Ebben et al., 2011, Cahan and Daley, 2013). Essentially the correct stem cell should be matched for the disease or use it is required for. There is of course an ongoing debate as to which stem cell is best for use. An example of improving the effectiveness of the stem cells is to pre-condition them. Such processes include pre-treating amniotic fluid stem cells with IL-1 β , with the aim of inhibiting the activation of T-lymphocytes thus altering the immune response and potentially reducing inflammation (Moorefield et al., 2011a). Furthermore, by increasing the lifespan of the stem cells once introduced to the patient, their effects are thought to be extended. This was done using a ROCK inhibitor, Y-27632, to enhance the life span of human-ESCs (Watanabe et al., 2007). Exposing the stem cells to hypoxic conditions prior to use has been shown to improve their therapeutic potential, thought to be due to an increased stress response (Hu et al., 2008), as explained later in more detail. Unfortunately, once injected into the body the concentrations of stem cell products and the stem cell activity is difficult to estimate, making the estimation of how many cells to inject in the first place a challenging task (Murphy et al., 2013). Stem cell therapies can use allogeneic or

autologous derived stem cells. Their effectiveness may depend on their immunogenicity. Allogeneic stem cells, cells from a non-self-donor, may cause an immunological response and therefore be destroyed before reaching their therapeutic potential but may also cause a harmful inflammatory response to the body. Furthermore, the use of allogeneic stem cells poses a risk of viral trans-infection from donor to recipient (Ikegame et al., 2014). Autogenic stem cell use may therefore overcome the disadvantages presented by allogeneic stem cell use and potentially aid the regenerative process and protect from necrosis rather than possibly inducing it further because of consequential inflammation.

Amniotic Fluid

At the start of the second week of human gestation the amniotic fluid materialises and thus forms a protective barrier around the developing embryo and foetus. In humans the volume of AF increases from 20ml at week 7 to 1000ml at week 34 and then subsequently reduces in volume to 800ml towards term (Beall et al., 2007). AF is known to contain foetal urine and foetal lung fluid, both of which increase over time (Brace et al., 1994, Rabinowitz et al., 1989). Post term pregnancies can pathologically present as oligohydramnios, where there is too little AF present, due to the 33% reduction in AF volume per ongoing week. In contrast, a condition where excessive AF is present, polyhydramnios usually occurs following twin-to-twin transfusion syndrome (Beall et al., 2007). Both extremes can cause birth complications and foetal defects. Amniocentesis is a procedure commonly used to remove a sample of AF whether this is to reduce the volume associated with polyhydramnios, sometimes around 4 litres, or often in the second trimester to remove around 2ml of AF for analytical processing. AF contains a wide variety of cell types originating from extra-embryonic structures such as the placenta but also foetal tissue (Gosden, 1983). The morphologies of cells found in AF can be characterised into fibroblastic, epithelioid and amniotic fluid in order of relative abundance (Hoehn et al., 1975).

Amniotic Fluid Stem Cells

In 2003 a small sub-population (0.1-0.5%) of AF cells were shown to express Oct-4, a transcription factor of undifferentiated cells (Prusa et al., 2003). This was later demonstrated to be the case as these AF Oct-4 cells were shown to be C-kit (CD117) positive and were able to differentiate into a number of lineages including osteogenic, myogenic, hepatic and neural (Tsai et al., 2006, Kim et al., 2007, De Coppi et al., 2007, Prusa et al., 2003). The surface antigen C-kit is used to characterise and isolate this small pluripotent population later called amniotic fluid stem cells, of which over ninety percent express Oct-4 (De Coppi et al., 2007). Isolation can be completed through the use of magnetic columns and magnetic beads selective for C-kit or a FACS cell sorting machine following the marking of the cells with C-kit selective antibodies. Furthermore the culturing of C-kit positive AFSCs is carried out in non-tissue treated flasks or dishes in order to provide optimum growing conditions for C-kit selected AFSCs, essentially adding a further selective measure. Karyotyping of AFSCs from male births showed that the AFSCs contained the Y chromosome and were therefore of foetal origin as opposed to maternal (De Coppi et al., 2007, Moschidou et al., 2012). Along with a rapid 36 hour doubling time, late passages of AFSCs still maintain a constant telomere length (De Coppi et al., 2007, Valli et al., 2010). Their characterisation revealed the presence of markers such as CD90, CD73, CD105, CD29, CD44 and MHC-I (De Coppi et al., 2007, Moorefield et al., 2011b). The presence of MHC-I may aid the cell with their immune-modulatory properties (Bailo et al., 2004). In contrast, markers including CD34, CD14, CD45, CD133, CD31 and MHC-II were not expressed (De Coppi et al., 2007, Ditadi et al., 2009, Chiavegato et al., 2007, Guan et al., 2011, Rota et al., 2012). Moreover, pluripotency markers such as Oct 4, SSEA3, SSEA4, NANOG, KLF4, Myc, TRA1-60 and TRA1-81 are expressed by the AFSCs (Moschidou et al., 2012, Zani et al., 2014, Wolfrum et al., 2010). Although AFSCs cannot be considered true pluripotent cells because of their lack of ability to produce tumours in immune-deficient mice, such as the SCID model (De Coppi et al., 2007, Moschidou et al., 2012, Carraro et al., 2008, Chiavegato et al., 2007, Gekas et al., 2010, Ma et al., 2012). However, Moschidou et al. proved that culturing AFSCs on matrigel in ES cell medium along with the histone deacetylase inhibitor (HDACi) Valproic acid without the use of ectopic reprogramming factors (AFiPS)

could induce their pluripotency (Moschidou et al., 2012). Furthermore, AF iPSCs were shown to produce tumours in SCID mice.

Advantages of Amniotic Fluid Stem Cells for the Use of Therapy

Advantages over other stem cells currently being researched, such as ESCs, make AFSCs highly favourable for stem cell based regenerative therapy. AFSCs can be obtained without ethical concern or interference with diagnostic procedures because they are retrieved through amniocentesis, which is required for diagnosis anyway, or amnio-drainage, which is often used as a protective measure for the baby and mother. Their use is seen to be safe because the AFSCs remain genomically stable and lack the ability to form tumours. However, if the need to reprogram them to pluripotency arose, the methods required are highly efficient, easy to follow and produce a set of cells whose pluripotent phenotype is stable. Furthermore, their use provides a reduced risk of random genetic integration of transgenes that could reprogram the host genome (Kaji et al., 2009, Warren et al., 2010). Additionally, AFSCs exhibit a phenotype and multi-lineage differentiation capacity similar to postnatal bone marrow (BM) derived mesenchymal stem cells (MSCs) (In 't Anker et al., 2003). Promisingly, expansion potentials of amniotic fluid-derived MSCs were also revealed to surpass that of BM-derived MSCs (In 't Anker et al., 2003), which therefore makes them an attractive cell source for future therapeutic approaches. Their extensive differentiation potential is mirrored by their ability to co-stain by over 75% with a minimum of two surface marker proteins such as Sox17 (an endodermal marker), SM22 α (a mesodermal marker) and Tubb3 (an ectodermal marker), thus making them stand out from other cell types (Maguire et al., 2013). The broad differentiation potential of AFSCs is reflected through their relatively successful use to treat diseased organs derived from all germ layers. Muscle, bone and heart (mesodermal in origin) disease models have been treated along with kidney and lung (endoderm in origin) disease models but also nervous system (ectoderm in origin) based diseases (Chiavegato et al., 2007, Guan et al., 2011, Carraro et al., 2008, Castellani et al., 2013, Perin et al., 2010, Hauser et al., 2010, Peister et al., 2011, Maraldi et al., 2011, Riccio et al., 2012, Calzarossa et al., 2013).

Conditioned Media

Studies that have focused on directly treating disease with stem cells have had issues with the targeting of the stem cells to the area of interest in order to promote regeneration. One such study that looked into treating nerve injuries with AFSCs noticed a large deposition of the cells in the lung after intravenous injection and consequently had to increase the expression of homing factors in the injured tissue to direct a larger proportion of the cells to the correct area of injury (Yang et al., 2012). The use of conditioned medium (CM) would bypass the problem of a lack of target tissue specificity by injecting the CM directly to the area without concern for the treatment actively relocating to an undesirable location in the body. Conversely, previous studies have shown that although injected stem cells did not reach the target tissue, for example were trapped in the muscle following intramuscular injection, a regenerative effect was still recorded (Shabbir et al., 2009). The injection of BM-MSCs into TO2 cardiomyopathy hamster models was compared to the less invasive intramuscular injection of BM-MSC extract, CM, which also significantly improved cardiac repair through reduced apoptosis and fibrosis (Shabbir et al., 2009). A paracrine mechanism of stem cell action was first hypothesised by Gneccchi et al (Gneccchi et al., 2005), who later provided evidence with the use of stem cell CM for the directed functional improvement of ischemic damaged cardiocytes in vitro (Gneccchi et al., 2006). Investigations into other disease models including spinal injury support a paracrine theory of stem cell action. Human umbilical mesenchymal stem cells were implanted into the lesion of pre-transected rat spinal cords (Yang et al., 2008). This resulted in an increase in the number of axons and reduced the number of microglia and astrocytes. However, a regenerative setting could not be attributed as being the result of stem cell differentiation because human MSC antigen did not overlap with the new neurons and oligodendrocytes, suggesting the stem cells lay undifferentiated (Yang et al., 2008). Instead large concentrations of cytokines and growth factors such as human basic fibroblast growth factor (bFGF), produced by stem cells, were believed to be the key to the stem cell transplant success (Yang et al., 2008, Lee et al., 1999, Teng et al., 1999).

As briefly discussed previously, preconditioning of cells is an important factor to remember when preparing to collect CM of stem cells. The belief that stem cells act as repair mechanisms in times of injury to tissues suggests that the stem cells are not constitutively producing paracrine factors which have the potential to induce regeneration. Instead stress signals from the stromal cells that are damaged or that neighbour the damaged cells are thought to reprogram the stem cells to awaken from a quiescent state. Such examples include the satellite cells of the skeletal muscle which activate following inflammation and damage to muscle fibres thus subsequently migrating to the area of damage to replace muscle fibres following myotube formation (Collins et al., 2005). The culture conditions of stem cells can vary greatly and therefore stem cell secretomes are highly likely to vary because of this. It may prove necessary to alter these conditions in order to retrieve the optimum set of trophic factors for the user's requirement.

Microvesicle and Exosome Biogenesis and Release

Small extracellular bodies produced by the stem cells constituting of both microvesicles and exosomes mediate the delivery of trophic factors within the conditioned media.. Exosomes are the smallest of the two vesicles (30-100nm). Their release (Figure 2a) is mediated through the fusion of multivesicular bodies with the cell membrane through exocytosis, thus releasing multiple exosomes into the environment (They et al., 2002b, They et al., 2009). Microvesicles are however larger in size (ranging from 100-1000nm) and released directly (Figure1.3.b) from the cells plasma membrane (They et al., 2009). Both vesicle types are found in various fluids such as blood, plasma, urine, saliva, breast milk, cerebral spinal fluid and amniotic fluid (Murakami et al., 2014, Hata et al., 2010, Kafian et al., 2014, Keller et al., 2007, Burgos et al., 2014, Xiao and Wong, 2012).

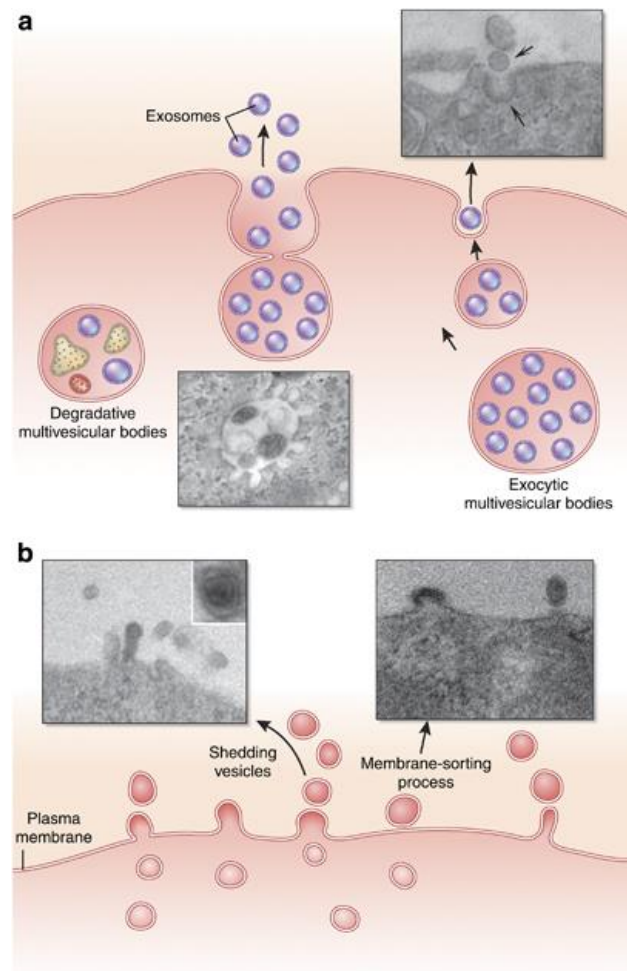


Figure 1.3: Mechanisms of exosome release. A depiction of how exosomes are released from the cell (a) compared to microvesicles (b). From Camussi, G., et al. (Camussi et al., 2010).

Although exosome release is thought to be regulated it also takes place constitutively, unlike microvesicles, which are mainly believed to be released in a regulated manner (Cocucci et al., 2009). Exosome release has been shown to be a p53 controlled process and is therefore thought to be up-regulated by stress (Yu et al., 2006). The activation of the p-53 pathway is likely to directly interact with tumour suppressor-activated pathway 6 (TSAP6), otherwise known as steap3, thus upregulating exosome release (Lespagnol et al., 2008). Exosome release is postulated to transfer stress linked receptors from one cell to another so that other cells may intercept signals indicating a hazardous environment, therefore inducing a more resilient cell (Yu et al., 2006). Using the ionophore treatment monensin (MON), exosome release was upregulated, providing evidence that this process

is partly calcium dependent, further backed up by the chelation of calcium with BAPTA-AM leading to reduced exosome release (Savina et al., 2003).

The endosomal sorting complex required for transport (ESCRT) mediates the inward budding of vesicles derived from the membrane of endosomes by weakening the endosomal membrane at isolated sites, via protein-protein and protein-lipid interactions. ESCRT I/II/III recognise monoubiquitinated cargoes and promote their inclusion in multivesicular bodies (MVBs) via an inward budding mechanism (Piper and Katzmann, 2007). ESCRT I/II orchestrates the clustering of ubiquitinated cargoes to the endosomal membrane following their binding to hepatocyte growth factor – regulated kinase substrate (Hrs), a component of ESCRT 0, on the clathrin coats surrounding the endosomal membrane (Hurley, 2008, Williams and Urbe, 2007). The role of ESCRT III proteins is to facilitate the removal of ubiquitin from cargo via de-ubiquitylating enzyme employment. Apoptosis linked 2 interacting protein X (Alix) is thought to link the various ESCRT complexes thus promoting their interactions (Babst, 2005). ESCRT then dissociates from MVB membranes aided by adenosine triphosphatase vacuolar protein sorting 4 (Vps 4), also recruited by ESCRT III, and is then recycled (Yeo et al., 2003).

Cholesterol and sphingomyelin rich micro domains, otherwise known as lipid rafts, have been shown to be important components of both microvesicle and exosome origins. A reduction in lipid rafts have led to reduced microvesicle budding (Del Conde et al., 2005, Lakkaraju and Rodriguez-Boulan, 2008). Lipid rafts are thought to cluster the proteins required for the release of both exosomes and microvesicles from the plasma membrane and are therefore not thought of as being specific to either exosome release or microvesicle release mechanisms (Cocucci et al., 2009). On the other hand, reducing cholesterol at the membrane or cholesterol synthesis has also been shown to increase exosome release, believed to be a result of removing associations between Rab7 and endosomes and instead allowing Rab 7 to associate with Rab4, which leads to increased endosomal recycling speed. Furthermore this is thought to result from an increase in endosomal migration to the positive pole of micro-tubules (Stoeck et al., 2006, Keller et al., 2007, Lebrand et al., 2002, Chen et al., 2008). Rab

proteins (small GTPases) promote exosome docking and membrane fusion events, specifically Rab35. Their inhibition leads to the accumulation of endosomal vesicles intracellularly and a reduction in exosome secretion (Ostrowski et al., 2010, Hsu et al., 2010).

In order for exosome release to take place the MVB must fuse with the plasma membrane. This is mediated by two main types of soluble N-ethylmaleimide-sensitive factor attachment protein receptors (SNAREs). The first resides on the MVB membrane, vesicular SNAREs (v-SNAREs), whilst the other presents itself on the intracellular side of the plasma membrane, a 'membrane-bridging SNARE complex' known as target SNAREs (t-SNAREs) (Südhof and Rothman, 2009, Urbanelli et al., 2013, Chaineau et al., 2009). Interaction between these two sets of SNARE proteins enables the coming together of the MVB membrane and plasma membrane.

Microvesicles as discussed are released via a blebbing like mechanism. The initiation of their formation and release is preceded by the translocation of phosphatidylserines (PS) from the intercellular side of the cells plasma membrane to the extracellular side, mediated by floppases (Zwaal and Schroit, 1997). A series of ERK facilitated phosphorylation follows. Conscripted by phospholipase-D at the membrane, myosin light chains activate and cytoskeletal organisations contract to allow microvesicle release (Muralidharan-Chari et al., 2009, McConnell et al., 2009).

Microvesicle and Exosome Isolation and Analysis

There are various techniques to isolate exosomes and microvesicles. Commonly, a two-step differential centrifugation is used. Centrifugation of the sample at a lower speed, around 17000g, removes cells and debris but not the vesicles, which are of too low a density and therefore remain in the supernatant. An ultracentrifugation step at 200,000g follows in order to pellet the vesicles. However, stepwise centrifugation is time consuming (Alvarez et al., 2012). Tamm-Horfall protein (THP) traps exosomes during initial low speed centrifugation (17000g). THP is reduced using DL-dithiothreitol to increase exosome yield (Alvarez et al., 2012). Furthermore, a sucrose density gradient technique can be used in which fractions of supernatant are formed following centrifugation. Each fraction contains specific particle masses and can therefore be collected through

simply pipetting (They et al., 2006). The use of immune-magnetic micro beads specific for markers (such as HLA-DP) found on exosomes or microvesicles have also been used for vesicle isolation. Light microscope based studies cannot confirm the purity of the selection and so an electron microscope is often used (Clayton et al., 2001). Exosomes carry lots of different molecules (Schorey and Bhatnagar, 2008). The exosomes themselves bring stability to their contents, more so than if they were found freely, for example in plasma. However, the correct storage of exosome containing supernatants at -20°C ensures the constant size of exosomes throughout storage (Yu et al., 2014). ExoQuick (Systems Biosciences) is a commercial precipitation reagent for high quality exosome isolation with high quality miRNA and mRNA (Beninson et al., 2014).

CD24, a protein often expressed on haematopoietic subpopulations of B and T lymphocytes, is a marker of exosomes in AF and urine (Keller et al., 2007). It is due to CD24's glycosyl-phosphatidylinositol (GPI) anchor, which specifically localises the associated protein to lipid rafts that largely increases CD24 concentration in exosomal membranes (de Gassart et al., 2003). However, other markers such as CD63, a membrane tetraspanning protein on exosomes, can also be used to quantitatively assess exosomes using an ELISA assay (Beninson et al., 2014). Markers such as IL-6, which are not expressed on exosomes, may also be used in tandem to act as a control measure (Beninson et al., 2014). Microvesicles unlike exosomes have a high concentration of PS and can therefore act as a marker to distinguish between the two.

Shuttle RNA

The first indication of miRNA detection came from the Ambros and Ruvkun labs who were working on *C.elegans* when a short RNA sequence was found to alter the time of transitions during the worm's development. The mechanism surrounding this outcome was found to be the miRNA complementarily binding to the bases of target mRNA (Lee et al., 1993, Wightman et al., 1993). Later research elaborated upon this process. Argonaute (AGO) proteins, the catalytic components of the RNA induced silencing complex (RISC), associate with miRNA. The miRNA directs AGO to complementary mRNAs to endonucleolytically cleave them, thus silencing their expression

(Hutvagner and Simard, 2008). A process of mRNA translational suppression is believed to be ensued by mRNA degradation. However, miRNAs were found not to be as specific as first thought with individual miRNAs targeting numerous mRNAs and the majority of mRNAs being targeted by multiple miRNAs (Chi et al., 2009). Both mRNA and miRNA are found in microvesicles and exosomes and may therefore be transferred to target cells to influence their behaviour. In the case of mRNA, a direct instruction for protein production could be transferred as opposed to miRNAs mechanism of action as explained. The selective trafficking of RNA binding proteins to vesicles is thought to play a major role in selectively transferring RNA to the exosomes and microvesicles (Valadi et al., 2007, Skog et al., 2008, Taylor and Gercel-Taylor, 2008, Mittelbrunn et al., 2011). Ribonucleoproteins (RNPs) are thought to act in such a manner (Figure 1.4.) as well as Gag proteins found in retroviral vesicle biogenesis processes to target larger RNAs to the budding vesicles (They et al., 2001, Alcazar et al., 2009).

mRNA contained in exosomes has been shown to be translated into protein production (Valadi et al., 2007). This field of work has become of high interest not only within areas of cancer biology but also stem cell biology (Ratajczak et al., 2006, Skog et al., 2008, Lotvall and Valadi, 2007, Valadi et al., 2007). In the case of stem cells, RNAs are believed to be a major mediator of regenerative potential of stem cell exosomes and microvesicles. The transfer of Oct-4 mRNA in microvesicles could handover a direct instruction for pluripotency and increased regenerative potential (Ratajczak et al., 2006). A point to note when studying miRNAs found in micro-vesicles and exosomes, if any at all, is that the miRNAs up-regulated in stressful conditions and times of disease often provide a large switch like effect as opposed to fine tuning, as suggested takes place in most cases (van Rooij et al., 2007). By analysing 47 gene products that derive from mRNA found in exosomes, the mRNA is believed to be involved in cellular growth, protein synthesis and the post transcriptional modification of RNA (Lotvall and Valadi, 2007). Furthermore, exosomal miRNA analysis shows a variety of functions related to stem cell properties such as differentiation, organogenesis (miR-1) and development (Let-7) (Alvarez-Garcia and Miska, 2005, Zhao et al., 2005, Eirin et al., 2014). The levels of these 'exosomal shuttle RNAs' could potentially decrease or increase depending on the

environment in which the cell they derive from is kept in. Introducing cells to a hypoxic environment is thought to stress cells and therefore modify the RNA which they express (Bussolati et al., 2012, Hu et al., 2008). Further research must be carried out to confirm whether the stress related RNAs are translocated to the microvesicles or exosomes of the cells following stress exposure.

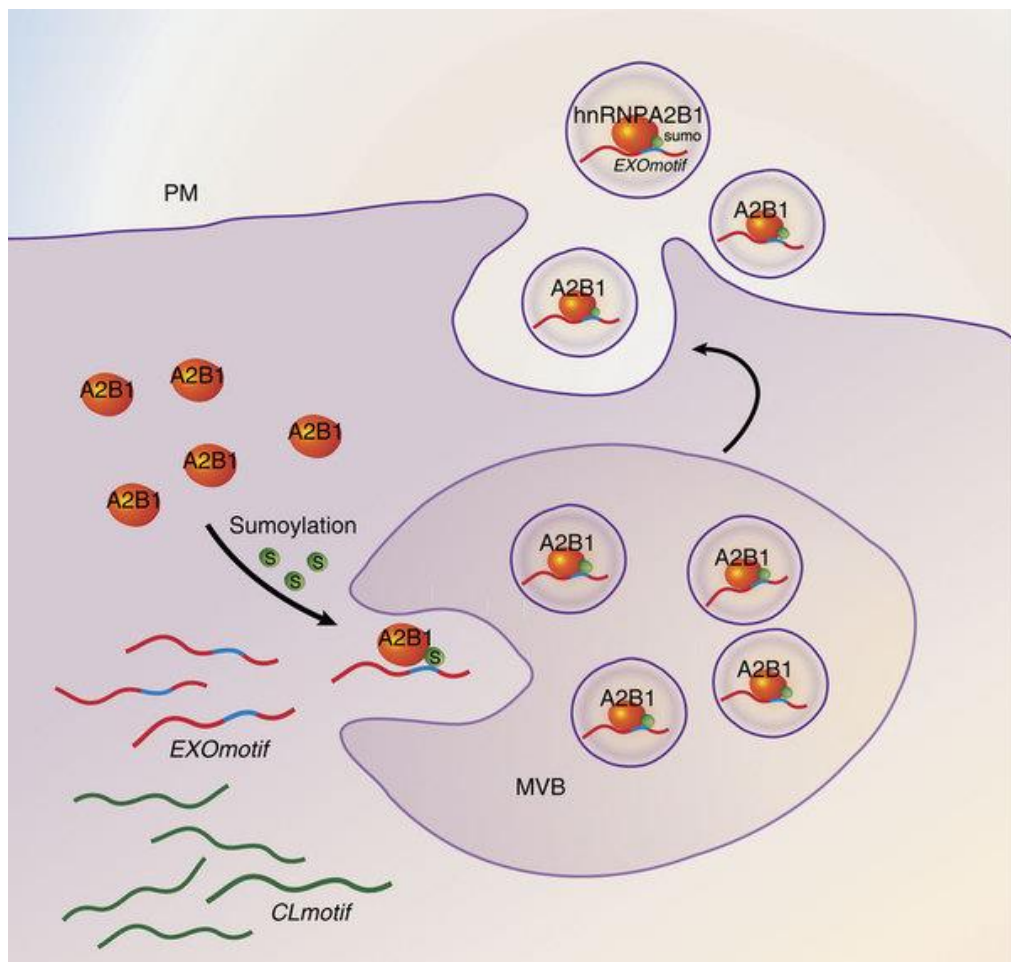


Figure 1.4: Packaging of miRNA into exosomes. Heterogeneous nuclear ribonucleoprotein A2B1 (hnRNPA2B1), a RNP, binds specifically to certain miRNA motifs following hnRNPA2B1 sumoylation (addition of a small ubiquitin-related modifier) allowing miRNA transportation into exosomes. From Villarroya-Beltri, C., et al. (Villarroya-Beltri et al., 2013).

Microvesicle Proteins

Targeting of proteins to the vesicles is aided via widely used cellular mechanisms such as myristoylation and palmitoylation of the protein thus anchoring them to the vesicle plasma membrane (Shen et al., 2011). Stressing cells through hypoxia changes the protein composition of

exosomes and microvesicles (Salomon et al., 2013). As discussed, common proteins found in exosomes and microvesicles include CD63 and CD24, however upon stress, cells may produce other proteins like the heat shock proteins (Hsp72) (Asea et al., 2008), which could provide signals to target cells to potentially protect them in a stressful environment. Moreover, the transport of embryonic related proteins including Oct-4, detected in embryonic stem cell microvesicles along with Wnt-3, may provide a means of inducing regeneration in target tissue (Rolf et al., 2012, Ratajczak et al., 2006). Furthermore as discussed, the protective coating provided by exosomes and microvesicles would allow these regenerative properties to affect wider reaches of the body. Another example of how stem cells may potentiate their effects comes from evidence of active Wnt proteins being discovered within exosomes derived from *Drosophila* cells but also a human Caco-2 colon cancer cell line and embryonic stem cells (Gross et al., 2012, Ratajczak et al., 2006). Their secretion via exosomes was also proven to be dependent on Ykt-6, a R-SNARE protein, providing further evidence that Wnt excretion is in at least partly due to exosome secretion (Gross et al., 2012). Wnt proteins are extremely important morphogens and thus play a role in the patterning of tissues during development. Although Gross's research shows that exosomal transfer of Wnt is not the only route of transfer, because Wnt secretion was still detected following exosome release was inhibited, it provides a possible hypothesis of how Wnt proteins are able to travel over long distances through the body to produce an effect without degrading. Insulin like growth factor binding protein (IGFBP) are also found to reside in microvesicles of C2C12 myoblast cells, a protein which regulates the action of insulin like growth factor (IGF) (Guescini et al., 2010). The transfer of IGFBP to target cells would alter the IGF activity acting to significantly alter signal transduction and therefore increase or decrease IGF activity, hence increasing or decreasing cell growth (Guescini et al., 2010). Understanding the protein content of vesicles excreted by cells would allow their use in regenerative medicine.

Cell Targeting

In order to specifically target cells, exosomes and microvesicles are thought to possess specific surface proteins which bind to complementary proteins on the target cell. Dendritic cell originating exosomes have been shown to express MHC proteins on their surface, which can present pathogen derived peptide fragments. This allows for specific binding of these exosomes to complementary T cell receptors on T cells leading to modulation of T cell activity (Nolte-'t Hoen et al., 2009, Admyre et al., 2006, They et al., 2002a).

Another potential mechanism of cell specificity may lie with the production of enzymes by the target cells. These enzymes could cleave a specific protein on the exosome or microvesicle membrane thus allowing the cleaved product to interact with the target cells surface receptors. Pro-CD46 shed by various cancer cells (in response to stress) on microvesicles for example is cleaved by metalloproteinases on other tumour cells to create an active CD46, which interacts with the enzyme producing tumour cell (Hakulinen et al., 2004). Cell signalling which follows is thought to lead to increased tumour resilience to the stress. This can be compared to a similar mechanism surrounding the actions of the aerolysin toxin produced by *Aeromonas spp.* Only when the furin enzyme is present on a cell does the inactivated toxin become active following its cleavage leading to its action on the target cell, in this case pore formation and apoptosis (Abrami et al., 1998).

A third potential mechanism of vesicle specificity relies on the pH of the tissue the vesicles enter. Tumours have been shown to be an acidic environment, one which is perfect for the fusion of exosomes and microvesicles to the plasma membrane of cells within the tumour in particular the cancerous cells themselves (Parolini et al., 2009). Although evidence is still required, if necrotic tissue is of a lower pH than normal healthy tissue, potentially due to an increase in anaerobic activity and consequential lactic acid production, it may provide a mechanism of targeted regenerative action for these vesicles. Regarding the use of CM as a therapy it is often an aim of researchers to modify the inflammation associated with the necrosis.

The role of inflammation in tissue regeneration

Inflammation has both a role in the aetiology behind pathogenesis but also regeneration of tissue. A sustained inflammatory state in tissue often leads to chronic disease of the tissue with pro-inflammation proving key to a positive feedback loop in which further necrosis of tissue is potentiated by pro-inflammatory factors. In a healthy tissue following injury, this pro-inflammatory response delivers a chemical flag for inflammatory cells, such as macrophages to enter the tissue and remove debris created through tissue destruction. Following debris clearance the pro-inflammatory response diminishes and is replaced by an anti-inflammatory response to spark regeneration. If this critical pro/anti-inflammatory substitution is in some way interrupted the process of regeneration can often be impaired, thus leading to a pathological state. Key to the mediation of an initial inflammatory response is the surrounding stromal cells of the damaged tissue. Following stress of necrotic cell death, cells will secrete chemokines and cytokines, which in turn act as a signal to activate and attract inflammatory cells.

Macrophages

Monocytes, the predecessors of macrophages, circulate in the circulatory systems until activated via stromal cell originating inflammatory signals. Upon activation monocytes migrate to enter the damaged tissue leading to their differentiation into macrophages. ECM breakdown facilitates macrophage infiltration of tissue. Plasminogen, activated by urokinase type plasminogen activator (uPA), enzymatically cleaves ECM. Expression of uPA in macrophages and its secretion promotes their migration into damaged tissue. The total expression of uPA in damaged muscle therefore increases. uPA is also known initiate regenerative signalling and macrophage uPA adds to the tissue regeneration (Novak et al., 2011). Classically, macrophages are known to phagocytose and clear tissue debris or foreign particles such as bacteria following infection. Consequentially the phagosome merges with the macrophages lysosomes. Enzymes and free radicals located or produced in the resulting phagolysosomes aid debris or bacterial breakdown. On the other hand, phagocytic macrophages provide no direct induction of regeneration. Their number gradually decline but are

replaced by anti-inflammatory macrophages thus outlining two major populations of macrophage, M1 macrophages otherwise described as the pro-inflammatory phagocytic type and M2 macrophages also known to be anti-inflammatory.

M1 and M2 macrophages

Exposure of M0 macrophages to IL-10 polarises macrophages towards an M2 phenotype, thought to be due to changes in arginine metabolism. These changes reduce pro-inflammatory nitric oxide production (Villalta et al., 2009). Furthermore P38/MKP-1 interactions with AKT have been proposed to co-ordinate the transition of macrophages from M1 to M2, therefore aiding resolution of inflammation and tissue repair (Perdiguero et al., 2011, Perdiguero et al., 2012). MKP-1, a phosphatase which reverses MAPK phosphorylation, restricts P38 MAPK activation pushing macrophages towards a M2 phenotype. M2 macrophages have been further categorised into M2a, M2b and M2c phenotypes, all of which have different but also overlapping roles to play in an anti-inflammatory response within different situations (Mantovani et al., 2004). Activation of M0 macrophages with IL-4 and IL-13 leads to macrophages that defend the body against parasites, have a role in allergy but also the classic type two inflammatory responses, the M2a macrophages, which secrete anti-inflammatory cytokines. M2b macrophages tend to be induced by TLR agonists and immune complexes. They aid in immune-regulation through cytokine production such as IL-6 and IL-1 but interestingly do not produce high levels of arginine, unlike M2a and M2c macrophages, when exposed to specific types of LPS and immune complexes (Mosser, 2003). M2c macrophages, polarised with IL-10, are also involved in immune-regulation however are heavily involved in promotion of tissue remodelling through matrix deposition. Work by Perdiguero et al. in mice suggests that hyperactivation of P38 due to a lack of MKP-1 activity leads to enhanced miR-21 expression and therefore reduced levels of PTEN mRNA being translated into functional PTEN proteins thus preventing AKT inactivation. Prolonged AKT activation is thought to promote an M1 state and prevent M2 onset (Perdiguero et al., 2011), a potential mechanism to potentiate chronic inflammatory diseases. On the other hand, the premature demise of M1 Macrophages, naissance of

M2 macrophages and expression of anti-inflammatory cytokines are also contributory to inefficient repair. This can lead to early macrophage exhaustion and 'cytokine silencing', characterised by termination of macrophage cytokine production, and inefficient activation of local stem cells whose role is to aid regeneration. Regeneration is also therefore compromised. The fine regulation of a M1 to M2 switch and finally overall macrophage exhaustion can therefore be seen as key to tissue healing and restoration. Altering the endogenous macrophage signalling seen in disease, where the switch is compromised, is suggested as being a therapeutic strategy to bring about favourable macrophage polarisation. Macrophages have been shown to have a greater propensity to take up exosomes compared to non-phagocytic cells therefore providing evidence that exosome uptake by macrophages may at least be mediated by phagocytosis (Feng et al., 2010). An increased susceptibility to take up exosomes may make macrophages a major target of stem cell exosomes and microvesicles, therefore making them potentially responsive to CM.

Alteration of Inflammatory state with Stem cells and conditioned media

With an increased interest in stem cell therapeutics a surge of data has suggested that along with improving regeneration within tissue a, reduction in inflammation is an important issue. Recently it has been proposed that MSCs are, like macrophages, polarisable and can exist as an anti-inflammatory phenotype, MSC2, or even an inflammatory phenotype, MSC1 (Waterman et al., 2010), a process influenced by environmental stimulation. For example if an MSC is injected into a site of pro-inflammatory significance it will adopt an inflammatory state, MSC1. If on the other hand the stem cell TLR3 is stimulated, as opposed to TLR4 in pro-inflammatory conditions, an anti-inflammatory status is assumed. The development of MSC1s may sound counterproductive, however inducing a pro-inflammatory state via their, or their secretomes, introduction into the site of early degeneration may accelerate initial responses to damage and therefore initiate an early regenerative response. It is unknown however whether exposure of stem cells to stress such as a hypoxic environment with little nutrition will push MSCs towards an MSC1 or MSC2 phenotype. Studies into MSC secretomes following this stress will expose any pro or anti-inflammatory mediators being

released and a total profile which can be determined and being pro or anti-inflammatory. Further investigation has uncovered a range of inflammatory modifying factors being released by stem cells. Co-culture of MSCs with macrophages has proven an increased secretion of anti-inflammatory cytokines such as IL-10, IL-4 and IL-13 (Adutler-Lieber et al., 2013). Furthermore, co-culture has shown a reduction in iNOS:Arg1 ratios of macrophages thus reducing NO production, suggesting a polarisation towards an M2 phenotype (Cho et al., 2014). In-vivo experiments also report reduced pro-inflammatory cytokines, such as TNF- α and IL-1 β , replaced by an increase in anti-inflammatory cytokines along with increased regeneration in models of lung, kidney and cardiac injury. Underlying mechanisms behind responses of stem cells to macrophages as described have been studied providing a wealth of data into how stem cells regulate regenerative signalling. Interaction of mouse derived macrophages with bone marrow derived stem cells shows an increase in IL-10 and Arg1 levels are due to alteration of the NF- κ B (figure 1.5.) and STAT3 pathways (Gao et al., 2014). Evidence of macrophage polarisation both *in vivo* and *in vitro* suggests that MSCs may have a role to play in determining M1:M2 ratios in the body and although an introduction of supplementary MSCs into a site of damage does not take place naturally, endogenous MSCs around the body could affect macrophage polarisation via paracrine factors. Additionally, monocytes may be attracted to an area of infection via a trace of secreted MCP-1 (monocyte chemotactic protein-1) from MSCs, which was observed to be exuded from BMDSCs. An increase in MCP-1 secretion follows an increase in TLR-4 expression allowing higher reception levels of its ligand LPS and downstream signals (Shi et al., 2007). As discussed previously paracrine factors, whether protein or RNA based, can be transferred via exosomes to circulating monocytes and macrophages. One such example includes Indoleamine 2,3-dioxygenase 1 (IDO1), an enzyme which catalyses the breakdown of L-tryptophan to N-formylkynurenine (Yeung et al., 2015). AFSCs have been found to secrete vesicles containing IDO1 following treatment with IFN- γ , a pro-inflammatory mediator (Romani et al., 2015). Increasing levels of N-formylkynurenine due to IDO1 action would suppress pro-inflammatory signalling in not only macrophages but also other inflammatory cells such as Th1-cells (Jalili et al., 2007).

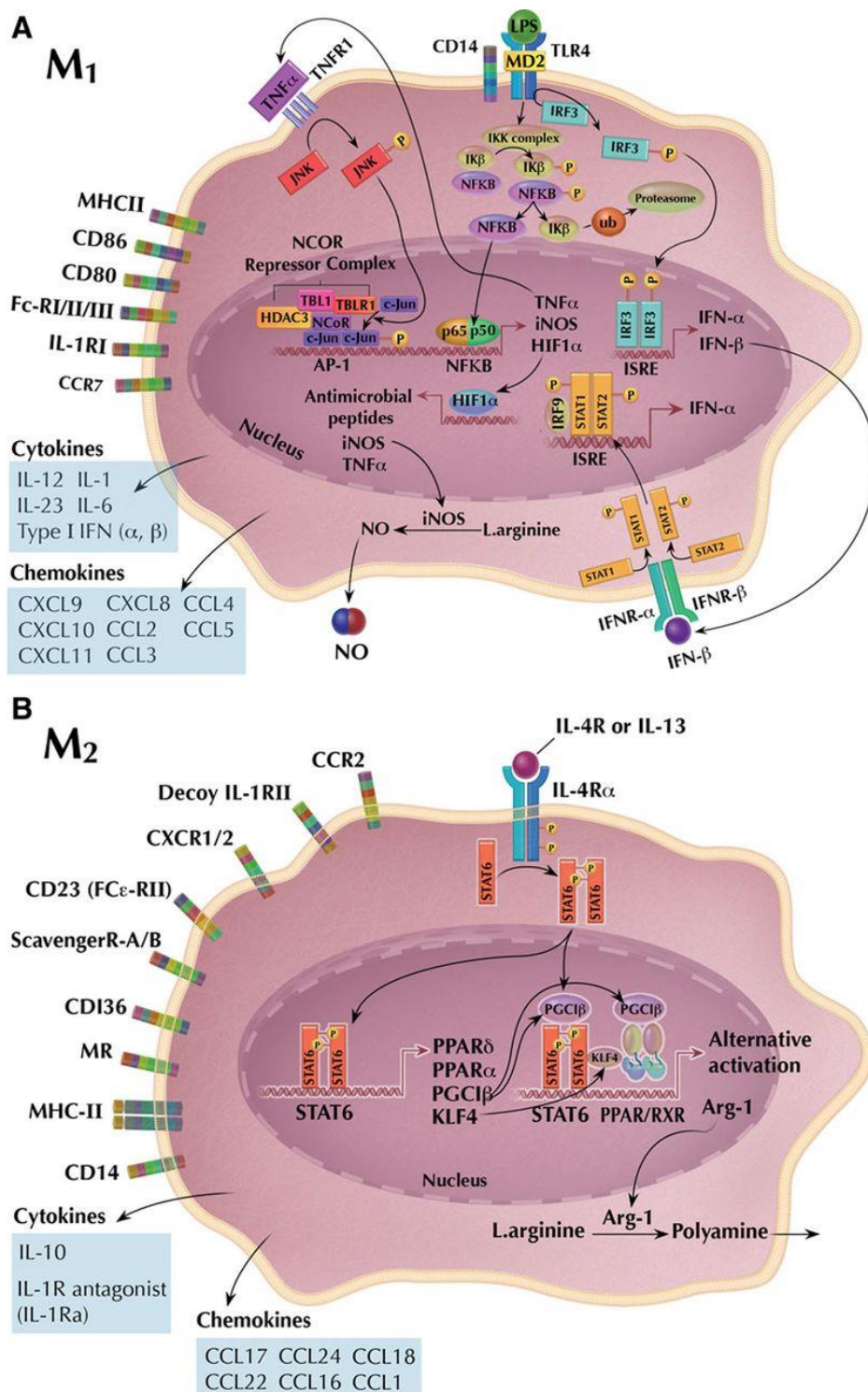


Figure 1.5: Macrophage inflammatory pathways, alteration of which can cause polarisation. Pro-inflammatory signalling pathways within M1 macrophages (A) leading to increased NF-κB (P65/P50) signalling and subsequent increased NO production via L-arginine conversion catalysed by iNOS. In contrast, a generic M2 macrophage (B) has reduced NO production due to the catalysis of L-arginine

to polyamines by Arg-1. Increased ARg-1 expression follows STAT6 phosphorylation and its co-operative DNA binding with KLF4 to the Arg-1 gene. From Tugal et al, 2013 (Tugal et al., 2013).

Treatment of NEC with AFSC CM

Research into the use of AFSCs as an NEC therapeutic was conducted in NEC rat models *in vivo* (Zani et al., 2014). IP injection of the GFP labelled AFSCs into 24 hour old NEC rats showed their integration into the intestinal wall. Furthermore, AFSC treatment led to increased survival and reduced incidence of NEC, which was not seen in BM-MSC treatment (Zani et al., 2014). AFSC treatment also corresponded with decreased gut damage and improved function as evaluated with an increase in intestinal motility and reduced permeability (Zani et al., 2014). Use of a COX-2 inhibitor, which inhibited the effects of AFSCs, showed that the AFSCs increased COX-2 expression helping to explain its protective effects (Zani et al., 2014). Often overexpressed in colorectal carcinomas, COX-2 acts as a major instigator of prostaglandin synthesis and therefore potentiates cell growth (Kaidi et al., 2006). In addition to this, the signalling pathways associated with COX-2 are known to cross talk with that of NF- κ B and is also known to regulate its activity positively and negatively (Poligone and Baldwin, 2001). Of particular interest, the beneficial effects seen with AFSC treatment were accompanied with a lack of total AFSC integration and was mirrored by the treatment with AFSC derived CM collected in α -mem for 30h under normal cell conditions (Zani et al., 2014). As previously hypothesised in studies using stem cells, much of the regenerative properties of AFSCs and the AFSC CM were therefore believed to derive from the paracrine factors released by the stem cells (Zani et al., 2014, Gnecchi et al., 2006, Gnecchi et al., 2005, Gnecchi et al., 2016).

Aims, Objectives and Hypotheses

Background:

Stem cells have been used in a range of necrotic and disease pathologies to promote regeneration (Gnecchi et al., 2006, Gnecchi et al., 2016, Zani et al., 2014). The mechanism of how the stem cells bring about the beneficial outcomes remains controversial. It was initially believed that the stem cells directly took part in the regeneration process by differentiating to replace dead tissue. However, much research has described the beneficial effects of stem cells yet at the same time demonstrating that these cells have not integrated into the damaged tissue (Gnecchi et al., 2006, Gnecchi et al., 2005). This has led to a paradigm shift in thinking and raised the possibility that stem cells bring about tissue repair by acting indirectly to promote regeneration. It is postulated that stem cells secrete paracrine acting molecules that influence the activity of resident stem cells or somatic cells, which facilitate the regeneration process. Paracrine factors from mesenchymal stem cells have been widely collected as part of conditioned media (CM). Data collected by an industrial partner has shown that a novel procedure for collecting CM produced under stressful conditions has enhanced therapeutic capabilities. However it has also become evident that many of these paracrine factors are secreted and packaged within extracellular vesicles (EV), such as exosomes and microvesicles (Eirin et al., 2014, Collino et al., 2010, Yu et al., 2014, Lee et al., 2012a). Packaging with the EV not only protects molecules from degradation and enables long distance cell-cell signalling but is also thought to aid in targeting regenerative factors to the appropriate cell type (Mathivanan et al., 2010). Nevertheless, the exact cocktail of paracrine factors within this AF-CM is still to be elucidated. Furthermore, the mechanisms by which this set of extracellular factors aid regeneration remains unknown.

Recently, Amniotic Fluid Stem Cells (AFSCs) have been shown through various studies to provide a particularly potent regenerative effect. In particular, Zani et al. 2014 showed that AFSCs increased survival following their introduction into a Necrotising enterocolitis rat model (Zani et al., 2014).

Furthermore this study and much of the literature surrounding how mesenchymal stem cells provide a regenerative effect have alluded to an anti-inflammatory mechanism of action therefore preventing widespread necrosis but also an ability to upregulate endogenous stem cell population regenerative properties (Gnecchi et al., 2016). It was also directly shown that an AFSC CM could mimic the whole AFSCs beneficial effects on NEC (Zani et al., 2014). However, this AFSC CM, like many other MSC CMs before, was created using non-stressed cells. It was therefore proposed that the use of AFSCs, developmentally naive cells, to create CM in a novel fashion under stressful conditions, discussed previously to enhance the quantity and quality of the secretome for regenerative purposes, would make a powerful therapeutic for tissue regeneration. Production of this AF-CM is such that, unlike many other types of CM detailed in previously published literature, it is free from animal derived serum or basal medium that contains uncharacterised constituents and a potential for inducing an immunological response following therapy.

Novelties of Project:

The industrial partners have extensive clinical evidence showing the efficacy of stem cell CM created under stressful conditions hypothesised to increase the regenerative potential of the secretome. However the mechanism by which this outcome is achieved remains to be elucidated. This project aims to define on the molecular and cellular level how a clinically relevant AF-CM created under stressful cellular conditions promotes regeneration. The AF-EV and their cargo will be characterised. Causal agents in the AF-CM will be attempted to be identified. The novelty of this project is that it will identify the mechanism by which a clinically relevant CM and its EV cargo promote regeneration. This will lead to the optimisation of regimes which ultimately could lead to an AF-CM regenerative therapeutic and in particular for NEC.

Overall Project Hypothesis:

AFSCs under non-physiological conditions (lacking nutrients and at a sub-optimal culture temperature) secrete protein or molecular species that act to support the host's regenerative mechanisms, in particular those controlling stem cell activity and/or the inflammatory process.

Overall Project aims:

- 1. To characterise AFSC CM/EV collected through a novel procedure developed by an industrial partner and the AFSCs after CM collection**
 - Characterise the multipotency of AFSCs following AFSC CM collection.
 - Study CM fractions such as the extracellular vesicle (EV) fraction using proteomic analysis and miRNA arrays to identify potentially regenerative molecules.
- 2. Establish the ability of AFSC CM/EV to alter stem cell properties and the state of inflammation**
 - Test AFSC CM/EV on a proliferation assay, migration assay, senescence assay, NF-kB reporter luciferase assay and a THP-1 macrophage polarisation assay.
- 3. To determine the influence of AFSC CM/EV on resident stem cells and its anti-inflammatory effects within *in vivo* or *ex vivo* models**
 - Test AFSC CM/EV on an established cardio-toxin induced acute injury mouse muscle model.
- 4. To determine the ability of AF-CM to modify altered signalling in LPS or TNF- α stressed mouse gut organoids which mimic NEC**
 - Create a reproducible model of LPS/ TNF- α stressed organoids
 - Treat LPS/ TNF- α stress induced mouse intestinal organoids with AF-CM
 - Analyses protein and gene expression levels of intestinal markers using western blotting and fluorescent staining as well as qPCR respectively.

Results Chapter 1: Characterisation of Amniotic Fluid Stem Cell Conditioned Media

Aims and objectives:

1. To Characterise AFSC CM/EV and AFSCs used for CM collection

- Collect CM at 24, 48 and 72 hours to provide three CM fractions.
- Recover AFSCs after CM collection and differentiate them towards osteogenic, adipogenic and chondrogenic lineages.
- Separate the EV fraction from the soluble CM fraction using step-wise ultracentrifugation.
- Characterise the proteome of AFSC CM fractions using SDS-PAGE and silver staining.
- Characterise in detail the proteomics of AFSC CM fractions using mass spectrometry.
- Bio-analyse samples for RNA using a pico-RNA chip before further Affymetrix array analysis of miRNA and or mRNA.

Outcome:

AFSCs will be shown to retain their multipotency following CM collection. AFSC CM and EV will contain a variety of molecules that are known to have regenerative properties such as being anti-inflammatory or pro-angiogenic.

Results Chapter 2: Investigation into the Regenerative Potential of AFSC CM *in Vitro*

Aims and objectives:

1. Establish the ability of AFSC CM to modify cell behaviour *in vitro*

- Test AFSC CM/EV on a stem cell migration assay.
- Test AFSC CM/EV on a stem cell proliferation assay.
- Test AFSC CM/EV on a stress induced cellular senescence assay.
- Inhibit energy production in target cells to identify if EV uptake is inhibited and
Identify the potential mechanisms of extracellular vesicle uptake in target cells

2. To determine the ability of AFSC CM to alter the inflammatory state of cells *in vitro*

- Test AFSC CM/EV on an NF-kB Luciferase reporter assay, which has had exposure to Salmonella LPS or human recombinant TNF- α .
- Compare the complete CM/EV against defined CM molecules NF-kB luciferase reporter assay.
- Test the alteration in inflammatory state of THP-1 macrophages treated with AFSC CM/EV.

Outcome:

An understanding of how AFSC CM can improve key mechanisms of non-autologous stem cells, provide a cyto-protective and an anti-inflammatory effect.

Results Chapter 3: Investigation into the Regenerative Potential of AFSC CM in an Acute CTX Damage Mouse Muscle Model in Vivo

Aims and objectives:

1. To determine if AFSC CM can enhance skeletal muscle regeneration *in vivo* following an acute injury

- Treat a Cardio-toxin induced acute TA damage mouse model with AFSC CM/EV or a Vehicle control.
- Dissect TA muscles 5 days after damage before cryo-embedding and sectioning.
- Stain muscle sections for H&E, Acid phosphatase, CD-68/F4-80 and embryonic Myosin Heavy Chain (eMHC) to analyse the level of damage and rate of regeneration.

Outcome:

Learn whether AFSC CM/EV provides a regenerative effect *in vivo* and accelerates the regeneration of muscle fibres following injury. Understand whether the AFSC EV has the same regenerative capabilities as whole AFSC CM.

Results Chapter 4: Establishment of an NEC Intestinal Organoid Model to Test the Regenerative Capability of AFSC CM

Aims and objectives:

- 1. To ascertain if AFSC CM/EV can enhance regeneration in acutely stressed mouse intestinal organoids specifically due to the protection of endogenous stem cells**
 - Mouse organoids will be stressed with E.coli LPS/ TNF- α stress and organoids will be treated with AFSC CM/EV.
 - Paraffin embed organoids and section for immunofluorescent staining and analysis of Indication of Ki-67, CC3 and Lysozyme markers of proliferation, apoptosis and Paneth cells respectively.

- 2. To establish if AFSC CM/EV can modify the inflammatory response seen in acutely stressed mouse intestinal organoids**
 - Measure the levels of NF-kB-p65 nuclear translocation within stressed organoids following AFSC treatment using immunofluorescent techniques.
 - Use qPCR to establish relative levels of pro-inflammatory and intestinal markers within the stressed organoids following AFSC CM treatment.

Outcome:

Understand whether AFSC CM/EV can also protect the endogenous stem cell population and reduce a pro-inflammatory state within an NEC organoid model. Results will suggest if this novel AFSC CM can assist in the regeneration of gut associated pathology as an anti-inflammatory and/or endogenous stem cell activity controlling therapy.

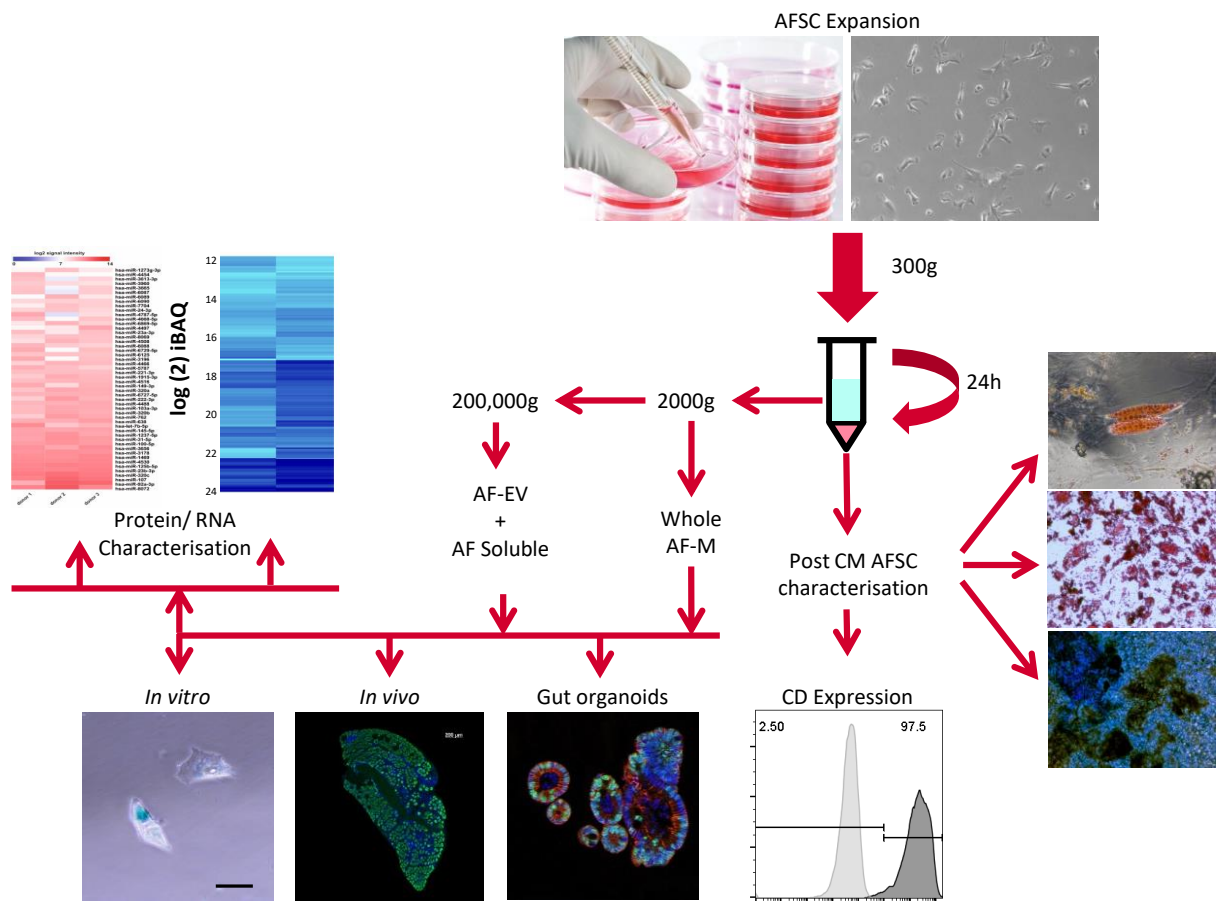


Figure 1.6: Overview of project plan and key steps undertaken.

2. Methods

Ethical Approval

Human amniotic fluid samples were collected from women having amniocentesis for prenatal diagnosis for therapeutic purposes in Foetal Medicine Unit of University College London Hospital (UCLH). All patients gave informed written consent to an approved researcher under ethical approval (UCL/UCLH Joint Committee for the Ethics of Human Research, REC Reference: 08/0304). Invasive procedures were performed under ultrasound guidance using sterile equipment. In vivo animal experiments were performed under a project license from the United Kingdom (UK) Home Office, in agreement with the Animals (Scientific Procedures) Act 1986.

Animal maintenance

Male wild-type C57BL/6 mice were obtained from Harlan Laboratories, UK and were maintained in accordance with the Animals (Scientific Procedures) Act 1986 (UK). Mice were housed under standard environmental conditions (20-22°C, 12h-light-12h-dark cycle) and were provided with food and water as libitum. Mice used for cardiotoxin injection experiments were aged 2-3 months (project licence - PA6190E59). Mice used for intestinal organoid isolation were aged 6 weeks.

Euthanasia procedure

All animals were culled via carbon dioxide asphyxiation with secondary cervical dislocation as per schedule 1 euthanasia protocol.

Cell culture and In-vitro experimentation

Cell culture conditions

All cells were cultured at 37°C with 5% CO₂ and passaged on reaching 70% confluency unless otherwise stated.

AFSCs

Human amniotic fluid stem cells were harvested from a single volume of second trimester amniotic fluid collected at 18 weeks pregnancy from a mother aged 38 via amniocentesis due to suspected

Down syndrome. Cells were of a normal karyotype. Amniotic fluid was centrifuged at 300g for 5 minutes and supernatant aspirated and discarded. Cells were re-suspended in 3ml AFSC media and seeded over a glass coverslip covering the inside of a 35mm × 10mm petri dish. Cells were incubated at 37°C, 5% CO₂ for 5-7 days until cells of a mesenchymal morphology could be identified. Media was then changed thus discarding any cells that had not adhered to the glass. Cells were passaged for immune-selection. Cells were purified according to positive selection of C-kit expression using MACS (Miltenyi Biotec) following 1 passage. MACS selection was carried out by washing cells in pre-cooled MACS buffer (1X PBS, pH 7.2, 0.5% bovine serum albumin (BSA), and 2mM EDTA). Cells were pelleted at 300g for 10 minutes, supernatant was aspirated and then cells were diluted in 300µL for every 1x10⁶ cells. 100µL of MACS FcR reagent was added for every 300µL buffer used. C-Kit microbeads were added using 100µL/1x10⁸ cells. Cells and solutions were mixed well before incubating for 15 minutes at 4°C. 2ml of buffer was then added to every 1x10⁸ cells and cells were centrifuged at 300g for 10 minutes. Supernatant was aspirated and cells were re-suspended in buffer at 1x10⁸/500µL. An MS MACS column was placed into a MiniMACS separator. The column was rinsed with 500µL of buffer before applying cells to the column. Cells that passed through the column were discarded. The column was removed was the separator and cells eluted from the column using 1ml buffer and the syringe/ plunger provided in the kit. C-kit⁺ AFSCs were cultured on non-tissue culture treated plastic in α-MEM medium containing 15% FBS, 1% glutamine and 1% pen/strep, supplemented with 18% Chang-B and 2% Chang –C (Pozzobon et al., 2013).

U251 NF-κB reporter cells

U251 NF-κB reporter cells were a gift of by D Widera (University of Reading). U251-NF-kappaB-Puro cells had been stably transduced using a lentivirus collected following the transfection of HEK293-FT cells with lentiviral package plasmids containing the pGreenFire-NF-κB-Puro vectors (Zeuner et al., 2017). They were selected for with puromycin for 2 weeks and clonally selected via serial dilution (Zeuner et al., 2017). Cells were cultured in antibiotics- free high glucose (4.5g/l) DMEM, FBS (10%) and L-glutamine (1%).

IMR-90 Lung Fibroblast cells

Human foetal IMR-90 Lung Fibroblast cells (IMR-90) were a gift of Dr. Debacq-Chainiaux (University of Namur, Belgium). Cells were used at 27-30 population doublings. IMR-90 cells were cultured in α -MEM medium containing FBS (10%), L-glutamine (1%) and pen/strep (1%).

Adipose Derived Stem Cells

StemPro[®] Human Adipose Derived Stem Cells, derived from a 49 year old female donor were from Stem Pro (Life technologies/ lot no. 2117- 510070). hADMSCs were cultured in MesenPro RSTM, L-glutamine (1%) and pen/strep (1%).

THP-1 Monocytes and Macrophages

THP-1 monocytes (ATCC) were cultured as a suspension in ATCC-formulated RPMI-1640 Medium, FBS (10%), L-glutamine (1%), pen/strep (1%) in non-tissue culture treated flasks.

Differentiation to M0 THP-1 macrophages:

THP-1 monocytes were stimulated with 25nM Phorbol 12-myristate 13-acetate (PMA) for 72 hours within a suitable tissue culture treated plate (40,000 cells/cm²). M0 macrophages were rested for at least 72h. Adherent cells were removed with a cell scraper.

Differentiation of M0 to M1 THP-1 macrophages:

M0 macrophages were treated with E.coli LPS (25ng/ml) and IFN γ (20ng/ml) in culture medium for 72h before flow cytometry analysis.

Differentiation of M0 to M2 THP-1 macrophages:

M0 macrophages were treated with IL-4 (20ng/ml) and IL-13 (20ng/ml) in culture medium for 72h before flow cytometry analysis.

Thawing of cells for culture

Cells were removed from liquid nitrogen and thawed in a 37°C water bath within 1 minute. Warm culture media (37°C, 1ml) was pipetted into the vial of thawed cells. Cells were transferred to warm

culture media (10ml) in a 15ml Falcon tube. Cells were centrifuged at 300g for 5 minutes and the resultant supernatant discarded. The cell pellet was re-suspended in 10ml culture media and transferred to a T75 culture flask. Cells were incubated under normal culture conditions for 24h, thus allowing cells to adhere, before changing media and removing non-viable cells.

Passaging cells

Media was removed on cells reaching 70% confluence (unless otherwise stated), media was removed. Cells were washed once with sterile 1X PBS. Cells were detached from the surface of the flask using TrypLE™ Select enzyme. Culture media was added to the cells in a 1:1 dilution and then transferred to a 15ml Falcon tube. A sample of cells was taken and Trypan blue along with a hemocytometer was used to determine a cell viability count. Stock cells were centrifuged at 300g for 5 minutes and supernatant discarded. Cells were re-suspended in a volume of media calculated so that a known number of cells could be transferred to new culture flasks.

Freezing of cells for storage

Cells were trypsinised, counted and pelleted as previously described. Passaged cells were re-suspended in freezing media (1ml/5x10³ cells) and transferred to cryogenic vials as 1ml aliquots. Aliquots were frozen at -80°C overnight within a Mr. Frosty™ freezing container before being stored long term in liquid nitrogen.

Conditioned media (CM) generation

Following a maximum of 10 passages, AFSCs were trypsinised and collected into 50ml Falcon tubes and centrifuged at 300g. Supernatant was discarded and the cell pellet re-suspended in 1-2ml sterile PBS. Centrifuging at 300g was repeated and supernatant discarded again. Wash in PBS was repeated. Cells were counted using a haemocytometer. Following centrifugation at 300g for 5 minutes, the PBS was discarded and cells re-suspended at 1x10⁶/ml cells of sterile ultra-centrifuged PBS (centrifuged at 100,000g). 1ml of cell suspension was pipetted into 1.5mL microfuge tubes at a density of 1x10⁶cells/tube. Microfuge tubes were centrifuged at 300g for 5 minutes, supernatant aspirated and

replaced with 400µl ultra-centrifuged sterile PBS. Cells were incubated 24 hours at room temperature. Following incubation the cells were centrifuged at 300g for 5 minutes, the supernatant was aspirated, pooled and centrifuged at 2,000 g for 20 minutes. The supernatant (AF-CM) was collected and stored at -20°C. Aspirated supernatant was replaced in equal amounts and incubation repeated for a 48h and 72h collection.

Extracellular vesicle (EV) isolation

AF-CM was made up to 8.9ml with ultra-centrifuged sterile PBS and transferred to a polyallomer centrifuge tube (Optiseal). AF-CM was centrifuged at 100,000g using a 70.1Ti fixed-angle rotor (Beckman Coulter) for 18h. Supernatant was carefully removed and discarded. EVs were re-suspended in ultra-centrifuged PBS at an equal volume to that of the AF-CM used to isolate them.

Fixation of cells

After the removal of culture medium, cells were fixed in 4% PFA/PBS for 15 minutes at RT. Fixative was aspirated and cells washed 3 times for 5 minutes in 1X PBS.

Flow Cytometry

AFSCs were trypsinised and collected in a 15ml Falcon tube. Cells were centrifuged at 300g, 5 minutes. Supernatant was removed and cells re-suspended in sterile PBS (1ml). 4% PFA (1ml) was added to cells for 15 minutes. Cells were centrifuged at 300g for 5 minutes and the supernatant discarded. Non-specific binding was blocked with 10% FBS/PBS at room temperature for 1h. Cells were centrifuged as before, supernatant discarded and cells washed once with PBS. Cells were transferred to a round bottom suspension cell plate (200µl/well, 2×10^5 cells/well). Cells were centrifuged at 500g for 5 minutes in a Heraeus Multifuge X3R using the plate attachment. Supernatant was removed, cells re-suspended in PBS. Antibodies were diluted in PBS (1:200) and incubated with the AFSCs for 1 hour at 4°C. Supernatant was removed; cells were re-suspended and washes were repeated 3 times. The 96 well plate containing re-suspended cells was placed in a BD Accuri C6 flow cytometer C-sampler and 10,000 events were captured and recorded. Unstained cells

were gated to remove debris using a side scatter area (SSC-A) vs forward scatter area (FSC-A) density plot. Subsequently a forward scatter height (FSC-H) vs. forward scatter area (FSC-A) density plot was used to gate and remove doublets from recordings. A single parameter histogram was then used to gate and remove effects of auto-fluorescence. Data was analysed using the FlowJo v10 analysis software (FlowJo LLC).

Adipogenic Differentiation

AFSCs cultured following CM collection were allowed to reach 70% confluency and then passaged into 24 well plates at 20000cells/well in Chang-C media and allowed to reach 95% confluency. Growth media was then removed, cells were washed once with PBS and cultured for 21 days with Stem XVivo Adipogenic Base Media (R&D Systems) supplemented with Stem XVivo Adipogenic Supplement (100X) made according to the suppliers instructions. Media was changed every 3 days without passaging. Differentiation medium was removed; cells washed once with PBS and fixed in 4% PFA/PBS and washed as previously described. PBS was removed and cells were washed with 70% isopropanol for 10 seconds. Isopropanol was removed and replaced with Oil Red O working solution for 30 minutes under gentle agitation. Stain was removed, replaced with 70% isopropanol for 10 seconds to remove excess stain and replaced with PBS. PBS was removed and cells allowed to air dry. Images were taken using a Zeiss A1 Inverted Epifluorescent Microscope and Zeiss Axiovision 4.8 software.

Osteogenic Differentiation

AFSCs cultured following CM collection were allowed to reach 70% confluency and then passaged into 24 well plates at 20000 cells/well using Chang C media and allowed to reach 95% confluency. Growth media was then removed, cells were washed once with PBS and cultured for 21 days with Stem XVivo Osteogenic Base Media supplemented with Stem Pro Osteocyte/Chondrocyte basal medium (Life Technologies) according to the supplier's instructions. Media was changed every 3 days without passaging. Differentiation medium was removed; cells washed once with PBS and fixed in 4% PFA/PBS and washed as previously described. PBS was removed and replaced with Alizarin Red S

working solution for 30 minutes under gentle agitation. Stain was removed and cells washed once with PBS and allowed to air dry. Images were captured using a Zeiss A1 Inverted Epifluorescent Microscope and Zeiss Axiovision 4.8 software.

Chondrogenic Differentiation

AFSCs cultured following CM collection were allowed to reach 70% confluency before trypsinising and collected in a 15 ml falcon tube. Cells were centrifuged at 300g, supernatant was removed and cells were re-suspended in 10 ml growth medium. 1×10^6 AFSCs were taken and pelleted at 300g for 5 minutes in a 15ml Falcon tube. Growth medium was removed and replaced with 1ml Stem Pro Osteocyte/Chondrocyte basal medium supplemented with StemPro Chondrogenesis supplement according to the supplier's instructions. Cells were centrifuged at 300g for 1 minute and then allowed to fall and sediment naturally to the bottom of the tube. Cells were incubated for 37°C, 5% CO₂ for 21 days, changing media every 3 days. Medium was removed, spheroids carefully washed once in PBS and fixed in 4% PFA/PBS and washed as previously described. Chondrogenic cultures were stained overnight with Alcian blue working solution at RT in the dark. Spheroids were washed 3 times for 2 hours in 6:4 ethanol/acetic acid de-stain solution. Pellets were washed once in ddH₂O before freezing and blocking in OCT. 10µm cryo-sections were taken using a Bright OT5000 cryostat and mounted on glass slides with Hydromount. Sections were imaged using a Zeiss Axioskope microscope.

Cellular Proliferation Assay

hADMSCs were seeded into 96-well culture plates at a density of 400 cells/well and allowed to adhere for 24 hours in growth media at 37°C, 5% CO₂. Subsequently, media was removed before replacing with corresponding treatments. Cells were treated for 48 hours, washed with PBS and fixed with 4% PFA/PBS for 15 minutes at RT. Fixative was removed and cells washed three times in PBS. Nuclei were stained with DAPI mounting medium and nuclei counted using a Zeiss Axioimager A1 microscope with an AxioCam digital camera and Zeiss Axiovision 4.8 software.

Migration Assay

ADMSCs were seeded and cultured in a 24 well plate at 40000 cells/well until 100% confluent. Then a 200ul pipette tip was used to scratch a single uniform line down each well to create an artificial wound. Media was removed and cells washed once with PBS to remove cell debris created through wound production. PBS was removed and corresponding treatments added. A hole was created in the side of the plate using a hot needle enabling the introduction of a 5% CO₂ line. Immediately after, 3 uniformly spaced and separate image co-ordinates were taken for each well along the scratch at a 10X magnification for T=0h. At T=9h images were retaken at exactly the same points as characterised previously. Using Fuji Image J software the area of the wound was analysed for T=0 and T=9 for each co-ordinate and the difference in wound area determined for wound closure.

Cellular Senescence Assay

IMR-90 cells used were between 27-32 population doublings, 50% of the Hayflick limit, and were seeded into 12 well plates at 30000cells/well and cultured until 70% confluency at 37°C, 5% CO₂. Media was removed and replaced with media containing AF-CM and left for 24 hours. Media was then removed and cells were washed once with PBS. PBS was removed and cells stressed for 2 hours with 100µM H₂O₂ in serum free media at 37°C, 5% CO₂. Media was removed and cells washed twice with PBS and replaced with growth media for 48 hours in normal culture conditions. Cells were passaged into 3 wells of a 24-well plate at 800cells/well. After 24 hours, media was removed and cells were fixed with 0.2% glutaraldehyde/ 2% PFA for 5 minutes at RT. Fixative was removed and cells washed twice in PBS. Cells were incubated with 2.5mg/ml X-Gal solution for 18 hours at 37°C in the dark with no additional CO₂. Wells were rinsed twice with PBS and then twice with methanol before air drying. Cells stained blue were considered senescent and counted to establish the percentage of senescent cells using a Zeiss A1 inverted Epi-fluorescent Microscope.

NF-κB p65 Nuclear Translocation Assay

U251 cells were cultivated on cell-culture treated cover slips at 4000cells/cm² for 24h. Media was removed and replaced with AF-CM containing media for 24h under normal culture conditions.

Treatment was removed and replaced with serum free media for 2 hours. Media was removed and cells were exposed to 10 ng/ml of TNF- α containing serum free media with AF-CM for 30 minutes. Treatment was removed and cells washed twice with PBS before being fixed in 4% PFA, 15 min, RT. Permeabilisation and blocking was carried out as described [24]. NF- κ B-p65 was detected by immunostaining overnight 4°C with p65 antibody (1:100, sc-8008, Santa Cruz Biotechnology). Primary antibody was removed and cells washed 3 times for 5 mins with wash buffer. Wash buffer was removed and cells incubated with Alexa fluor 488 goat anti-mouse IgG secondary antibody (Molecular probes 1:200) in wash buffer for 1h at RT. Secondary Ab was removed, cells washed 3 times for 5 minutes and mounted in DAPI mounting medium. Imaging was carried out using Zeiss Axioimager Epifluorescence microscope at the same exposure and p65 nuclear pixel intensity was measured using ImageJ software.

NF- κ B luciferase gene reporter assays

U251 NF- κ B reporter cells were seeded into 24 well plates at 4000cells/cm². After 24h cells media was removed and replaced with AF-CM containing culture medium for 24h. Pre-treatment was removed and cells were treated with 10ng/ml TNF- α or 1 μ g/ml of ultrapure *E.coli* LPS containing serum free media with AF-CM for 24h. GFP expression of cells of positive control assays were checked to ensure suitable expression. Cells were rinsed with PBS and 100ul of 1X passive lysis buffer was then added to each well. Plates were gently shaken for 15 minutes at room temperature before lysates were collected into separate tubes. 10 μ l of each lysate was pipetted into a separate well of a white, clear bottom, non-treated 96-well BRAND plate. 40ul of LAR II was quickly added to each well before measuring firefly luciferase activity in a Lucy 1 luminometric plate reader (Anthos).

Uptake of PKH26-stained EVs by IMR-90 cells

AF-EV (1ml) was diluted in Diluent (1ml - PKH26 Red Fluorescent Cell Linker Kit). PKH26 stain (2 μ L) was diluted in diluent (1ml) as described in the PKH26 Red Fluorescent Cell Linker Kit (Sigma) and added to dilute AF-EV for 3 minutes. BSA/PBS (0.1%, 1ml) was added to the stained AF-EV for 5 minutes. Stained AF-EV were made up to 8.9ml with sterile ultra-centrifuged PBS and pipetted into a

polyallomer centrifuge tube. AF-EV was centrifuged at 100,000g using a 70.1Ti fixed-angle rotor (Beckman Coulter) for 18h. Supernatant was carefully removed and discarded. EVs were re-suspended in ultra-centrifuged PBS (1ml). U251 cells were cultured in a 12 well cell culture plate until 70% confluency was reached. Media was removed and cells were washed twice with PBS. Cells were treated for 3 hours with stained AF-EVs (10%) in serum free media for 3 hours. Cells were washed twice with PBS and EV uptake visualised using a Zeiss Axioimager Epifluorescence microscope.

Intestinal organoid Culture and Isolation

Complete Medium without growth factors (AddMEM) containing advanced DMEM/F12, GlutaMax (1:100), HEPES (10mM) and pen/strep (1%) was made up in advance. C57BL/6 mice were culled by schedule 1 killing as described. A 10cm stretch of small intestine was dissected 1cm below the stomach, halved into two 5cm lengths transferred to ice cold PBS in a 10cm dish. Fat was removed from the outside of the two portions of small intestine with small scissors. Using a syringe the intestines were flushed with cold PBS. A cut was made longitudinally down one side. Villi were gently scraped off from the inside of the intestines with a glass microscope slide. Intestines were transferred to a 50ml Falcon tube containing 20ml ice cold PBS and briefly vortexed. Intestines were transferred to a new 50ml tube and washed repeated 10X, each with fresh PBS. The intestines were transferred to fresh 50ml falcon tubes containing 30ml EDTA (2mM) in cold PBS and put on a rotating mixer for 30 minutes at 4°C. Intestines were placed into a new 50ml tube containing 30ml cold PBS and inverted 5X. Intestines were transferred to a new 50ml tube with 10ml cold PBS and shaken 5X to create supernatant 1. Intestines were transferred to a new tube containing 10ml cold PBS and shaking repeated as before to create supernatant 2. This process was repeated to create 12X separate supernatants for each 5cm length of intestine. A 50ml sample from each supernatant was placed on a 10cm petri dish and each checked for crypts. Crypt containing supernatants were pooled in 50ml Falcon tubes and filled with cold AddMEM. Crypts were spun at 200g for 10 min. Supernatant was removed carefully and pellet re-suspended in 5ml cold AddMEM. Crypts were pipetted onto a 70µm cell strainer over a 50ml tube. Suspension was transferred to a 15ml falcon

tube and spun at 300g for 5 min. Supernatant was discarded pellet put on ice. Pellet was re-suspended in growth factor reduced phenol red free Matrigel (50ul for each intended well). Matrigel-crypt suspensions were pipetted into a pre-warmed 24-well plate (50µl/well) and incubated for 8-10 minutes at 37°C 5% CO₂ until matrix solidified. To each well 500µl of adDMEM containing freshly added N2 Supplement (1:100), B27 Supplement (1:50), N-Acetylcysteine (1µM), Mouse-rEGF (50ng/ml), Mouse rNoggin (100ng/ml), human rR-spondin1 (500ng/ml), Valproic acid (1mM) and CT99021 (3µM) and incubated at at 37°C 5% CO₂ . After 3 days medium was refreshed without the addition of Valproic acid and CT99021.

Passage of Matrigel containing Crypts

Before starting the tips of glass pipettes were stretched over a naked flame, broken to form a fine end and edges smoothed over fire. Waste media was removed from around Matrigel. Cold Cell recovery solution (500µl) was pipetted in wells and over Matrigel to break it up. Cell recovery solution/Matrigel/Crypt mix from each well was pooled into a 15ml Falcon tube and left for 30 minutes on ice, occasionally inverting the tube. Crypts were centrifuged at 300g for 3 min. Waste was removed. Crypts were re-suspended in 1ml PBS and with a pre-wetted glass tip pipette the crypts pipetted up and down 5-6X to mechanically break them up. Crypts were centrifuged for 3 minutes at 300g. Waste supernatant was removed and crypts re-suspended in Matrigel. Crypt containing Matrigel was pipetted and media added as previously described into pre-warmed 24-well plates.

Fixing of organoids

Media was removed from around Matrigel. Organoids and Matrigel were fixed with 500ul of 4% PFA/PBS overnight at RT. Fixative was removed and organoids washed three times with PBS as to not disturb Matrigel. Agarose gel (2%) made up in PBS was pipetted over Matrigel in each well and allowed to set. Agarose was removed with forceps, thus also removing embedded Matrigel/organoids, and stored in 70% ethanol until paraffin embedding.

Molecular analysis:

SDS-PAGE:

Sample protein concentration was established using the BioRad DC protein assay as instructed. The volume required for loading a specific number of μg of protein was calculated. Knowing the protein concentration of each sample, loading samples were prepared ensuring each contained equal totals of protein. 3.4ul of 6X RSTB reducing buffer was added to each sample and then made up to 20ul total volume per sample using ultrapure dH₂O. Samples were heated to 100°C for 15 minutes using a heat block, briefly vortexed and centrifuged for 1 minute at 300g before immediately placing on ice. Stamps were taken out of pre-cast 1.0mm NuPAGE 4-12% Bis-Tris gels (Novex by Life Technologies) and wells washed with running buffer to remove bubbles. Tape from the base of the gel was removed and XCell SureLock (Novex by Life Technologies) electrophoresis apparatus set up with the prepared gel as instructed by the manufacturer. The central chamber was filled with 200ml of antioxidant 1X running buffer (check for leaks) and outer chamber with 800ml 1X running buffer. A volume, corresponding to the future requirements of the gel as instructed by the manufacturer, of protein ladder was loaded into the desired wells. All 20 μL of each loading sample was then loaded into a well. The apparatus lid and circuit connections were fitted and the electric field applied to 80V for the first 15 minutes until samples until dye had passed the stacking gel. The voltage was then increased to 120-150V for at least 1h until sample dyes reach the very edge of the gel before the electrophoresis was switched off and gel retrieved (CM samples should be run at 100V due to the high salt content).

Silver staining

Silver Staining was carried out using the SilverXpress[®] silver staining kit. Protein bands were imaged using a Syngene G:Box and GeneSys software.

Western Blotting

Wet 5 sponges (XCell II Blot module kit – Novex), blot and 4 filter papers (cut equal to size of blot equipment) in transfer buffer and methanol (only for the blot paper). Materials were placed in the XCell II Blot module in the order from the anode (negative charge): 2 sponges, (complex of 2 filter papers), gel, blot, (complex of 2 filter papers), rest of sponges. Bubbles were rolled out carefully and the cathode portion of the blot module assembled thus sandwiching materials and it was assembled again in the XCELL SureLock tank as instructed by the manufacturer. Blots were run at 30V for 3 hours.

Western Blot Staining and visualisation

Blot was removed and placed in blocking buffer for 40 minutes. Primary Antibody was prepared by diluting as required in blocking buffer. The blot was cut as desired and placed into 50ml falcon with 3ml primary antibody containing blocking buffer to be left overnight on a rotator at 4°C. Blots were washed three times with PBS-T (5 minute/wash). The 2nd Antibody was diluted in blocking buffer and 3ml pipetted into the blot containing 50ml falcon for 40 minutes on a rotator at room temperature. Washes in PBS-T were repeated 3 times. The blot was placed on a black imaging tray and 500µl of a 1:1 solution Amersham ECL prime western blotting detection reagent kit was pipetted on and a clear plastic film was placed over the top to ensure a uniform spread before imaging in an ImageQuant LAS 4000 mini and corresponding software.

Real Time- Quantitative Polymerase Chain Reaction

Organoid RNA was collected using buffer RLT lysis buffer (Qiagen, RNeasy mini kit) and transferred to 1.5 mL microfuge tubes. Total RNA was isolated and purified following the protocol included in the RNeasy Mini Kit (Qiagen-74104) and RNase-Free DNase set (Qiagen-79254). The Nanodrop 2000 (Thermo Scientific) was used to quantify RNA concentrations.

Sample RNA concentrations were normalised to the sample with the lowest total RNA content using nuclease free water up to a total volume of 11µl. Oligo(dT)18 primers (1µl) were added to each sample totalling 12µl. 5x reaction buffer (4µl), RiboLock RNase inhibitor (1µl), 10mM dNTP mix (2µl)

and RevertAid H minus MULV Reverse Transcriptase (1 μ l) were added to each sample respectively. Samples were gently mixed and briefly centrifuged. Samples were incubated at 42°C for 60 minutes. The reaction was terminated by heating samples at 70°C for 5 Minutes. Samples were incubated at 65°C for 5 mins, chilled on ice and briefly centrifuged. cDNA samples were analysed for quantitative real-time RT-PCR on a StepOnePlus™ Real-Time PCR system using the Applied Biosystems SYBR Green PCR Master Mix (Applied Biosystems 4309155) and StepOne software v.2.1. Primers were designed using the primer designing tool on the NCBI website. Primer efficiencies were quantified from serial dilutions made with nuclease free water and mixture of all sample. A standard curve was created to identify an R value and equation for the line of best fit. Individual sample quantification was carried out using a 1:20 sample dilution. Reactions were carried out using SYBR® Green PCR master mix. All data were normalised to Hypoxanthine Phosphoribosyltransferase 1 (HPRT) and Cyclo expression.

Sample preparation for Mass Spectrometry (MS)

AF-EV and non-EV fraction isolated from AFSCs secretome were obtained as described above. Proteins were suspended in SDS-PAGE loading buffer 1x (NuPAGE, Invitrogen, Darmstadt, Germany), denaturated and reduced with 1 mM DTT for 10 minutes at 95°C then, alkylated using 5.5 mM iodoacetamide for 30 minutes at 25°C in the dark. Proteins were resolved by SDS-PAGE using 4-12% Bis-Tris mini gradient gels (NuPAGE, Life Technologies). Each lane was cut into 10 equal slices, proteins therein were in-gel digested with trypsin (Promega). Peptides were extracted, purified by STAGE tips, dried to less than 5 μ l and re-suspended in 15 μ l of 0.5% acetic acid for the MS analysis.

Mass Spectrometry Analysis

LTQ Orbitrap XL mass spectrometers (Thermo Fisher Scientific) coupled to an Agilent 1200 nanoflow-HPLC (Agilent Technologies GmbH) were used to measure peptides derived from trypsin digestion. Samples, applied directly onto self-packed HPLC-column tips of around 20 cm, were subjected to a gradient formed by solution A (0.5% acetic acid in LC-MS grade water) and by increasing organic proportion of solution B (0.5% acetic acid in 80% LC-MS grade ACN in water) within 120 minutes [25]. MaxQuant software version 1.4.1.2 was used to identify proteins based on peptides and to

perform label-free quantification [26]. Both mass spectrometry and MaxQuant parameters were set as previously described [27]. The analysis of Molecular Function GO terms was performed through Perseus software version 1.5.8.5 using Fisher's exact test with a p-value threshold of 0.02 [28].

miRNA Array and analysis

GeneChip® miRNA 4.0 Arrays were used to analyze the miRNA content of AF-EVs using FlashTag™ Biotin HSR RNA Labeling Kits according to the manufacturer's instructions.

Probe cell intensity data (CEL) from Affymetrix GeneChip miRNA 4.0 Arrays were analyzed in the Affymetrix Expression Console™ software. Normalization was performed using the Robust Multichip Analysis (RMA) + DABG algorithm [29]. Only miRNAs calculated as present in all 3 samples were declared as generally expressed after 24 hours. Focus was given to the miRNAs present with the highest signal intensities (top 50). For these top 50 miRNAs validated target mRNAs were amalgamated using miRWalk2.0 software [30]. In the next step, GO Slim classification for biological process was performed using WebGestalt software to provide a high-level functional classification for validated target mRNAs [31]. Morpheus software was used to design the Heat-map showing intensity variability between biological replica (n=3) for the top 50.

Transmission Electron Microscopy

For TEM extracellular vesicle pellets were re-suspended in 40 µl of 0.1M PBS. Drops of the suspensions were placed on parafilm. Carbon-coated copper meshed grids (Plano, Germany) were placed on the drops for 5 minutes for probe adsorption. After five minutes of fixation on drops of 1% glutaraldehyde (Roth, Germany) grids were washed 4 times for 30 seconds and negative contrasted using 1% uranyl acetate. Grids were air dried and analysed using a Zeiss 906 transmission microscope (Zeiss, Germany).

In-Vivo* experimentation:*In Vivo Cardiotoxin induced Mouse TA Injury and AFSC CM/EV Treatment**

C57BL/6 mice (12 week old) were placed under general anaesthetic using isoflurane. Mice were tail vein injected with 100µL either hAFSC CM, hAFSC EV or ultra-centrifuged PBS. After 30 minutes, hind limb fur was shaved and then the exposed skin sprayed with 70% ethanol. TA muscles located on the anterior-medial surface were chosen for their anatomical location allowing ease of injection. Three separate IM injections of 10µl 50mg/ml *Naja pallida* cardiotoxin (CTX) were carried out in the right TA muscle of the mice, one injection in the distal portion and one either side of the muscle situated proximally. This same procedure was repeated with a vehicle (PBS) in the left hind limb. Mice were left 5 days to recover before culling. Muscle was collected and frozen on frozen isopentane.

Dissection of Tibialis anterior (TA):

Mice were culled by schedule 1 killing as described. Once death was confirmed animals were weighed. Hind limbs were shaved fully and cleaned with 70% ethanol. TA muscles were taken from the hind limb following a circular incision around the proximal end of the thigh through the skin using a sterile scalpel blade. The TA was then exposed by pulling isolated skin distally towards and over the ankle joint. Slicing down the foot plate allowed skin to be fully removed exposing further the foot and tendons. Insertion of forceps between the EDL and TA distal tendons allowed the removal of the fascia covering the TA by drawing it up towards the knee. The distal tendon, situated above the tarsal and metatarsal bone, was cut. Holding the cut distal tendon, the TA was pulled proximally to the tibial tuberosity. Cutting the muscle at the proximal end allowed the muscle to be freely transferred immediately into PBS.

Preparation of Muscles for Cryo-sectioning:

TA muscles were transferred from PBS onto aluminium foil anterior side down, which was then placed on frozen isopentane allowing them to snap-freeze. Muscles were then transferred to pre-cooled Eppendorfs for storage at -80°C using dry ice pre-cooled forceps. Tissue-TEK® Optimal Cutting

temperature compound (OCT) (PST) was used to fill aluminium foil wells. OCT containing wells were then placed into dry ice super cooled in 100% ethanol allowing OCT to freeze. As quick as possible frozen muscles were placed into the OCT as it began to freeze. OCT was then used to cover the muscle and allowed to freeze as one continual process. OCT-muscle blocks were stored at -80°C ready for cryo-sectioning. Blocks were mounted on pre-cooled chucks in a cryo-sectioning chamber (-20°C) (Bright 5040 Cryostat) using OCT. Sections of 12µm were cut from the mid-region of the muscle and transferred to poly-L-lysine coated slides. After 1 hour at room temperature sections on slides were stored at -80°C or directly used for analytical staining.

Histology:

Paraffin embedding and processing:

Agarose/Matrigel/organoid complex was placed into an embedding/processing cassette and transferred to the following solutions in the designated order:

- 70% Ethanol – 1h
- 70% Ethanol – 1h
- 80% Ethanol – 1h
- 95% Ethanol – 1h
- 95% Ethanol – 1h
- 100% Ethanol – 1h
- 100% Ethanol – 1h
- 100% Ethanol – 1h
- Xylene – 2h
- Xylene – 2h
- Paraffin – 2h
- Paraffin – 2h

Paraffin permeated agarose/organoids were placed in plastic moulds and embedded in paraffin before allowing to cool on ice until solid. Sections were cut (5µm thick) using a Leica RN 2155 microtome and floated in a water bath at 37°C so that they could be floated onto a positively charged glass slide. Sections were allowed to dry at 45°C overnight.

De-paraffinisation and rehydration:

Section perimeters were marked with a diamond tip pen showing organoids location before de-paraffinization. Sections were placed in the following solutions in the designated order:

- Xyline – 5mins
- Xyline – 5mins
- Xyline – 5mins
- Xyline – 5mins
- 99% EtOH – 5 min
- 99% EtOH – 5 min
- Ethanol series (few seconds each) 99%, 96%, 70%, 50%
- ddH₂O (2X 5 min)

Antigen retrieval

Slides were placed in a plastic box and covered with citrate buffer (10mM pH6). Slides were boiled for 4-5 minutes (maximum wattage) in a microwave. Slides were boiled at 600 Watt for 8 minutes before adding the remaining buffer and repeating for another 8 minutes. Slides were allowed to cool for 25 minutes before continuing with immuno-histology protocol.

Haematoxylin and Eosin staining

Following 10 minutes of drying sectioned slides were washed for 2 minutes in PBS then placed in Mayers Haematoxylin for 18 minutes. Slides were then washed with distilled water for 2 minutes

before immersing slides in acidic alcohol (0.1% HCL) and then rinsing with running tap water for 5 minutes. For 2 minutes slides were submerged in Eosin stain and then washed in 70% ethanol for 1 minute, 90% ethanol for 2 minutes and 100% ethanol three times for 2 minutes. Sections were then washed twice in xylene for 3 minutes and then immediately mounted and cover-slipped using DPX medium.

Acid phosphatase staining

Frozen sections were washed three times with PBS (5 minutes/wash) to remove OCT. 150ul-200ul of acid phosphatase staining solution was pipetted/slide onto sections. Sections were incubated at 37°C (no additional CO₂) for 90 minutes or until desired staining was reached. Sections were washed three times with dH₂O. Sections were then incubated with Mayers haematoxylin solution (1:30 dilution in dH₂O) for 1 minute. Sections were then rinsed with dH₂O and then placed in a slide bath in order to run tap water over them for 3-5 minutes. Sections were then rinsed with dH₂O before mounting with hydro-mount and covering with a glass cover-slip.

Immuno-histochemical staining

Sectioned slides were allowed to dry for 10 minutes before an ImmEdge Hydrophobic barrier pen (Vector) was used to draw around sections to reduce the amount of antibodies and solutions used. Sections were washed twice for 5 minutes with PBS to remove surrounding OCT, which was then poured off and replaced with permeabilisation buffer for 15 minutes. Permeabilisation buffer was washed off with three 5 minute PBS washes. Incubation of sections for 30 minute in wash buffer was then used to block non-specific antibody binding. Whilst incubating in wash buffer, primary antibodies were diluted in wash buffer and then used to incubate sections overnight at 4°C or 1 hour at room temperature. Primary antibody was then removed with 5 washes of wash buffer. Corresponding Alexa Fluor 488 or 594 secondary antibodies were diluted and then sections incubated in them for 45 minutes in the dark. Another 3 washes in wash buffer was repeated and the sections mounted with 2.5µg/ml DAPI and then cover slipped for visualisation.

Pearson's co-localisation statistical test

Images were opened in Image J Fiji and colour channels split. The Analyse tab was selected, followed by the subsequent co-localisation option and then Coloc 2. Channel colours of interest were selected in the drop down selection menu before running the test. The Pearson's R value was taken as a measure of co-localisation between the two channels.

Statistics

Experiments were repeated in triplicate unless otherwise stated. Statistical analysis was performed using GraphPad Prism software. Data analysed between multiple groups was tested using one-way ANOVA followed by Tukey's post-hoc testing. For comparison between two groups, independent sample t-tests were completed. Significance values were always set at the 95% confidence interval. All p values were indicated as $p < 0.05$ (*), $p < 0.01$ (**) or $p < 0.001$ (***). All data are displayed as mean \pm SEM.

3. Chapter 3

Characterisation of Amniotic Fluid Stem Cell

Conditioned Media

Introduction

The enthusiasm surrounding the use of stem cells for regenerative therapy, especially MSCs has stemmed from an ability to differentiate into a number of different cell types. Originally found to differentiate down osteogenic and chondrogenic lineages, these cells were proposed to be able to replace lost or damaged tissues following their differentiation into a desired cell type (Caplan, 1991). Following these discoveries and others, which exhibited the differentiation potential and potency of other MSCs such as umbilical cord MSCs, BM-MSCs and AFSCs, research into their use for regenerative therapy increased (Honmou et al., 2011, Rodrigues et al., 2017, Piccoli et al., 2012, Zani et al., 2014). The characteristics which are used to define and select for MSCs prior to use have been outlined in 'The International Society for Cellular Therapy' position statement. Minimal criteria for classification of a MSC include being plastic-adherent when sustained in standard culture conditions (Lv et al., 2014, Dominici et al., 2006). Secondly, relating to surface markers, MSCs must express markers such as CD73, CD105, CD-44 and CD90, but lack expression of CD45, CD34, CD14, CD11b, CD79alpha, CD19 and/or HLA-DR (Lv et al., 2014, Dominici et al., 2006). Furthermore, an MSC must be proven *in vitro* to differentiate into osteogenic, adipogenic and chondrogenic cells (Dominici et al., 2006, Lv et al., 2014). CD73, an ecto-5'-nucleotidase and CD90, also known as Thy1, are known to mediate the transduction of signals within immune cells but also provide cell-cell and cell-extracellular matrix interactions (Barker and Hagoood, 2009, Hunsucker et al., 2005). CD105, also known as Endoglin, binds to the TGF- β family of receptors and is also known to interact with Activin and therefore has an important role in regulating differentiation and growth of cells (Barbara et al., 1999). CD105 has been classically used as a marker of MSCs, however it has recently been shown to vary in expression between MSCs of which some do not express this marker at all (Mark et al., 2013, Barbara et al., 1999, Anderson et al., 2013). CD 44, a cell-cell interacting glycoprotein has also been identified as a marker of stem cells, it's function is believed to provide many known stem cell properties including resistance to stress, such as hypoxia (Zöller, 2015). However, it is understood that phenotypic profiles of MSCs, as with most cells, vary depending on the environment in which they exist (Pozzobon et al., 2014, Bussolati et al., 2012, Lv et al., 2014).

The application of AFSCs for regenerative therapy has become a focus for a number of researchers (Prusa and Hengstschlager, 2002, Moorefield et al., 2011a, Piccoli et al., 2012, Ramachandra et al., 2014, Zani et al., 2014, Mellows et al., 2017). AFSCs are isolated from AF and therefore inherently originate from an early developmental time-frame compared to their adult MSC counterparts (De Coppi et al., 2007). CD117 is used to select for the AFSCs following isolation from AF (Di Trapani et al., 2015, Pozzobon et al., 2014, Zani et al., 2014). CD117, otherwise known as C-kit, is a surface tyrosine kinase receptor which binds to 'stem cell factor'. Due to their foetal origins, AFSCs are hypothesised to be more comparable to embryonic stem cells, which are believed to be the gold standard in stem cell research (De Coppi et al., 2007). Furthermore, the ability to isolate the AFSCs with little ethical constraint from second trimester AF makes them a strong candidate for therapeutic purposes. However, the use of whole AFSC and other MSCs for therapeutic research has led to the conclusion that the regenerative capabilities of the MSCs mainly reside in the paracrine factors that they secrete into the environment (Shabbir et al., 2010, Zani et al., 2014, Mellows et al., 2017).

Paracrine factors secreted by stem cells have been reported to consist of a variety of cellular products ranging from growth factors to RNA based transcripts (Waszak et al., 2012, Robinson et al., 2014, Balbi et al., Gneccchi et al., 2005, Gneccchi et al., 2016, Mellows et al., 2017). Furthermore, collection of the MSC paracrine factors and then introducing them to an area of significant pathology may provide a more efficient form of therapy compared to the whole stem cell alone. Introduction of whole stem cells has shown that few survive to graft and differentiate to replace lost tissue due to host rejection (Ikegame et al., 2014). Rejection not only reduces the efficacy of the population of MSCs but may also cause an unwanted and damaging cytokine response. Injected MSCs, such as AFSCs, find themselves in other organs like the lungs and spleen as opposed to the tissue of interest (Zani et al., 2014, Ikegame et al., 2014). Therefore injection of the paracrine factors collected in CM to the site of interest would deliver a more targeted and efficient approach without the risk of immune rejection.

Protocols developed by our industrial collaborators led to the development of a method consisting of pelleting cells, here in particular AFSCs, in PBS with the aim of collecting an AF-CM free of serum and therefore making them clinically compliant. Pelleting of the cells is hypothesised to create a hypoxic environment in which cell-cell contact is also amplified due to the increased cell density (Balbi et al., Roemeling-van Rhijn et al., 2013). Along with the lack of nutrients, brought about by the use of PBS and lack of normal culture medium, it is believed that the AFSCs experience a high level of cellular stress. Heightened levels of stress are also known to increase the exosome release from cells. Therefore, the collection of CM from AFSCs under these conditions is proposed to contain higher levels of exosomes and other EVs, which are imbued with cyto-protective properties (Lee et al., 2012a, Balbi et al., Yu et al., 2006). Additionally, the literature surrounding the stress responses of cells and their resultant exosome release would also suggest that the method of CM collection used for this study may increase protein concentrations which could further change with increased stress exposure (Waszak et al., 2012, Yu et al., 2006).

Furthermore, the exact nature of the paracrine factors released from each type of MSC will most likely vary. An extensive characterisation of AFSCs and more specifically under the stated CM collection protocol has not been previously carried out. Techniques such as silver staining of SDS-PAGE gels run with samples of AFSC CM provide a sensitive means of detecting protein in the CM at ng concentrations, unlike staining techniques such as Coomassie, but also enable further processing of proteins within the gel such as mass spectrometry. However, pooling conclusions from the literature surrounding AFSC paracrine factors would suggest that it is likely that CM produced from AFSC will have a multitude of proteins and RNA species likely to have advantageous properties (Savickiene et al., 2015, Liang et al., 2014, Zani et al., 2014, Lo Sicco et al., 2017, Ti et al., 2015, Collino et al., 2010). Work here aims to establish whether the AFSCs used to create AF-CM are indeed MSCs and therefore differentiate down the described lineages as well as expressing correct levels of MSC markers. Additionally, the nature of any EVs are hoped to be elucidated along with their protein and RNA based cargo. Any proteins and RNA identified will aid the clarification of any signalling processes that the AF-CM may modify or effect in target cells.

Results

Flow Cytometric Analysis of AFSCs Before and After AF-CM Collection

To ensure the AFSCs used to collect AF-CM are MSCs, the expression of surface markers identifiable as MSC markers must be confirmed. Further to this, a lack of surface markers not attributable to mesenchymal stem cells must be proven. Flow cytometry analysis of AFSCs was therefore carried out for positive (CD-44, CD-73, CD-90) and negative (CD-45 and CD34) mesenchymal stem cell markers (Figure 3.1. A-E). All AFSCs expressed the cell surface glycoprotein CD-44, whilst most (98.2%) expressed CD-73. The majority of cells were positive (64.6%) for CD-90. Fewer than 10% expressed CD-34 and fewer than 5% expressed CD-45.

Collection of CM is designed to induce stress in the pelleted AFSCs. We established the CD profile of cells after the period of induced stress. Expression of CD-44 and CD-73 on AFSCs after CM collection dropped very marginally to 97.5% and 92.7% respectively. CD-90 expression of AFSCs post-CM generation was found in 42.7% of cells. Furthermore a reduction of over 99.9% and 94% of AFSCs were shown to be negative for CD-45 and CD-34 respectively.

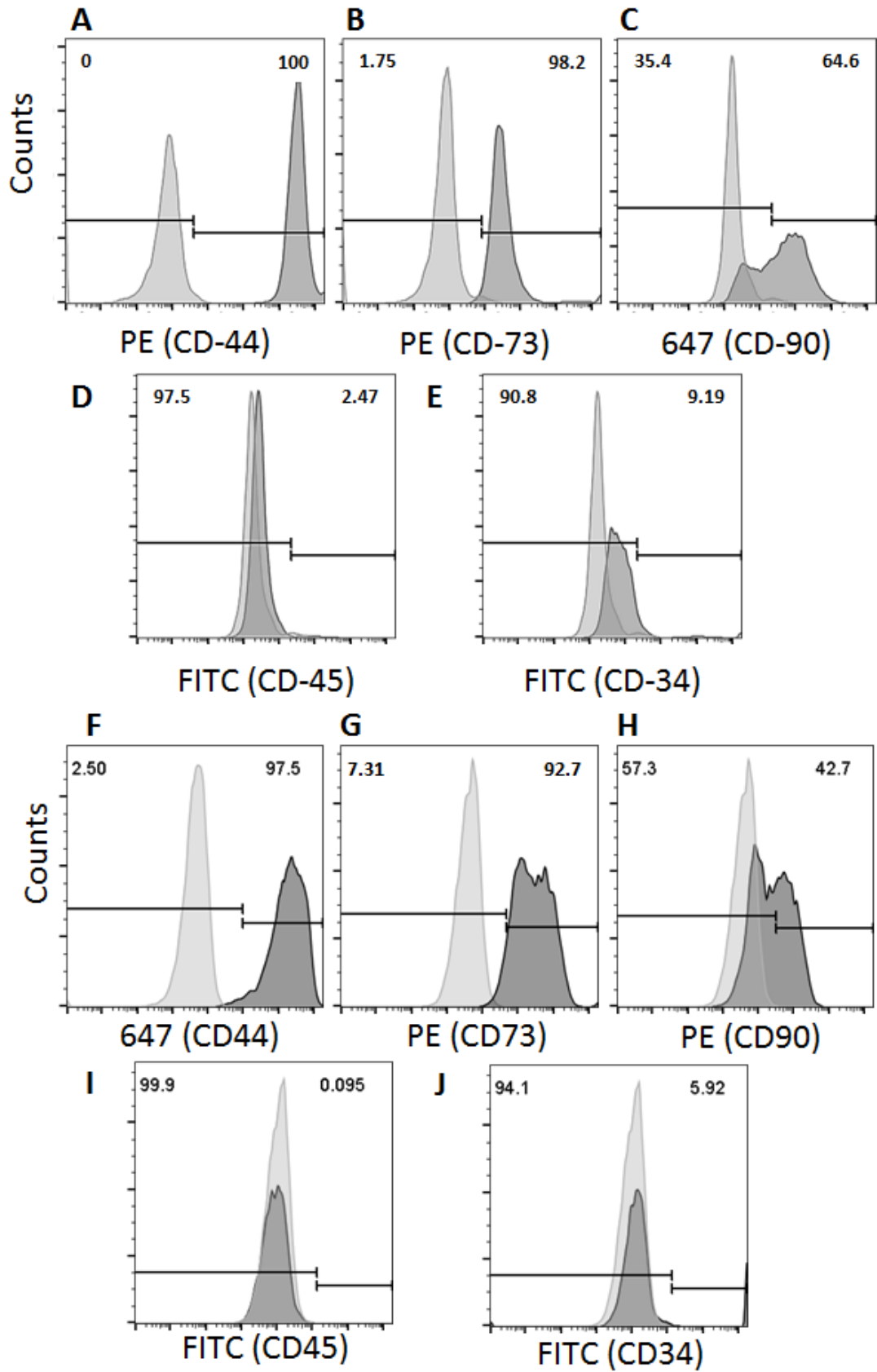


Figure 3.1

Figure 3.1: Surface marker expression analysis of AFSCs before and after CM collection. Flow cytometry analysis of AFSCs before CM collection for (A) CD44, (B) CD-73, (C) CD-90, (D) CD-45) and (E) CD-34. Flow cytometry analysis of AFSCs after CM collection for (A) CD44, (B) CD-73, (C) CD-90, (D) CD-45) and (E) CD-34.

Differentiation of AFSCs Post AF-CM Collection

A key characteristic of mesenchymal stem cells is that they can differentiate into a variety of cell types. AFSCs not only successfully survived the CM collection protocol but were able to proliferate once returned to normal culture conditions. AFSCs in differentiating conditions after CM collection underwent adipogenesis, osteogenesis and Chondrogenesis (Figure 3.2.A-C').

AF-EV Size Distribution

It is well known that the environment in which the cell exists influences the type of EV secreted. TEM images of the AF-CM were taken in order to identify the type of EV being secreted into the AF-CM (Figure 3.3.A). The average AF-EV diameter was 97.8 ± 4.9 and therefore lay within the known boundaries of exosome size. Size distribution of AF-EVs also suggested that the majority consisted of exosomes, with over 92% being under 150nm in diameter. Although low, the presence of larger EVs suggested that other EV species were present within the AF-CM.

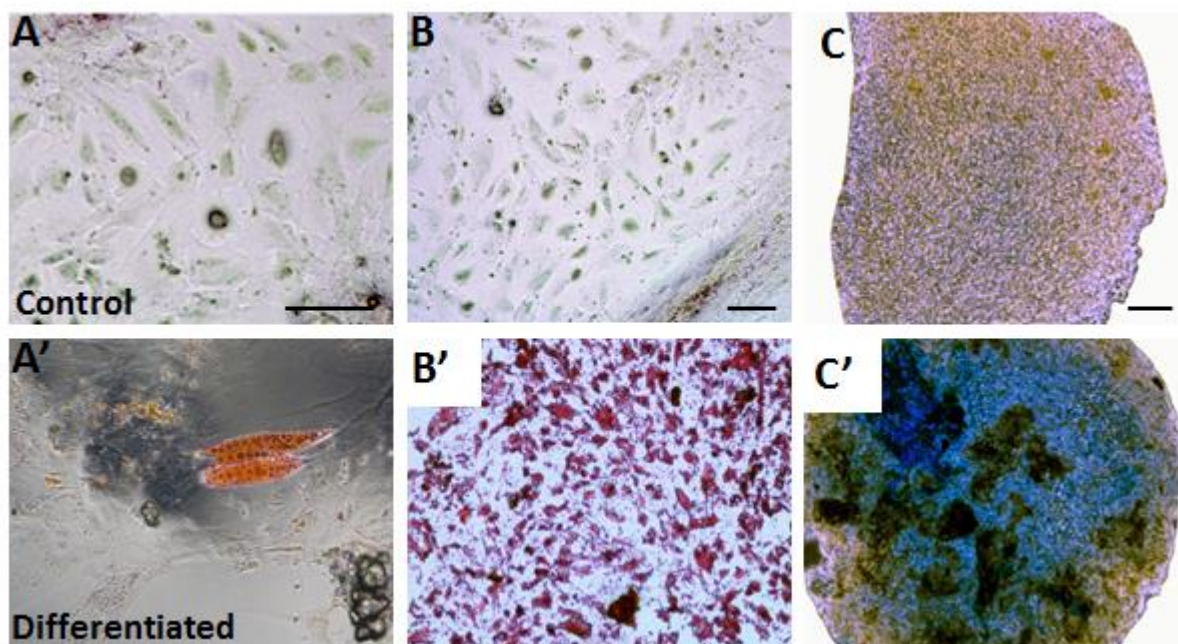


Figure 3.2: Multipotency of post-CM generated AFSCs. AFSCs cultured in (A') adipogenic, (B') osteogenic and (C') chondrogenic media. (A, B) scale bar equal to 50µm, (C) equal to 100µm.

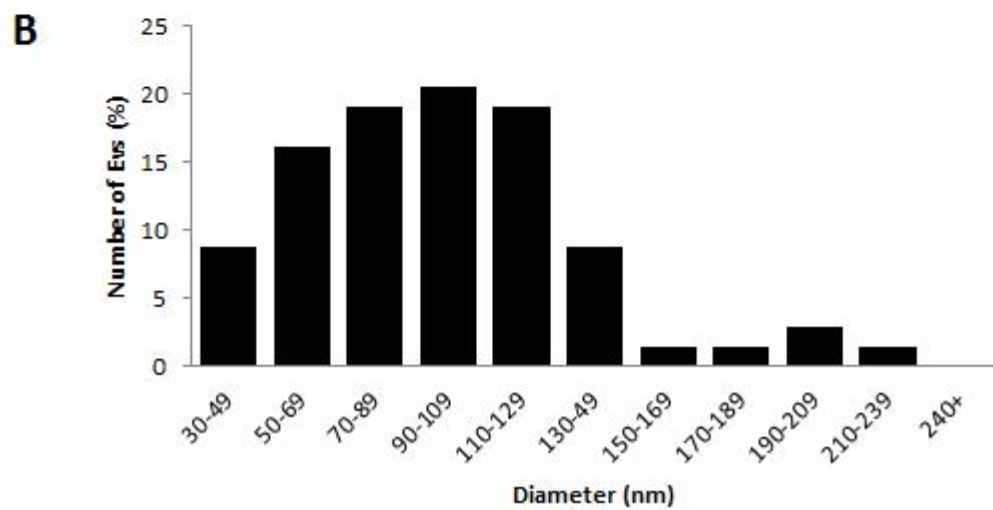
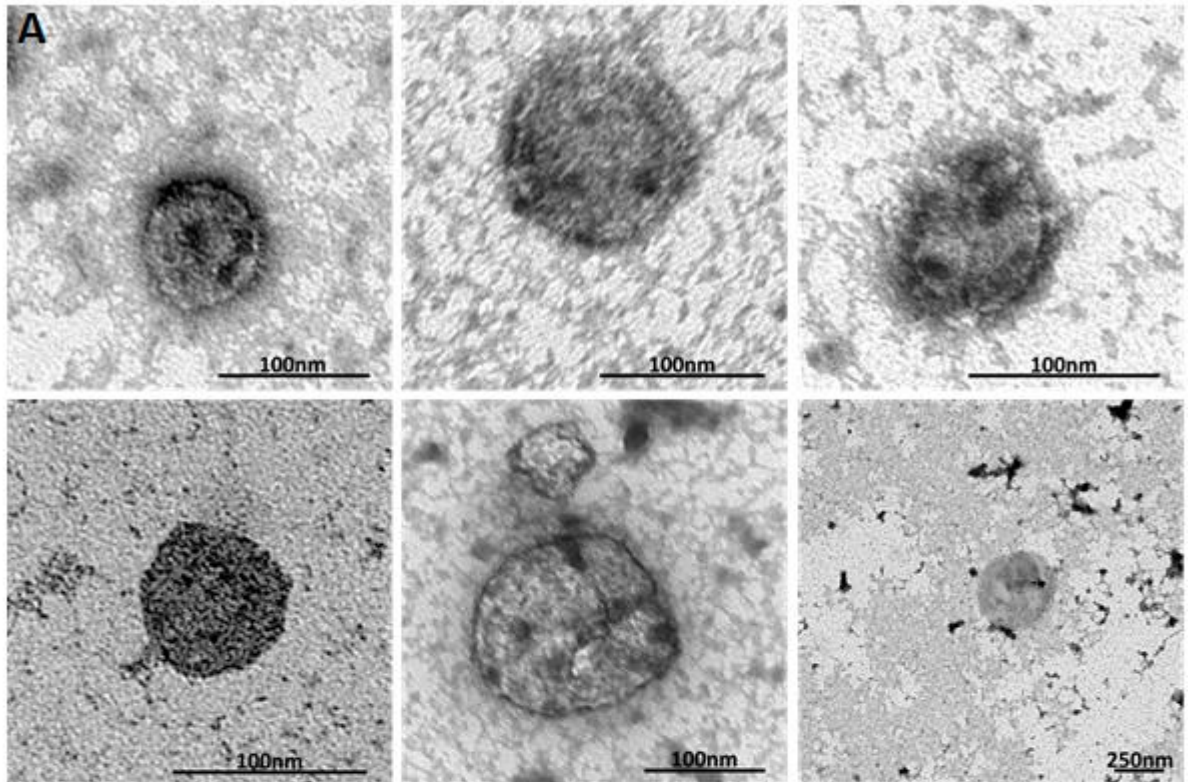


Figure 3.3: Characterisation of AF-EV type and size (N=3). (A) TEM images of AF-EVs. (B) AF-EV size distribution from TEM images.

Basic Protein and Nucleic Acid Analysis of AF-CM

Collection of AF-CM was carried out every 24 hours over a 72 hour period thus providing three fractions, T24, T48 and T72. Basic analysis of secretome composition was carried out to determine the protein and nucleic acid concentrations within each fraction. Nucleic acid concentrations between T24, T48 and T72 AF-CM samples did not differ significantly (Figure 3.4.A) with an average of $21.93\text{ng}/\mu\text{l} \pm 2.23$ (n=4), $14.88\text{ng}/\mu\text{l} \pm 1.23$ (n=4) and $19.93\text{ng}/\mu\text{l} \pm 3.88$ (n=4) at 24, 48 and 72 hours respectively. Average protein concentration of AF-CM (Figure 3.4.B) were $834.25\mu\text{g}/\text{ml} \pm 72.73$ (n=3) and $889.25\mu\text{g}/\text{ml} \pm 162.62$ (n=3) at T24 and T48 respectively. However, both had significantly higher protein concentrations compared to that of AF-CM collected at T72 ($241.75\mu\text{g}/\text{ml} \pm 5.20$ (n=3, $P < 0.05$)). Silver staining of proteins within AF-CM fractions was carried out to compare their size profiles. Comparison of T24, T48 and T72 silver staining profiles suggested that fractions did not differ in protein composition (Figure 3.4.C). However, differences in protein band intensities between each fraction were discernible. T24 AF-CM containing bands with higher intensities compared to T48 and T72. Differences in silver staining profiles were also compared between T24 AF-CM and its constitutive AF-EV fraction (Figure 3.4.D). Silver stain comparisons between whole AF-CM and AF-EV suggested that a lot of the protein in the AF-CM was to be located in the subsequent soluble fractions as opposed to the AF-EV. The AF-EV silver stain profile also showed that the majority of the proteins in the 40-50KDa range.

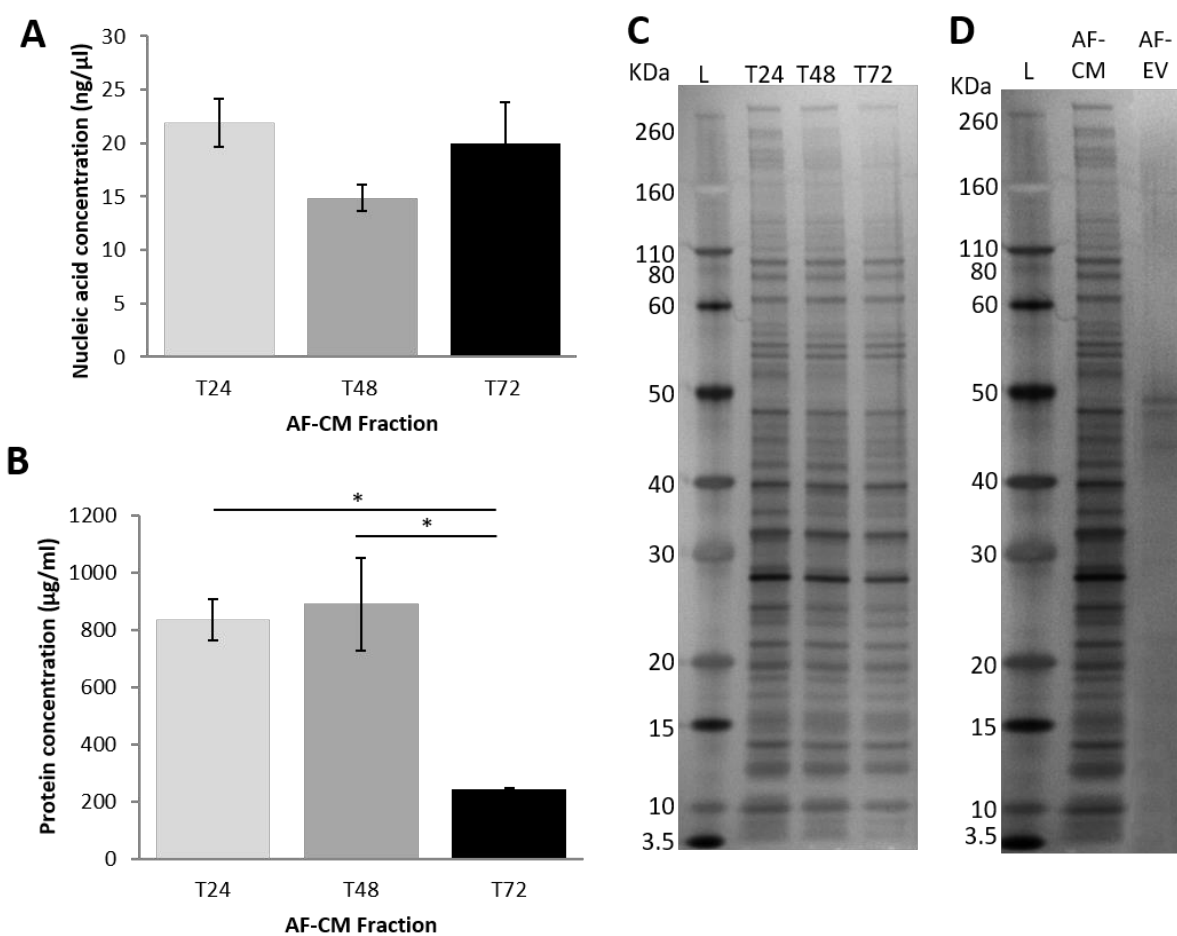


Figure 3.4: Basic protein and nucleic acid content characterisation of AF-CM fractions. (n=3) (A) Nucleic acid concentrations of AF-CM taken at 24 hours (T24), 48 hours (T48) and 72 hours (T72). (B) Protein concentrations of AF-CM taken at T24, T48 and T72. (C) Silver staining of AF-CM taken at T24, T48 and T72. (D) Silver staining of T24 AF-CM vs T24 AF-EV. L, Ladder.

Mass Spectrometry Analysis of AF-CM Protein Content

Mass spectrometry was performed in order to identify protein species and compare any differences in the species of protein contained within the AF-EV and the soluble fraction. A total of 856 proteins were identified between the AF-EV and soluble fraction (Figure 3.5.A). In addition to this, 416 of these protein species were found in both fractions. However, many of the proteins (190) were found to be specific to the AF-EV fraction and even more (250) specific to the soluble fraction. This stark contrast in protein distribution is illustrated in the heat map (Figure 3.5.B) which shows that some proteins found in the AF-EV are of a high concentration whilst they are low in the soluble fraction and vice versa. Gene ontology molecular function terms (GOMF) describe the ability of the proteins found and therefore reveals how the proteins could interact with target cells following a treatment with AF-CM. Although proteins were found to be enriched in the different AF-CM fractions, many potentiated the functioning of shared cellular processes (Table 3.1.) and therefore were identified under GOMFs including many global RNA metabolic processes such as the metabolic processing of tRNA and ncRNA. In contrast, many of the proteins found solely in the soluble or AF-EV fraction were shown to be involved in distinctly different cellular processes. Proteins highly enriched within the soluble fraction (Table 3.2.) were involved in processes such as translational initiation and its regulation. Proteins enriched within the AF-EV fraction only were shown to be implicated in pathways constructive of viral transcription and membrane targeting. A large number of heat-shock protein (HSP) species were found within the AF-CM. Similarly to other proteins found, some of the HSPs were found only within the AF-EV and not the soluble fraction, specifically HSPA (70KDa)-4L. Other HSPs were found specifically within the AF-CM soluble fraction such as the mitochondrial 60KDa heat shock protein (HSPD-1). HSP species were also found to be conserved across both fractions and included HSPA-6 protein. In addition, other proteins of interest present within the AF-CM include CD63, HSP70, HSP90, ACTB, GAPDH, 14-3-3 protein zeta/delta (YWHAZ) and the 'Alarmin' protein HMGB1. Further to this, the AF-EV fraction was found to contain the A2B1 ribonucleoprotein although no member of the RNA-induced silencing complex (RISC) associated proteins were found either the AF-EV or soluble fraction.

Much of the literature surrounding EVs has suggested that they may retain receptors on their membrane that enable specific targeting to cellular membranes (Montecalvo et al., 2012, Mathivanan et al., 2010, Wiklander et al., 2015, Mulcahy et al., 2014). Many proteins within the AF-EV fraction were found to be enriched towards processes commonly known to aid viral infectious cycles. At the individual protein level it was found that transmembrane transporters and receptors were enriched within the AF-EV (Figure 3C), including ABCE1, ABCF1, ABR, AP2A1, CYFIP1, CYFIP2, DNM1, DNM2, DNM3, HDAC2, HDAC1, HK1, MAPK1, NCKAP1, PPP1CB, ROCK2, RTN4, STRAP, USP9X, USP9Y and XPO1.

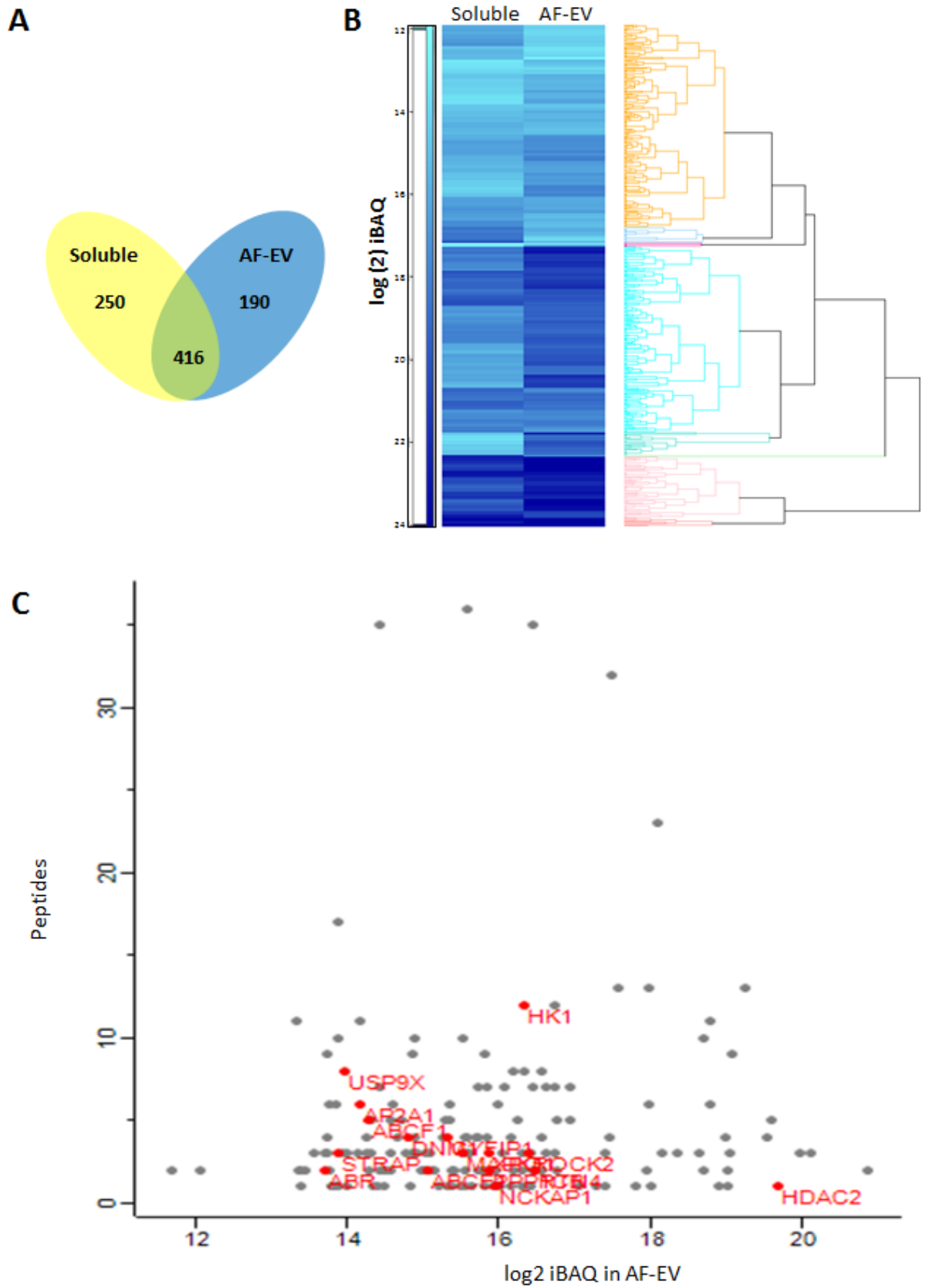


Figure 3.5

Figure 3.5: Mass spectrometry analysis of AF-CMs soluble and EV fraction. **(A)** Comparison of the number of unique and shared proteins between the AF-soluble and AF-EV fractions. **(B)** Heat map of the GO terms found within the AF-EV and AF-soluble fraction. **(C)** GO terms of transmembrane transporters and receptors enriched within the AF-EV. GO, gene ontology.

Category value	Selection size	Category size	Enrichment factor	P value	Benj. Hoch. FDR
nucleic acid metabolic process	112	126	2,5057	2,66E-33	8,10E-27
RNA metabolic process	112	105	2,6531	2,88E-30	4,38E-24
metabolic process	192	297	1,3423	9,33E-28	9,46E-22
proteolysis	32	42	8,3571	8,10E-27	4,92E-21
Aminoacyl-tRNA biosynthesis	13	13	32	6,73E-25	8,87E-20
proteolysis	21	42	9,9048	4,58E-24	9,29E-19
small molecule metabolic process	192	112	1,8571	5,27E-24	1,00E-18
tRNA metabolic process	13	14	29,714	9,43E-24	1,51E-18
nucleobase-containing compound metabolic process	112	159	2,0323	1,03E-23	1,56E-18
ribonucleoprotein complex	78	58	3,8621	3,95E-23	1,74E-17
regulation of gene expression	112	107	2,3605	1,74E-21	2,52E-16
cytoskeleton	49	81	3,9829	1,24E-21	2,73E-16
nucleic acid metabolic process	48	126	3,0265	2,17E-21	3,00E-16
ncRNA metabolic process	13	18	23,111	5,77E-21	7,02E-16
primary metabolic process	192	279	1,3357	6,13E-21	7,17E-16
regulation of RNA metabolic process	112	78	2,619	1,05E-19	1,18E-14
RNA processing	78	42	4,1905	1,85E-19	2,01E-14
regulation of catalytic activity	29	62	5,7842	2,53E-19	2,66E-14
nitrogen compound metabolic process	112	183	1,8064	3,14E-19	3,19E-14
cellular nitrogen compound metabolic process	112	180	1,8159	4,90E-19	4,81E-14
regulation of RNA metabolic process	48	78	3,8889	6,94E-19	6,59E-14
mRNA metabolic process	78	46	3,942	1,33E-18	1,23E-13
RNA processing	112	42	3,2721	1,44E-18	1,29E-13
mRNA metabolic process	112	46	3,1491	2,33E-18	2,02E-13

Table 3.1: Soluble and Extracellular Vesicles GOMF terms enrichment.

Category value	Selection	Category	Enrichment factor	P value	Benj. Hoch. FDR
translational initiation	13	12	17,628	1,94E-16	3,05E-10
regulation of translational initiation	13	10	19,231	1,31E-15	1,02E-09
translational initiation	15	12	15,278	3,37E-15	1,76E-09
regulation of gene expression	46	63	2,9331	4,56E-15	1,79E-09
regulation of translational initiation	15	10	16,667	1,37E-14	3,07E-09
regulation of macromolecule biosynthetic process	46	53	3,1788	1,21E-14	3,16E-09
regulation of cellular macromolecule biosynthetic process	46	53	3,1788	1,21E-14	3,79E-09
regulation of cellular biosynthetic process	46	55	3,0632	5,54E-14	9,66E-09
regulation of biosynthetic process	46	55	3,0632	5,54E-14	1,09E-08
nucleic acid metabolic process	23	47	4,6253	6,93E-14	1,09E-08
translational initiation	26	12	9,6154	1,01E-13	1,33E-08
regulation of translation	15	14	13,095	9,88E-14	1,41E-08
regulation of transcription, DNA-dependent	23	38	5,1487	5,90E-13	7,12E-08
translation	13	10	17,308	7,74E-13	8,67E-08
regulation of translation	13	14	13,736	1,24E-12	1,30E-07

Table 3.2: Soluble only GOMF terms enrichment.

Category value	Selection	Category	Enrichment factor	P value	Benj. Hoch. FDR
Ribosome	28	28	6,7857	3,87E-34	2,17E-29
viral transcription	28	28	6,7857	3,87E-34	8,96E-29
translational termination	28	28	6,7857	3,87E-34	1,20E-28
protein complex disassembly	28	28	6,7857	3,87E-34	1,79E-28
cellular protein complex disassembly	28	28	6,7857	3,87E-34	3,58E-28
viral reproductive process	28	29	6,5517	1,12E-32	1,16E-27
viral infectious cycle	28	29	6,5517	1,12E-32	1,30E-27
translational elongation	28	29	6,5517	1,12E-32	1,49E-27
macromolecular complex disassembly	28	29	6,5517	1,12E-32	1,73E-27
cellular macromolecular complex disassembly	28	29	6,5517	1,12E-32	2,08E-27
SRP-dependent cotranslational protein targeting to membrane	28	30	6,3333	1,68E-31	1,04E-26
protein targeting to membrane	28	30	6,3333	1,68E-31	1,11E-26
protein targeting to ER	28	30	6,3333	1,68E-31	1,20E-26
nuclear-transcribed mRNA catabolic process	28	30	6,3333	1,68E-31	1,30E-26
establishment of protein localization in endoplasmic reticulum	28	30	6,3333	1,68E-31	1,42E-26

Table 3.3: Extracellular Vesicles only GOMF terms enrichment

AF-CM RNA Content

EVs are able to alter target cell signalling through the activity of RNA molecules (Lotvall and Valadi, 2007, Ratajczak et al., 2006, Valadi et al., 2007, Villarroya-Beltri et al., 2013). Bioanalyser RNA profiling of the AF-EV collected at T24 was therefore carried out (Figure 3.6.A). Evidently the RNA species found within the AF-EV consisted almost entirely of small species about 21-25 nucleotides in length. Due to the size of the RNA species found within the AF-EV further analysis was carried out into to specific miRNA species present. Through detailed analysis of the miRNA species, 586 species of miRNA were identified. 21399 pathway targets were found from the miRNA species identified (Figure 3.6.C). Metabolic processing was found to be how most of the miRNAs were known to influence signalling pathways. More precisely, 21.87% of miRNAs found were known to be involved in responding to stress and 10.2% in immune system processes. A list of top 50 miRNAs present within all 3 batches of AF-EV used was compiled (Figure 3.6.B). Many of the miRNAs within the top 50 identified are believed to support proliferation, migration, differentiation, angiogenesis and autophagy for example miR3960, miR24-3p and miR382 (Seok et al., 2014, Yu et al., 2017, Xia et al., 2015). Inhibition of apoptosis is known to be achieved with miR3196, miR125b-5p, miR1273-3p and miR762 also found to be present within AF-EV (Xu et al., 2016, Ma et al., 2016, Yang et al., 2016, Niu et al., 2016). Similarly present was miRNA Let-7b-5p recognised as retaining anti-inflammatory properties (Ti et al., 2015, Landskroner-Eiger et al., 2013). On the other hand, other miRNAs present such as miR-1273g-3p have been known to induce injury via inhibited proliferation facilitated by acute glucose fluctuation (Guo et al., 2016).

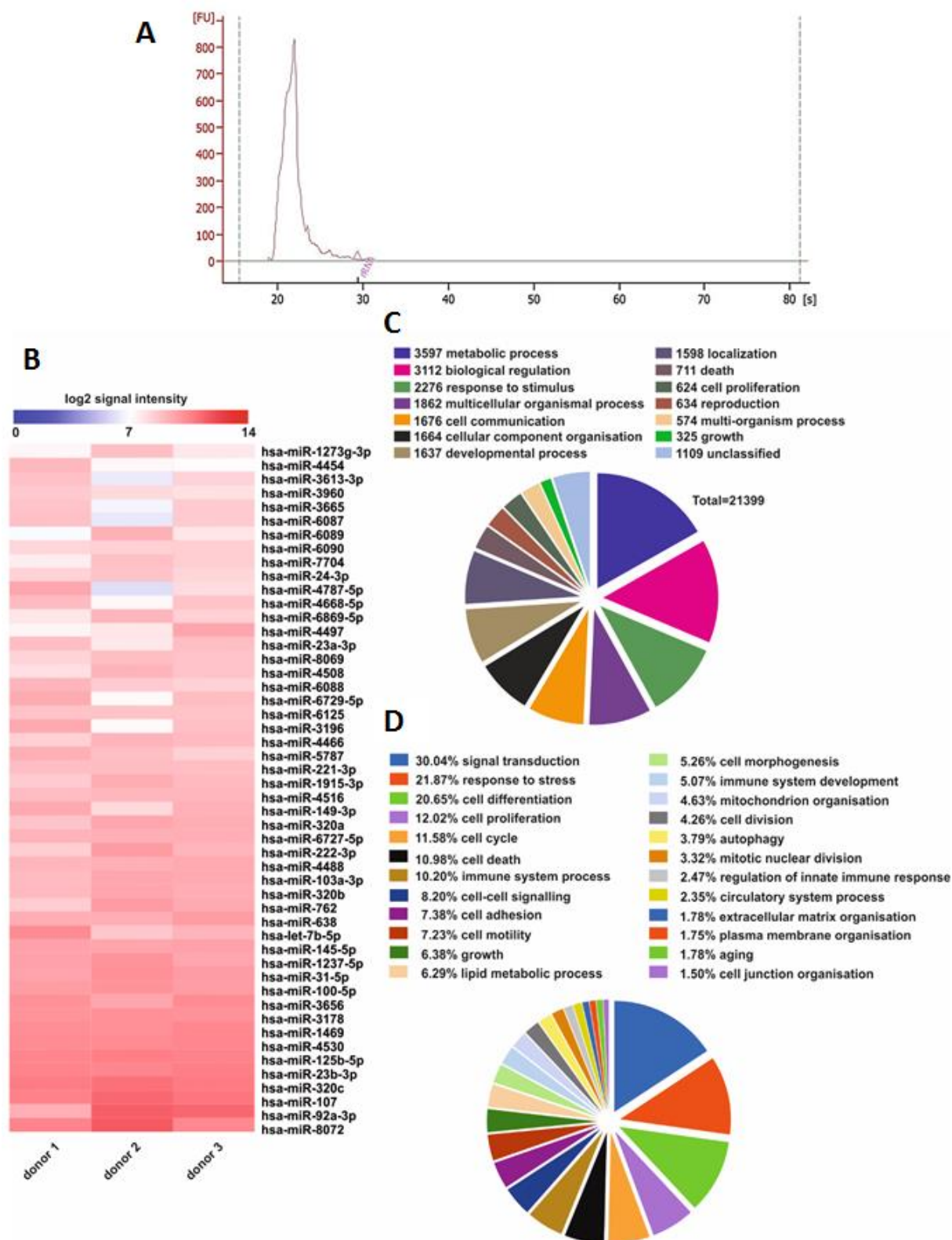


Figure 3.6: RNA profiling of T24 AF-EV. (A) Bioanalyzer profile of AF-EV RNA size (s) and frequency (FU). (B) Top 50 expressed miRNAs in AF-EV (n=3). (C) General cell process targets of miRNA found within AF-EV. (D) Specific cellular processes targeted by miRNA present within AF-EV.

Discussion

Ensuring MSC Characteristics of AFSCs

Much controversy surrounds the use of stem cells for therapy. One aspect of this debate is the validation of the stem cell nature of the cell in question. It is now recognised that a number of cellular membrane expressed markers can be used to identify a mesenchymal stem cell. It was therefore important that the AFSCs used to generate CM were characterised according to guidelines published (Lv et al., 2014, Dominici et al., 2006). The initial isolation of AFSCs involved culturing them on non-tissue culture treated plastic is a characteristic attributable to stem cells. Furthermore, the collection of CD-117⁺ (C-Kit) cells via MACS sorting isolated a population of cells previously characterised as AFSCs (De Coppi et al., 2007). Finally, flow cytometric characterisation of the cell membrane markers clearly showed that most cells expressed the positive MSC markers; CD-44, CD-73 and CD-90 (Figure 3.1.A-C). AFSCs also expressed low levels of CD-45 and CD-34 (Figure 3.1.D-E).

In summary of these expression profiles, the AFSCs expressed markers of MSCs and very low levels of markers believed to be negatively expressed in MSCs. However, the levels of CD-45 and especially CD-34 were not completely absent and the level of CD-90 was not expressed in 100% of the population. This exemplifies the heterogeneity of the population of cells as is found with most cell populations, even that of a clonal population where micro-environments around individual cells will affect phenotypic profiles (Singh et al., 2014). Furthermore, the frequently changing stance towards expression of specific markers for MSCs is reflected by the growing evidence that there are exceptions when it comes to the expression of, or lack of expression of specific membrane markers. There are inconsistencies in the acceptance of CD34 as a positive or negative marker for MSCs (P et al., 2011). Furthermore, the accepted positive MSC marker, CD-105 expression is suggested to diminish over time in serum free culture, something that should be considered as the need to reduce cell contact with animal derived serum increases in order to become therapeutically compliant (Mark et al., 2013). The growing evidence for marker expression variability between different MSCs may simply suggest that the current rules for defining a mesenchymal stem cell must be altered.

AFSCs Retain Stem Cell Characteristics Following CM Collection

Ensuring the absence of animal derived products such as serum, is one of the first steps in creating a clinically compliant cell derived therapeutic. The collection of the AFSC secretome was therefore collected within PBS to negate the use of basal or growth medium as others have previously done. Use of animal derived serum and products, without steps to remove their traces later on in the production line will lead to levels higher than that of the FDA's code of regulations acceptable level of 1ppm (Carmen et al., 2012). Due to the removal of the AFSCs from their normal culture conditions throughout the CM collection for 24-72 hours, it was imperative to ensure that the AFSCs had not become less stem cell like or worse had differentiated and were therefore no longer stem cells.

Following CM collection, AFSCs were once again characterised for the phenotypic expression of CD-44, CD-73, CD-90, CD-45 and CD-34. The maintenance of high levels of CD-44 and CD-73 positivity went some way to show that the AFSCs retained their stem cellness. This was further illustrated by the fact that the populations expression of CD-45 and CD-34 reduced further. This further reduction in the negative MSC markers suggests that the CM collection protocol may have led to a slight selection in the cells that survived and therefore led to a purer stem cell population. On the other hand, levels of CD-90 had also diminished and may reflect the increased mechanical stimulation on the cells during the pellet phase of CM collection (Wiesmann et al., 2006). This increased mechanical stimulation and therefore reduced CD-90 expression may have also started to drive the AFSCs towards an osteogenic pathway (Moraes et al., 2016). The reduction in CD-90 expression can almost certainly be hypothesised as accumulating over the 72h period and therefore would be important to recognise when looking at the most suitable time fraction of AF-CM in order to consider which is more potent and stem cell derived.

However, consistent with current guidelines, AFSCs following CM collection were also shown to differentiate and undergo adipogenesis, osteogenesis and chondrogenesis when placed in the correct environments to promote differentiation (Figure 3.2.). Although a reduced CD-90 expression

was seen, the AFSCs must still retain the stem cell potency to differentiate down all of the three lineages tested.

Extracellular Vesicles within the AFSC CM

An increasing number of EVs are being characterised, of which have been grouped into certain size ranges (Willms et al., 2016, Zhang et al., 2018). Many of these different types of EVs are known to have different origins within the cell and can be generated in response to certain changes in environmental cues or secreted constitutively. TEM imaging of the AF-CM clearly showed that most of the EVs collected within the AF-CM were relatively small and under 150nm in diameter, with an average diameter of 97.8nm (Figure 3.3.A-B). Exosomes are known to be the main extracellular vesicle of this size. As discussed previously, exosomes are known to be secreted constitutively but also at an increased rate following periods of stress. The ratio of these small EVs, hypothesised to be exosomes, corresponds with the prediction that the CM collection process would induce stress upon the AFSCs leading to an AF-CM with increased exosome concentrations (Yu et al., 2006).

Basic Nucleic acid and Protein Content of AF-CM Fractions

AF-CM collected at different time-points was assayed for nucleic acid and protein. Interestingly, nucleic acid content did not significantly differ between fractions (Figure 3.4.A). This suggests that the signalling pathways involved in the alteration of nucleic acid secretions is not visibly affected over the time course selected. However, it cannot be ruled out that some nucleic acids are being produced at higher levels, whilst the production of other species is reduced. This would lead to no overall net change in nucleic acid concentration.

On the other hand, protein concentrations dropped off dramatically after 48 hours of the cells being pelleted (Figure 3.4.B). Due to the reduction in cell viability at T72 following CM it is suggested that an increase in cell death has a negative effect on AF-CM protein concentration. Although the levels of Protein differ between T24 and T72 or T48 and T72, the profile created following silver staining of the AF-CM taken at the differing time-points did not. It was therefore evident that the two fractions to concentrate experimentation on were at the two extreme time-points, T24 and T72. T24 did not

seem to differ significantly in both nucleic acid and protein content to T48 but the T72 fraction was believed to have more extreme differences to the T24 fraction due to significant levels of apoptosis.

AF-EV isolation and subsequent profiling of its proteins via silver stain implied that the majority of proteins were retained within the soluble fraction of AF-CM as opposed to the AF-EV. Secretion of these freely secreted proteins can be anticipated as having a shorter half-life when alone compared to those protected within an EV and therefore more likely to have an effect on the local milieu of cells as opposed to the distant tissues within the body if introduced as a therapy. However, free proteins could be bound to albumin, one of the main binding proteins within the circulation, thus protecting soluble factors from being degraded rapidly. It would therefore be suggested that protein based soluble paracrine factors could act over larger distances if bound to albumin. On the other hand, diseases leading to damaged kidneys and liver reduce the level of freely available albumin (Klammt et al., 2012). This therefore shows the importance of the EVs within the AF-CM as a protector of cargo if injected into a patient presenting with a multitude of dysfunctions and potentially reduced albumin levels as a consequence.

Extensive Characterisation of AF-CM Protein Content

Identifying the specific protein in the AF-CM was carried out using mass spectrometry. The mass spectrometry analysis revealed that both AF-EV and soluble fraction shared 416 protein species and the AF-EV contained 190 species specific to this fraction (Figure 3.5.A). The soluble fraction of AF-CM contained only 60 more species of protein specific to that fraction. Furthermore, the relative levels of proteins found within the AF-EV were comparatively high when looking at the heat map of the two fractions (Figure 3.5.B). However, the potential therapeutic value of both the AF-EV and soluble fraction is exemplified in the fact that both contain proteins specific to that fraction and therefore both could provide differing advantages for use. This is in contrast to many other studies which suggest that an EV fraction is superior for therapy and retains all that is needed to promote regeneration (Balbi et al.).

Further evidence of exosomes within the AF-EV fraction was shown with the existence of exosome specific markers such as CD-63, HSP70, HSP90, GAPDH, ACTB and 14-3-3 protein zeta/delta (YWHAZ) (Mathivanan and Simpson, 2009, Lötvald et al., 2014). The presence of HSPs is of particular interest because they are believed to have dramatic effects on cellular signalling processes involved in the stress response. Although many studies show an increase in HSPs during pathogenesis, which would suggest that they potentially play a factor in creating or amplifying the pathology, much of our understanding now revolves around them preparing the unaffected tissues for incoming stress (Bangen et al., 2007, Danzer et al., 2011, Bianchi, 2007). A cycle of damage, necrosis and inflammation could hypothetically be curbed. Preparatory responses to stress through the inhibition of cell death and reduced inflammatory responses would therefore halt or slow the spread of damage making it easier to regenerate or resect the affected area.

A number of ABC binding cassette transporters were found including ABCE1. ABCE1 protein is also known as an RNase L inhibitor and is therefore capable of inhibiting the catalysis of ribonuclease-L and thus in turn promotes the upregulation of protein synthesis (Bisbal et al., 1995). The promotion of protein synthesis is mirrored by the fact that many proteins within the AF-EV fraction were enriched within cellular processes that are shared in viral reproduction and the viral infectious cycle. Viral replication associated proteins are hypothesised to be present due to the EV manufacturing and shedding processes but may also endorse EV uptake as would be required for viral dissemination. Additionally many proteins within the soluble fraction of AF-CM were enriched in processes such as translational initiation and regulation of translation. On the other hand, proteins enriched in processes shared by the soluble and AF-EV such as proteolysis may reflect the cell death seen during the CM collection process. However, this cell death was seen to be minimal at T24 and the majority of apoptotic bodies were removed. In contrast, if AF-CM contains factors that also direct autophagy signalling, which controls proteolysis, it can be hypothesised that it could help to remove diseased organelles and dysfunctional cell machinery thus being beneficial for maintaining functional regeneration (Nichenko et al., 2016, Garcia-Prat et al., 2016).

Identification of a number of receptor proteins in the AF-CM and more specifically the AF-EV is important in identifying how AF-EVs are targeted to the membranes of cells thus potentiating some or all of its contents paracrine activity. However, no proteins were found to specifically target the EVs to a particular cell type. This is in contrast to the literature which suggests that EVs target specific cell types or tissues (Camussi et al., 2010). However, a number of integrins such as integrin- β -1 and integrins- α -1/2/3/5 were found to be present in the AF-CM and highly present within the AF-EV suggesting that mechanisms are in place to initiate EV-cell membrane contact and binding. This EV membrane to cell membrane binding could facilitate the uptake of AF-EVs and their contents into the cell. Many receptors or membrane bound proteins on the surface of the EVs reflect what is found within or on the membrane of the cell they originate from (Deregibus et al., 2007).

Interestingly, A2B1 ribonucleoprotein was found in the AF-EV. A2B1 ribonucleoprotein has been described as being important for the transport of miRNA into EVs during the production and packaging process (Villarroya-Beltri et al., 2013). The presence of A2B1 therefore indicated that there may be miRNA within the AF-CM and that it has been loaded into EVs. To further this evidence, RISC complex proteins were not detected within the expanse of proteins identified. RISC complex proteins both aid as a transport protein and serve as protection for the miRNA from enzymatic degradation. The lack of RISC proteins therefore provided supplementary proof that any miRNA present would be packaged within the AF-EV fraction. The controlling of mRNA levels is further exaggerated with the enrichment of proteins known to be important for nuclear-transcribed mRNA catabolic processes (Table 3).

Extensive Characterisation of AF-CM RNA Content

The identification of RNA species within MSC EVs has been noted on many occasions (Eirin et al., 2014, Collino et al., 2010). A bioanalyzer profile of RNA content revealed that RNA was present but remarkably was almost entirely made up of RNA of around 20-25 nucleotides (Figure 3.6.A). RNA of 21-25 nucleotides corresponds to the size of miRNA and not the larger mRNA. This finding is especially important because the majority of research has detailed the presence of high quantities of

mRNA within MSC EV fractions (Eirin et al., 2014, Deregibus et al., 2007, Alvarez et al., 2012, Valadi et al., 2007). The presence of miRNA and not mRNA would also suggest that the AF-EVs are more likely to regulate already existing endogenous mRNA within the target cell and not impress new mRNA and its subsequent protein production upon the cell. Following the confirmation that miRNA were the predominant species present within the AF-EV, 586 species of miRNA were identified using the miRNA arrays. Subsequent to this, 21399 pathway targets of the miRNA were revealed and exhibited the potential of a single miRNA species being complimentary to a number of mRNAs as opposed to a single mRNA species within the target cell.

Many of the identified targets of the miRNAs found (Figure 3.6.D) were attributed to stress responses. It can therefore be speculated that the pelleting of AFSCs and removal of them from their normal culture environment with sufficient nutrients had induced the production or secretion of these miRNAs. Furthermore once in the target cell they may enhance the protective mechanisms to incoming stress and increase the chance of cell survival thus reducing widespread cell death. Such miRNAs identified capable of pro-survival included miR3196, miR125b-5p, miR1273-3p and miR762 found within the AF-EV (Xu et al., 2016, Yang et al., 2016, Ma et al., 2016, Niu et al., 2016, Mendell and Olson, 2012). This can be achieved in a number of ways. The miRNA may lead to the direct translational downregulation of proteins involved in promoting stress response pathways such as p53 and PTEN, which could have otherwise induced apoptosis (Niu et al., 2016, Xu et al., 2016). Alternatively the miRNA may downregulate the synthesis of proteins which buffer pro-survival signalling processes thus allowing hyper-activation of pro-survival proteins (Mendell and Olson, 2012, Xu et al., 2016, Ma et al., 2016, Yang et al., 2016, Niu et al., 2016).

As well as preventing apoptosis miRNAs identified were found to be important in promoting proliferation, migration, differentiation, angiogenesis and autophagy such as miR3960, miR24-3p and miR382 (Villarroya-Beltri et al., 2013, Xia et al., 2015, Valadi et al., 2007). Regulated by hypoxia and HIF1 α , miR382 is hypothesised to be upregulated within the ASFSC due to the pelleting process which induces reduced oxygen levels, especially in those cells at the centre of the pellet. Through the

direct targeting of the tumour suppressor PTEN translation, miR-382 is believed to promote AKT and mTOR signalling and subsequent VEGF production leading to endorsement of angiogenesis (Seok et al., 2014). Increased angiogenesis and therefore increased blood flow to the site of injury would provide a significant boost to the regenerative process. Translational suppression of the death effector domain-containing protein DEDD by miR24-3p has been shown to increase autophagy, proliferation, migration and inhibit apoptosis within bladder cancer cells (Yu et al., 2017). Reduced DEDD inhibition of the LC3/ p62 autophagy signalling pathway would lead to increased autophagy and potentially remove damaged and pathological organelles promoting regeneration (Nichenko et al., 2016, Yu et al., 2017). Due to the resultant increase in p62 activity, an increase in cellular migration and proliferation is implicated. This alteration in cell activity may be potentiated through the binding and subsequent stabilisation of Twist1 (Qiang et al., 2014). An increase in cellular migration and proliferation of cells in the milieu local to damage or from distant sites may be sufficient to replace tissue lost to disease. However, the introduction of cells outside the locally affected area is not always beneficial in the case of an exaggerated immune response. Immune system processes made-up 10.2% of the targets for the identified miRNAs. One of the most researched of these miRNAs includes Let-7b-5p. Let-7b-5p, as previously stated is recognised as primarily an anti-inflammatory miRNA as are many of the Let-7 miRNA species (Ti et al., 2015). Let-7b in LPS pre-conditioned human umbilical cord MSC derived exosomes has been shown to inhibit TLR4/NF- κ B-p65 signalling whilst supporting the phosphorylation of Akt and STAT3. As previously identified, Let-7b was discovered to target the mRNA of TLR4 (Bao et al., 2013). Reduced TLR4 signalling would mean that less NF- κ B-p65 is phosphorylated and therefore unable to translocate into the nucleus to up-regulate pro-inflammatory gene transcription (Ghosh and Dass, 2016). On the other hand, disruption of p65 signalling can increase STAT3/ Akt phosphorylation further potentiating the negative feedback loop which controls and hinders NF- κ B signalling (Ti et al., 2015). Reduced pro-inflammatory signalling in the face of massive infiltration of M1 macrophages within a diseased tissue may attenuate the destructive power of these cell types.

4. Chapter 4

Investigation into the Regenerative Potential of AFSC *CM in Vitro*

Introduction

It was found that AF-CM contained a wide variety of constituents from proteins to miRNA, some of which were contained within EVs. However it was important to establish how the mixture of these soluble components along with the EVs and their cargo interacted with a variety of cells types and if they altered their properties. Changes to the cell properties following AF-CM treatment would help us understand if AF-CM has regenerative capabilities. Regeneration of tissue can be influenced by a number of factors; namely proliferation, migration, senescence and inflammatory status. However, it is the role of a multitude of cell types ranging from those found within the milieu, such as the local stem cells and other stromal cells, to those that are foreign to the damaged tissue to aid the facilitation of this regeneration. Furthermore, the inflammatory status of the damaged tissue and how it transitions towards that found in regenerating tissue is of the utmost importance. Overzealous inflammatory signalling as well as too little signalling will often cause further damage and hinder regeneration. As discussed local paracrine and autocrine signalling within the damaged region and from distant sites in the body have a significant influence on how these cellular processes and signalling events prevail.

Proliferation of resident stem cells provides a source of cells for tissue repair. Stem and progenitor cells are capable of differentiating into specific cell types to replace lost or damaged mature cell types (Lee et al., 2009). For example, skeletal muscle satellite stem cells must proliferate upon activation to replace those lost from the stem cell pool after they begin to differentiate and fuse with others to form muscle fibres. Similarly, proliferation of Lgr5⁺ stem cells within the crypts of the intestine serve to replace lost cells within the villi as well as due to normal homeostatic sloughing or damage (Yan et al., 2012, Sato et al., 2011, Zani et al., 2014). Increasing the proliferation of intestinal stem cells during a pathogenic state when more tissue is being lost than replaced is believed ameliorate the disease (Zani et al., 2014). Additionally, the ability to proliferate is especially important for terminally differentiated cell types, such as endothelial cells, which must divide to extend the vasculature within a tissue thus providing blood supply (Rahbarghazi et al., 2013). Often

stimulation of cells to proliferation comes from molecules such as cytokines released by the locally damaged stromal cells. Following stimulation, a variety of signalling pathways can be activated such as those involving the upregulation of PI3Kinase, Akt, NF- κ B, Wnt, notch, Oct4, C-Myc (Zani et al., 2014, Neal et al., 2012, Zhao et al., 2014, Widera et al., 2006, Lee et al., 2009). It is recognised that proteins, heavily recognised as being regulators of inflammation such as the Myd88 and NF- κ B pathways and their regulators, also assist in modulating proliferation levels (Brown et al., 2007, Kaltschmidt et al., 1999, Widera et al., 2006). The dual role and function of these pathways stresses the importance of their tight homeostatic control and regulation as to not induce exaggerated pro-inflammation or too little proliferation.

The capacity to migrate is important for stem cells to locate themselves to an area of damage from where they reside. Migrating to an area of damage both provides more efficient localising of paracrine factors but also positions the stem cell to replace the damaged cells upon its differentiation. Resident stem cells such as the satellite cells within muscle not only migrate from under the basal lamina of muscle fibres but also travel along the fibre to an area of damage utilising an amoeboid type migration (Otto et al., 2011). Once the target location is reached the satellite cell can begin to differentiate, fuse with others to form myotubes and mature to eventually new muscle fibres (Otto et al., 2011). Although, classically thought of as scar forming cells, fibroblasts provide a trophic environment for the stromal cells within a tissue (Jung et al., 2007). Migration of fibroblasts to an area of damage is therefore vital for the regeneration of that tissue following damage. Cytoskeletal rearrangements permit migration and this is often triggered through chemokine and cytokine induced signalling. Chemokines exist as soluble molecules or transmembrane proteins (Hattermann et al., 2016, Ludwig et al., 2005). Binding of the chemokines such as CXCL16 or cytokines such as TNF- α to their appropriate receptor often leads to an increase in NF- κ B signalling. Ultimately NF- κ B will either translocate to the nucleus where it can alter gene expression important for migration, or potentiate post-translational modifications important for actin mobilisation (Prisco et al., 2016).

However, following an initial acute injury or during a chronic pathological state, inflammatory factors along with other stressors are continually released by the local milieu. One such response to these factors, other than cell death, is for the cell to become senescent. Levels of senescent cells increase with aging [10]. Sometimes the senescent state is triggered by an increase in the production of reactive oxygen species (ROS). ROS are damaging to DNA and can therefore cause mutagenesis. A senescent like state is an attempt by the cell to prevent cell division and therefore the proliferation of a cell with mutated DNA (Campisi and d'Adda di Fagagna, 2007). Although not clearly understood, a marker found to increase within senescent cells is β -galactosidase. This enzyme is found in the lysosomes of senescent cells and it is important in energy production. β -galactosidase catalyses the breakdown of lactose into glucose and galactose. This breakdown is potentially important to the alteration of metabolism and creating a state of senescence (Campisi and d'Adda di Fagagna, 2007, Gary and Kindell, 2005). However, senescent cells are also known to produce above basal levels of pro-inflammatory factors thus slowly causing damage to other surrounding cells (Salminen et al., 2008). Furthermore, the ability of a tissue to regenerate following damage is diminished if a large proportion of the cell population is senescent and therefore unable to proliferate or hindered in their ability to migrate.

Inflammation and the signalling pathways that facilitate it are important for the initiation of the regenerative response. However an overpowering pro-inflammatory response following an acute injury or persistence of chronic inflammation can cause further damage. A bacterial infection or imbalance in the body's microflora in favour of more pathogenic bacteria can often lead to the introduction of higher toxin concentrations, such as gram-negative bacterially derived lipopolysaccharide (LPS). LPS is known to bind to a number of receptors, including toll like receptors (TLR) such as TLR2 and TLR4 (Andreakos et al., 2004). Use of ultrapure LPS from bacterial species such as *E.coli* or *S. minnesota* ensures the specific activation of downstream responses from TLR4 activation alone. The main and most widely described signalling pathways associated with TLR4 signalling is that involving NF- κ B (Kawai and Akira, 2007). In addition TNF- α , a pro-inflammatory cytokine often released by cells as a consequence to damage or LPS/ TLR4 signalling, also has a

strong influence on NF- κ B signalling following its binding to the TNF receptor (TNFR). Alternatively, heightened NF- κ B activity can lead to increased TNF- α gene transcription. Heightened signalling via these toxins, cytokines and pathways can lead to both regulated cell death like apoptosis and or cell death classically defined as being unregulated, such as necrosis.

LPS stimulation of TLR4 is capable of activating both myeloid differentiation primary response gene 88 (MyD88) dependent and independent pathways. The MyD88 dependent pathway triggers NF- κ B activation and therefore pro-inflammatory gene expression (Kawai and Akira, 2007, Kawai et al., 1999). On the other hand signalling via the MyD88 independent pathway, via Toll-interleukin receptor-domain-containing adapter-inducing interferon- β (TRIF), results in the anti-viral and anti-inflammatory associated IRF3 activation (Tarassishin et al., 2013, Zeuner et al., 2016, Fitzgerald et al., 2003). Use of *S. minnesota* LPS to stimulate TLR4 signalling has been shown to initially induce higher levels of IRF3 activation but is then replaced by MyD88 dependent NF- κ B-p65 nuclear translocation after a longer period of stimulation (Zeuner et al., 2016). However, *E.coli* LPS has been shown to elevate NF- κ B-p65 nuclear translocation from the start of TLR4 stimulation (Zeuner et al., 2016). The differences in LPS mediated signalling have been hypothesised to be attributed to the type of membrane micro-domain binding within the same TLR-4 (Zeuner et al., 2016).

Activation of inflammatory signalling pathways including NF- κ B by stimulants such as LPS or acute stressors often potentiates the transcription and translation of cytokines such as TNF- α . TNF- α can also further enhance pro-inflammatory signalling, for example via NF- κ B in an autocrine and paracrine manner. For TNF- α to facilitate downstream signalling it must bind to either TNFR-1 or TNFR-2 (Chen and Goeddel, 2002). Binding to TNFR-1 leads to the assembly and recruitment of a protein complex containing TNF-R1-associated death domain (TRADD) protein, FAS-associated death domain (FADD) protein, the TNF receptor-associated factor 2 (TRAF2), and then finally the receptor-interacting protein kinase RIP1 (Hsu et al., 1996b, Hsu et al., 1996a). As with most signalling, a range of signalling pathways and effects can follow from this phenomenon. An apoptotic programme is initiated with the association of FADD with TRADD (Hsu et al., 1996b). On the other hand, binding of

TRAF2 and RIP to TRADD triggers the association of the I κ B kinase (IKK) complex and Jun N-terminal kinase (JNK), ultimately leading to NF- κ B-p65 translocation to the nucleus as described. The activation of NEMO, the major subunit of IKK also known as IKK γ , is suggested to be aided via the poly-ubiquitination of RIP-1 at Lys-377 and subsequent binding of the ubiquitin binding domain of NEMO (Ea et al., 2006).

An increase in proliferation and migration capacity of cells is believed to improve the efficiency of regeneration. Protection from senescence is thought to aid tissue regeneration by maintaining the number of cells, in particular stem cells, able to facilitate regeneration. If these factors can be regulated by paracrine activity, potentially capable of AFSC CM, then overall regenerative capabilities should also increase.

Results

Proliferation Assays

After identifying specific protein and miRNA components within the AF-CM it was important to show that AF-CM could also modify cell function. T24 and T72 AF-CM fractions were collected and they could therefore have very different effects on how cells operate because of the varying time-points at which they were collected. The effect of AF-CM was first tested on cellular proliferation. Cellular proliferation is known to be an important component within the regenerative process. Proliferation levels of the local stem cell population within or near to an area of damage can prove critical to the replacement of dead or damaged tissue (Brown et al., 2007, Collins et al., 2005, Zani et al., 2014). Increasing concentrations of AF-CM fractions, T24 and T72, were tested to see if they could increase the proliferation of an allogeneic MSC, in this case adipose derived MSCs (ADMSCs).

Varying concentrations of T24 AF-CM were first tested (Figure 4.1.A). The supplementing of ADMSC culture media with 2.5% T24 AF-CM significantly increased the relative cell number by 23.1% (from 1.10 ± 0.04 to 1.43 ± 0.04 ($n=6$, $p<0.001$)). Increasing the concentration of T24 AF-CM also led to a significant increase in relative cell number to 1.43 ± 0.03 ($n=6$, $p<0.001$) compared to the control. Finally, a concentration of 10% T24 AF-CM significantly increased relative cell numbers by 24% from the control to 1.44 ± 0.08 ($n=6$, $p<0.001$). However, no significant differences in relative cell number were found between the varying concentrations of T24 AF-CM treatment.

As T24 AF-CM was found to increase relative numbers of ADMSCs, the same concentrations of T72 AF-CM were tested to find out whether ADMSC proliferation was increased with treatment. A significant increase from the control, 1.51 ± 0.14 , to 2.13 ± 0.06 with 2.5% T72 AF-CM was found ($n=6$, $p<0.001$). 5% treatment of T72 AF-CM also led to a significant increase in relative cell number, by 26% to 2.04 ± 0.07 ($n=6$, $p<0.01$). Likewise, a treatment of 10% T72 AF-CM was seen to increase relative cell numbers by 26% to 2.03 ± 0.05 ($n=6$, $p<0.01$). A comparison of the T72 AF-CM concentrations showed no significant difference in relative ADMSC number.

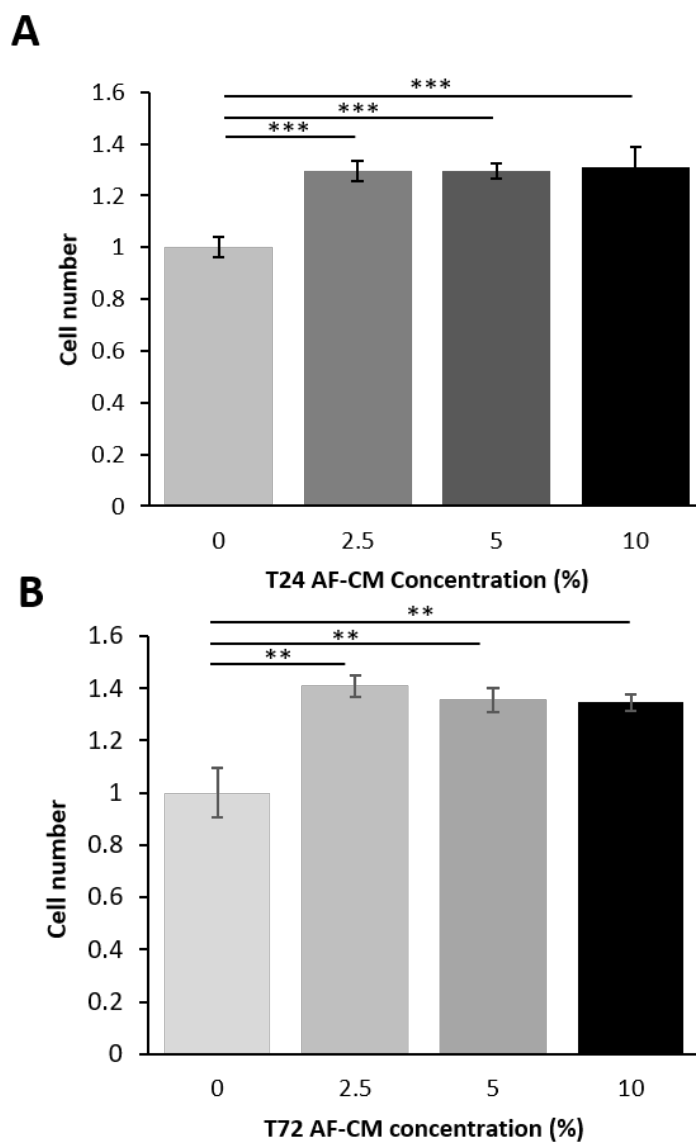


Figure 4.1: ADMSC proliferation over 72 hours following AF-CM treatment. (A) Relative number of ADMSCs with increasing concentrations of T24 AF-CM. (B) Relative number of ADMSCs with increasing concentrations of T72 AF-CM. Values are expressed as means \pm SEM (n=6). $p < 0.05$ (*), $p < 0.01$ (**) or $p < 0.001$ (***)

Migration Assays

The ability of cells to migrate is an important feature of the regeneration. AF-CM fractions were tested to determine whether they facilitated a change in artificial wound closure and therefore a change in migration behaviour of ADMSCs (Figure 4.2.A-B). Firstly increasing concentrations of T24 AF-CM were used to treat the ADMSCs following the creation of a wound (Figure 2C). Only the 2.5% concentration of T24 AF-CM increased the extent of wound closure. T24 AF-CM at 2.5% concentration increased relative wound closure by 25% from 2.68 ± 0.33 to 3.57 ± 0.14 ($n=6$, $p < 0.05$). On the other hand, concentrations of 1, 5 and 10% did not increase relative levels of wound closure significantly. ADMSCs were then treated with increasing concentrations of T72 AF-CM (Figure 4.2.D). After 9 hours of wound closure none of the tested concentrations of T72 AF-CM increased the level of relative wound closure from the control treated with 0% AF-CM.

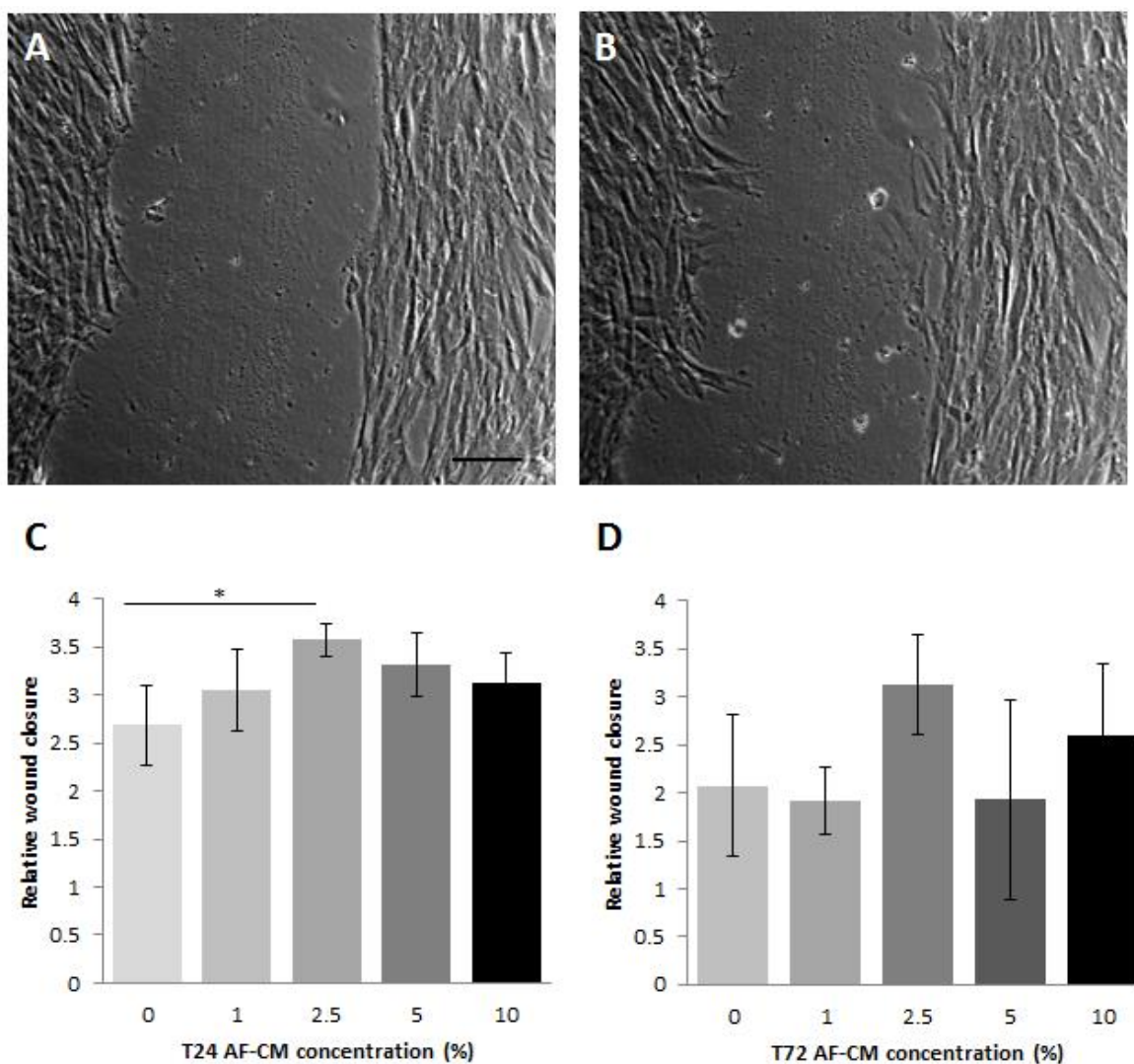


Figure 4.2: Closure of an artificial wound over 9 hours created within a confluent population of ADMSCs with AF-CM treatment. (A) Artificial wound at T=0 hours. **(B)** Artificial wound at T=9 hours. **(C)** Relative wound closure with increasing concentrations of T24 AF-CM. **(D)** Relative wound closure with increasing concentrations of T72 AF-CM. Scale bar representative of 100µm. Values are expressed as means ± SEM (n=4). p < 0.05 (*), p < 0.01 (**), or p < 0.001 (***)

Senescence Assays

Acute and high levels of stress such as a physical trauma can lead to necrosis. Chronic but high exposure to a stressor such as a chemical damage may lead to a more regulated type of cell death such as apoptosis. On the other hand, lower exposures to stress can cause cells to become senescent. Senescence, a form of permanent growth arrest, whereby cells will no longer divide will occur with age induced telomere shortening or is forced through stress exposure (Campisi and d'Adda di Fagagna, 2007). Treatment of cells with low but damaging levels of H_2O_2 can also induce senescence. IMR90 lung fibroblast cells are a cell line especially susceptible to damage and can be driven into senescence with $100\mu M H_2O_2$ (Debacq-Chainiaux et al., 2009). Furthermore, staining cells blue with X-gal (5-Bromo-4-Chloro-3-Indolyl β -D-Galactopyranoside) for the substrate β -galactosidase, found in lysosomes, permits the identification of senescent cells (Figure 3A)(Debacq-Chainiaux et al., 2009).

IMR90 cells were treated with varying concentrations of AF-CM before and after being stressed with $100\mu M H_2O_2$ in a bid to determine whether AF-CM protected the cells from senescence. Firstly, increasing concentrations of T24 AF-CM was tested to identify if it reduced the percentage of senescence within the IMR-90 population (Figure 4.3.B). The positive control group, treated only with PBS, showed a significant increase in the percentage of senescent cells by 24.6% following exposure to H_2O_2 from $67\pm 6.48\%$ to $88.75\pm 4.36\%$ ($n=4$, $P<0.01$). Although a stepwise decrease in the levels of senescence can be seen with increasing concentrations of T24 AF-CM, no significant decrease was seen with 2.5% and 5% concentrations of AF-CM treatment, $80.5\pm 3.80\%$ and $76.75\pm 1.11\%$ respectively. However, treatment of IMR-90 cells with 10% T24 AF-CM led to a significant decrease in the percentage of senescent cells compared to the stressed untreated cells by 17.5% to $73.25\pm 1.89\%$ ($n=4$, $p<0.05$). Furthermore, all concentrations of T24 AF-CM led to levels of senescence non-significantly different to that of the non-stressed control.

The protection from senescence afforded by T24 AF-CM was compared to that of the T72 fraction and (Figure 4.3.C). The positive stress control also increased the level of senescence as seen previously from $21.08\pm 1.75\%$ to $85.58\pm 0.61\%$ ($n=4$, $P<0.001$). The senescent levels of T24 and T72

fraction treated cells were also significantly increased from the non-stress control to $50.75 \pm 0.79\%$ ($n=4$, $p<0.001$) and $42.92 \pm 1.64\%$ ($n=4$, $p<0.001$), respectively. However, both the T24 and T72 AF-CM fraction treatments led to a reduction in the number of senescent cells, although this time insignificant. In addition, the T72 fraction led to a significantly reduced level of senescence compared to the T24 fraction ($n=4$, $p<0.01$). Further to this result, a mix of T24 and T72 (T24/T72) was compared to the individual fractions (Figure 4.3.D). T24/T72 treatment further significantly reduced the level of senescence from T24 AF-CM by 52.12% compared to the T72 fraction which showed on average 33.6% less senescence; $19.83 \pm 4.09\%$, $41.42 \pm 4.32\%$ and $27.5 \pm 2.79\%$ respectively ($n=4$, $p<0.01$).

Following the isolation of AF-EVs from the T24 AF-CM, AF-EV was also tested and compared to the AF-CM in its ability to alter the levels of senescence (Figure 4.3.E). All stressed groups of cells such as the positive control, AF-CM and AF-EV treated cells showed significantly higher levels of senescence to the non-stressed control which had basal levels of $0.83 \pm 0.27\%$ senescence, at $35.50 \pm 1.99\%$, $6.17 \pm 1.06\%$ and $7.58 \pm 6.94\%$ respectively ($n=4$, $p<0.001$; $p<0.05$; $p<0.01$). As shown previously the whole AF-CM significantly reduced the level of senescent cells from the positive control, by 82.6% ($n=4$, $p<0.001$). Additionally, the AF-EV fraction also significantly reduced the percentage of senescent cells, by 78.6% ($n=4$, $p<0.001$). On the other hand, comparison between the AF-CM and AF-EV treatments showed no significant difference in senescence levels.

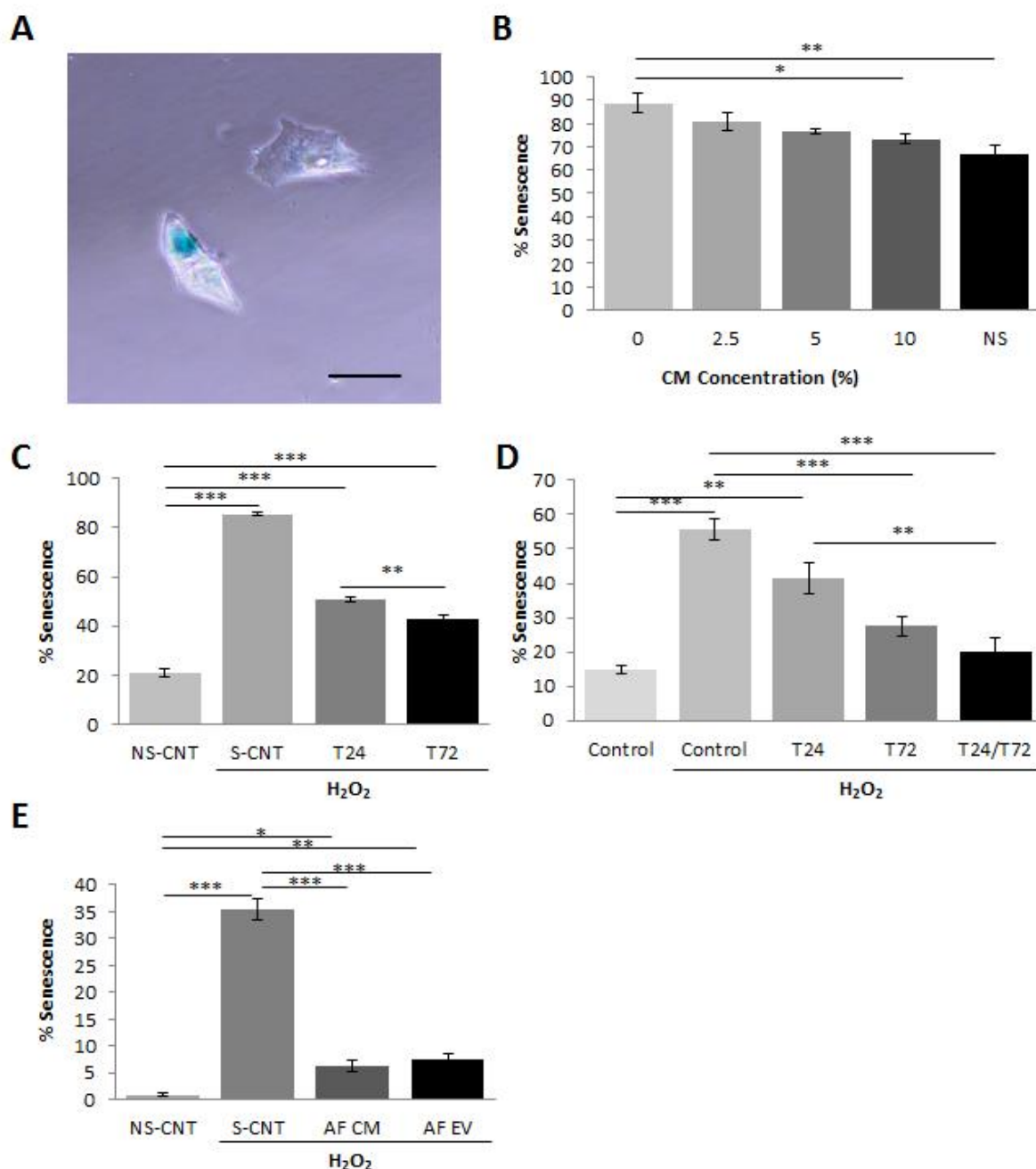


Figure 4.3: H₂O₂ induced senescence within a population of IMR-90 lung fibroblasts. (A) A non-senescent and senescent (blue) IMR-90 cell stained for β -galactosidase. **(B)** Percentage of senescent cells following treatment with increasing concentrations of T24 AF-CM. **(C)** Comparison in protection against senescence between 10% T24 and T72 AF-CM compared to a non-stressed vehicle (PBS) treated control without AF-CM or 100 μ M H₂O₂ (NS-CNT) and a vehicle treated (PBS) H₂O₂ stressed control without AF-CM (S-CNT). **(D)** Comparison in protection against senescence between 10% T24, T72 AF-CM and a 1:1 T24/T72 AF-CM mix (T24/T72) compared to a non-stressed control (NS-CNT)

and a stressed control (S-CNT). (E) Comparison in protection against senescence between AF-CM and its AF-EV fraction compared to a non-stressed control (NS-CNT) and a stressed control (S-CNT). Scale bar representative of 20 μ m. Values are expressed as means \pm SEM (n=4). p < 0.05 (*), p < 0.01 (**), or p < 0.001 (***)

NF- κ B Nuclear Translocation and Transcription

As previously discussed, the level and type of inflammatory response is important not only in promoting and aiding regeneration but can also cause further damage if uncontrolled. Uncontrolled pro-inflammation usually occurs due to widespread necrosis and cytokine release both from the damaged or dead cells but also from infiltrating macrophages. Such cytokines include TNF- α , a strong stimulus of the NF- κ B pathway subsequent to it binding to the TNF- α receptor (Ea et al., 2006). NF- κ B is a key regulator of inflammatory signalling along with its major sub-unit p65. Phosphorylation of I κ B and the revealing of the nuclear translocation site on NF- κ B leading to the subsequent nuclear translocation are known to facilitate the up-regulation of pro-inflammatory genes and therefore a downstream pro-inflammatory cell response (Ghosh and Dass, 2016). A reduction in NF- κ B-p65 nuclear translocation or a reduction in NF- κ B protein is known to reduce the level of this pro-inflammatory response.

MSCs and their paracrine factors have been shown to have anti-inflammatory properties. Therefore we determined whether the AF-CM had anti-inflammatory properties (Zhang et al., 2013, Liu et al., 2014, Cho et al., 2014, Lo Sicco et al., 2017). Treatment of U251 cells with 10ng/ml TNF- α was used to induce p65 nuclear translocation (Figure 4.4.A-D). As seen in the immunofluorescent images (Figure 4.4.A), control cells without inflammatory stimulation had only cytoplasmic p65. Upon the addition of the strong pro-inflammatory stimulus, cells had a high level of nuclear p65 (Figure 4.4.B). The nuclear p65 stain intensity was shown to be 76.7% higher in the positive control compared to the unstimulated control, 2.28 ± 0.02 and 1.29 ± 0.11 respectively ($n=5$, $p < 0.001$). Treatment of cells with 1% AF-CM before and during inflammatory stimulation led to a significant decrease in nuclear p65 intensity from the positive control to 1.31 ± 0.11 (figure 4C-D; $n=5$, $p < 0.001$). The level of nuclear p65 intensity between the non-stimulated control and that of the AF-CM treated (TNF- α stimulated) cells were not significantly different.

U251 NF- κ B reporter cells which had been previously transfected produce cumulative levels of luciferase and short lasting levels of GFP following NF- κ B gene expression. Lysates of treated cells

were used to quantitatively determine luciferase levels within the population which is therefore indicative of the NF- κ B activity. U251 reporter cells were utilised to show a significant increase in NF- κ B dependent luciferase activity following TNF- α stimulation to 47.26 ± 2.02 times that of the unstimulated control, 1 ± 0.67 (Figure 4E; $n=3$, $p < 0.001$). The level of luciferase activity was also measured for AF-CM treatment alone and showed no significant difference between that and the non-stimulated control. Treatment with T24 AF-CM before and during TNF- α stimulation led to a significant decrease in NF- κ B dependent luciferase activity to 40.00 ± 1.63 , a decrease of 15.4% from the positive control ($n=4$, $p < 0.05$). This was also decreased with T72 and T24/T72 mix treatment, 38.25 ± 2.21 and 36.22 ± 1.84 ($n=4$, $p < 0.01$). However, luciferase activity of AF-CM fraction treated cells following TNF- α stimulation remained significantly higher than that of the non-stimulated control ($n=4$, $p < 0.001$). Finally, we found that without any TNF- α stimulation that T72 AF-CM treatment alone, unlike the T24 or T24/T72 mix, led to a small but significant increase in luciferase expression 4.72 ± 0.86 ($n=4$, $p < 0.05$).

In addition, U251 reporter cells were stimulated with *S. minnesota* LPS for 24 hours (Figure 4.4.F). Ultrapure LPS is known to stimulate only TLR-4, unlike TNF- α (Zeuner et al., 2016). *S. minnesota* LPS stimulation also leads to an increase in NF- κ B activity as seen with the positive control versus the non-stimulated control, 6.84 ± 0.49 and 1 ± 0.36 respectively ($n=4$, $p < 0.001$). A step-wise decrease in NF- κ B dependent luciferase was seen with T24, T72 and T24/T72 treatment although no significant reduction was seen with the T24 treatment; 6.45 ± 0.27 , 5.18 ± 0.26 and 3.87 ± 0.20 . Furthermore, T24/T72 treatment led to a significantly lower level of luciferase compared to that of U251 cells treated with T24 AF-CM ($n=4$, $p < 0.001$).

The AF-EV fraction was compared to whole AF-CM (Figure 4.5.). AF-EV was shown to be significantly more potent at reducing the level of p65 nuclear translocation compared to the whole AF-CM ($n=5$, $P < 0.001$). AF-EV showed 38.5% less p65 nuclear translocation compared to AF-CM, 1.46 ± 0.16 and 2.39 ± 0.12 respectively. However, comparison between the whole and AF-EV fraction looking at NF- κ B dependent luciferase activity showed no significant difference between the two treatments.

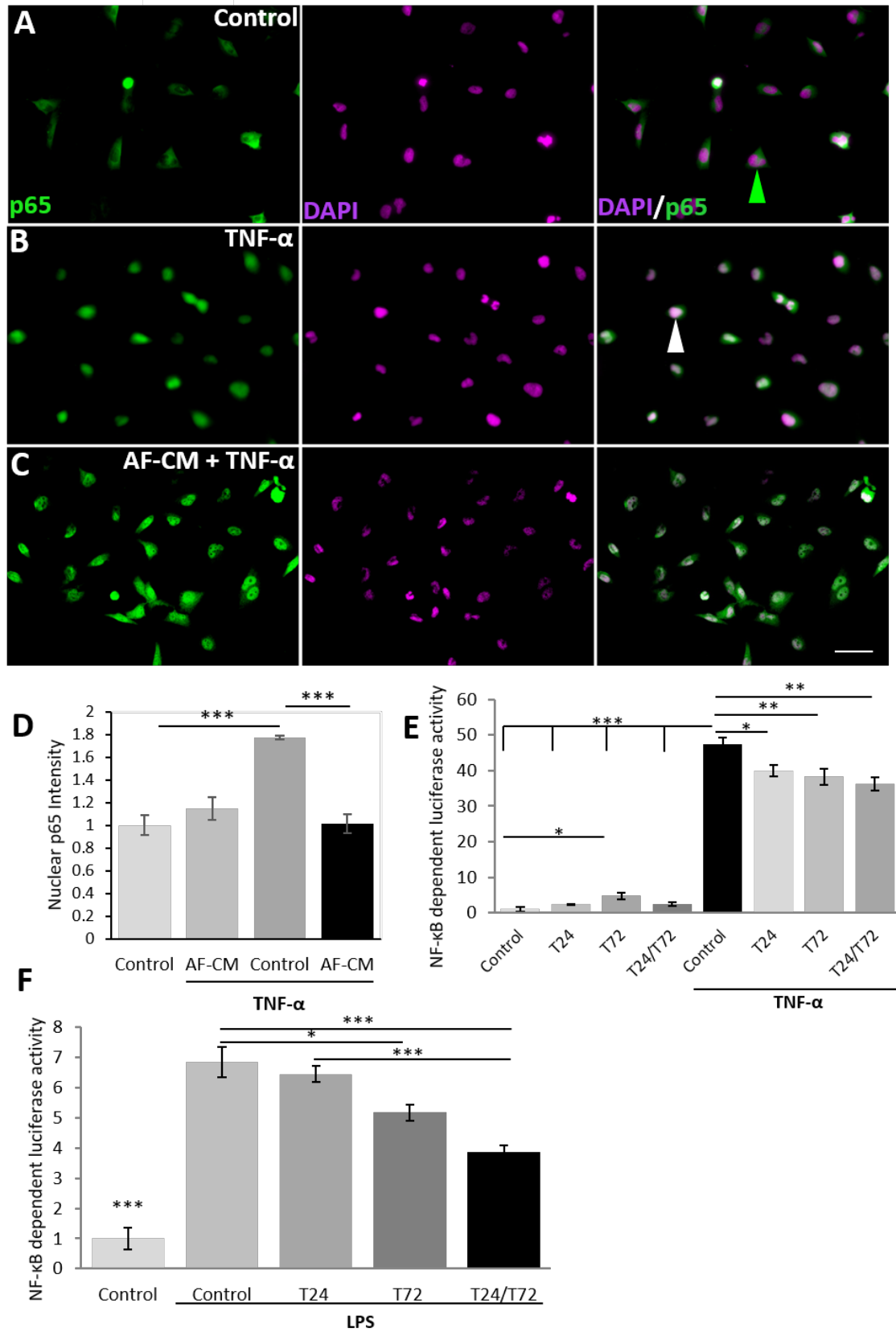


Figure 4.4

Figure 4.4: Modulation of NF- κ B activity by AF-CM. (A-C) Malignant U251 Glioblastoma cells stimulated with 10ng/ml TNF- α and treated with 1% AF-CM, stained for NF- κ B-p65 (green) and DAPI (blue) immunofluorescence (n=4). (D) Nuclear translocation of p65 analysed by mean nuclear p65 staining intensity. (E) Lentiviral transfected U251-NF- κ B- GFP-Luciferase cells were used to quantitatively assess the ability of AF-CM collected at T24 and T72 to modulate NF- κ B signalling following 10ng/ml TNF- α stimulation over 24 hours. (F) Ability of AF-CM collected at T24 and T72 to alter NF- κ B dependent luciferase activity was further assessed following *S. Minnesota* LPS stimulation of U251 cells. Images were taken at a 20x Magnification. Green and white arrows representative of weak and strong nuclear localisation respectively. Scale bar representative of 50 μ m. Values are expressed as means \pm SEM (n=4). p < 0.05 (*), p < 0.01 (**) or p < 0.001 (***)

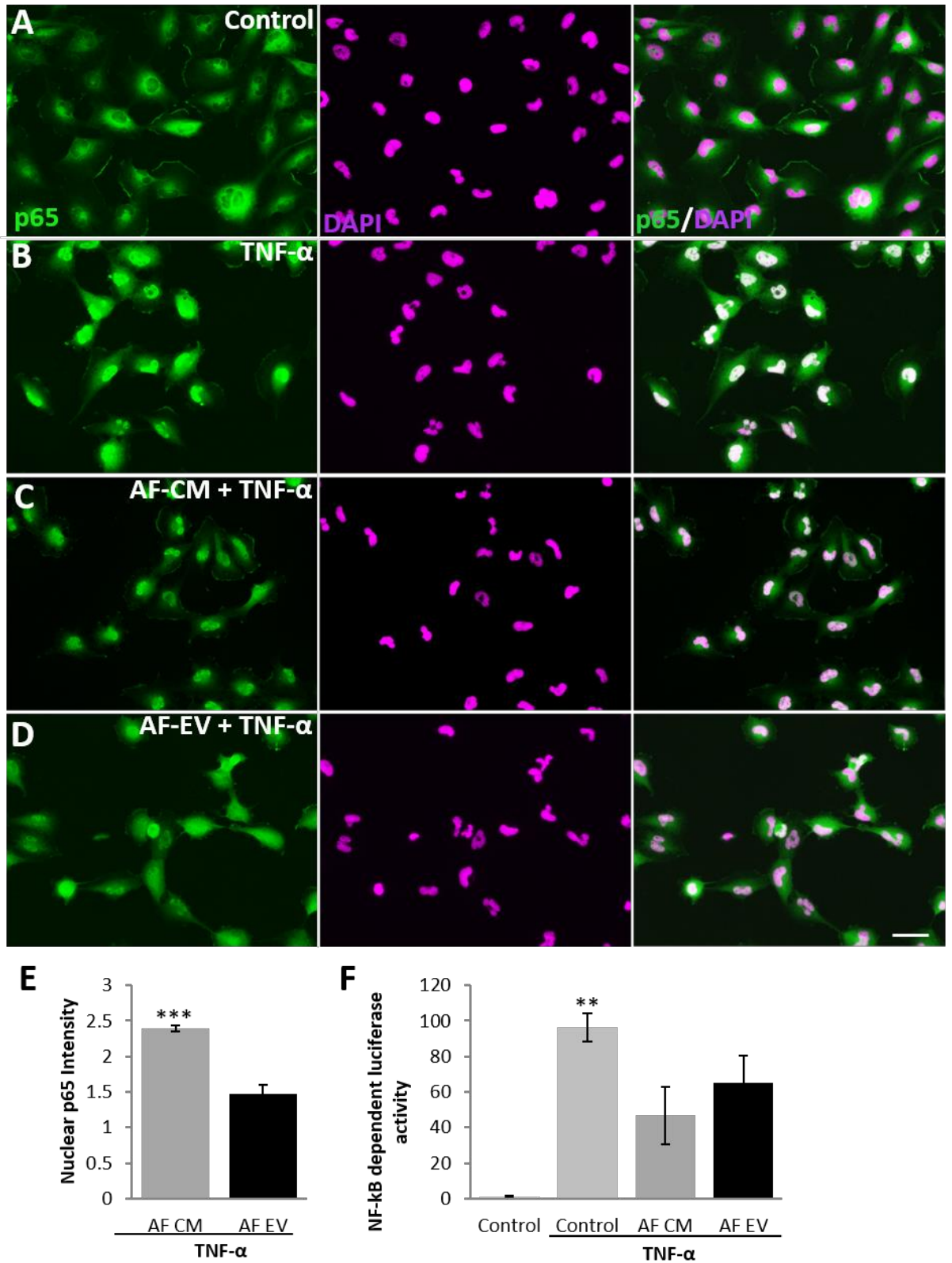


Figure 4.5

Figure 4.5: Comparison of AF-CM and AF-EV effects of NF- κ B activity. (A-D) Malignant U251 Glioblastoma cells stimulated with 10ng/ml TNF- α and treated with AF-CM or AF-EV, stained for NF- κ B-p65 (green) and DAPI (blue) immunofluorescence (n=4). (E) Comparison between AF-CM and AF-EV treated U251 cell nuclear translocation of p65 analysed by mean nuclear p65 staining intensity. (F) Lentiviral transfected U251-NF- κ B- GFP-Luciferase cells were used to quantitatively assess the ability of AF-CM and AF-EV to modulate NF- κ B signalling following 10ng/ml TNF- α stimulation over 24 hours. Images were taken at a 20x Magnification. Green and white arrows representative of weak and strong nuclear localisation respectively. Scale bar representative of 50 μ m. Values are expressed as means \pm SEM (n=4). $p < 0.05$ (*), $p < 0.01$ (**) or $p < 0.001$ (***)

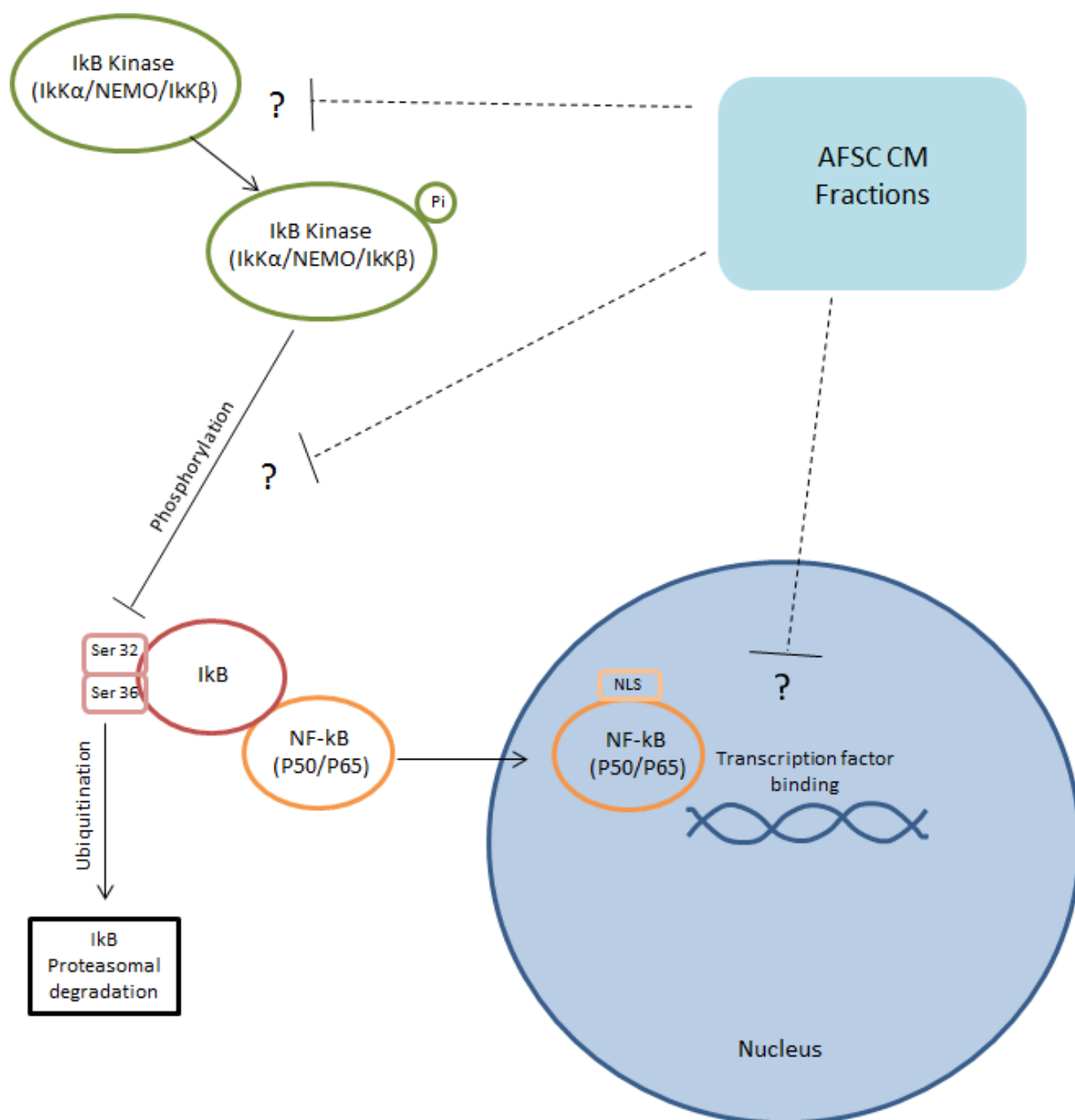


Figure 4.6: Potential sites of action within the NF-κB pathway that AF-CM may be acting. AF-CM may prevent the phosphorylation and therefore activation of IκB Kinase by effecting any one or a multitude of IκB kinases subunits; IκKα, IκKβ and IκKγ (commonly known as NEMO). Active IκB kinase phosphorylates IκB at amino acid residues Serine 32 and 36 thereby inhibiting its binding to NF-κB. Subsequently, IκB is poly-ubiquitinated and therefore destined for proteasomal degradation. The nuclear localisation site (NLS) of NF-κB is uncovered following its split from IκB and NF-κB is therefore transported into the nucleus to act as a transcription factor. The ability of AF-CM to inhibit the phosphorylation of IκB directly or indirectly would facilitate the binding of NF-κB to IκB and thus

prevent NF- κ B nuclear translocation. AF-CM could also inhibit NF- κ B activity by directly or indirectly preventing NF- κ B gene transcription, translation and/or post-translational modification.

AF-CM Treatment of Polarised THP-1 Macrophages

To identify whether AF-CM had the ability to alter the inflammatory state of inflammatory cells, THP-1 monocytes were differentiated into macrophages and polarised towards a pro-inflammatory M1 status and treated with AF-CM (Figure 4.7.). CD80, a molecule found on the surface of macrophages and known to aid the facilitation of T cell activation, is increased in macrophages driven towards and M1 pro-inflammatory state (Peach et al., 1995, Genin et al., 2015). The level of THP-1 cells was therefore examined. Levels of CD80⁺ cells did not increase upon CM treatment of M0 cells or upon M2 polarisation compared to an M0 control. On the other hand, polarisation towards an M1 like state led to a significant increase in CD80⁺ with or without AF-CM by at least 78.0% (n=3, p<0.001). However, although AF-CM treatment of M0 cells before and during polarisation had not led to a change in CD80⁺ cells, AF-CM treatment only during polarisation significantly reduced CD80⁺ cell levels by 11.1% (n=3, p<0.05).

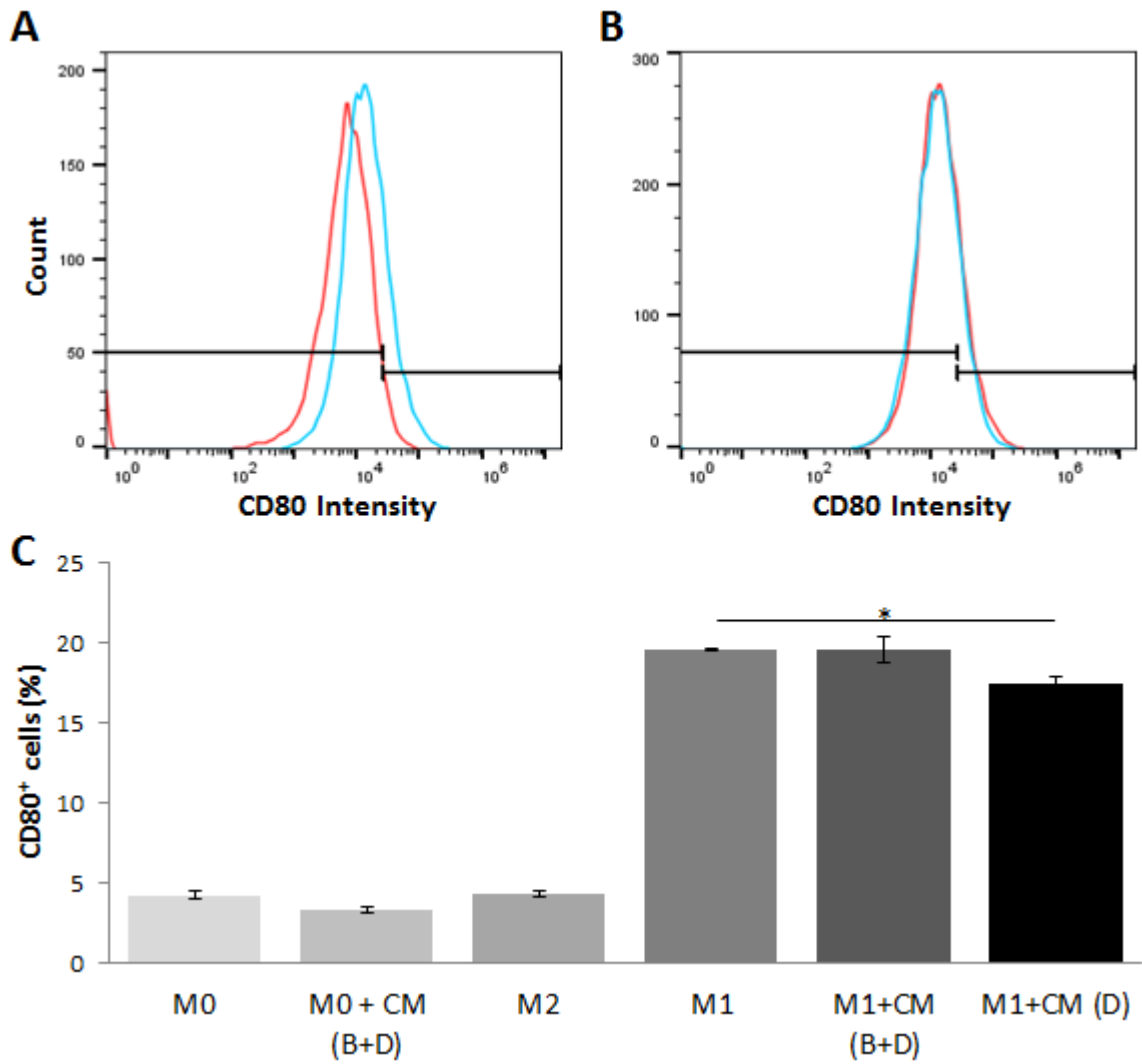


Figure 4.7: AF-CM treatment of pro-inflammatory polarised THP-1 macrophages. THP-1 count vs CD80 intensity for (A) M0 THP-1 cells (red) vs M1 THP-1 cells (blue), (B) M1 THP-1 cells (red) vs M1 THP-1 cells treated with AF-CM (CM) only during (D) polarisation. (C) % of CD80 expressing THP-1 cells after differentiation to M0 and subsequent polarisation towards M2 and M1 states with or without AF-CM treatment either 24 hours before and during polarisation (B+D) or just during (D). Values are expressed as means \pm SEM (n=4). $p < 0.05$ (*), $p < 0.01$ (**), $p < 0.001$ (***)

Cellular Uptake of AF-EVs

Many potential mechanisms have been identified for the interaction of EVs with their target cells (Mathivanan et al., 2010, Urbanelli et al., 2013). Firstly EV membrane bound receptors may simply bind to ligands on the surface of the target cell leading to the activation of downstream signalling pathways and vice versa without any EV uptake. On the other hand, cell membranes could fuse with that of the EV allowing EV cargo to be released into the cells cytoplasm. Additionally an endocytic process where the EV is enveloped by the target cell membrane and internalised could be facilitated through mechanisms such as phagocytosis, pinocytosis and receptor-mediated endocytosis. Fluorescent dyes such as PKH that bind to the lipid membrane can be used to stain EVs (Balbi et al.). Once stained, EVs up taken by a cell and their location once target cell interaction can be determined.

AF-EVs were therefore stained with PKH26, a long lasting red fluorescent dye suitable for EV tracking. U251 cells were treated with PKH26 stained EVs (Figure 4.8.). Images of U251 cells after treatment showed that AF-EVs had been taken up into the cell cytoplasm (Figure 4.8.B-C). The uptake of stained AF-EVs was then analysed in single cells by examining PKH26 intensity throughout the cell (Figure 4.8.D). Control cell membranes were stained with PKH26 without AF-EV treatment and showed that the cells had an average relative PKH26 fluorescent intensity of 74.90 ± 8.35 . Staining the target cell membrane directly as a positive control led to a significantly higher fluorescent intensity to that of cells treated with PKH26 stained AF-EVs or NaAzide and PKH26 AF-EVs, 11.68 ± 1.04 and 5.56 ± 0.95 respectively ($n=4$, $p < 0.001$). Cells were treated with NaAzide, a mitochondrial ATP production inhibitor, to reduce the level of any actively regulated endocytic like pathways (Harvey et al., 1999, Schwoebel et al., 2002). Comparison of the PKH26 relative intensity within the cells using ANOVA statistical analysis with the control cells did not show any significant reduction compared to AF-EV treated cells without NaAzide. On the other hand, a statistical T-test comparing just the PKH26 AF-EV treated cells and cells treated with NaAzide and the PKH26 stained AF-EV did show a significant reduction in relative fluorescent intensity ($n=4$, $P < 0.01$).

Flow cytometric analysis was carried out to identify the percentage of cells taking up the PKH26 stained AF-EVs in the population of U251 cells. Cells were treated with PBS that had been introduced to PKH26 stain and ultra-centrifuged as carried out with the AF-EVs, thus acting as a negative control. After treatment with the negative control $1.68 \pm 0.95\%$ of U251 cells proved positive for PKH26 staining. The percentage of cells proving positive for PKH26 were significantly higher in the positive control where cells were stained directly beforehand with PKH26, $99.6 \pm 0.15\%$ ($n=3$, $p < 0.001$). Both treatments with PKH26 stained AF-EVs with and without NaAzide showed a significant increase in the percentage of cells positive for PKH26 compared to the negative control, $79.93 \pm 0.15\%$ without NaAzide and $77.6 \pm 1.92\%$ with NaAzide ($n=4$, $p < 0.001$). On the other hand, both AF-EV treatment groups showed a significant reduction in PKH26 stained cells compared to the positive control ($n=4$, $p < 0.001$). However, there was no significant difference in the level of stained cells between that of the AF-EV treated cells and those treated with both NaAzide and the AF-EVs.

Overall results showed that AF-CM and its resulting AF-EV modulated a number of cellular properties both in stem cells and non-stem cells. Ability of ADMSCs to proliferate was increased by all concentrations of AF-CM tested. Migration capacity of ADMSCs was increased by the T24 AF-CM, although only at the lower 2.5% concentration. Although the T72 AF-CM fraction proved more potent, both T24 and T72 AF-CM fractions protected IMR-90 cells from H_2O_2 induced senescence. Additionally, the AF-EV fraction similarly showed protective properties against senescence. Fractions of AF-CM were also shown to reduce NF- κ B activity in U251 cells. Finally the uptake of AF-EVs in U251 cells was proven and shown to reduce following treatment of cells with a known mitochondrial toxin, NaAzide.

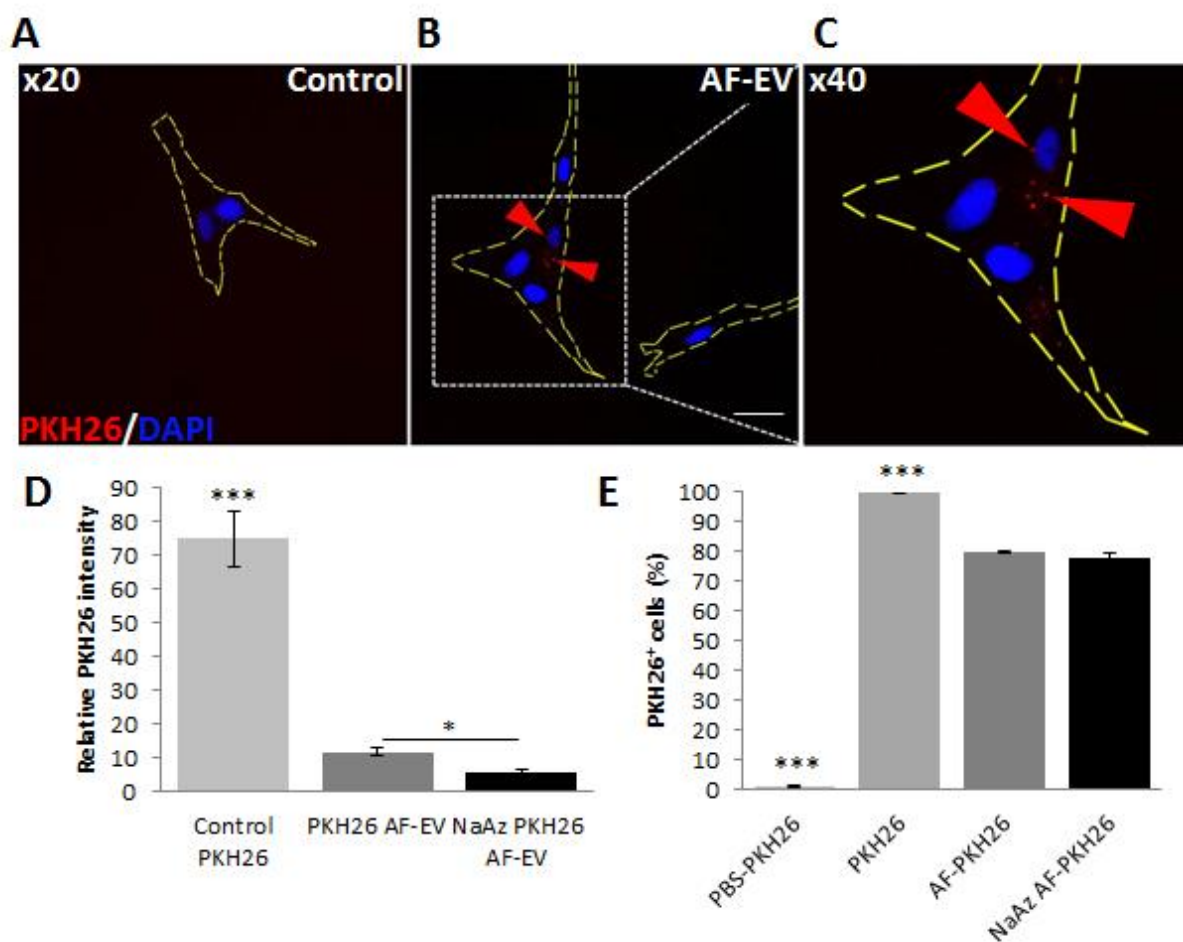


Figure 4.8: Uptake of PKH26 stained AF-EVs by U251 cells. (A-C) Uptake of PKH26⁺ AF-EVs (red) by U251 cells (outlined in yellow) as indicated with red arrows. (D) The relative uptake of PKH26 stained AF-EVs per cell compared to cells treated with sodium azide (NaAz) to inhibit ATP production. (E) The percentage of U251 cells within a population to take up PKH26 stained AF-EVs compared to cells treated with NaAz. Scale bar is representative of 20 μ m. Values are expressed as means \pm SEM (n=4). $p < 0.05$ (*), $p < 0.01$ (**) or $p < 0.001$ (***).

Discussion

Numerous cellular properties contribute to the outcome of a diseased and damaged tissue and whether it regenerates. Often upon damage a wave of pro-inflammatory cytokines and molecules are released from the damaged area (Karalaki et al., 2009). The pro-inflammatory response triggers the initiation of a regenerative programme. Proliferation, migration, senescence and inflammatory status play a large role in the regeneration process.

AF-CM Increases Allogeneic Stem Cell Proliferation Capacity

The first phase of regeneration usually consists of the proliferation of the local stem cell pool. In order to maintain the native stem cell population of the tissue, they must undergo asymmetric division, thus producing daughter cells for stem cell pool replenishment but also another for lost/damaged cell replacement. Treatment of ADMSCs with AF-CM showed a marked increase in MSC proliferation (Figure 4.1.A-B). Both the T24 and T72 fraction of AF-CM proved to be effective at increasing the proliferation of the ADMSCs by more than 20%. Interestingly, all of the tested concentrations of AF-CM led to a significant increase in cell number and the lowest concentration tested, 2.5%, did not significantly differ in its effect on cell number to the highest concentration, 10%. This suggests that the AF-CM is potent enough at low concentrations to induce an increase in MSC numbers and that this effect seems to plateau at this low concentration. This may be explained by a complete saturation of the signalling molecules required for proliferation. The results also suggest that no negative feedback mechanisms have been initiated by the higher concentrations of AF-CM therefore preventing a decrease in proliferation. Furthermore, because AF-CM had led to an increase in cell number within the ADMSC population, an allogeneic MSC population, it would be expected to also improve the proliferation of other allogeneic stem cells found within the location of damaged tissue. Increasing the proliferation of the local stem cell population would create a higher capacity for cell replacement improving regenerative efficiency.

AF-CM Improves the Ability of ADMSCs to Close an Artificial Wound

Following or prior to the proliferation of the local stem cell population, the ability of an MSC to reach its target destination so that it may aid regeneration is dependent on its ability to migrate. Application of an artificial wound closure assay enabled the ability of ADMSCs to migrate into an unoccupied and damaged area within the cell population to be measured (Figure 4.2.A-D). Results showed that the 2.5% concentration of T24 AF-CM was optimum for increasing wound closure. None of the other concentrations of AF-CM led to a significant increase in wound closure. The difference in effects between the different concentrations may arise due to homeostatic control mechanisms in place within the cell. Too much AF-CM may initiate negative feedback loops in signalling required for migration therefore reducing migration. Too little AF-CM is simply hypothesised to be not enough to provide a significant effect. On the other hand, treatment of ADMSCs with T72 AF-CM did not lead to any significant increases in relative wound closure. This suggests that the T72 fraction contains lower concentrations of migration capacity enhancing cargo to the T24 fraction of AF-CM. However, looking at the pattern of results produced by the T72 treatment, the 2.5% promoted the largest mean wound closure. All other concentrations of T72 AF-CM showed noticeably comparable levels of wound closure to that of the control. Higher levels may have initiated negative feedback signalling pathways thus leading to lower levels of migration in comparison to the 2.5% treatment. Differences in potency towards enhancing migration between the two fractions may stem from stress levels within the AFSCs during the CM collection process. Upon culturing cells to a higher confluency it can be noted that cells become more static. The longer exposure of the AFSCs to being at a high density during CM collection may therefore have initiated a response within the cell to inhibit migration. The secretome of the AFSCs at this stage is therefore expected to mirror that of the mother cells state and thus does not promote migration. In conclusion, the T24 AF-CM provided an increase in cellular migration unlike the T72 fraction. Many pathways can affect the outcome of migration such as the type of migration and/ or speed of migration. Actin remodelling is arguable the most important of these mechanisms potentiating migration. The extent of actin filament extension, recycling and branching promotes the polarisation of the cells lamellipodia or bleb formation thus directing the cell

(Otto et al., 2011). The degree of actin re-organisation can be partly attributed to the type and level of chemokine reception. Activation of Src kinase via growth factor binding to its receptor such as that of epidermal growth factor or integrin – integrin receptor binding would activate Src kinase thus phosphorylating FAK. Consequentially, Calpain mediated disassembly of the focal adhesion complex is activated therefore enabling migration (Westhoff et al., 2004). The activation of Src/ FAK signalling is also known, although not well understood, to promote cell survival (Westhoff et al., 2004, Park et al., 2004). If the AF-CM AF-EVs contain growth factors and or integrins, it may be stimulating Src kinase and FAK dependent signalling therefore promoting migration but also acting to protecting cells from apoptosis.

Protection from Senescence Following AF-CM or AF-EV Treatment

The ability of a cell to both proliferate and migrate can be severely compromised or completely inhibited if a cell becomes senescent. As discussed, in the event of ageing or cellular stress a cell may be driven into a senescent state. Therefore protection from senescence would be hypothesised to both maintain proliferation and migration of the local stem cell population or stromal cells. Unlike, the previous proliferation and migration assays, T24 AF-CM was shown to be more effective at reducing senescence at the higher concentration tested, 10% (Figure 4.3.B). It was also noted that in comparison to the T24 fraction the T72 fraction protected IMR-90 cells more so from senescence (Figure 3C). This may be because AFSCs used to collect the AF-CM at T72 had simply been exposed to stress for longer than that collected at T24. The AFSCs at T72 may therefore be producing more paracrine factors aimed at protecting from the imminent stress as opposed to that collected at T24 warning of a stress to potentially come. However, it was also found that the AF-CM was able to modulate NF- κ B activity and therefore has the potential to reduce inflammation. Cells in a senescent state are known to produce above basal levels of pro-inflammatory factors (Rodrigues et al., 2017). It is therefore suggested that the AF-CM is reducing inflammation via the dampening of NF- κ B signalling in the IMR-90 cells following their stress exposure. When the T24 and T72 were mixed they provided even more protection from senescence (Figure 4.3.D). Although not significantly different

to the T72 fraction protection, the result reflects the differences in T24 and T72 constituent make-up. In unison the T24 and T72 fractions seem to work synergistically. In addition, the AF-EV fraction also provided a protective effect and did not significantly differ from the whole AF-CM (Figure 4.3.E). This suggests that the AF-EV contains most if not all of the capacity to protect IMR-90 cells from senescence.

The combined results from the proliferation, migration and senescence assays suggest that a multitude of paracrine effectors may provide a role in controlling these processes. Much of the signalling which leads to increased migration and proliferation is also involved in driving the cell towards a senescent state when signalling activity is increased. Therefore, it could be hypothesised that to drive both an increase in proliferation and migration whilst protecting from senescence, the signalling in differing pathways to those common to all three features may also be modified by the AF-CM.

AF-CM and AF-EV Treatment Reduces NF- κ B Activity

One of the main signalling molecules important in regulating the three previously described cell characteristics is NF- κ B. Furthermore, NF- κ B serves as an important hub protein controlling the inflammatory status of a cell and therefore subsequent to this, that of others (Figure 4.6.). The tightly controlled homeostatic regulation of NF- κ B is very important in keeping not only inflammation in check but also the level of cellular proliferation, migration and senescence.

Significantly the AF-CM was shown to reduce the level of NF- κ B-p65 nuclear translocation when cells were stimulated with TNF- α (Figure 4.4.A-D). Signalling involving the p65 subunit of NF- κ B, also known as RelA, is controlled through the NF- κ B canonical pathway as described previously (Siebenlist et al., 1994). Reduced p65 nuclear translocation would correspond to an increased level of I κ B α binding. The increase in binding and therefore p65 inhibition may be induced at several different levels within the canonical pathway (Figure 4.6.). The first would be that the AF-CM decreased the level of I κ B phosphorylation by the inhibitor of I κ B, I κ B kinase (IKK) and its main subdomain NEMO at serine 32 and 36 thus leading to more p65 nuclear translocation domain

coverage by I κ B α . Secondly, AF-CM may cause a decrease in p65 transcription and/or translation. However, many more regulatory processes such as ubiquitination and acetylation of NF- κ B and its subunits which control and modify its signalling function may be affected.

Further to the reduced p65 nuclear translocation, NF- κ B dependent luciferase expression subsequent to TNF- α stimulation, was also reduced with AF-CM treatment (Figure 4.4.E). This suggests that AF-CM has a direct effect on NF- κ B gene expression. As explained, a reduced level of NF- κ B subunit gene expression could lead to reduced levels of p65 and therefore explain at least in part why reduced p65 nuclear translocation was seen with AF-CM treatment. Less p65 would enable easier sequestration by I κ B. Comparison between the two fractions, T24 and T72, as well as treatment with a T24/T72 mix showed no significant differences in luciferase expression. However, a step-wise decrease in luciferase expression can be seen with the T24, T72 and T24/T72 mix respectively. Additionally, the effect of stimulation of U251 cells with *S. minnesota* LPS to increase NF- κ B dependent luciferase expression levels was seen to decrease in the same manner with the various fractions (Figure 4.4.F). Conversely, T24 AF-CM did not significantly reduce luciferase levels unlike the T72 fraction and T24/T72 mix. Although not significant in this case, the mix of the two fractions is seen to be more potent at reducing NF- κ B activity. This suggests that the T24 and T72 fraction have differing components and when mixed are able to act on independent pathways or levels within the same pathway to bring about a more desirable effect. For example it has been shown that hypoxia induced release of factors such as HIF have an anti-senescent effect through mechanisms such as TWIST activated E2A-p21 signalling downregulation (Tsai et al., 2011). Downregulation of p21 is known to reduce senescence and therefore it's associated inflammation via NF- κ B (Tsai et al., 2011, Yao et al., 2008). Increased exposure to hypoxia as would be expected from the cells used to collect T72 AF-CM would therefore be expected to contain more hypoxia related factors such as HIF compared to the T24 fraction. On the other hand, the T24 fraction may contain factors that reduce NF- κ B signalling that are not strictly associated with hypoxia. Therefore a mix of the two fractions would provide a number of different mechanisms of action to reduce inflammation, more so than that of any single fraction alone. The ability to reduce the LPS and TNF- α stimulated NF- κ B escalation suggests that the

AF-CM is acting further down from the receptor level in the signalling pathway where both TLR-4 and TNFR share signalling proteins. Overlap between the two pathways is most evident from IKK activation and therefore a change in NF- κ B signalling is suggested to be altered from here to the genetic level of NF- κ B. Furthermore, AF-CM may have the potential to reduce NF- κ B signalling through a reduction in CD80 expression. Reduced CD80 expression in M1 pro-inflammatory macrophages would reduce their ability to bind to CD28 thus activating downstream NF- κ B signalling in other inflammatory cells which would otherwise potentiate the inflammatory response (Schulze-Luehrmann and Ghosh, 2006, Peach et al., 1995).

Additionally, when the AF-CM was compared to its AF-EV fraction in their ability to reduce p65 nuclear translocation, AF-EV was shown to be more potent (Figure 4.5.A-E). On the other hand, the AF-EV was shown to be comparable to the whole AF-CM when looking at NF- κ B dependent luciferase levels. These results suggest that the AF-EV cargo may provide the majority of the NF- κ B activity modulation.

Further analysis of the NF- κ B dependent luciferase expression shows that the inhibition of NF- κ B gene expression by AF-CM is not sufficient to reduce it to levels comparable to that of non-stimulated cells. This may explain why the AF-CM is also able to increase the level of proliferation and migration whilst protecting from senescence and reducing NF- κ B signalling in a simulated stress condition. It can be hypothesised that AF-CM is able to reduce levels of NF- κ B activity, decreasing potentially damaging pro-inflammatory signalling and subsequent senescence, but also not too low which could have an inhibitory effect on proliferation and migration levels (Kaltschmidt et al., 1999). It could therefore be concluded that AF-CM and the AF-EV fraction help to bring the homeostatic regulation of NF- κ B back under control but also to a level optimum for regenerative purposes.

AF-EV Uptake by Target Cells is at Least Partly Dependent on Active Processes

Facilitation of the signalling modifications discussed by the AF-CM and AF-EVs is dependent on how the AF-EV interacts with the target cells. PKH26 stained AF-EVs were found within the cytoplasm of U251 cells (Figure 4.8.A). This suggests that the AF-EV has been taken up by the target cell. However,

ANOVA statistical analysis showed that treatment of cells with NaAzide prior to exposure to the AF-EVs did not lead to a significant decrease in AF-EV uptake per cell or the percentage of cells overall taking up the AF-EVs (Figure 4.8.D). This would suggest that this uptake is not entirely an active process as previously suggested by others (Ronquist et al., 2016, Mulcahy et al., 2014, Camussi et al., 2010, Urbanelli et al., 2013). However statistical testing between the AF-EV treated and NaAzide affected AF-EV treated cells only did show a significant decrease in AF-EV uptake due to the NaAzide treatment. Some of the pathways expected to decrease following NaAzide induced ATP depletion include pinocytosis but also phagocytosis. Pinocytosis has been shown to be the major mechanism in the uptake of small complex particles below 250nm as opposed to phagocytosis which is employed with those over this size (Panariti et al., 2012). The NaAzide may not have blocked all active transport into the target cell thus leading to a lack of a complete block of AF-EV uptake. Furthermore, any uptake at all within a cell would lead to a cell being counted as positive within the flow cytometric readout (Figure 4.8.E). Due to a significant drop in AF-EV uptake per cell within the NaAz treated U251 cells it can be concluded that AF-EV uptake is at least partly dependent on active processes. On the other hand the occurrence of some PKH26 uptake in NaAz treated cells may also illustrate the variety of AF-EV types or subtypes present within the AF-EV. Some AF-EVs may therefore be taken up into the cell via integration of their phospholipid membrane with the cell plasma membrane in a non-energy dependent manner. A difference in AF-EV structure and membrane make-up could influence the mechanisms of uptake.

5. Chapter 5

Investigation into the Regenerative Potential of AFSC CM in an Acute CTX Damage Mouse Muscle Model *in* *Vivo*

Introduction:

In-vitro results had shown that the AF-CM contained a diverse range of molecular protein species but also miRNA. Some of these molecules were not only found to be in a soluble fraction of AF-CM but were also contained as cargo within or on small EVs. Furthermore, treatment of a number of different cell types *in-vitro* with AF-CM, suggested that the AF-CM potentiated some key cellular properties. Cell migration, proliferation and enhanced protection from stress induced senescence were increased by the AF-CM and or its resulting fractions. Additionally, some of the AF-CMs effects were suggested to derive from its ability to reduce NF- κ B signalling and therefore inflammation. Because AF-CM and its fractions could enhance cellular properties known to be important in regeneration, it was therefore proposed that AF-CM could accelerate regeneration *in-vivo*. Testing the effectiveness of AF-CM regenerative capabilities *in-vivo* would potentially aid the identification of any single or multi mechanistic mode of action using histological techniques. Furthermore, an acute injury to regeneration model would allow the gathering of information about whether the AF-CM could accelerate regeneration *in-vivo* over a short period of time and clues as to how. The major stages that can be described to take place within such an *in-vivo* scenario are well documented and include the initial trauma to the tissue, inflammation and regeneration of tissue through remodelling and maturation. In this particular case, the use of a myotoxic phospholipase A2 cardiotoxin (CTX) from a species of Cobra, *Naja Pallida*, can be utilised to create an acute injury within the skeletal muscle of a mouse. This initial damage is followed up, as described, with various phases of inflammation and then regeneration.

Regeneration in Muscle

Muscle is a large and important organ of the body derived from the mesoderm, which not only allows movement, but is also essential for the body's glucose regulation, respiratory functions such as diaphragm mobility and metabolism. Degeneration of this organ can take place due to genetic defects including muscular dystrophies, neurodegenerative diseases leading to lack of motor end plate activity or acute trauma, which can occur physically for example due to a sporting injury or

blunt trauma. Skeletal muscle consists of a number of major cell types, forming both the fibres themselves (derived from the mesoderm) and the stromal tissue, all of which interact to provide healthy function (Murphy et al., 2011). Upon the muscle fibres exists a small population of stem cells, known as satellite cells, important for regeneration of muscle fibres following necrosis. Within the milieu of cells are resident fibroblasts whose main role is to provide an environment perfect for the existence of cells within the tissue by producing ECM, such as collagen and growth factors. However, fibroblasts also play a major role in scar formation following damage and induce pathological fibrosis (Li et al., 2008). Blood vessels penetrate the tissue thus providing the surrounding cells with oxygen and nutrients from around the body and are made up mainly of endothelial cells, which line the vessels. Endothelial cell health is also maintained by pericytes which lie upon the capillaries to ensure vessels maintain adequate blood to tissue junctions (Bergers and Song, 2005). Angiogenesis, the process of blood vessel growth and development is vital for revitalisation of not only skeletal muscle but all tissues, and hindrance due to necrosis or inflammation can have major consequences for regeneration. Following injury otherwise non-resident cells such as inflammatory cells (mainly macrophages) infiltrate muscle adding to the interplay of cell to cell signalling.

Following damage and initiation of a pro-inflammatory response, satellite cells awaken from a quiescent state and commence a proliferative stage in muscle regeneration. In a quiescent state, satellite cells reside under the basal laminae of the myofibre. This quiescent state is believed to be maintained through environmental niche derived Notch ligand binding with Notch receptors on the satellite cells, and in particular downstream RBP-J (Bjornson et al., 2012, Mourikis et al., 2012). Upon damage to the tissue and the initiation of a pro-inflammatory phase, cytokines such as $\text{INF-}\gamma$ lead to the activation of the satellite cells (Qin and Zhang, 2017, Collins et al., 2005). Activation of satellite cells usually occurs between 6-12 hours after damage (Vater et al., 1994). The stem cells will then proliferate in an asymmetric manner producing two daughter cells, one to replace the mother stem cell and replenish the stem cell pool whilst the other can be used for tissue replacement and repair (Zammit et al., 2004, Ono et al., 2011, Collins et al., 2005). Activation is switched on through p38-

MAPK signalling, known to be associated with stress and growth factors binding to their receptor such as HGF, leading to increased expression of genes including MyoD (Tatsumi et al., 2002, Jones et al., 2005). Satellite cell proliferation coincides with expression of MyoD and Myf5 (figure 5.1.), a basic helix-loop-helix family (bHLH) of protein which bind muscle specific genes (Cornelison et al., 2000, Cornelison and Wold, 1997).

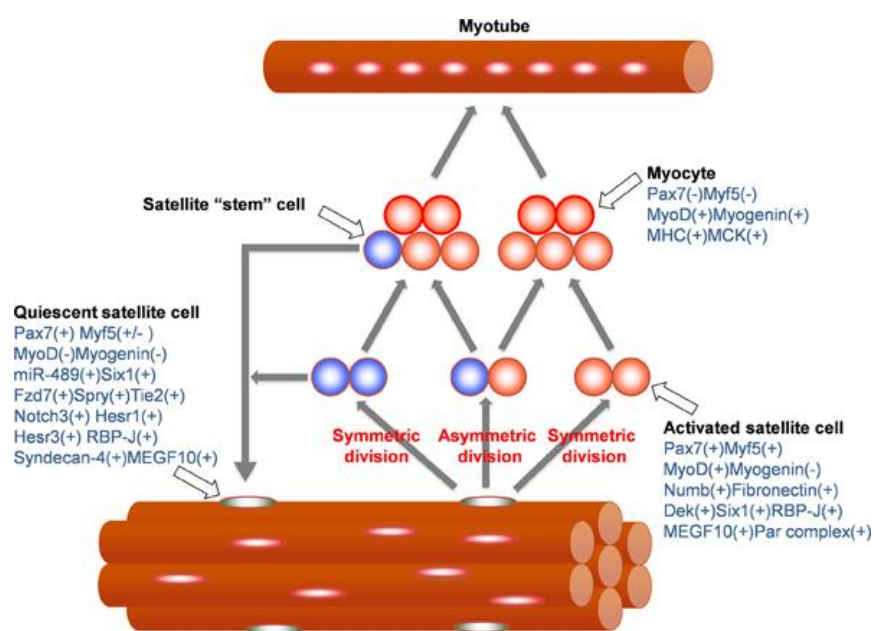


Figure 5.1: Expression markers of satellite cells from the point of quiescence to activation and then differentiation into myocytes prior to myotube formation. Modified from Motohashi and Asakura, 2014 (Motohashi and Asakura, 2014).

Acute or chronic damage can however lead to the exhaustion of a stem cell population because of over activation and the overwhelming need of stem cells for replacement of damaged cells (Yue et al., 2016). However, exhaustion of this critical cell population stifles the regeneration of the tissue in chronic disease (Heslop et al., 2000). Active stem cells that have migrated to or localise in the area of damage undergo differentiation. Initially residing under the myofibre basal lamina, the satellite cells migrate via lamellipodia towards the fibre surface. Upon reaching the surface, lamellipodia based migration is replaced by amoeboid migration mediated through blebbing (Otto et al., 2011). Satellite

cells will then progress towards the area of damage before differentiating, which does not take place until pro-inflammatory M1 macrophage levels have dropped and are at least partly replaced with M2 macrophages classically defined as anti-inflammatory (Perdiguero et al., 2011, Perdiguero et al., 2012).

At the stage of differentiation MyoD and Myf 5 become activated and lead to the expression of myogenin and Myf4 (Molkentin et al., 1995, Cornelison et al., 2000, Cornelison and Wold, 1997). This differentiation of satellite cells is however tightly regulated by the inflammatory status of the environment which in turn is highly dependent of the infiltration and type of macrophages. The infiltration of macrophages depends on the influx and differentiation of monocytes in the local vasculature. The initial pro-inflammatory response created by the necrosing cells and, in the case of muscle, the myofibre acts as the driving force behind this macrophage assault. In an attempt to clear the scene of cellular debris as a result of damage, M1 macrophages classically known to be pro-inflammatory remove fragments via phagocytosis. Markers highly attributed to the M1 macrophage state and function includes Ly6, iNOS and CD80 (Arnold et al., 2007, Daigneault et al., 2010). M1 macrophages also secrete large quantities of pro-inflammatory cytokines both recruiting further waves of macrophages and increasing the activity of other cells types within the vicinity.

On the other hand differentiation of the activated satellite cells is triggered by a reduction in pro-inflammatory cytokines, M1 macrophages that are associated with them but also clearance of debris. Following the clearance of debris a timely transition takes place whereby M1 macrophages are slowly replaced by M2 macrophages, generally thought of as being anti-inflammatory (Perdiguero et al., 2011, Perdiguero et al., 2012, Arnold et al., 2007). This transition from M1 to M2 is believed to be under the control of the p38 MAPK and the MAPK phosphatase, MKP-1 (Perdiguero et al., 2011, Perdiguero et al., 2012). Reduction in MKP-1 activity and therefore increased p38-MAPK phosphorylation leading to its increased signalling is suggested to facilitate the anti-inflammatory state of the macrophage population. The development of the M2 response brings about tissue remodelling and differentiation of cells because of the secretion of cytokines including TGF- β (Arnold

et al., 2007, Lefaucheur and Sebillé, 1995). In particular the M2 response promotes satellite cell differentiation and fusion with other satellite cells into a myotube structure. The myotube will eventually mature and materialise into a functional myofibre.

Classically, satellite cells will differentiate into myoblasts, which fuse to form multi-nucleated myotubes and finally differentiate into myofibres, thus replacing those previously lost (Motohashi and Asakura, 2014). Nevertheless, satellite cells appear to possess multipotent properties and can also differentiate into other cell types including adipocytes and osteocytes, although for this to take place they must not have been pushed towards a myogenic lineage (Asakura et al., 2001). Expression of the transcription factor Pax-7 is indicative of satellite cells and can be seen to be expressed in cells of regenerated muscle fibres following injury (Lepper et al., 2009, Lepper and Fan, 2010, Seale et al., 2000). In mice at least the ability to express Pax-7 has been shown to maintain the satellite cell population prior to an age of P21 (Oustanina et al., 2004). Moreover as with most stem cells, satellite cells will produce paracrine acting factors to stimulate and direct other cell types within the environment and presumably throughout the body if secreted factors enter and circulate the blood stream (Rahbarghazi et al., 2013, Rhoads et al., 2009, Fry et al., 2014).

Cardiotoxin Induced Muscle Damage

CTX can be used to create an acute muscle injury model. CTX is an amphiphilic polypeptide, defined as having a polar water-soluble terminal group attached to a water insoluble hydrocarbon chain, it is able to penetrate cellular membranes leading to osmotic shock, lysis and widespread necrosis within the tissue (Wang et al., 1997). Furthermore, cells that survive lysis can be additionally affected by mitochondria membrane disruption, which similarly to whole cell osmotic shock can cause cell fragmentation (Wang and Wu, 2005, Ramadasan-Nair et al., 2014). The spike in intracellular calcium following sarcolemma disruption leads to sustained high levels of Ca^{2+} , prompting muscle fibres to change morphologically from a rod shape to becoming round due to hypercontraction (Wang et al., 1997). Ca^{2+} -dependent proteases are activated and wreak havoc within the cell leading to mass protein breakdown. Mitochondria can also take up Ca^{2+} , which is exaggerated by the increased

intracellular levels created by CTX leading to dysregulation of mitochondrial homeostasis (Ramadasan-Nair et al., 2014). As a consequence of abnormal Ca^{2+} levels in mitochondria, an increase in the production of damaging ROS follows and the ability of mitochondria to effectively undertake respiration fails. However, not only does CTX IM injection provide a model of acute degeneration within muscle it also presents with many pathological features observed in chronic disease, including that of many muscular dystrophies, which can be experimentally evaluated. Characteristics include sustained pro-inflammation, apoptosis and loss of sarcoplasm and structure. Importantly, the satellite cells are not killed by CTX and drive regeneration in the following days after CTX muscle exposure (Harris, 2003).

The Satellite cells of skeletal muscle are highly resilient, this along with the position they reside between the plasma membrane and basal lamina of the muscle fibre whilst quiescent means that they are protected and not killed by CTX (Harris, 2003). Due to the sparing of satellite cells from CTX induced damage, the stem cell pool stays intact. Furthermore the CTX, which is comprised mainly of phospholipases as opposed to enzymes such as collagenases that catalyse the breakdown of the ECM, is therefore sparing of the subsequent basal laminae tubes after fibre death. Activated satellite cells can therefore use the leftover fibre 'skeleton' not only as highway for travelling along but also as a scaffold developing fibres following satellite cell differentiation (Harris, 2003). Depending on the turnover of cells within the tissue the local stem cells can stay in a quiescent state until damage occurs and they are activated (Fu et al., 2015, Villalta et al., 2009, Karalaki et al., 2009).

As discussed, CTX has been found not to affect the ECM of the muscle fibres. The ECM and its elasticity is an important regulator of stem cell differentiation and its lineage specification (Engler et al., 2006, Kundu and Putnam, 2006, Kuang et al., 2008). Therefore preservation of the ECM following CTX damage plays an important role in directing the satellite cell down a myogenic lineage and ultimately its ability to facilitate regeneration. In addition to this preservation, the innervation of fibres has been found not to be affected by CTX. It has been suggested as being at least in part the reason why the transition of regenerating fibres (following CTX) to express adult myosins from

embryonic forms is that much quicker than the transition in normally developing fibres (d'Albis et al., 1988). Finally, during the stages of differentiation a state of macrophage exhaustion and dispersal from the tissue follows, as correlated by the complete loss of MKP-1 activity in the macrophages (Perdiguero et al., 2011, Perdiguero et al., 2012).

As discussed, the delivery of macrophages to the damaged area relies heavily on the vasculature. The capillary network in the given area also provides a source of oxygen and nutrients for both the healthy and regenerating tissue. Inflammation and hypoxia due to damage in the existing vasculature initiates an angiogenic programme (Szade et al., 2015). A necrotic and therefore often hypoxic environment leads to the stabilisation and dimerization of hypoxic inducible factor (HIF) family members HIF α and HIF β (Schofield and Ratcliffe, 2004, Szade et al., 2015). Acting as a transcription factor the dimerised forms of HIF induce gene transcription of genes such as NF- κ B, VEGF and COX2 (Kaidi et al., 2006, Ceradini et al., 2004, Cummins et al., 2006, Oliver et al., 2009). Like-wise, inflammatory signalling such as that via NF- κ B leads to the upregulation of HIF genes (Oliver et al., 2009, Cummins et al., 2006). VEGF or more specifically VEGF-A, in the case of angiogenesis, binds to VEGF receptors (VEGFR-1/2) (Shibuya, 2011). Under the VEGFR-2 receptor signalling pathway the PLC γ -PKC-MAPK signalling pathway is highly active (Takahashi et al., 1999, Takahashi et al., 2001). Activation of this signalling pathway is known to induce mitogenesis and differentiation of vascular endothelial cells.

Results

AF-CM Treatment in an Acute Damage Model

To determine if AF-CM can promote regeneration *in vivo* in an acute damage model, treatment with AF-CM was carried out on mice with cardiotoxin (CTX) induced muscle injury. Damage to the mouse Tibialis Anterior muscle with 100µM *Naja Pallida* CTX is known to generate localised necrosis within the muscle followed by regeneration. The extent to which AF-CM could accelerate regeneration was therefore analysed. Mice TA muscles were either damaged with CTX and treated with a vehicle (PBS) or damaged with CTX and treated with AF-CM and collected 5 days after damage.

Haematoxylin/ Eosin and Acid Phosphatase Staining of Damaged Muscle

First, the extent and location of damage was assessed using haematoxylin and eosin staining (H&E) (Figure 5.2.A-C). The set of negative control muscles showed no damage and normal muscle fibre morphology as seen by the coverage of tissue pink in colour. On the other hand, CTX damaged muscles presented with regions depleted of the pinkish haematoxylin staining and appeared more purplish thus indicating the regions of interest. At a higher magnification, the damaged regions contained many small fibres with centrally located nuclei (Figure 1C high magnification). In addition, a clear increase in the concentration of nuclei within the area surrounding the myofibres could be seen compared to undamaged regions and that of the undamaged control sections of muscle.

The extent of necrosis and inflammation was determined using acid phosphatase staining (Figure 5.2.D-F). Present within the lysosomes, acid phosphatase can be found in a number of tissues, in particular tartrate-resistant acid phosphatase (TRAP5a) is found in cells such as macrophages. Naphthol acid phosphate within the staining solution is hydrolysed by acid phosphatases within the tissue producing naphthol derivatives. The unstable diazonium salt, hexazonium pararosanilin, within the stain couples with the naphthol derivatives thus creating a red azo dye. A deep red stain correlated to the regions described in the H&E stained sections with fibres consisting of centrally located nuclei.

Images of acid phosphatase stained sections were blindly assessed for intensity and coverage (Figure 5.2.G). No significant differences between other parameters were found.

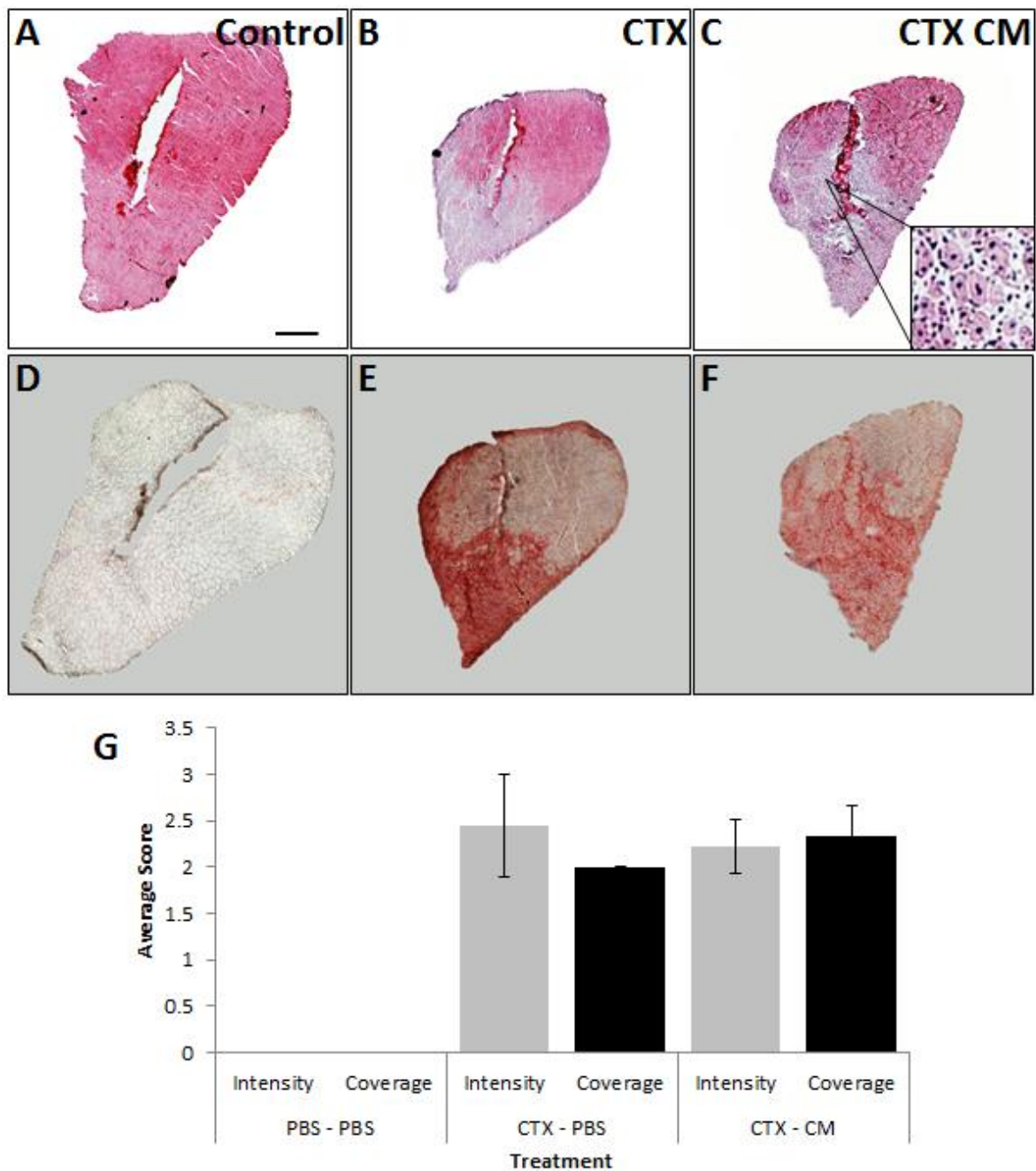


Figure 5.2: Cardiotoxin induced muscle damage histology after 5 days. Haematoxylin and Eosin staining of (A) non-damaged control TA muscle sections, (B) CTX damaged vehicle treated control TA muscle sections and (C) CTX damaged AF-CM treated TA muscle section. Acid phosphatase staining of (D) non-damaged control TA muscle sections, (E) CTX damaged vehicle treated control TA muscle sections and (F) CTX damaged AF-CM treated TA muscle sections. (G) Acid phosphatase stain scores

carried out blindly for stain intensity and coverage with 0 = no stain/coverage and 5 = highly stained/complete coverage. Scale bar represents 500 μm . Values are expressed as means \pm SEM (n=5). $p < 0.05$ (*), $p < 0.01$ (**) or $p < 0.001$ (***)).

Cross-Sectional Area of Newly Regenerated Fibres

Embryonic Myosin heavy chain (eMHC), also known as MHC3, is expressed in developing muscle fibres before being replaced by the mature forms of myosin heavy chain (Schiaffino et al., 2015). However, following damage eMHC gene expression is switched back on within newly forming muscle fibres and can therefore be used to identify newly regenerating myofibres. Once identified, the sizes of these newly regenerating fibres were compared to understand whether AF-CM treatment had accelerated the regeneration process (figure 5.3.A-B).

Comparison between the two CTX damaged groups of muscles showed that treatment with AF-CM (CTX-CM) led to a significant increase in newly regenerating fibre size compared to the vehicle treated (CTX). Fibres in the deep region (Figure 5.3.C) were 74.84% larger in the AF-CM treated muscle compared to the vehicle treated, ($630.79 \pm 10.36 \mu\text{m}^2$ and $360.79 \pm 6.10 \mu\text{m}^2$ (n=5, $p < 0.001$)). Within the superficial region of the TA, AF-CM treatment also led to a significant increase in newly regenerating fibre size (Figure 5.3.D). (67.29% from $405.07 \pm 7.49 \mu\text{m}^2$ in the vehicle treated to $677.63 \pm 12.59 \mu\text{m}^2$ (n=5, $p < 0.001$)). Collating data from the deep and superficial regions of muscle (Figure 2E), newly regenerating fibres from AF-CM treated mice were 73.59% larger than in the vehicle treated muscles, $661.66 \pm 11.93 \mu\text{m}^2$ and $381.16 \pm 6.66 \mu\text{m}^2$ respectively (n=5, $p < 0.001$).

Frequency-distribution profiles of fibres from the AF-CM treated and vehicle treated muscles damaged due to CTX were also developed. The majority of fibres within the vehicle treated group 200-400 μm^2 . On the other hand, the majority of fibres within the AF-CM treated group were 400-600 μm^2 . The majority of AF-CM treated fibres had a larger cross-sectional area than muscles damaged with CTX but not treated with AF-CM. This was further corroborated by a statistical Chi test of variance which showed a significant difference in variance between the AF-CM treated and vehicle treated.

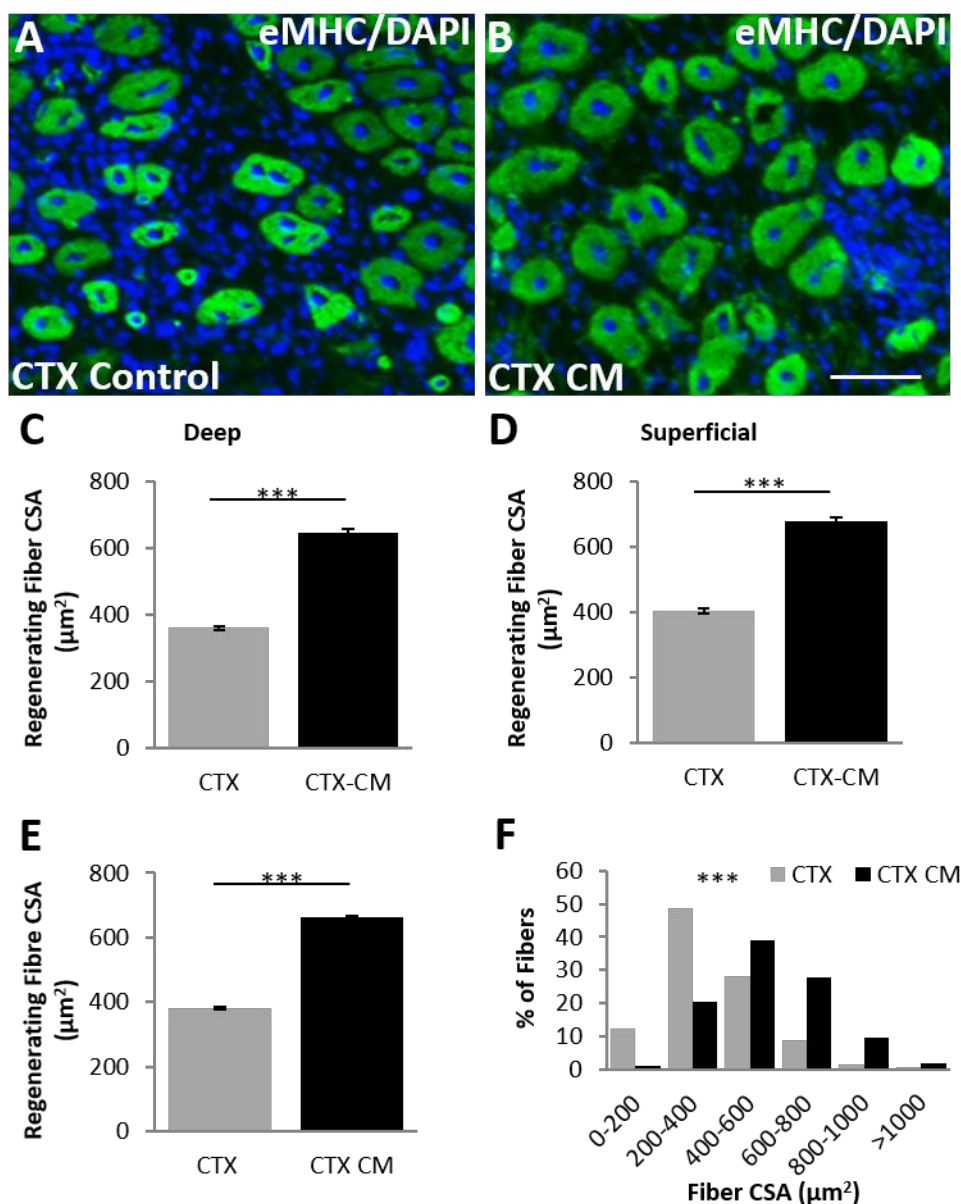


Figure 5.3: Newly regenerated TA muscle fibres following CTX damage. (A-B) embryonic Myosin heavy chain expression in damaged muscle (green) with DAPI (blue staining comparing CTX damaged vehicle treated muscles (CTX Control) and CTX damaged AF-CM treated muscles (CTX CM). (C) Quantification of cross-sectional area of newly regenerated fibres in the deep region of the TA muscle sections. (D) Quantification of cross-sectional area of newly regenerated fibres in the superficial region of the TA muscle sections. (E) Quantification of cross-sectional-area of newly regenerated fibres across the total TA muscle sections. (F) Frequency distribution graph of regenerated muscle fibres. Scale bar represents 50µm. Values are expressed as means \pm SEM (n=5). $p < 0.05$ (*), $p < 0.01$ (**) or $p < 0.001$ (***).

Satellite Cell Activity within the Regenerating Tissue

In muscle, the number of quiescent and active satellite cells along with their transition down the myogenic lineage is a key factor in muscle fibre replacement. The expression of Pax7, a transcription factor, in the absence of MyoD expression represents these quiescent satellite cells as they reside under the basal laminae of the muscle fibre. Upon satellite cell activation, MyoD gene expression is switched on and begins to repress the expression of Pax7 as the satellite cell begins to differentiate towards the mature muscle cell. Upon differentiation, Pax7 expression becomes absent and the cell fuses with other myoblasts forming a syncytium of cells and providing the classic morphology of a muscle fibre. Following CTX damage no significant differences were found between the AF-CM treated and vehicle treated groups in terms of the number of quiescent (Pax7⁺/MyoD⁻) cells or the number of activated (Pax7⁺/MyoD⁺) cells (Figure 5.4.B). However, a significant increase in the number of committed progenitor cells (Pax7/MyoD⁺) from the AF-CM treated group of muscles was found compared to that of the vehicle treated, 50.20±5.62 cells/mm² and 28.45±4.65 cells/mm² respectively (n=5, P<0.05).

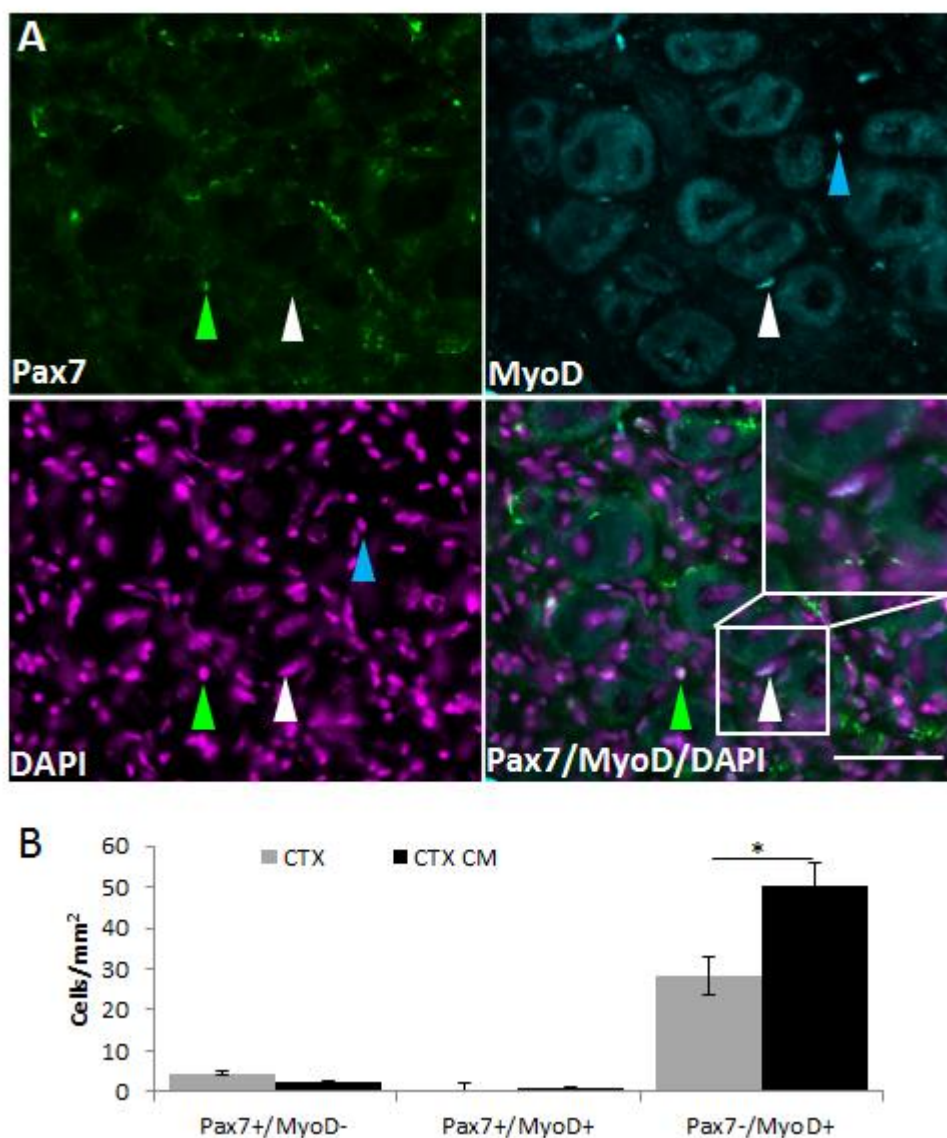


Figure 5.4: Assessment of regeneration with CTX damaged muscle treated with vehicle or AF-CM.

(A) Immunofluorescent staining for Pax7 (green), MyoD (Cyan) and DAPI (Magenta) in TA muscle damaged with CTX. (B) Quantification of quiescent satellite Pax7⁺/MyoD⁻, activated satellite cells Pax7⁺/MyoD⁺ and muscle lineage committed progenitor cells Pax7⁻/MyoD⁺ within vehicle and AF-CM treated muscles damaged with CTX. (A) Scale bars are equal to 100μm. Values are expressed as means ± SEM (n=5). p < 0.05 (*), p < 0.01 (**), or p < 0.001 (***).

Blood Supply to the Regenerating Tissue

In addition to satellite cell activities, the ability to provide a source of blood, oxygen and the nutrient content that comes with it is critical for regeneration of tissue. The smallest of the blood vessels that provide this source of blood, capillaries, and the endothelial cells that make them up undergo angiogenesis following the initial cytokine response along with VEGF and HIF signalling pathway stimulation due to stressors such as hypoxia. CD31, also known as platelet endothelial cell adhesion molecule (PECAM-1), is highly expressed at endothelial cell junctions. CD31 is widely used as a marker for capillaries and the endothelial cells that comprise them (Figure 5.5.A). The number of CD31⁺ vessels were analysed within a given area of the treatment groups to understand the extent of vascularisation within the regenerating muscle (Figure 5.5.B). Although not significant between both CTX damaged muscle groups, the number of CD31⁺ vessels had increased following CTX damage compared to the non-damaged control muscles. There was however a significant increase in the number of CD31⁺ vessels/mm² in the AF-CM treated (1008.86 ± 116.33 cells/mm²) CTX damaged muscles compared to the non-damaged muscles (494.68 ± 17.90 cells/mm²). On the other hand, a decrease in the number of CD-31⁺ cells/fibre was found upon CTX damage with treatment with the vehicle, although not significant (Figure 5.5.C). However, treatment with AF-CM increased the number of CD31⁺ vessels from the damaged control by 71.43% from 0.98 ± 0.10 CD31⁺ vessels/ fibre to 1.68 ± 0.25 CD31⁺ vessels/ fibre ($n=5$, $p<0.05$). The increase in vessels from the damaged control with AF-CM treatment brought levels of CD31⁺ vessels to a level that was not significantly different to that of the undamaged control.

Macrophage Infiltration

Many of the processes involved in regeneration as well as degeneration are profoundly affected by the inflammatory status of the tissue affected. In the case of the skeletal muscle as with many tissues following damage, inflammation is further increased by the infiltration of macrophages following their differentiation from monocytes in the circulating blood. Although not believed to be necessary for development of macrophages, F4-80 an extensively characterised marker commonly used for mouse macrophages is thought to play a key role in their function, such as adhesion and activation of other cell types including natural killer cells and those of the immune system (Lin et al., 2005). The number of F4-80⁺ cells/mm² in the CTX damaged AF-CM treated muscles were significantly higher than that of the vehicle treated CTX damaged muscles by 19.3% ((n=5, p<0.05)(Figure 5.5.D-E)).

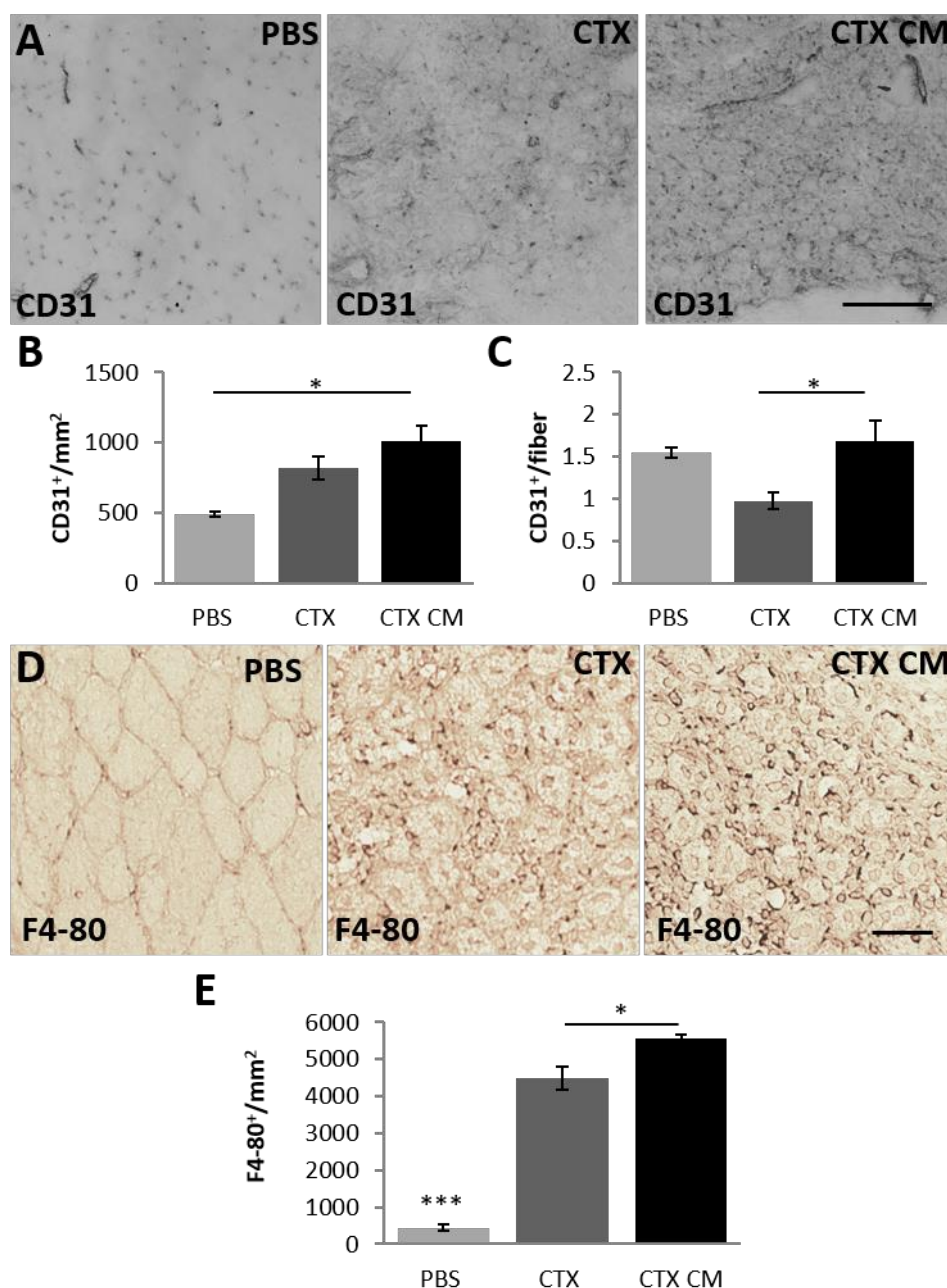


Figure 5.5: Assessment of regeneration with CTX damaged muscle treated with vehicle or AF-CM.

(A) CD31 staining for capillaries in healthy (PBS) and regenerating muscle treated with vehicle (CTX) or AF-CM (CTX CM). (B) Quantification of capillary density (no. per mm²) and (C) quantification per fibre. (D) F4-80 staining for macrophages in healthy (PBS) and regenerating muscle treated with vehicle (CTX) or AF-CM (CTX CM). (E) Damaged areas assessed for the number of F4-80⁺ cells. Black arrows indicate F4-80⁺ cells. (A, D) Scale bar represents 50µm. Values are expressed as means ± SEM (n=5). p < 0.05 (*), p < 0.01 (**), p < 0.001 (***).

AF-EV Treatment in an Acute Damage Model

Next, we examined the ability of the AF-EV to accelerate regeneration in the damage model *in vivo* (Figure 5.6.). Firstly, staining of eMHC was carried out. The CSA of eMHC stained fibres were analysed (Figure 5.6.A-B). A significantly larger newly regenerating fibre CSA was recorded from muscle treated with AF-EV compared to those treated with the vehicle (n=5, p<0.001). Vehicle treated mice with CTX damaged muscles had an average eMHC stained fibre CSA of $484.51 \pm 68.27 \mu\text{m}^2$ whereas AF-EV treated Mice with CTX damaged muscles had an average eMHC stained fibre CSA of $926.66 \pm 24.23 \mu\text{m}^2$, 91.26% larger.

Furthermore, analysis showed that AF-EV treatment had also brought levels of CD31⁺ vessels/fibre back to a level that was not significantly different to that of the non-damaged muscles, 1.31 ± 0.07 CD31⁺/fibre and 1.37 ± 0.10 CD31⁺/fibre respectively (Figure 5.6.C-D). Also, AF-EV treatment in CTX damaged muscles had significantly higher level of CD31⁺/fibre than the vehicle treated CTX damaged muscles, 1.01 ± 0.08 CD31⁺/fibre (n=5, p<0.05).

On the other hand, counts of F4-80⁺ cells/mm² showed no significant differences between the AF-EV and vehicle treated CTX damaged muscles, 3437 ± 240.91 F4-80⁺ cells/mm² and 3606.67 ± 250.64 F4-80⁺ cells/mm² (Figure 5.6.E-F). However, a significant increase in F4-80⁺ cells were seen within CTX damaged muscles from that of the undamaged, 666.67 ± 88.19 F4-80⁺ cells/mm² (n=5, P<0.001).

Further investigation into how AF-EV could enhance regeneration was carried out into the satellite cell and committed progenitor cell status. Levels of quiescent Pax7⁺/MyoD⁻ cells did not differ between the vehicle treated, 0.56 ± 0.29 cells/mm², and AF-EV treated, 1.43 ± 0.53 cells/mm², CTX damaged muscles. On the other hand, the level of activated Pax7⁺/MyoD⁺ cells were significantly higher in the AF-EV treated, 1.15 ± 0.27 cells/mm², compared to the vehicle treated, 0.33 ± 0.33 cells/mm² (n=5, p<0.05). However, committed Pax7⁻/MyoD⁺ cell levels did not differ between the vehicle and AF-EV treated CTX damaged groups of muscles, 0.22 ± 0.22 cell/mm² and 0.71 ± 0.29 cells/mm².

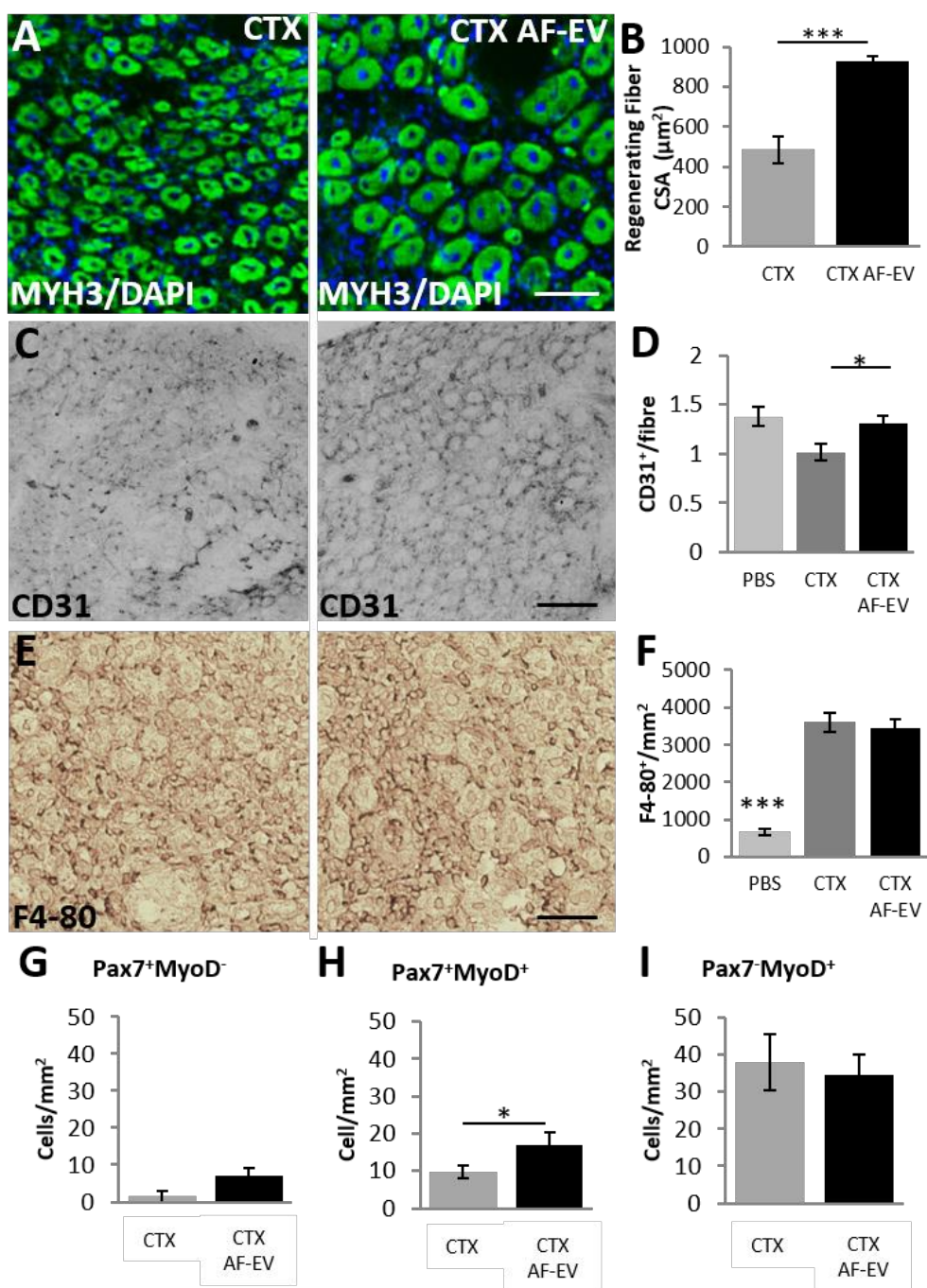


Figure 5.6: Muscle regeneration following AF-EV treatment. (A) Embryonic Myosin heavy chain expression in damaged muscle (green). (B) Quantification of cross-sectional area of newly regenerated fibres. (C) CD31 staining for capillaries in regenerating muscle. (D) Quantification of CD31⁺ capillaries per fibre. (E) F4-80 staining for macrophages. (F) Damaged areas assessed for the number of positive F4-80 cells/mm². Comparison of the number of Pax-7⁺/MyoD⁻ quiescent satellite cells (G), Pax-7⁺/MyoD⁺ activated satellite cells (H) and Pax-7⁻/MyoD⁺ muscle lineage committed progenitor cells (I) per mm² between treated groups. Values are expressed as means \pm SEM (n=5). (A)

Scale bar equal to 100 μ m. (C, E) Scale bar represent 50 μ m. $p < 0.05$ (*), $p < 0.01$ (**) or $p < 0.001$ (**).

Comparison of AF-CM, AF-EV and Soluble Fraction in an Acute Damage Model

Each of the fractions that make up the AF-CM may have different regenerative qualities following acute damage *in vivo*. Both the AF-EV and resultant soluble fraction were used as treatments along with the whole AF-CM. Treatments were compared to each other and a vehicle treated CTX damaged positive control. First we compared average CSA of eMHC stained fibres from across the total TA muscle section (Figure 5.7.A). A significant increase in CSA could be seen compared to the vehicle treated control ($475.22 \pm 2.65 \mu\text{m}^2$) with the AF-CM treatment ($775.39 \pm 28.30 \mu\text{m}^2$), AF-EV treatment ($735.74 \pm 55.35 \mu\text{m}^2$) and soluble fraction treatment ($790.47 \pm 72.20 \mu\text{m}^2$) ($n=5$, $p < 0.01$, 0.05 and 0.01 respectively). However, no significant difference was detected between the AF-CM derived treatments. A more detailed inspection into the CSA of newly regenerating fibres within the superficial and deep area was also carried out to identify if the AF-CM and its derived fractions had differing effects on these areas (Figure 5.7.B-C). Within the superficial area AF-CM, AF-EV and the soluble fraction treatment led to a significantly larger average CSA in eMHC stained fibres compared to the vehicle treated control; $759.93 \pm 54.21 \mu\text{m}^2$, $759.50 \pm 46.34 \mu\text{m}^2$, $820.24 \pm 87.53 \mu\text{m}^2$ and $450.48 \pm 28.18 \mu\text{m}^2$ respectively ($n=5$, $p < 0.05$, 0.05 and 0.01). On the other hand, within the deep region of the TA muscle sections only the whole AF-CM treatment ($789.41 \pm 38.39 \mu\text{m}^2$) and the soluble fraction ($763.15 \pm 60.92 \mu\text{m}^2$) treatment led to a significantly larger CSA in eMHC stained fibres compared to the control, $498.19 \pm 25.35 \mu\text{m}^2$ ($n=5$, $p < 0.05$). The AF-EV fraction on the other hand, $713.06 \pm 84.39 \mu\text{m}^2$, did not show a significantly higher CSA compared to the control. Additionally, there were no significant differences in CSA between the AF-CM derived treatments in either of the superficial or deep regions of the muscle.

Analysis into the number of CD31⁺ vessels/ fibre showed that only the whole AF-CM significantly increased the numbers to 1.36 ± 0.20 CD31⁺/fibre from 0.75 ± 0.07 CD31⁺/fibre in the control ($n=5$, $p < 0.05$). Whole AF-CM treatment also showed significantly higher levels of CD31⁺ vessels/fibre compared to the soluble fraction treated group, 0.79 ± 0.08 CD31⁺/fibre ($n=5$, $p < 0.05$). However, neither AF-EV treatment (1.07 ± 0.10 CD31⁺/fibre) nor the soluble fraction treatment led to a

significant increase in CD31⁺ vessels/fibre from the control. Moreover, when profiling Pax7/MyoD expression of cells within the sections, only AF-EV (3.52±1.00 cells/mm²) and treatment with the soluble fraction (4.92±1.03 cells/mm²) led to a significantly larger number of Pax7⁺/MyoD⁺ cells compared to the vehicle treated CTX control, 0.97±0.59 cells/mm² (n=5, p<0.05). No other significant effect from the control was seen with other treatments or within that counted for Pax7⁺/MyoD⁻ or Pax7⁻/MyoD⁺ expression.

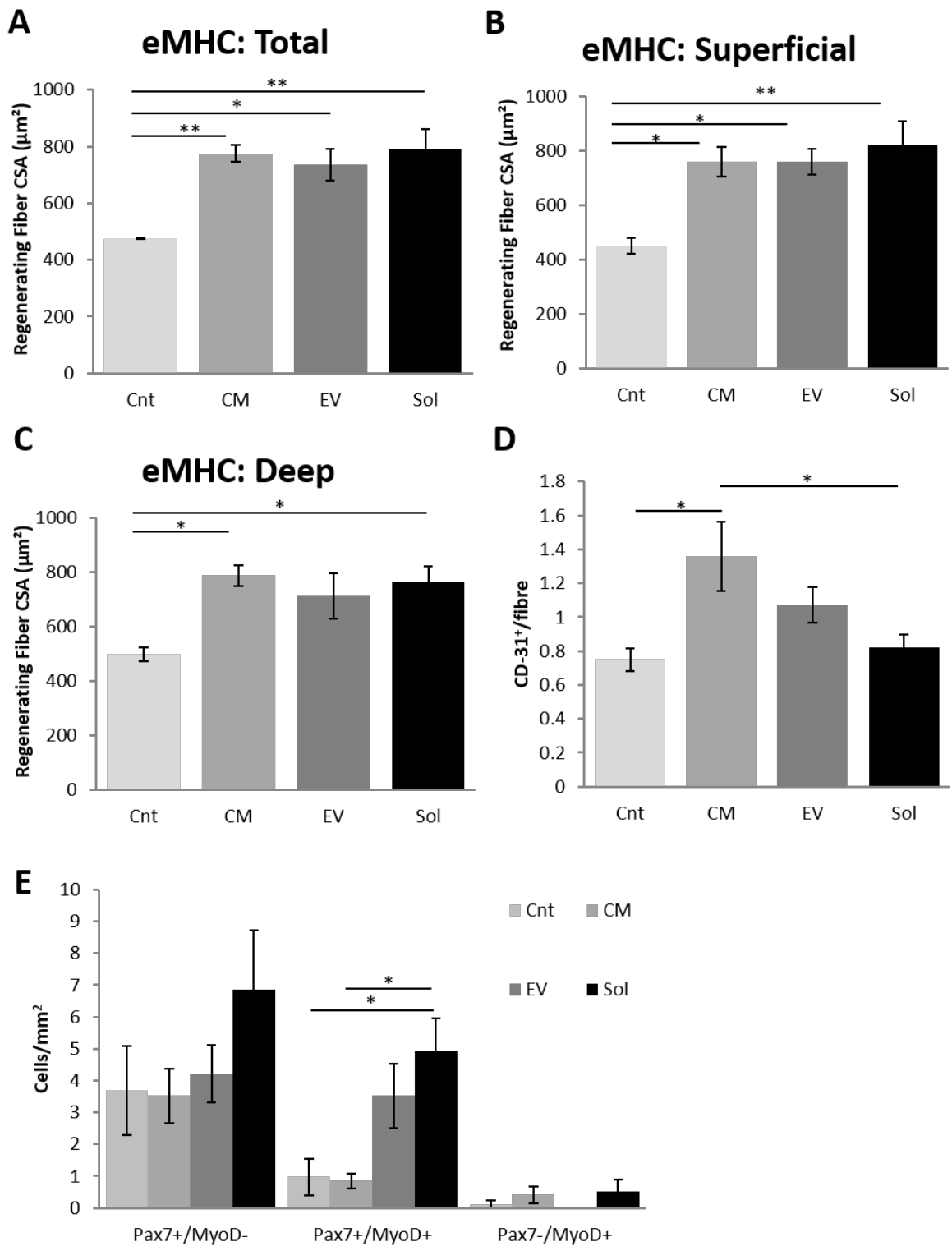


Figure 5.7

Figure 5.7: Comparison between whole AF-CM, AF-EV and soluble fraction treatment in a model of CTX damage. (A) Quantification of cross-sectional area of newly regenerated fibres across the total TA muscle sections. (B) Quantification of cross-sectional area of newly regenerated fibres in the superficial region of the TA muscle sections. (C) Quantification of cross-sectional area of newly regenerated fibres in the deep region of the TA muscle sections. (D) Comparison of the number of CD31⁺ capillaries per fibre. (E) comparison of the number of Pax-7⁺/MyoD⁻ quiescent satellite cells, Pax-7⁺/MyoD⁺ activated satellite cells and Pax-7⁻/MyoD⁺ muscle lineage committed progenitor cells per mm². Values are expressed as means \pm SEM (n=5). p < 0.05 (*), p < 0.01 (**), or p < 0.001 (***)

Discussion

Histological analysis of CTX damaged TA muscles from mice treated with or without AF-CM or its resulting fractions were carried out. Results showed that although the CTX damage model presented with regenerating fibres, muscles also showed widespread macrophage infiltration. In comparison to those untreated damaged muscles, muscles treated with the AF-CM displayed newly regenerating fibres of dramatically larger cross sectional areas. Furthermore, the number of active muscle precursors was noticeably higher within those treated with AF-CM. Regarding inspection of the vasculature within damaged muscles; the treatment of AF-CM had not only increased the number of blood vessels within a given damaged area but had also increased the number of blood vessels per muscle fibre. Interestingly, the AF-CM treatment was suggested to have increased the total number of macrophages within the damaged muscle. Upon replacement of AF-CM treatment with its resulting AF-EV fraction, damaged muscles still showed similar regenerative characteristics to its originating AF-CM. However, following comparison between AF-EV and the AF-CM soluble fraction, it was evident that treatment would benefit from the mixture of the two fractions because each was not as potent under the measures tested. It was therefore concluded that the whole AF-CM may be the more beneficial for use as a regenerative therapeutic and could not be replaced entirely by one of its fractions.

Widespread Inflammation and Tissue Damage Following Cardiotoxin Injection

Initially, mice were either treated with vehicle or whole AF-CM just prior to CTX induced TA muscle damage. Histological analysis of sections taken from the TA muscles, were stained using H&E techniques. Images provided the location of direct damage as indicated by the alteration in colour from the normal bright pink colouration towards a darker purplish colouration. This change in colouration can be explained by the reduction in cytoplasmic surface area, which would usually stain pink due to Eosin in the staining process staining the eosinophilic proteins within the cytoplasm of cells and fibres. Furthermore, an increase in the number of smaller cellular structures, most likely to be made up of infiltrating inflammatory cells, is apparent and provides an increase in the number of

purple haematoxylin stained nuclei within the region. In addition to this change in colouration within the predicted damaged region, the presence of centrally located nuclei within small fibres provides a tell-tale sign of regeneration and in this case, as a consequence of damage. Centralisation of the nucleus within early myotubes and also immature myofibres results from the microtubule network driving, along with its regulator Cdc42, the nuclei towards the nuclear envelope of other nuclei within the myotube (Roman and Gomes, 2017). The microtubule network organising centre is located at the nuclear envelope in differentiating myoblasts and myotubes, as opposed to the cytoplasm, in which it would normally be located in the majority of other cell types (Roman and Gomes, 2017). Another reason for the central location of the nucleus stems from the lack of organisation of neuro muscular junctions yet to be established during regeneration, a key aspect of a mature functioning myofibre. Further analysis into the status of the muscle sections and the damaged now regenerating areas was taken from acid phosphatase staining. No significant differences in acid phosphatase staining were established between the vehicle and AF-CM treated mice that had been affected with CTX. There was however a clear difference between those affected with CTX and those that were not. The strong presence of staining within the damaged regions suggests the presence of a large infiltration of inflammatory cells, thought to be macrophages, as well as the prolific inflammatory status of the tissue. The current inflammatory status could be attributed to previous necrotic events and or infiltration of inflammatory cells.

AF-CM Treatment Accelerated Newly Regenerating Fibre Growth

Although the presence of centrally located nuclei indicates regenerating myofibres, the presence of eMHC can be used to identify newly regenerating myofibres. It was noted that some larger fibres contained centrally located nuclei and yet lacked notable levels of eMHC. As the myofibres mature the expression of eMHC is replaced by a mature form of MHC however the presence of centrally located nuclei must still exist for some time after this switch until true maturation is reached. Analysis into the deep, superficial and the total area of the eMHC stained fibres unveiled that AF-CM treatment had led to a significantly larger CSA compared to the CTX damage control. The larger CSA

in AF-CM treated muscles therefore suggests that the AF-CM had accelerated the regenerative process and therefore sped up the maturation of the newly regenerating fibres towards a larger fibre of healthy status. Furthermore, because AF-CM increased the CSA of newly regenerating fibres of both the deep and superficial region of muscle it is suggested that acceleration of skeletal muscle fibres due to AF-CM treatment is not notably affected by metabolic state. Similar results would suggest that AF-EV contained at least some of the AF-CMs regenerative effects. The results showed that AF-EV treatment led to significantly larger newly regenerating fibre CSAs. This therefore suggested that the binding of the AF-EVs or indeed the effects of their cargo led to acceleration in the development of newly regenerating fibres.

Increased Numbers of Macrophages in AF-CM Treated Muscles

As substantiated by the acid phosphatase staining, a large infiltration of macrophages can be seen within the muscles of those damaged with CTX. This was even more exaggerated within those originally treated with AF-CM. In contrast to the AF-CM, the level of F4-80 cells in AF-EV treated muscles were shown to not change and once again suggests that the soluble fraction has an important part to play in altering the level of macrophages and therefore the inflammatory state of the tissue. Furthermore, it has been previously been shown that MSC-EVs have lower levels of cytokines such as IL-6 (Nakamura et al., 2015). It was also found within a model of necrotising enterocolitis that treatment with AFSCs increased the levels of COX2, known to be involved in inflammatory signalling (Zani et al., 2014). Increases in COX2 activity was believed to aid the enhancement of gut stem cell proliferation and therefore replace intestinal cells lost due to widespread necrosis. Classically pro-inflammatory cytokines or induced signalling may also exist in or be promoted by the AF-CM in the same manner. It is proposed that a spike in these cytokines due to AF-CM could induce a larger M1 macrophage response and therefore facilitates the clearing of debris more efficiently thus clearing the way for M2 cells to accelerate regeneration (Arnold et al., 2007).

Due to the time-span in which the muscles were collected it could be hypothesised that many of the macrophages seen to be stained were M2 macrophages and therefore classically anti-inflammatory.

Levels of M1 macrophages are known to spike within the first 48h followed by their replacement by M2 cells as the spike diminishes (Villalta et al., 2009, Arnold et al., 2007, Perdiguero et al., 2011, Perdiguero et al., 2012). However, although both M1 and M2 macrophages have differing ratios of classically M1 or M2 surface markers they still both retain positivity for these markers regardless (Daigneault et al., 2010, Chanput et al., 2013, Akagawa, 2002, Verreck et al., 2006). Staining of muscle sections for an M2 marker, such as Mannose receptor, would therefore stain most if not all macrophages because most macrophages would retain this marker even in an M1 state, just at lower levels. Therefore clarification as to whether the AF-CM altered macrophage polarisation is difficult histologically and therefore requires isolation of macrophages from the muscle, which could be analysed for the ratio of M1/ M2 marker expression using flow cytometry.

AF-CM Treatment Increased the Number of Committed Muscle Progenitor Cells

To understand how the AF-CM potentiates the acceleration of the myofibre regeneration, it was also necessary to ascertain if the satellite cell activity had been altered. No significant difference between the numbers of quiescent or active satellite cells could be seen. On the other hand, there was a significantly higher level of committed progenitor cells. The muscles were collected 5 days after injury which would suggest that the majority of satellite cell activation had already taken place and had already begun to commit to myogenic differentiation. AF-CM could therefore have already led to increased satellite cell activation in the initial stages of damage providing more active cells for commitment. However, this cannot be confirmed with this data. On the other hand, a higher number of committed myoblasts would provide a greater number of cells to fuse together to form myotubes and thus accelerate myotube/fibre formation.

It was however interesting to note that the AF-EV treatment unlike the whole AF-CM led to significantly more activated Pax7⁺/MyoD⁺ cells within the damaged region compared to the vehicle treated damaged muscles. No differences were seen however in the committed Pax7⁺/MyoD⁺ cell population, unlike that seen with AF-CM treatment. These results suggest that paracrine factors within the soluble fraction of the AF-CM are overriding that of the AF-EV thus driving increased levels

of committed cells. On the other hand, the combined effects of the soluble fraction and AF-EV might be required for increasing the level of the committed cell population.

The use of bone marrow derived MSCs in previous research on C2C12 cells showed that the MSC-CM caused increased proliferation and differentiation as indicated by the increased cell numbers and then increased expression of MyoD1 and Myogenin (Nakamura et al., 2015). This effect could therefore also be caused by the AF-CM treatment. Additionally it is widely accepted that the use of an MSC secretome as a therapeutic would most probably have a large short term effect as opposed to lasting over the time of a week (Balbi et al.). The majority of EVs or solubilised proteins would already be intercepted and therefore have produced an effect within the first 24 hours. This suggests that because the AF-CM treatment took place once and on the first day of damage, its effects are most likely to have increased the proliferation and therefore the numbers of active satellite cells. This, as discussed, would provide a larger number of committed cells as seen after 5 days in these results.

AF-CM Increased the Number of blood Vessels within the Regenerating Tissue

Damage within muscle usually leads to the activation of an angiogenic programme to provide enough nutrients and oxygen to the regenerating area. An increase in the number of fibres within a given area can be accounted for by the increase in small regenerating fibres and therefore an ability to fit more fibres in the area of damage. Each fibre is dependent on the local capillary network for its supply of nutrients. In an undamaged muscle, around 500 capillaries infiltrate the TA within a mm^2 area and each fibre was shown to have about 1 capillary within its immediate vicinity as evidenced by the data in Figure 3D-E. It was however clear that although the angiogenic programme pursued following damage increased the number of what was believed to be capillaries within the given damaged area, the number of these vessels/ fibre diminished. Furthermore, AF-EV treatment instigated increased vascularisation, bringing about levels of CD31⁺ vessels significantly higher than found in the damaged control and to a level that was comparable to the non-damaged control. Similarly to what was seen with the whole AF-CM, this increase in vascularisation can be suggested as

being a major factor contributing to the enlarged regenerating fibres because of an increased supply of blood, nutrients and oxygen.

It has been shown previously that treatment with AFSC, other MSCs and their EV content promotes angiogenesis (Rahbarghazi et al., 2013, Gneccchi et al., 2016, Balbi et al., Lee et al., 2009, Lee et al., 2012a). An increase in both the level of CD31⁺ vessels in the given area as well as per fibre due to AF-CM treatment is believed to provide further nutrients and oxygen to those newly regenerating fibres. This improved vascularisation is suggested to be due to the AF-CM treatment and that it has at least in part accelerated fibre regeneration. The metabolism of regenerating fibres throughout the muscle, both within the deep and superficial area, would be hypothesised as being more similar than those of mature fibres within the two differing regions. The need for oxygen and nutrients at this stage of regeneration would therefore also be similar and accounts for newly regenerating fibres in both the deep and superficial region having been similarly positively affected by the AF-CM. Furthermore, a higher level of oxygen would maintain the oxidative metabolism of differentiating myoblasts thus accounting for higher levels of committed Pax 7⁻/MyoD⁺ cells discussed previously (Koopman et al., 2014, Folmes et al., 2011, Zhang et al., 2011, Zhang et al., 2012).

Both AF-EV and the Soluble Fraction are Important for Improved Regeneration

To further provide evidence that the soluble fraction has a key role to play in the regenerative actions of the AF-CM, mice were treated with either the whole AF-CM or one of the two fractions, AF-EV or the soluble fraction. All three AF-CM based treatments resulted in larger newly regenerating fibre CSAs across the total damaged region suggesting that key components required for this accelerated increase in CSA is shared by both fractions. This result was mirrored in the superficial region. However, in the deep region only the AF-CM and soluble fraction provided significant increases in CSA. Increases in superficial fibre size but not deep fibre size with the AF-EV fraction suggests that the AF-EV is lacking a component of the soluble fraction that is able to utilise signalling found mainly in superficial fibres. The superficial region of a healthy muscle is documented as consisting of mainly glycolytic type IIB MHC containing fast twitch fibres as opposed to the deep

region which consists mainly of oxidative fast twitch fibres containing type IIA MHC (Omairi et al., 2017). If the soluble fraction and therefore the AF-CM contain more paracrine factors that aid regeneration via metabolic pathways compared to the AF-EV they may be more suited to regenerating the deep portion of the muscle. The AF-EV on the other hand could be hypothesised to not contain these unknown factors and can only improve regeneration significantly in the glycolytic superficial region which is not as dependent on oxidative metabolism. Only AF-CM treatment created a significantly larger vascularisation compared to the damaged control and further evidences its role through the enhancement of oxidative metabolism. The variation between experiments when looking at treatment of the mice with fractions of the AF-CM solidifies the idea that the fractions alone do not provide a reliable therapeutic effect. Therefore a combination of the fractions, such as that found in the whole AF-CM, would be suggested as being the most reliable route for therapeutic treatment with a mind to accelerate regeneration following necrotic damage.

6. Chapter 6

Establishment of an NEC Intestinal Organoid Model to

Test the Regenerative Capability of AFSC CM

Introduction

Due to advances in healthcare more pre-term born infants are surviving to full term. However, because more infants are initially surviving premature birth with under-developed respiratory, immune and cardiovascular systems, the level of those being affected by NEC is increasing. There is around a 35% mortality rate in those affected. The need to identify a treatment for NEC other than just surgical resection of the affected gut, which can lead to long term health problems for the child if they do survive, is becoming ever more important. The use of AF, subsequently AFSCs and their paracrine factors has been previously suggested as a potential therapy for NEC (Zani et al., 2014). However, an AF-CM that is created in such a way that is suitable for future clinical use had not been tested. The AF-CM used here, as discussed therefore needed a model of NEC to test its regenerative capabilities and ability to inhibit any pathological affects associated with the environment of the gut in NEC patients. However, the production and use of an *in-vivo* rodent model by others that mimics NEC leads to animals presenting with an extremely severe condition that is often perceived as being too harsh to allow in the UK. Therefore the use of 3D intestinal organoids treated with either LPS or TNF- α , acting as inflammatory stimuli, was believed to be the next best option.

NEC Background

Although the causes are complex, the main reason for its onset is believed to be due to a lack of respiratory, intestinal and immune system development (Sharma and Hudak, 2013). Often an underdeveloped respiratory system causes onset of ischemia upon birth. Aggressive feeding leads to an increased demand for blood flow to the intestine, however the need for oxygen in the rest of the body reduces the oxygen levels available in the intestine, which is relatively less important than that of other organs such as the heart (Sharma and Hudak, 2013). As a consequence the gut becomes hypoxic and homeostasis of cell turnover compromised. Increased stasis eventually leads to microbial dysbiosis and the normal cross-talk between the intestinal epithelium and microflora is disrupted (Emami et al., 2009). High levels of LPS derived from the gram-negative bacterial colonisation is believed to induce a leaky intestine making the infant vulnerable to sepsis (Guo et al., 2013). An

elevated level of cytokines and inflammatory signalling not only leads to widespread apoptosis and necrosis but also triggers the infiltration of innate immune cells such as macrophages. Such cytokines include IL-6 and TNF- α (Sharma and Hudak, 2013, Zani et al., 2014, McElroy et al., 2011). Overzealous macrophages due to an immature immune system hyper-respond to the inflammation. LPS and presence of bacteria further exacerbate the pro-inflammation within the gut and therefore the cycle of inflammation and cell death is intensified.

Cell Types of the Intestine and Their Role in NEC

Severe NEC affected intestines present with extreme sloughing of the epithelial layer and therefore a loss of villi architecture (Koike et al., 2017). To some extent the severity of NEC has been postulated as being due to reduced gastric motility, which in itself is caused by a number of factors (Koike et al., 2017). The intestinal epithelial layer is composed of a number of cell types. One is the Goblet cell, which produces mucus through the production of a range of Mucins, including Mucin-2. Mucus production in the gut serves not only as a primary barrier to protect from excessive sloughing, but also acts to prevent over colonisation by bacteria, prevents direct bacteria contact with the epithelia and also aids the motility of food through the intestine. High levels of inflammatory factors, in particular TNF- α have been shown to deplete the level of mucus production within the intestine and have therefore been hypothesised as playing a key role in the induction of NEC (Ahn et al., 2005, McElroy et al., 2011).

Furthermore, stresses imposed on the intestine leading to NEC have a profound effect on the local stem cells. Although a reserve population of Bmi1 expressing stem cells have been found to exist, and rapidly proliferate to replace those lost due to stress, overwhelming, continuous and excessive inflammation is thought to exhaust the stem cell population (Yan et al., 2012, Tian et al., 2011, Zhu et al., 2013). Reduced stem cell levels due to exhaustion and cell death dramatically decreases the ability of the intestine to replace lost epithelia.

Interplay between the resident stem cell population and Paneth cells provide signalling for the stem cells to proliferate and retain a healthy population of multipotent stem cells. Short range Wnt

signalling from the Paneth cells is detected by the adjacent stem cells thus retaining stem cells in their proliferative and progenitor state (Sato et al., 2011). MyD88 signalling and its downstream effects, presumably including NF- κ B, following TLR activation triggers the production of multiple anti-bacterial factors by the Paneth cell, such as Reg-III γ (Vaishnava et al., 2008). Reduced Paneth cell numbers and their juxtacrine signalling, negatively impacts not only on the stem cell pool but also the hosts defences.

Gut motility is also regulated by mesenteric neuronal stimulation. Enteroendocrine cells within the villi secrete a range of hormones and paracrine factors that not only communicate with the local nervous system but also help to regulate normal cell homeostasis (Moran et al., 2008, Bohórquez et al., 2015). An important secreted peptide of the enteroendocrine cells is Chromogranin-A (ChA). ChA is also a pre-cursor to a number of other secreted proteins required for signalling such as vasostatin and chromostatin (D'amico et al., 2014, Rumio et al., 2012, Eissa et al., 2018). Increases in ChA in patients and models of IBD and colitis are believed to have an immuno-regulatory role (Eissa et al., 2018). Interestingly, although ChA has a low affinity for Ca²⁺, it has a high capacity to do so (Eissa et al., 2018). The ability to mop up extracellular Ca²⁺ has been suggested to play a key role in regulating the functionality of smooth muscle contractions around the gut as well as that required for T-cell inflammatory responses (Eissa et al., 2018). Oral administration of vasostatin, the N-terminal derivative of ChA, in mouse models of dextran sodium salt (DSS)-induced colitis was shown to inhibit the production of inflammatory cytokines and chemokines whilst also maintaining tight junction permeability (Rumio et al., 2012).

Disadvantages of In Vivo NEC Models

Rats induced to NEC through gavage-feeding with hyperosmolar formula, hypoxia and oral administration of LPS had been shown to have under a 20% survival at 7 days, all of which had died before 15 days (Zani et al., 2014). Due to the extremely high mortality rate of the *in-vivo* models, studies require large numbers of animals to ensure that they are statistically powerful enough even if animals die prior to experimental endpoints. It is therefore beneficial to have a model which retains

many of the cell types important within the intestine, in particular the epithelial layer of the villi and its crypts thus retaining an ability to undergo high levels of inflammation and cell death but also capable of regenerating.

Intestinal Organoids

With the knowledge that the local stem cell population within the crypts of the intestine were capable of differentiating into most of the varying cell types within the villi the idea of reconstituting this same system in culture was tested (Sato et al., 2009). Two approaches to creating mini intestinal organoids have been established. The first utilises the ability of the Lgr5⁺ stem cells to reconstitute the cell niche within a 3D matrix, such as Matrigel, whilst supplementing cultures with essential growth factors such as EGF, Noggin, and R-spondin (Sato et al., 2009). This approach either uses sorted and isolated Lgr5⁺ stem cells or develops organoids from primary isolation of intestinal crypts containing these stem cells without the need of sorting. On the other hand, iPSCs have also been shown to be effective at providing a source of intestinal like stem cell that can also reconstitute the cells found naturally *in-vivo*. iPSCs can be directed towards an endodermal lineage with Activin and then subsequently hindgut maturation with FGF-4 and Wnt3A (Spence et al., 2010, Date and Sato, 2015). Interestingly, the mesenchymal cells are also capitulated simultaneously, of which cells attach to the budding epithelia monolayer that forms from the developing spheroids. This additional mesenchymal layer provides a further intestinal niche and is thought to provide paracrine factors such as R-spondin and Wnt proteins thus promoting stem cell self-renewal (Date and Sato, 2015, Spence et al., 2010). Furthermore, iPSC derived intestinal organoids are believed to resemble foetal epithelium as opposed to the adult like epithelium created through the first method discussed (Date and Sato, 2015). In common with both systems is the ability of intestinal organoids to produce crypt like structures with villus architecture and a simple but enclosed lumen.

Intestinal Organoids for Models of NEC

The ability to create intestinal organoid systems replicating the environment of the intestine *in-vivo* meant that additional factors could be added to culture to create models of pathology or organoids.

Furthermore, stem cells used to create organoids could be isolated from transgenic mice to create transgenic organoids. In addition to this, the self-replicating ability of organoids decreases animal usage. Taking what was known about the pathology surrounding NEC, the use of LPS or hypoxia had been used to replicate the NEC condition in organoids (Chen et al., 2012, Neal et al., 2012, Egan et al., 2015). Significantly smaller organoids were found to develop under hypoxic conditions compared to those cultured under normoxia (Chen et al., 2012) Furthermore, the use of *E.coli* LPS and subsequent TLR-4 signalling was also separately shown to induce significant increases in CC3 and decreases in PCNA suggestive of increased apoptosis and decreased proliferation (Neal et al., 2012).

The use of organoids to model NEC allows the testing of AF-CM, by-passing to a certain extent the need to use the harsh as well as still developing *in-vivo* models. We wanted to first replicate what has been shown by other work, such as that produced by Neal et al, that shows LPS mimicking an NEC like cell death in organoids following LPS exposure (Neal et al., 2012). Furthermore, the use of TNF- α was also hoped to bring about a similar response. It was also hoped that differences in stress associated protein synthesis and autophagy signalling could be identified following stimulation of organoids along with AF-CM bringing about a reversal in this signalling back to that seen in unstimulated control organoids.

Results

LPS and TNF- α Stimulation of Organoids

Previous studies show the effectiveness of AFSCs to hinder the damage caused by, as well as extending life-span of those affected by the pre-term neonatal disease NEC (Zani et al., 2014). The potential of the AF-CM to treat NEC was also tested (Zani et al., 2014). An *in-vitro* 3D mouse model of the intestine was established and introduced to acute levels of inflammatory stimuli in a bid to mimic the cellular environment seen in NEC. Intestinal organoids from 6 week old mice had a lumen, villus domain and crypts all characteristic of an intestine *in-vivo* (Figure 6.1.A). Organoids were cultured with media containing either 10ng/ml TNF- α or 10 μ g/ml *E.coli* LPS from 30 minutes to 2 hours and differences in selected gene expression compared (Figure 6.1.B-E). Following treatment of organoids with TNF- α from 30 minutes to 2 hours, organoids showed a significantly elevated level of *TNF- α* gene expression compared to both the non-treated control and other tested conditions (n=3, P<0.01). After 1 hour of TNF- α treatment organoids had 12.6 times the *TNF- α* level compared to the control and over twice the level seen at 30 minute and 2 hour exposures. *TNF- α* gene expression did not significantly differ from the control between 30 minutes to 2 hours. On the other hand, treatment of organoids with LPS showed no significant alterations in *TNF- α* gene expression at 30 minute and 1 hour exposures. However, after 2 hours of LPS treatment organoids showed significantly reduced levels of *TNF- α* gene expression compared to all other treatments and in particular 69.7% less expression compared to the non-treated control organoids (n=3, p<0.05).

In the case of *TGF- β* gene expression, neither the TNF- α treatment or LPS treatment at any exposure tested showed any significant changes from the control. Furthermore, none of the treatments showed any significant differences in *TGF- β* gene expression between the different exposure timings.

Next expression of *Mucin-2* was examined. After 30 minutes exposure to TNF- α organoids showed significantly higher levels of *Mucin-2* expression compared to that of the non-treated control (n=3, p<0.05). *Mucin-2* gene expression levels were 36% higher after 1h exposure to TNF- α compared to the untreated control. Furthermore, *Mucin-2* expression after 30 minutes exposure of TNF- α was

significantly higher than that seen after 2 hours, which was 45% lower than that at 30 minutes ($n=3$, $p<0.05$). However, treatment of organoids with LPS showed no significant change in *Mucin-2* expression compared to any other treatment or length of LPS exposure.

To understand whether LPS or TNF- α had induced apoptosis, organoids were exposed to varying concentrations of LPS at 10 $\mu\text{g/ml}$, 50 $\mu\text{g/ml}$ and 100 $\mu\text{g/ml}$ LPS or 20ng/ml TNF- α for 2 hours (Figure 6.1.E). The level of cleaved- caspase-3 (CC3) protein, associated with apoptosis, was measured. The lowest concentration of LPS used (10 $\mu\text{g/ml}$) which has previously been shown to induce cell death in the organoids produced no significant changes in the level of CC3 compared to the non-treated control or other treatment groups (Egan et al., 2015). However stimulation with 50 $\mu\text{g/ml}$ LPS led to significantly higher levels of CC3 compared to both the untreated control and those treated with 10 $\mu\text{g/ml}$ LPS but also those treated with TNF- α ($n=3/ p<0.05$). Levels of CC3 after 50 $\mu\text{g/ml}$ LPS treatment were 4.8 times higher than that of the untreated control and 10 $\mu\text{g/ml}$ LPS treated organoids and 6.4 times higher than those treated with TNF- α . Additionally, treatment with 100 $\mu\text{g/ml}$ LPS significantly increased CC3 protein expression compared to that of the control, 10 $\mu\text{g/ml}$ LPS treated and TNF- α treated ($n=3$, $p<0.01$). CC3 levels after 100 $\mu\text{g/ml}$ LPS treatment were 2.5 times more than the non-treated and 10 $\mu\text{g/ml}$ LPS treated organoids and 3.3 times higher than the TNF- α treated organoids. Treatment with 20ng/ml TNF- α did not lead to significant changes in CC3 levels compared to the untreated control.

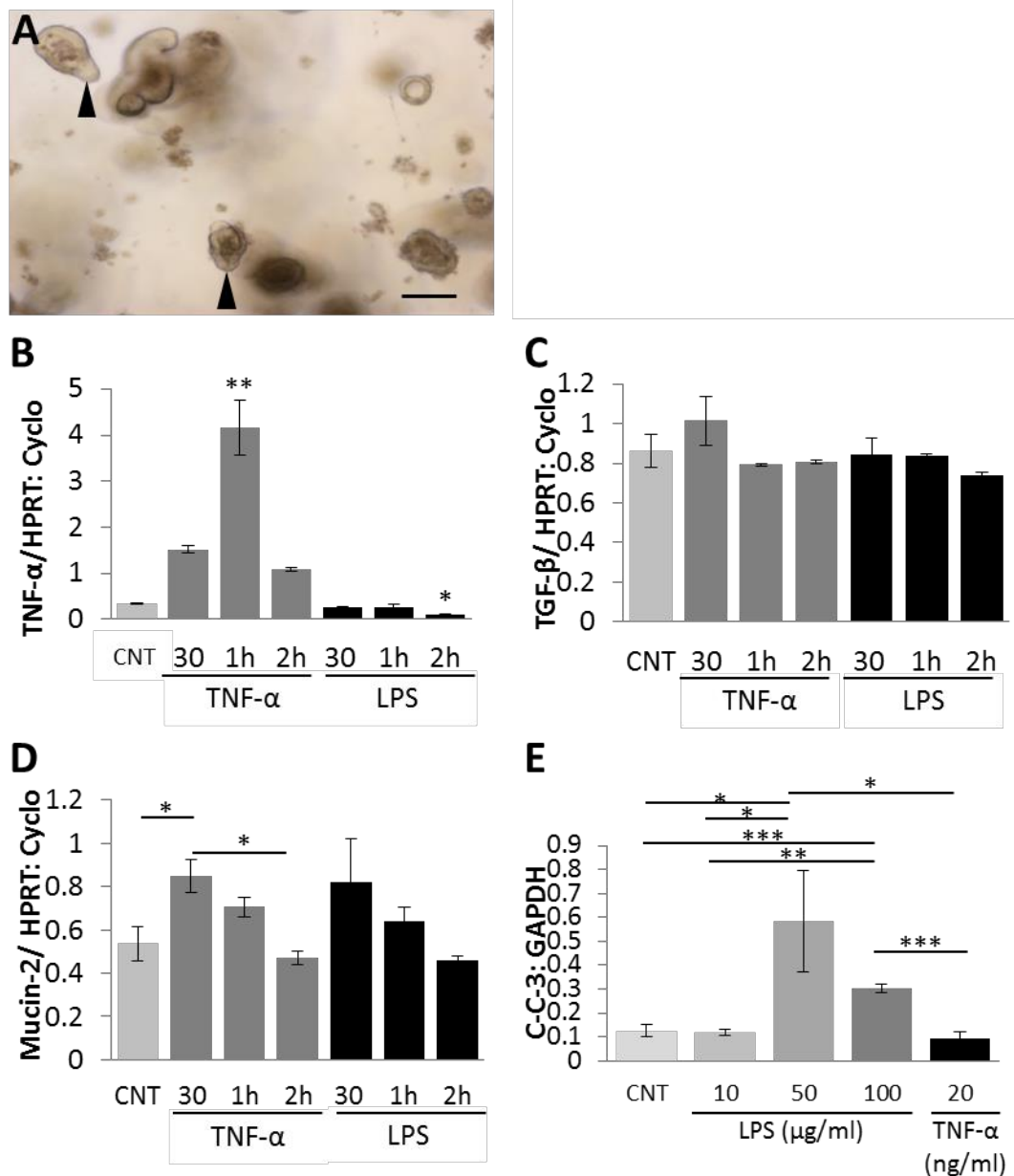


Figure 6.1: Organoids stimulated with *E. coli* LPS or TNF- α for up to 2 hours and at different concentration. (A) Organoids derived from the small intestine of C57BL/6 mice 3 days after harvest. Images a) and b) were taken at different focal points to visualise the depth of the organoids 3D morphology. (A) Scale bar representative of 100 μ m. Gene expression values of TNF- α (B), TGF- β (C) and Mucin-2 (D) in organoids stimulated with 10ng/ml TNF- α (TNF) or 10 μ g/ml LPS for either 30 minutes, 1 hour or 2 hours. (E) Protein expression of cleaved caspase-3 (CC3) in organoids stimulated with either 10 μ g/ml, 50 μ g/ml or 100 μ g/ml LPS for 2 hours. Arrows indicate crypt domains forming with the organoids. Values are expressed as means \pm SEM (n=4). p < 0.05 (*), p < 0.01 (**) or p < 0.001 (***).

Histological analysis of organoids treated with the varying concentrations of LPS for 2 hours was also carried out because of the increased CC3 seen at this time-point (Figure 6.2.A-F). Non-treated organoids and organoids treated with 10µg/ml, 50µg/ml and 100µg/ml LPS were stained for the proliferation marker Ki-67 along with the transmembrane adhesion molecule E-cadherin and nucleic marker stain DAPI. Statistical analysis showed the extent of co-localisation between the Ki-67 stain and DAPI staining. A significant increase of 42% in co-localisation was seen following the 10µg/ml LPS treatment compared to the non-treated control (n=4, p<0.05). This increase was also significantly higher than that seen following treatment with 100µg/ml LPS; 82.0% higher than the 100µg/ml treatment (n=4, p<0.05). No difference was seen between those treated with 50µg/ml and the other groups. Relative intensity of E-cadherin was analysed between groups. However, no differences between LPS treatments of the non-treated control were seen.

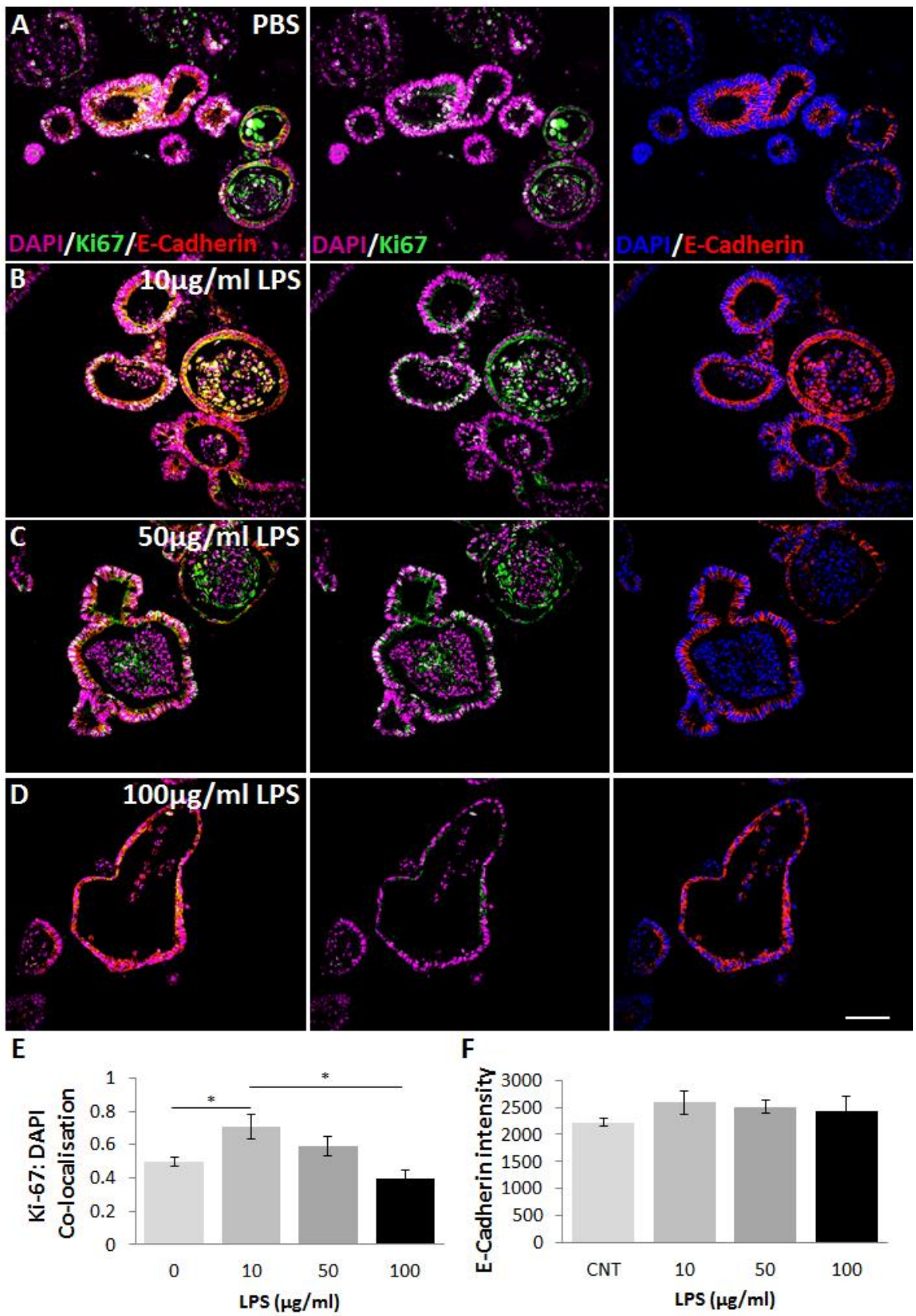


Figure 6.2

Figure 6.2: Immuno-fluorescent analysis of organoids stimulated with E.coli LPS 2 hours. Organoids stimulated with (A) PBS, (B) 10µg/ml, (C) 50µg/ml or (D) 100µg/ml LPS for 2 hours, sectioned and stained for DAPI (magenta/ blue) Ki-67 (green) and E-cadherin (red). (E) Statistical co-localisation of Ki-67 and the nucleus (DAPI) using Pearson's' R values from stained samples. (F) Comparison of E-cadherin intensity within the cellular membrane of stained organoids. (D) Scale bar is representative of 500µM. Values are expressed as means ± SEM (n=4). p < 0.05 (*), p < 0.01 (**) or p < 0.001 (***).

Following short term exposure of organoids to LPS and TNF- α , organoids were exposed to 10 μ g/ml LPS or 10ng/ml TNF- α for 48 hours (Figure 6.3.A-D). Gene expressions of key proteins associated with the cells that make up the organoids were measured. *Mucin-2*, as previously discussed plays a key role in Goblet cell function. LPS significantly increased levels of *Mucin-2* expression from the non-treated control and also led to significantly higher levels compared to the TNF- α treated organoids (n=4, p<0.05). LPS treatment after 48 hours led to 50.5% more *Mucin-2* expression than the untreated control, whilst the TNF- α treatment led to levels 49.0% of that produced with the LPS treatment. TNF- α treatment produced no significant alteration in *Mucin-2* expression compared to the non-treated control.

Gene expression of *Lysozyme-1*, a protein encoded and secreted by Paneth cells, was analysed. LPS significantly increased *Lysozyme* expression by 50.0% from the non-treated control (n=4, p<0.01). Furthermore, the expression of *Lysozyme* following LPS treatment was 26.3% higher than that produced by the TNF- α treatment (n=4, p<0.05). TNF- α treatment produced no significant alteration in *Lysozyme-1* expression compared to the non-treated control.

The gene expression of *Lgr5*, a marker of intestinal stem cells and a receptor known to promote Wnt signalling was also analysed. Stimulation of the organoids with LPS led to significantly increased levels of *Lgr5* gene expression compared to the non-treated control by 22% (n=4, p<0.05). Treatment with TNF- α also led to a significantly higher level of *Lgr5* gene expression but by 26% compared to the non-treated control (n=4, p<0.01). On the other hand, there were no significant differences in *Lgr5* expression between the LPS and TNF- α treated organoids.

Finally, the gene expression of *ChA*, a frequently used marker of enteroendocrine cells of the intestine, was analysed. No significant differences were seen between the non-treated control organoids and those treated with LPS for *ChA* expression. On the other hand, the TNF- α treatment significantly increased expression levels of *ChA* by 35.4% from the non-treated control (n=4, p<0.05). No significant differences were seen between the LPS and TNF- α treatment. Overall, it was shown

that differing concentrations of LPS and TNF- α could modulate the gene expression of organoids over differing time-points as well as altering levels of the apoptotic marker CC3.

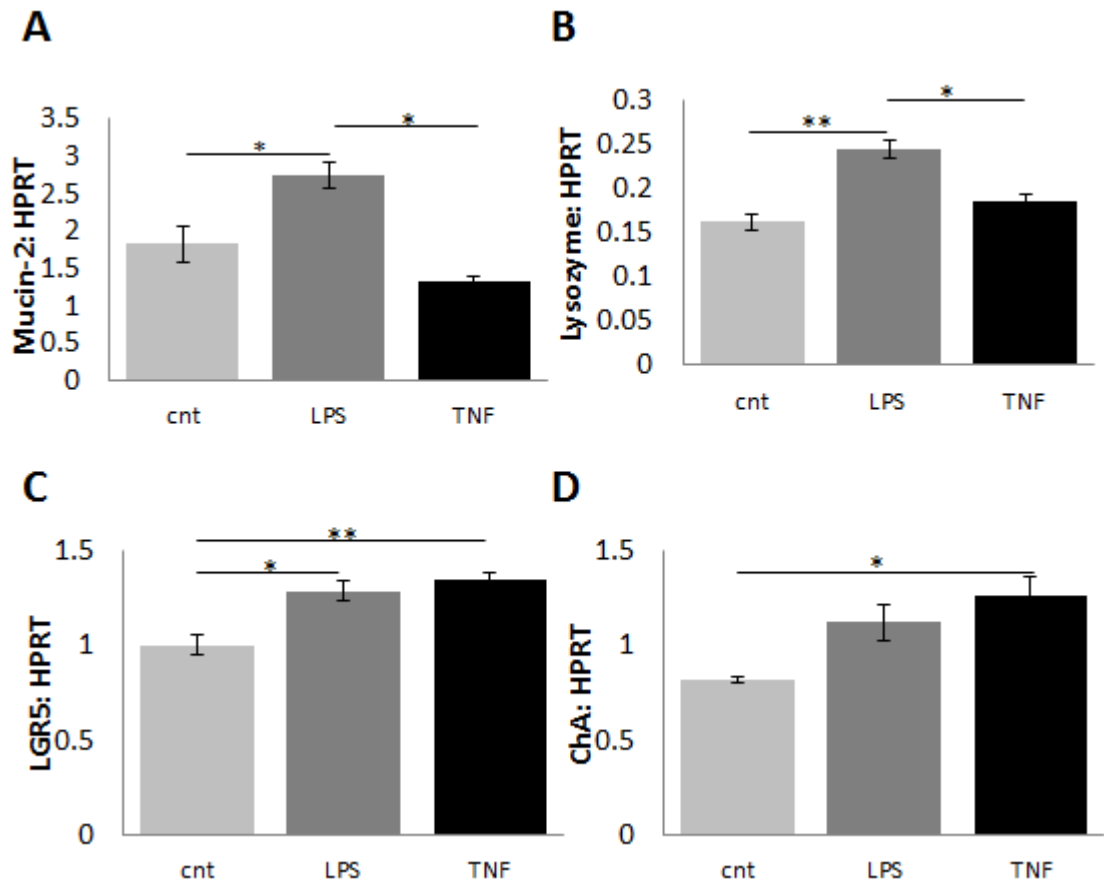


Figure 6.3: Expression of genes commonly expressed in intestinal cells within organoids following stimulation of organoids with 10 μ g/ml E. coli LPS or 10ng/ml TNF- α for 48 hours. Gene expression of (A) Mucin-2, (B) Lysozyme-1, (C) Lgr5 and (D) Chromogranin-A. Values are expressed as means \pm SEM (n=4). p < 0.05 (*), p < 0.01 (**), or p < 0.001 (***).

Gene Expression after Acute Stimulation and AF-CM Treatment

After establishing how short exposures to LPS and TNF- α affected the organoids, organoid exposures to 10ng/ml TNF- α were repeated for 30 minutes and 1 hour. However, organoids were also treated with AF-CM for 24 hours before and the time during this TNF- α exposure. Gene expression of organoids was analysed and compared between the groups (Figure 6.4.A-E). TNF- α stimulation for 30 minutes on its own did not significantly alter the levels of *TNF- α* gene expression from the control (PBS treatment). TNF- α stimulation for 30 minutes along with AF-CM treatment also showed no significant difference from the control or from the TNF- α stimulation for 30 minutes alone. On the other hand, both organoid groups stimulated with TNF- α for 1 hour showed significantly higher levels of *TNF- α* gene expression compared to the control as well as those treated with TNF- α for 30 minutes, with or without AF-CM ($n=3$, $p<0.001$). The organoids stimulated with TNF- α for 1 hour without AF-CM treatment had gene expression levels 11.5, 6.6 and 5.7 times higher than that of the PBS controls, organoids stimulated with TNF- α alone for 30 minutes and organoids stimulated with TNF- α for 30 minutes and treated with AF-CM respectively. No significant difference between the 1 hour stimulated positive control and the 1 hour stimulated AF-CM treated organoids was seen with *TNF- α* gene expression.

Analysis of *TGF- β* gene expression produced data with no significant differences between any of the treatment groups. No significant changes between groups were also seen with *Lgr5* expression, *Mucin-2* gene expression or the subsequently tested Lysozyme-1 expression.

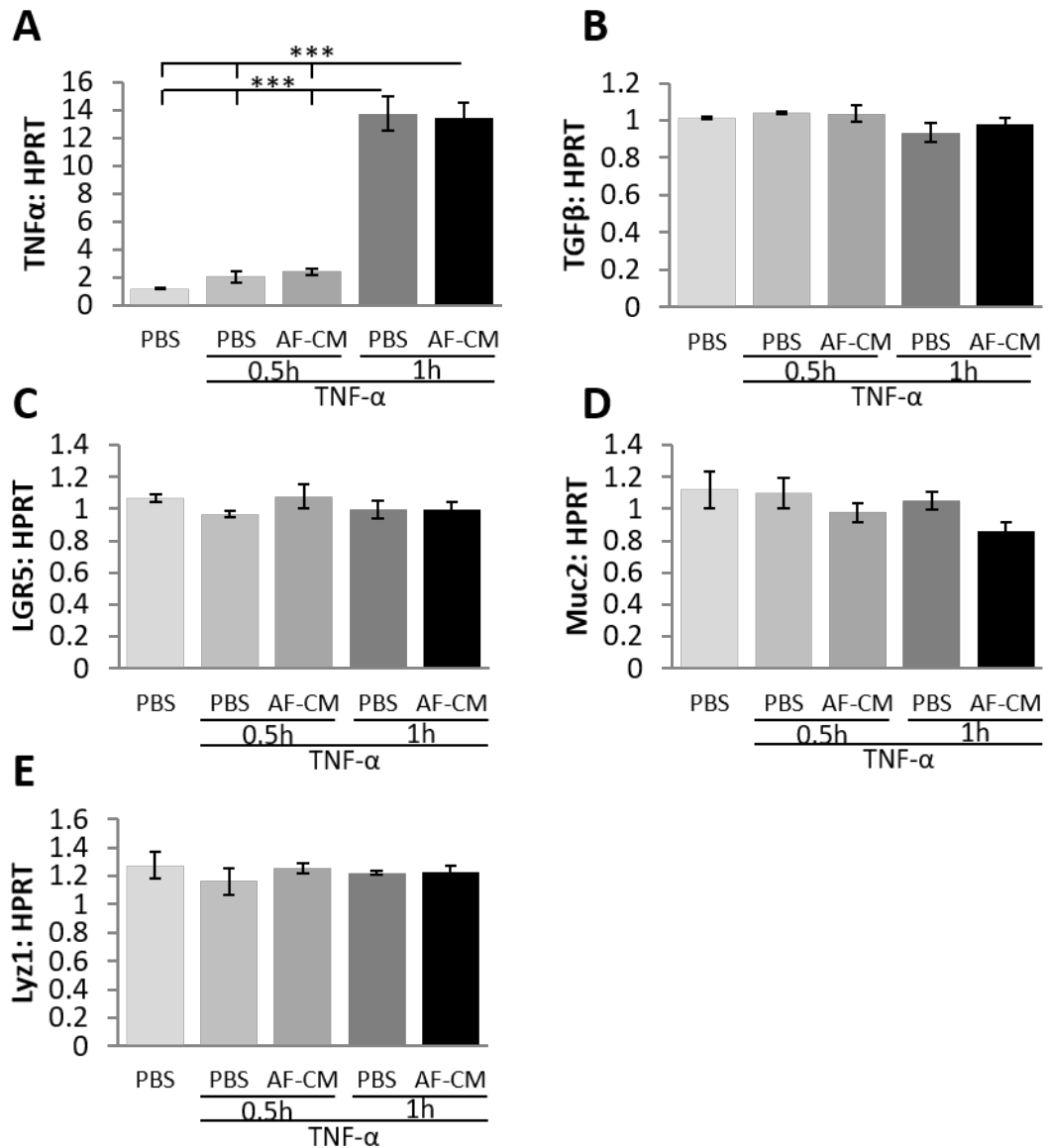


Figure 6.4: Gene expression of organoids stimulated with 10ng/ml TNF- α for 0.5 hours or 1 hour with AF-CM treatment. Gene expression of (A) TNF- α , (B) TGF- β , (C) Lgr5, (D) Mucin-2 and (E) Lysozyme-1. Values are expressed as means \pm SEM (n=4). $p < 0.05$ (*), $p < 0.01$ (**) or $p < 0.001$ (***).

Comparison of AF-CM to AF-EV and AD-CM

Next we examined the impact of AF-EV treatment on organoid gene expression and signalling following TNF- α stimulation. It was also important to ascertain whether CM produced from other stem cells, in particular adult derived stem cells, had the same potency as AF-CM in the way it affected organoids that were stimulated with TNF- α (Figure 6.5.A-D). Organoids were therefore stimulated with 10ng/ml TNF- α for 1 hour with or without treatments of AF-CM, AD-CM or AF-EV and compared to a non- TNF- α stimulated control. All groups of organoids stimulated with TNF- α presented with significantly elevated levels of *TNF- α* gene expression compared to the non-stimulated control (n=3, p<0.01 and p<0.001). Levels of *TNF- α* gene expression in organoids stimulated with TNF- α with or without treatments were at least 5.5 times higher than that of the non-stimulated control. However, none of the CM treatments differed significantly between each other or the positive control. *Mucin-2* gene expression was also measured. Only AF-EV treatment of organoids stimulated with TNF- α significantly differed from the non-stimulated control (n=3, n<0.05). AF-EV treatment with TNF- α stimulation led to a 28% increase in *Mucin-2* gene expression from the non-stimulated control. However, no significant differences in *Mucin-2* gene expression were seen between the other groups.

Due to previous results suggesting that AF-CM could alter NF- κ B signalling, organoids were examined for NF- κ B-p65. Nuclear intensity of p65 staining was measured and compared between the treatment groups discussed. Although p65 intensity did not significantly increased with TNF- α stimulation alone, all CM treatments significantly reduced nuclear intensity compared to that of the positive control (n=5, p<0.001 and 0.05). CM treatments did not show significant differences in p65 nuclear intensity between each other however reduced levels to at least 23.4% of the positive control. Treatment with AF-EV did not significantly differ from the non-stimulated control whereas AD-CM and AF-CM showed significantly lower levels of p65 nuclear intensity compared to the non-stimulated control (n=5, p<0.05).

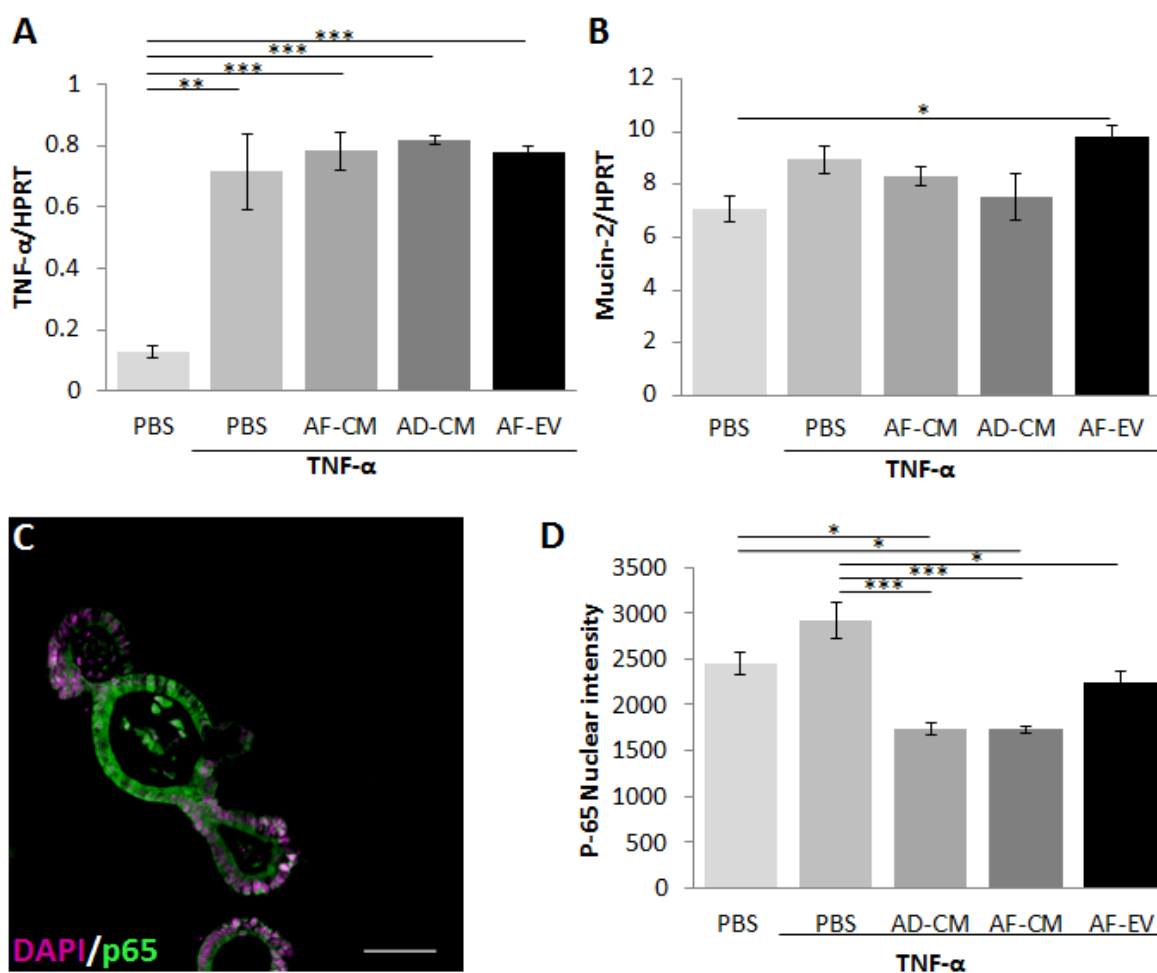


Figure 6.5: Inflammation and NF- κ B signalling in organoids stimulated with 10ng/ml TNF- α for 1 hour with AF-CM, AD-CM or AF-EV treatment. Gene expression of (A) TNF- α and (B) Mucin-2. (C) Organoid stimulated with 10ng/ml TNF- α and stained for NF- κ B-p65 (p65) (green) and DAPI (magenta) (D) Comparison of the level of NF- κ B-p65 nuclear intensity between AF-CM, AD-CM and AF-EV as a treatment following TNF- α stimulation of organoids. (C) Scale bar is representative of 500 μ M. Values are expressed as means \pm SEM (n=4). $p < 0.05$ (*), $p < 0.01$ (), $p < 0.001$ (***)**

Protein Expression after Acute LPS Stimulation and AF-CM Treatment

Protein levels were measured after organoids were stimulated with 50 μ g/ml and 100 μ g/ml LPS for 2 hours with or without AF-CM (Figure 6.6-8.). Organoids treated with 50 μ g/ml LPS with or without AF-CM presented with significantly lower levels of CC3 compared to the unstimulated control (n=4, p<0.01). Although organoids stimulated with 50 μ g/ml LPS without or with AF-CM did not differ between each other, treatments reduced CC3 protein levels by 57.2% and 51.7% from the unstimulated control. On the other hand treatment with 100 μ g/ml LPS without AF-CM treatment did lead to a significant increase in CC3 from the unstimulated control as well as being significantly higher than that of the 50 μ g/ml LPS treated organoid group (n=4, p<0.001). 100 μ g/ml LPS without AF-CM treatment in organoids showed 22.3% higher levels of CC3 compared to the unstimulated control and 66.7% higher levels compared to the 50 μ g/ml LPS without AF-CM treated organoids. Additionally, treatment of 100 μ g/ml LPS stimulated organoids with AF-CM led to a significantly reduced level of CC3 compared to the 100 μ g/ml LPS stimulated positive controls to one that was similar to the unstimulated control (n=4, p<0.05). AF-CM treatment of 100 μ g/ml LPS stimulated organoids reduced levels of CC3 by 42.3% compared to the positive control.

Protein levels of E-cadherin did not significantly differ between organoids stimulated with or without 50 μ g/ml LPS and the unstimulated control. However, stimulation with 100 μ g/ml LPS alone, organoids showed significantly elevated levels of E-cadherin compared to the unstimulated control (n=4, p<0.05). 100 μ g/ml LPS stimulated and increased E-cadherin levels from the unstimulated control by 60.3%. Furthermore, treatment 100 μ g/ml LPS stimulated organoids with AF-CM showed levels of E-cadherin similar and therefore not different to that of the unstimulated control but also not different to the positive control.

Lysozyme-1 protein levels were shown to be significantly higher in those stimulated with 50 μ g/ml LPS alone compared to the unstimulated control, by 56.0% (n=4, p,0.05). Stimulation with LPS at 50 μ g/ml also led to significantly higher levels of Lysozyme-1 compared to organoids stimulated with 100 μ g/ml LPS with or without AF-CM treatment (n=4, p<0.01 and 0.05 respectively). However,

treatment of 50µg/ml LPS stimulated organoids with AF-CM led to significantly less Lysozyme-1 protein levels compared to its positive control and to a level that did not significantly differ to the unstimulated control (n=4, p<0.01). AF-CM treatment had reduced levels to 26% of that seen in the 50µg/ml LPS stimulated positive control. No significant change in Lysozyme-1 protein levels were seen following 100µg/ml LPS stimulation with or without AF-CM compared to the unstimulated control, neither were there differences between the 100µg/ml LPS stimulated groups.

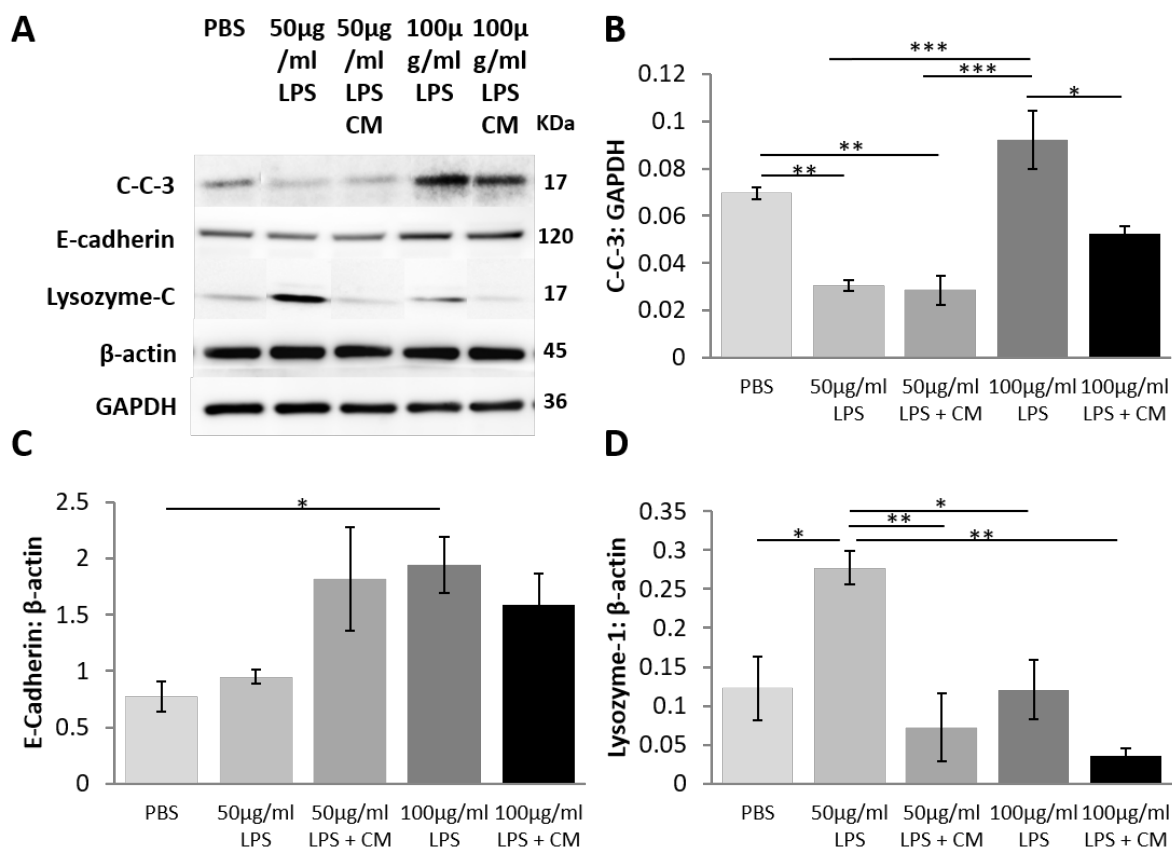


Figure 6.6: Protein expression of organoids stimulated with either 50µg/ml or 100µg/ml E.coli LPS for 2 hours and treated with AF-CM. (A) Western blots of protein analysed. Protein expression of (B) cleaved Caspase-3 (CC3) (C) E-cadherin and (D) Lysozyme. Values are expressed as means ± SEM (n=4). $p < 0.05$ (*), $p < 0.01$ () or $p < 0.001$ (***).**

Protein Synthesis Signalling after Acute LPS Stimulation

Stress associated with NEC affects the function of the endoplasmic reticulum, in particular following maternal separation (Li et al., 2016). Any stress associated with the endoplasmic reticulum would potentially affect protein synthesis, thus potentially affecting autophagy related pathways. Key proteins involved in protein synthesis, as well as some known to cross talk with autophagy signalling, investigated (Figure 6.7.A-N). A summary of results can be found in Table 6.1. The size of a cells nucleolus, were often indicative of the level of rRNA and therefore mRNA translation, can be determined with the nucleoli marker Fibrillarin. Levels of Fibrillarin protein were also examined and the 50µg/ml LPs with AF-CM treatment led to a significant decrease from the positive control by 52.6% (n=4, p<0.05). Additionally, the 100µg/ml LPS alone showed significantly lower levels of Fibrillarin compared to the 50µg/ml LPS stimulation alone by 58.1% (n=4, p<0.05).

No significant changes between groups were seen for the key protein synthesis regulating kinase AKT, its phosphorylated (pAKT) state levels or the calculated ratios from the two states. Another regulator of many signalling pathways and in particular protein breakdown is FOXO3a. pFOXO3a levels were shown to be significantly increased from the unstimulated control when organoids were stimulated with 50µg/ml LPS (n=4, p<0.05). Furthermore, this increase was shown to drive levels of FOXO3a significantly higher than its AF-CM treated counterpart but also of organoids stimulated with 100µg/ml LPS with or without AF-CM treatment (n=4, p<0.01). 50µg/ml LPS alone increased FOXO3a levels up by 50.0% from the unstimulated control and were 62.8% higher than the 50µg/ml LPS AF-CM treated organoids. Additionally, 50µg/ml LPS led to levels being 71.4% and higher than organoids stimulated with 100µg/ml LPS. The 50µg/ml LPS stimulated AF-CM treated organoids had levels of FOXO3a similar to that of the unstimulated control. No significant differences were however seen between the two 100µg/ml LPS stimulated groups of organoids or to the unstimulated control. On the other hand no differences were seen between any of the groups when looking at the levels of un-phosphorylated FOXO3a. Upon calculating pFOXO3a/ FOXO3a ratios a significantly larger value compared to the unstimulated control was seen for the organoids stimulated with 50µg/ml LPS alone (n=4, p<0.05). This value was also significantly higher than that of 100µg/ml LPS stimulated organoids

without AF-CM treatment (n=4, p<0.05). Calculated ratios for 50µg/ml LPS stimulation were 81.5% and 93.7% larger than that of the unstimulated control and 100µg/ml LPS stimulated organoids without AF-CM treatment respectively.

4EBP-1, which inhibits mRNA translation until it becomes phosphorylated, was also investigated. p4EBP-1 was significantly decreased from the control by 45.1% with 100µg/ml LPS alone (n=4, p<0.01). This increase was also significantly lower than those stimulated with the lower concentration of LPS and treated with AF-CM (n=4, p<0.01). Levels of 4EBP-1 were significantly decreased with 100µg/ml LPS alone by 84.6% from the control (n=4, p<0.05). Although the level achieved from 50µg/ml LPS stimulation alone did not differ from the control its levels were significantly higher than the other stimulated groups by at least 55.6% (n=4, p<0.05 and <0.001). On the other hand regarding the ratios of p4EBP-1/ 4EBP-1, none of the groups differed from each other or the control.

Additionally, analysis of the protein synthesis regulator Eif2α and its phosphorylated state pEif2α showed no significant differences between the treatment groups or the control. However upon calculating the ratio between these two protein states, pEif2α/ Eif2α, it was found that organoids stimulated with 50µg/ml LPS alone were 12.2 times lower than and had significantly lower calculated ratios compared to the unstimulated control (n=4, p<0.05). No other calculated ratios showed any significant differences between groups.

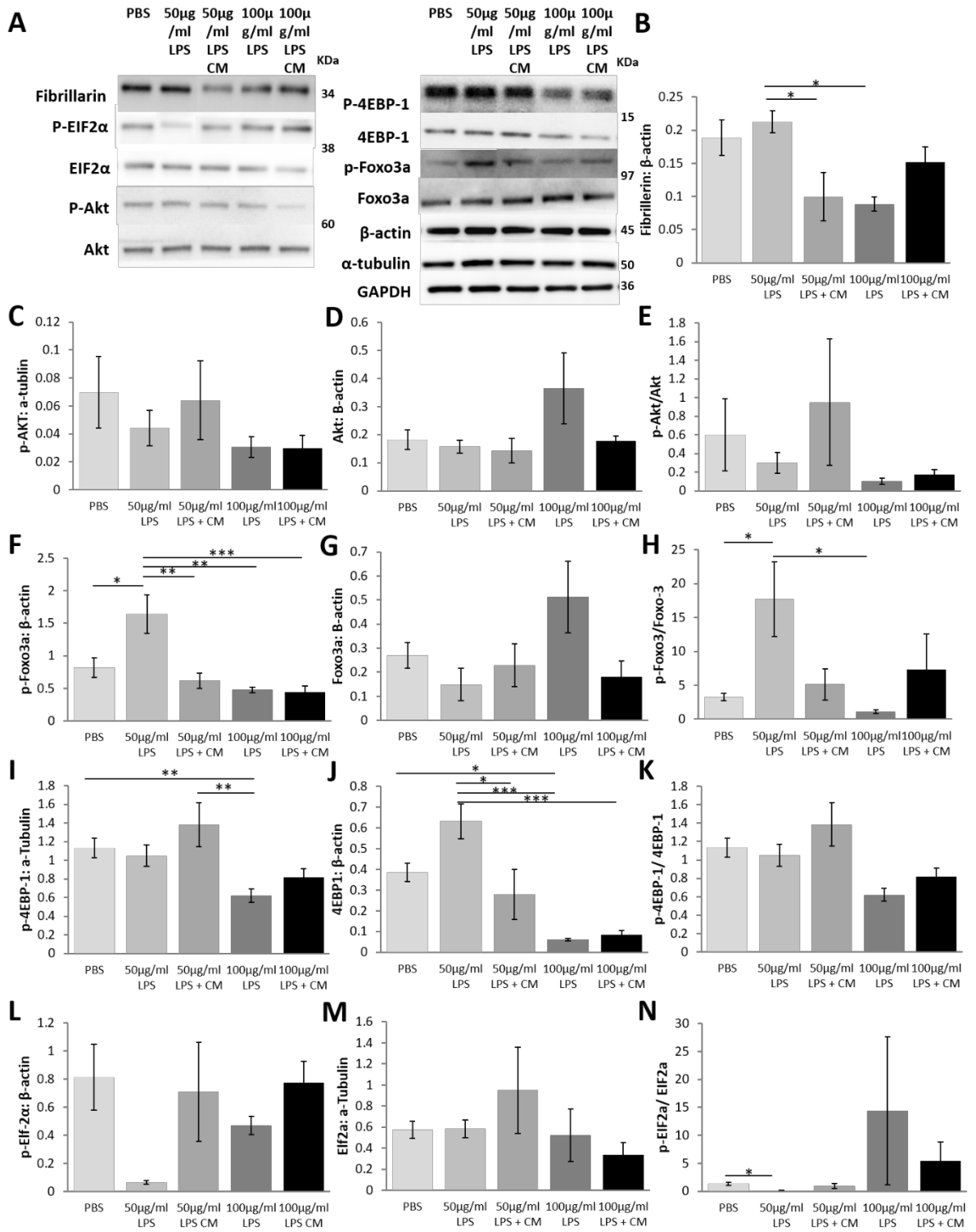


Figure 6.7

Figure 6.7: Expression of protein synthesis signalling proteins in organoids stimulated with either 50µg/ml or 100µg/ml E.coli LPS for 2 hours and treated with AF-CM. (A) Western blots of proteins analysed. Protein expression of **(B)** Fibrillarin. Protein expression of **(C)** pAkt, **(D)** Akt and **(E)** the levels of calculated pAkt/ Akt ratios. Protein expression of **(F)** pFoxo3a, **(G)** Foxo3a and **(H)** the levels of calculated pFoxo3a/ Foxo3a ratios. Protein expression of **(I)** p4EBP-1 and **(J)** 4EBP-1 and **(K)** the levels of calculated p-4EBP-1/ 4EBP-1 ratios. Protein expression of **(L)** pEif2α, **(M)** Eif2α and **(N)** the levels of calculated pEif2α / Eif2α ratios. Values are expressed as means ± SEM (n=4). p < 0.05 (*), p < 0.01 (**) or p < 0.001 (***)

Autophagy Signalling after Acute LPS Stimulation

Autophagy signalling was then analysed (Figure 6.8.A-D). p62, also known as sequestosome 1 (SQSTM 1), is often used to gauge the degree of autophagy. None of the treatment groups tested significantly affected p62 levels. Autophagy signalling can often occur in response to stress as a mechanism to clear unwanted and damaged organelles (Nichenko et al., 2016, Garcia-Prat et al., 2016). LC3BII/ LC3BII ratios showed no significant differences from the unstimulated control. On the other hand, AF-CM treatment of 50µg/ml LPS stimulated organoids had significantly higher LC3BII/ LC3BI compared to their positive control by 50% (n=4, p<0.05). Furthermore, AF-CM treated 50µg/ml LPS stimulated organoids presented with significantly higher values compared to the 50µg/ml LPS stimulated positive controls but did not significantly differ to their own positive control. Finally, C/EBP homologous protein (CHOP) was analysed. Levels of CHOP were significantly reduced from the control by at least 79.4% when organoids were stimulated with 100µg/ml LPS with or without AF-CM treatment (n=4, p<0.01). No difference in CHOP levels was found between the treatment groups.

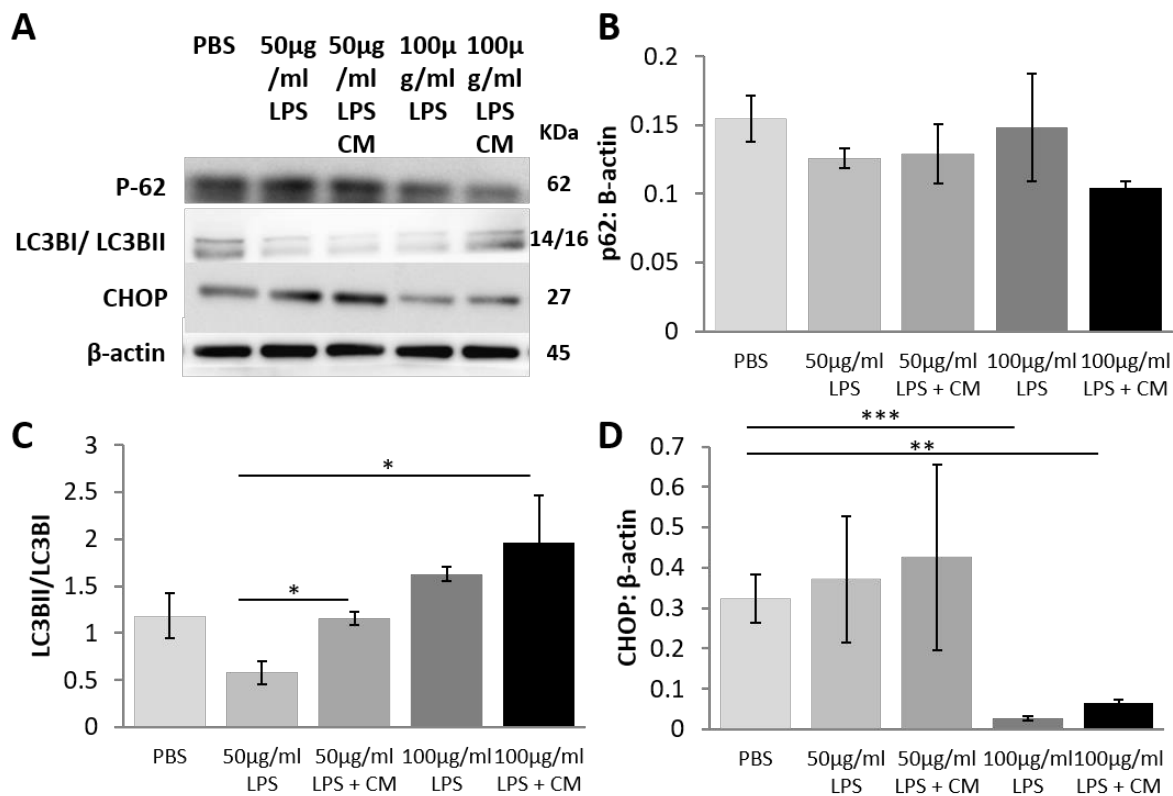


Figure 6.8: Expression of autophagy signalling proteins in organoids stimulated with either 50µg/ml or 100µg/ml E.coli LPS for 2 hours and treated with AF-CM. (A) Western blots of proteins analysed. Protein expression of (B) p62, (C) calculated ratios of LC3BII/ LC3BI and (D) CHOP. Values are expressed as means \pm SEM (n=4). $p < 0.05$ (*), $p < 0.01$ () or $p < 0.001$ (***).**

Gene Expression after 24 hour Long Stimulation and AF-CM Treatment

Organoids were then stimulated for 24 hours with one of two pro-inflammatory proteins, 10ng/ml TNF- α or 10 μ g/ml LPS and their gene expression levels examined after AF-CM treatments (figure 6.9.A-G). A summary of results can be found in Table 6.1. First the gene expression of the inflammatory cytokine *TNF- α* was analysed. TNF- α stimulation with and without AF-CM treatment led to a significant increase in *TNF- α* gene expression compared to the non-stimulated, although differences between the two TNF- α stimulated groups was not (n=4, p<0.001). TNF- α stimulation with and without AF-CM treatment increased *TNF- α* gene expression by 88.1% and 84.3% respectively.

TGF- β gene expression was next investigated and found that TNF- α stimulation significantly increased its expression by 35.5% compared to the control (n=4, p<0.001). AF-CM treatment of organoids stimulated with TNF- α increased its expression by another 8.3%, totalling 43.8% higher gene expression compared to the unstimulated control and 12.9% higher than that of the positive control. (n=4, p<0.05). Although the LPS stimulation alone didn't significantly alter *TGF- β* gene expression from the control, the AF-CM treated counterpart was significantly less than the unstimulated control and LPS stimulated control (n=4, p<0.01). AF-CM of LPS stimulated organoids reduced their *TGF- β* gene expression by 20.0% from the unstimulated control and 23.4% from the positive control.

Angiogenesis associated genes related to the VEGF group of proteins were next analysed. Gene expression of *VEGFA*, which binds to both VEGFR1 and VEGFR2, was not altered in any of the tested groups. Furthermore, gene expression of *VEGFB*, known to bind only to VEGFR1, also was not changed by treatment.

Analysis into the level of *Lgr5* gene expression revealed that all treatment groups had significantly lower levels compared to the unstimulated control (n=4, p<0.001). At the very least, in the case of the TNF- α stimulated organoids without AF-CM treatment, *Lgr5* expression levels were reduced by

19.0% from the control. However, no significant changes within and between the two TNF- α stimulated groups or LPS stimulated groups were detected.

In the case of the Goblet cell specific *Mucin-2* gene expression, TNF- α stimulation reduced levels significantly from the unstimulated control by 25.2% (n=4, p<0.05 and <0.001). However, AF-CM treatment made no difference to its expression. AF-CM treatment of those stimulated with TNF- α had led to a significantly smaller level of *Mucin-2* gene expression compared to its positive control (n=4, p<0.05). Addition of AF-CM treatment reduced the level from the unstimulated control by 53.2%, which was 37.3% less than that of the organoids stimulated with TNF- α but without AF-CM treatment. Additionally, LPS stimulation significantly reduced *Mucin-2* gene expression levels (n=4, p<0.001). However, AF-CM treatment did not bring gene expression back towards normal levels. The LPS stimulation had reduced expression levels by at least 48.6% in the case of the LPS stimulation alone.

Finally, analysis of *Lysozyme-1* gene expression was performed. TNF- α stimulated organoids showed significant reductions in gene expression compared to the control (n=4, p<0.01 and <0.001). However, AF-CM did not change expression from this level. Reductions from the unstimulated control with TNF- α stimulation was at least 23.6%. In addition, the LPS stimulation alone significantly reduced *Lysozyme* gene expression by 16.3% from the control (n=4, p<0.05). No significant differences between the two LPS stimulated groups were seen either however the organoids stimulated with TNF- α and had been treated with AF-CM presented with significantly lower levels of *Lysozyme-1* expression compared to both LPS stimulated organoid groups by at least 18.5% (n=4, p<0.05 and <0.01).

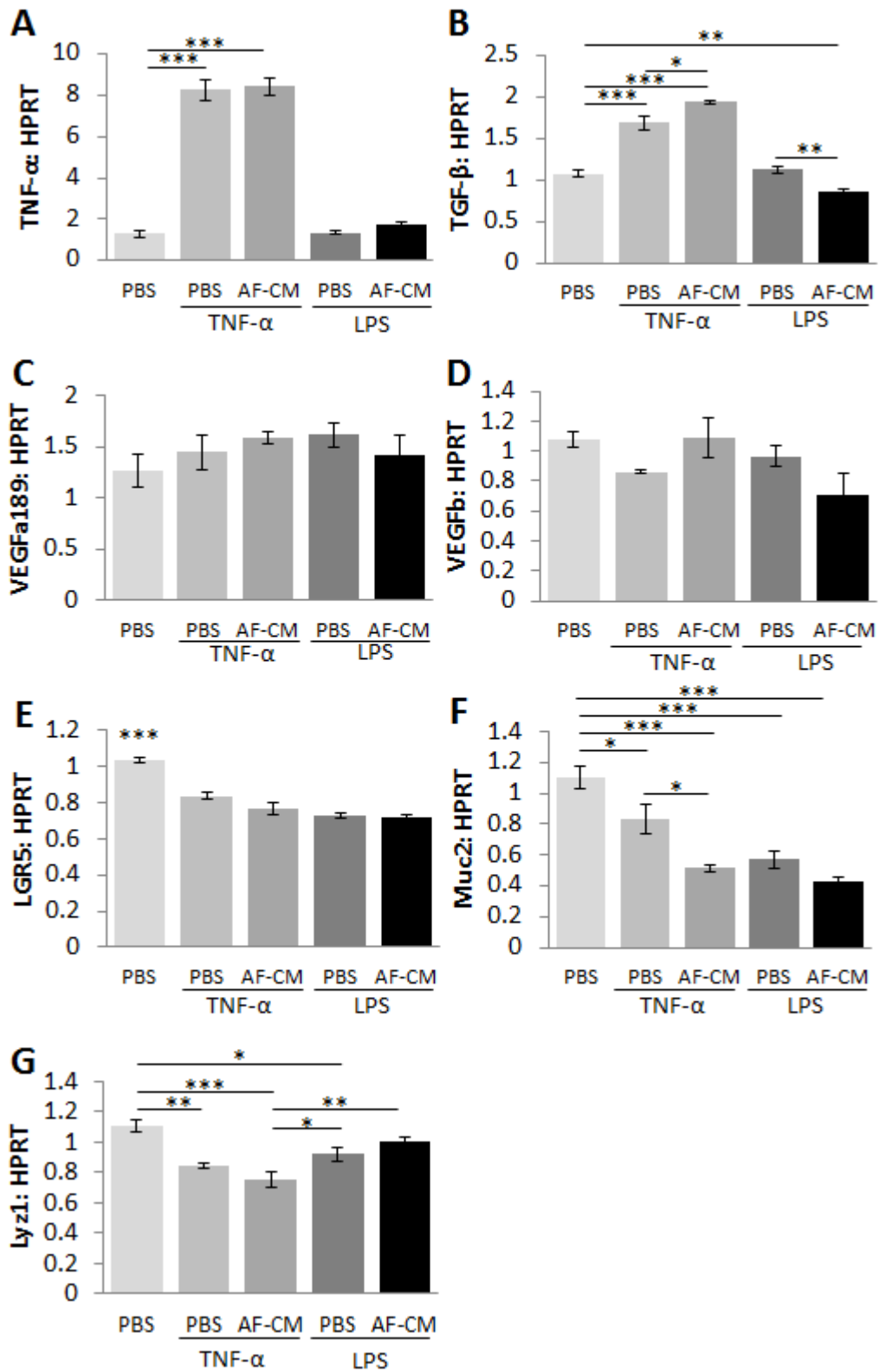


Figure 6.9

Figure 6.9: Gene expression in organoids stimulated with either 10ng/ml TNF- α or 10 μ g/ml E.coli LPS for 24 hours and treated with AF-CM. Gene expression of (A) TNF- α , (B) TGF- β , (C) VEGFa189, (D) VEGFb, (E) LGR5, (F) Mucin-2 and (G) Lysozyme-1. Values are expressed as means \pm SEM (n=4). p < 0.05 (*), p < 0.01 (**) or p < 0.001 (***)

AF-CM Treatment of 48 hour LPS or TNF- α Stimulated Organoids

Timings of organoid stimulation with a higher concentration of 50 μ g/ml LPS and 10ng/ml TNF-stimulation were further increased to 48h to understand if protein levels could be further altered by the stimuli and whether AF-CM could inhibit these changes (Figure 6.10.A-D). A summary of results can be found in Table 6.1. In addition to protein levels, the level of TNF- α gene expression was measured to understand if these changes could be related to inflammatory signalling (Figure 6.10.E). Mucin-2 gene expression was also measured to provide a read-out of Goblet cell activity in the organoids after this longer stimulation period with or without AF-CM treatment (Figure 6.10.F). In relation to gene expression values organoids were stimulated with only TNF- α and the AF-CM treatment was compared to AD-CM and AF-EV to identify whether AF-CM provided a more potent effect than AF-AD and if AF-EV provided the effect of AF-CM if any.

In the case of CC3 protein levels LPS stimulation with or without AF-CM treatment led no significant change from the unstimulated control. However, E-cadherin was significantly reduced from both the control and LPS positive control with AF-CM treatment by 41.3% and 36% respectively (n=4, p<0.05). On the other hand, both LPS and TNF positive controls treatment did not differ in E-cadherin expression from the unstimulated control. Regarding CC3, stimulation with TNF- α alone prompted a significant increase in CC3 compared to the LPS stimulated organoids by at least 60.0% (n=4, p<0.01 and <0.05). This increase was also shown to be significantly higher than that of the TNF- α stimulated AF-CM treated organoids, which although showed a similar level of CC3 to the unstimulated control was 60% less than the TNF- α stimulated groups CC3 level too (n=4, p<0.05). However, the AF-CM treated TNF- α stimulated organoids showed significantly higher levels of E-cadherin compared to the TNF- α stimulation alone by 40.6% (n=4, p<0.05). In relation to Lysozyme-1 protein levels, all groups of organoids showed significantly lower levels of protein compared to the unstimulated control (n=4, p<0.05, <0.01 and <0.001). LPS stimulation alone had reduced levels by 42.0% whilst the addition of AF-CM treatment had reduced levels by 43.0%. Moreover, TNF- α stimulation alone and with AF-CM treatment reduced Lysozyme-1 protein levels by 59.3% and 74.1% respectively.

Analysis of the *TNF- α* gene expression concluded that the organoids stimulated with *TNF- α* regardless of CM treatment showed significantly elevated expression (n=4, p<0.01 and <0.001). *TNF- α* stimulation had increased *TNF- α* gene expression by at least 94%. Furthermore, only the organoid group treated with AF-CM showed significant increases in *Mucin-2* expression from the AD-CM treated organoids (n=4, p<0.05). The data here showed a 41.0% increase from the unstimulated control. None of the other treatment groups differed significantly from each other or the unstimulated control.

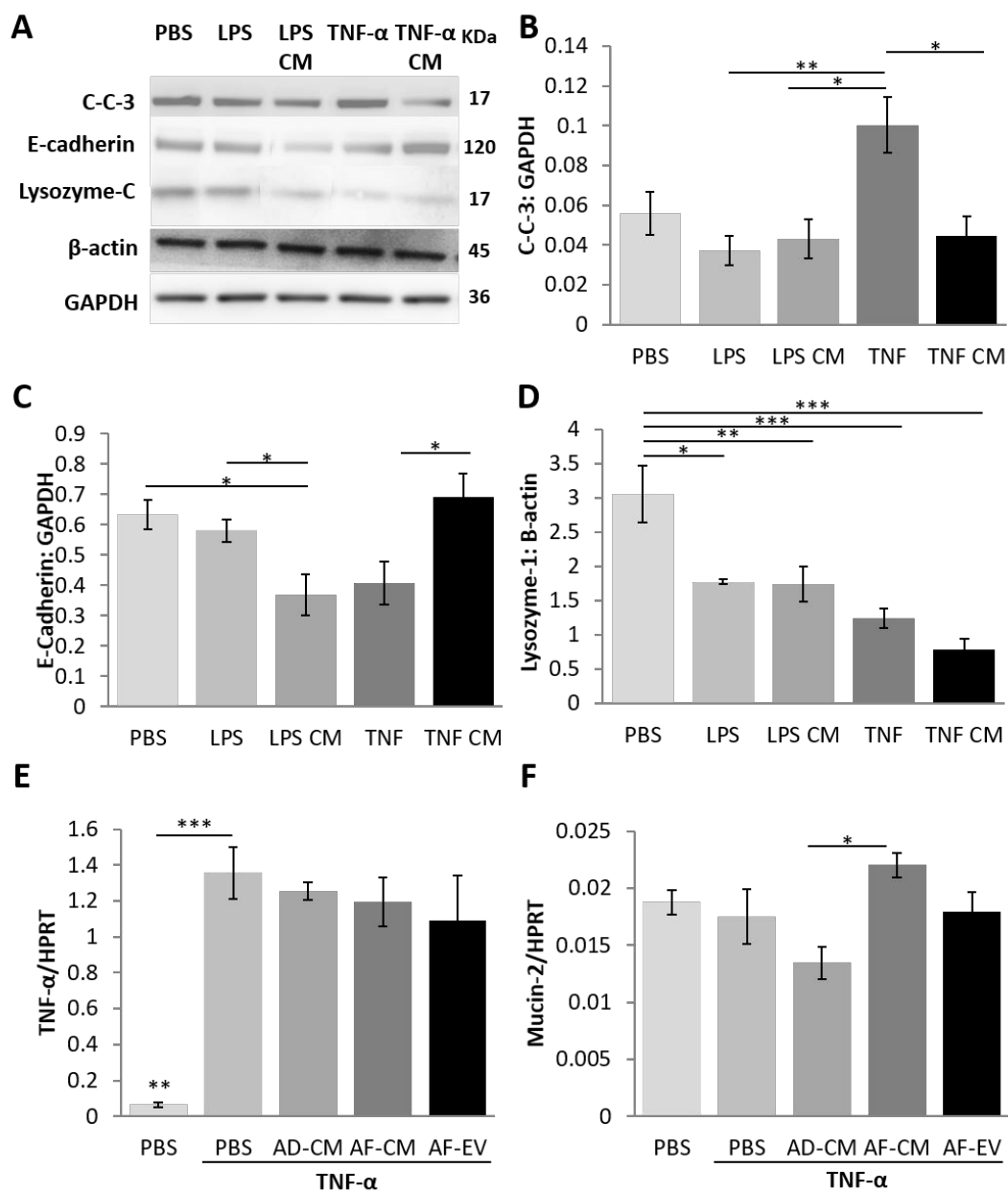


Figure 6.10: Protein and gene expression of organoids stimulated with either 50 μ g/ml E.coli LPS or 10ng/ml TNF- α for 48 hours and treated with AF-CM. (A) Western blots of proteins analysed. Protein expression of (B) cleaved Caspase-3 (CC3), (C) E-cadherin and (D) Lysozyme. Gene expression of (E) TNF- α and (F) Mucin-2. Values are expressed as means \pm SEM (n=4). p < 0.05 (*), p < 0.01 () or p < 0.001 (***).**

Protein Synthesis and Autophagy in 48 hour Stimulated Organoids

Continuing from the 48 hour experiment described further western blots were carried out to analyse key autophagy and protein synthesis signalling pathway related proteins (Figure 6.11.A-N and 6.12.A-E). A summary of results can be found in Table 6.1. Fibrillarin levels did not differ between the control and positive controls. However, the level of Fibrillarin was significantly lower in organoids stimulated with LPS and treated with AF-CM compared to LPS alone by 29.3% (n=4, p<0.05). Levels in organoids with TNF- α stimulation alone also had lower levels compared to the LPS AF-CM treated organoids by 12.2% (n=4, p<0.05).

No significant differences were found between any of the tested groups of organoids when looking at levels of AKT, pAKT/ AKT, 4EBP-1, p4EBP-1/ 4EBP1, EIF2 α , pEIF2 α or pEIF2 α / EIF2 α .

On the other hand, LPS stimulation alone led to a significant decrease in the level of pAKT from the control by 72.7% (n=4, p<0.01). This reduction was also shown to be significantly less than that of organoids also stimulated with LPS but treated with AF-CM by 65.9%. The level of pAkt in LPS stimulated AF-CM treated organoids was not dissimilar to that of the unstimulated control.

AF-CM treatment of LPS stimulated organoids showed a significant increase on FOXO3a from the unstimulated control by 86.2%, its corresponding positive control by 78.9% as well as that seen in the AF-CM treated organoids stimulated with TNF- α by 61% (n=4, p<0.001). Furthermore, the TNF- α stimulation alone significantly increased levels from the control by 82% (n=4, p<0.001). Treatment of the TNF- α stimulated organoids led to a significant decrease in FOXO3a by 48.9% to a level similar to that of the unstimulated control (n=4, p<0.05). Analysis of pFOXO3a showed no significant changes with LPS stimulation until AF-CM treatment was carried out, increasing levels by 23.8%, which was also significantly higher than those produced by organoids stimulated with TNF- α and treated with AF-CM by 68.5% (n=4, p<0.05). The addition of AF-CM treatment to LPS stimulated organoids and both TNF- α stimulated groups of organoids had significantly lower pFOXO3a/ FOXO3a ratios compared to the control (n=4, p<0.05). Those that did significantly differ from the unstimulated control were at least 85.2% lower but did not significantly differ from each other. AF-CM treated

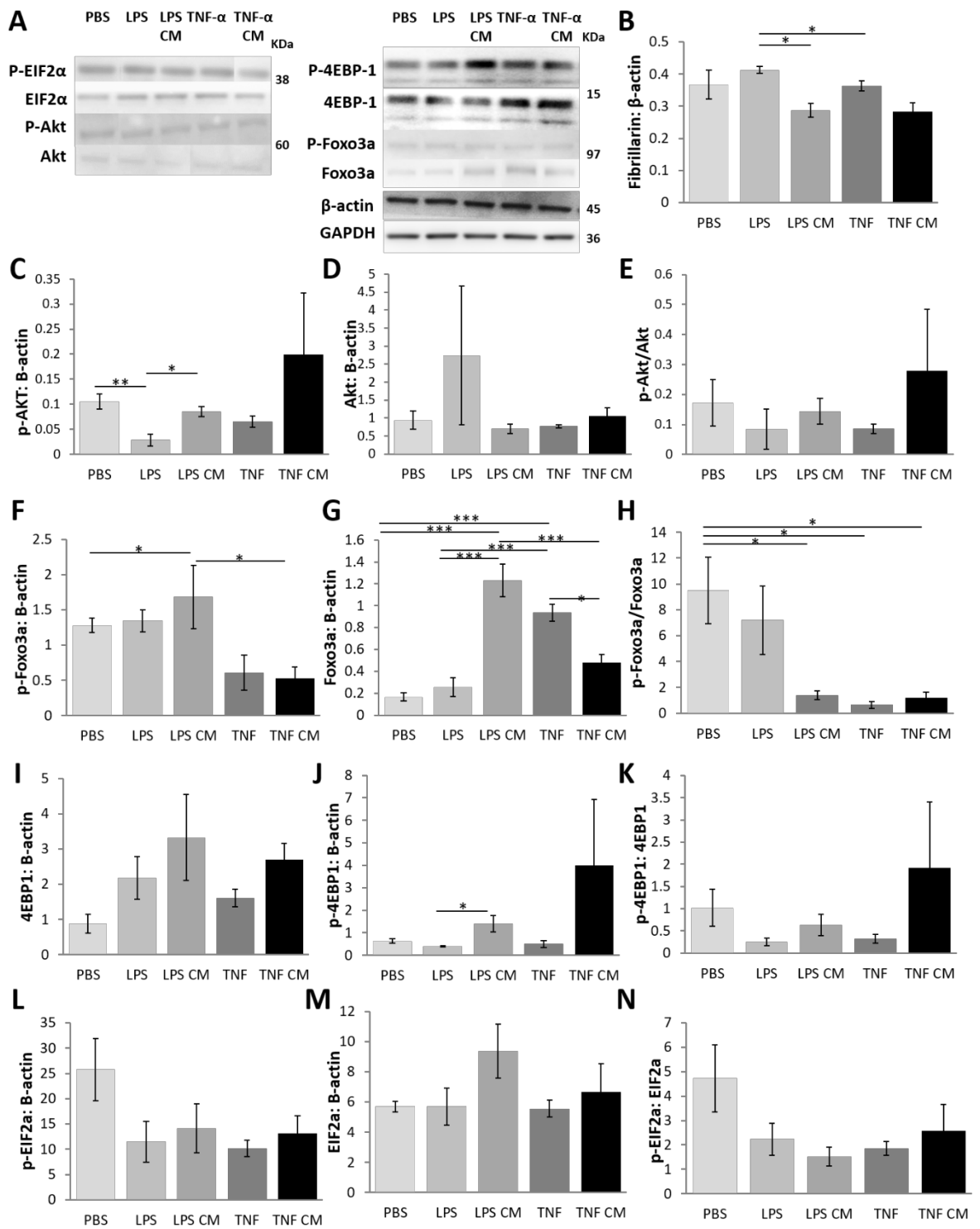


Figure 6.11

Figure 6.11: Expression of protein synthesis signalling proteins in organoids stimulated with either 50µg/ml E.coli LPS or 10ng/ml TNF-α for 48 hours and treated with AF-CM. (A) Western blots of proteins analysed. Protein expression of (B) Fibrillarlin. Protein expression of (C) pAkt, (D) Akt and (E) the levels of calculated pAkt/ Akt ratios. Protein expression of (F) pFoxo3a, (G) Foxo3a and (H) the levels of calculated pFoxo3a/ Foxo3a ratios. Protein expression of (I) p4EBP-1 and (J) 4EBP-1 and (K) the levels of calculated p4EBP-1/ 4EBP-1 ratios. Protein expression of (L) pEif2α, (M) Eif2α and (N) the levels of calculated pEif2α / Eif2α ratios. Values are expressed as means ± SEM (n=4). p < 0.05 (*), p < 0.01 () or p < 0.001 (***)**.

organoids that had been stimulated with LPS had significantly higher levels of p4EBP1 compared to its positive control by 71.6% (n=4, p<0.05).

Regarding autophagy (Figure 6.12.A-E), p62 protein levels showed significant increases from the control with AF-CM treatment in the LPS stimulated organoids (n=4, p<0.05). AF-CM treatment had increased levels from the norm following LPS stimulation by 55.1%. Calculated ratios for LC3BII/LC3BI were significantly higher for organoids stimulated with TNF- α and treated with AF-CM compared to those stimulated with LPS and treated with AF-CM by 42.9% (n=4, p<0.05). No differences were observed between other treatment groups and the control. Levels of BIP were significantly decreased from the control by 78.0% with the TNF- α AF-CM treatment (n=4, p<0.05). However the level of BIP after this treatment did not differ from its positive control or that of the LPS stimulated organoids. On the other hand, the level of CHOP was significantly decreased by the LPS AF-CM treatment by 45.2% (n=4, p<0.05). TNF- α stimulation with or without AF-CM treatment also decreased levels of CHOP from the control by at least 69.0% (n=4, p<0.001). The TNF- α stimulation with or without AF-CM showed levels of CHOP significantly lower than that of the LPS stimulation alone by at least 56.7% (n=4, p<0.05).

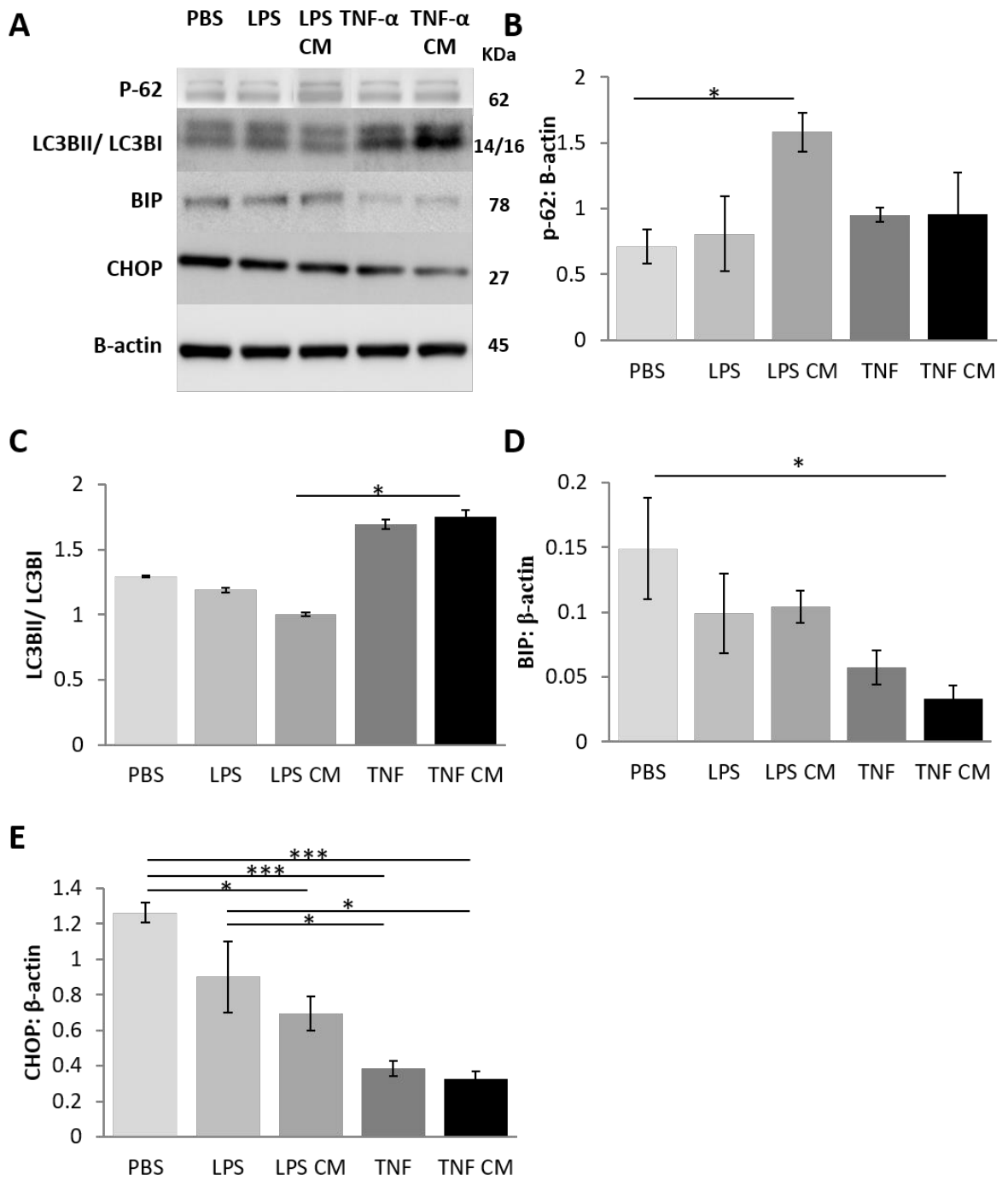


Figure 6.12: Expression of autophagy signalling proteins in organoids stimulated with either 50 μ g/ml E.coli LPS or 10ng/ml TNF- α for 48 hours and treated with AF-CM. (A) Western blots of proteins analysed. Protein expression of (B) p62, (C) calculated ratios of LC3BII/ LC3BI, (D) BIP and (E) CHOP. Values are expressed as means \pm SEM (n=4). p < 0.05 (*), p < 0.01 () or p < 0.001 (***).**

Immuno-histological Analysis of 72 hour Stimulated Organoids

In a bid to further mimic the inflammatory and damaging conditions found in NEC without the need to passage the organoids, the time frame for 50 μ g/ml LPS and 10ng/ml TNF- α stimulation was stretched to 72h. Once again stimulated organoids were also treated with or without AF-CM. Firstly immune-fluorescent analysis of the organoids was conducted and they were therefore stained for nucleic acid (DAPI), Lysozyme and E-cadherin (Figure 6.13.A-G).

From the images it is apparent that lysozyme staining is restricted to the crypts of the organoids. As lysozyme is secreted by the Paneth cells, the densometric level of lysozyme per Paneth cell was calculated (Figure 6.13.F). The only treatment group to significantly differ from that of the unstimulated control were the 10ng/ml TNF- α stimulated AF-CM treated organoids, in which levels of Lysozyme/ Paneth cell were reduced by 60.3% (n=4, p<0.05). Furthermore, the TNF- α stimulated AF-CM treated levels were significantly lower than its positive control as well as the two LPS stimulated groups of organoids alone and with AF-CM treatment (n=4, p<0.01, <0.05 and <0.01).

E-cadherin intensity was also analysed as a measure of barrier function, known to be affected in NEC (Guo et al., 2013, McElroy et al., 2011, Khailova et al., 2009). LPS stimulation showed no change in E-cadherin intensity from the control. However stimulation with TNF- α alone led to a significant reduction in E-cadherin intensity (n=4, p<0.01). Levels following TNF- α stimulation were reduced by 20.8% from the control. Furthermore, treatment of organoids that had been stimulated with TNF- α with AF-CM led to a significant increase in E-cadherin intensity from those not treated by 13.2% (n=4, p<0.05). AF-CM treatment therefore increased levels of E-cadherin intensity back to a level similar to that of the unstimulated.

In addition to analysis of Lysozyme and E-cadherin, immunofluorescent analysis was carried out for Ki-67 to detect any changes in proliferation capacity (Figure 6.13.A-F). The only cells of the epithelial layer in the intestine that proliferate are the resident stem cells. Statistical analysis of Ki-67 co-localisation with the nucleus (DAPI stained nucleic acid) was performed (Figure 6.14.A-F). Organoids stimulated with LPS with or without AF-CM showed no difference in co-localisation compared to the

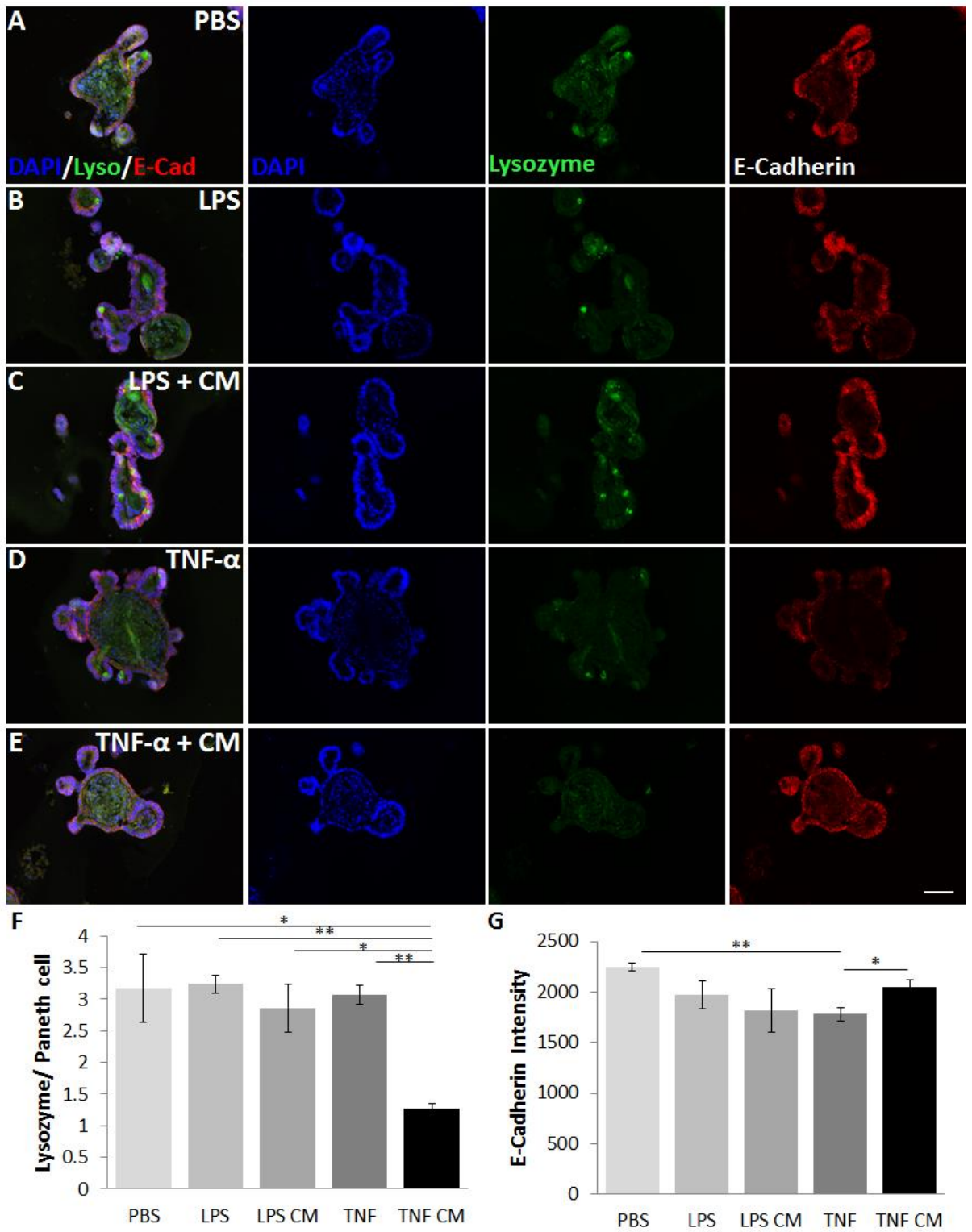


Figure 6.13

Figure 6.13: Immuno-fluorescent analysis of organoids stimulated with either 50 μ g/ml E.coli LPS or 10ng/ml TNF- α for 72 hours and treated with AF-CM. (A) Organoids sectioned and stained for DAPI (blue), Lysozyme (green), and E-cadherin (red). **(B)** Densiometric analysis of Lysozyme staining within Paneth cells. **(C)** Comparison of E-cadherin intensity within cellular membranes of stained organoids. **(A)** Scale bar representative of 500 μ m. Values are expressed as means \pm SEM (n=4). $p < 0.05$ (*), $p < 0.01$ (**) or $p < 0.001$ (***).

unstimulated control. However, stimulation with TNF- α alone significantly reduced levels of Ki-67 co-localisation from the unstimulated control and those stimulated with LPS (n=4, p<0.05 and <0.01). Levels of co-localisation following TNF- α stimulation alone had reduced by 7.5%, 8.6% and 11.9% from the unstimulated control, LPS positive control and those stimulated with LPS but treated with AF-CM respectively. AF-CM treatment of TNF- α stimulated organoids did not change levels of Ki-67 co-localisation from the positive control and levels were significantly lower than that of the LPS stimulated organoids treated with AF-CM by 10.7% (n=4, p<0.01).

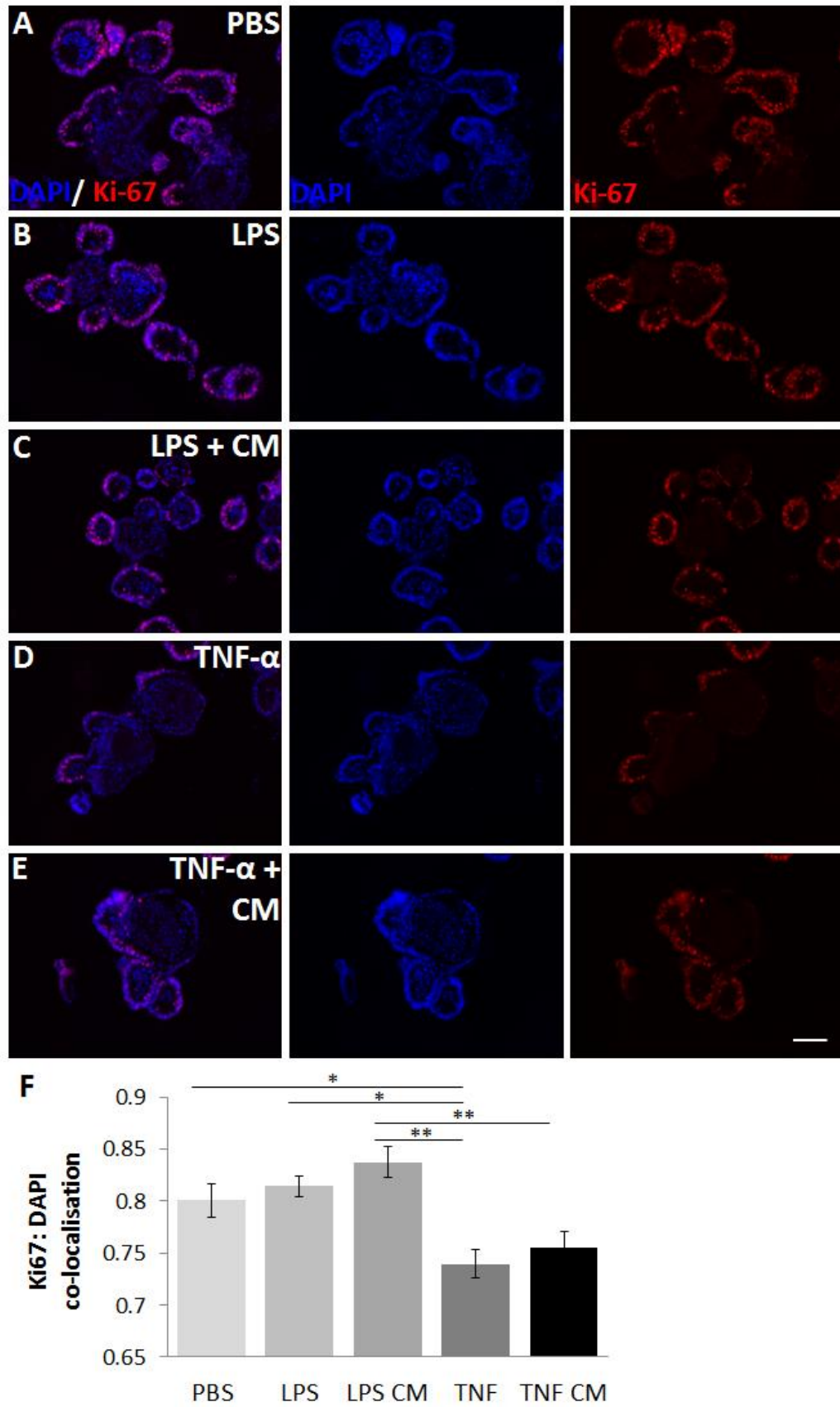


Figure 6.14

Figure 6.14: Immuno-fluorescent analysis of organoids stimulated with either 50µg/ml E.coli LPS or 10ng/ml TNF-α for 72 hours and treated with AF-CM. (A) Organoids sectioned and stained for DAPI (blue) and Ki-67 (red). (B) Statistical co-localisation of Ki-67 and the nucleus (DAPI) using Pearson's R values from stained samples. (A) Scale bar representative of 500µm. Values are expressed as means ± SEM (n=4). p < 0.05 (*), p < 0.01 (), or p < 0.001 (***).**

Protein Translation of 72 hour Long Stimulated Organoids

To assess any changes in protein synthesis that may have occurred with the increase in exposure time to the inflammatory stimuli the culture media or organoids was briefly labelled with puromycin. A summary of results can be found in Table 6.1. Puromycin is a structural analogue of aminoacyl-transfer RNA. In the short time cells are introduced to puromycin, puromycin is incorporated via the peptide bonds into the lengthening peptide chains (Schmidt et al., 2009). This so-called SUNSET technique was carried out and normalised to the total protein content (Figure 6.15.A, C). Although LPS stimulation alone showed no change in puromycin incorporation, the level was significantly increased with AF-CM treatment both from the control and positive control ($n=4$, $p<0.01$ and <0.05). The AF-CM treatment of LPS stimulated organoids increased levels by 33.4% and 22.3% from the control and the positive control respectively. Those stimulated with TNF- α with or without treatment did not differ from the control. However AF-CM treated LPS stimulated organoids significantly higher puromycin incorporation levels compared to those stimulated with TNF- α alone by 32.6% ($n=4$, $p<0.01$). On the other hand, Fibrillarlin and E-cadherin levels were not changed significantly between any of the treatment groups (Figure 6.15.D and G).

Western blotting was also carried out for the apoptotic marker, CC3 and Paneth cell marker Lysozyme (figure 16.15.B, E-F). In relation to CC3, LPS stimulation with or without AF-CM treatment provided no change in CC3 levels. However, stimulation with TNF- α alone and with AF-CM did significantly increase levels of CC3 by at least 52.7% ($n=4$, $p<0.01$ and <0.05). Although the AF-CM did not bring levels back towards that of the unstimulated control. Levels of Lysozyme-1 were significantly increased by LPS alone by 43.3% from the control ($n=4$, $p<0.05$). Lysozyme-1 levels of those stimulated with LPS and treated with AF-CM along with both TNF- α stimulated group were shown to not-significantly differ from the control.

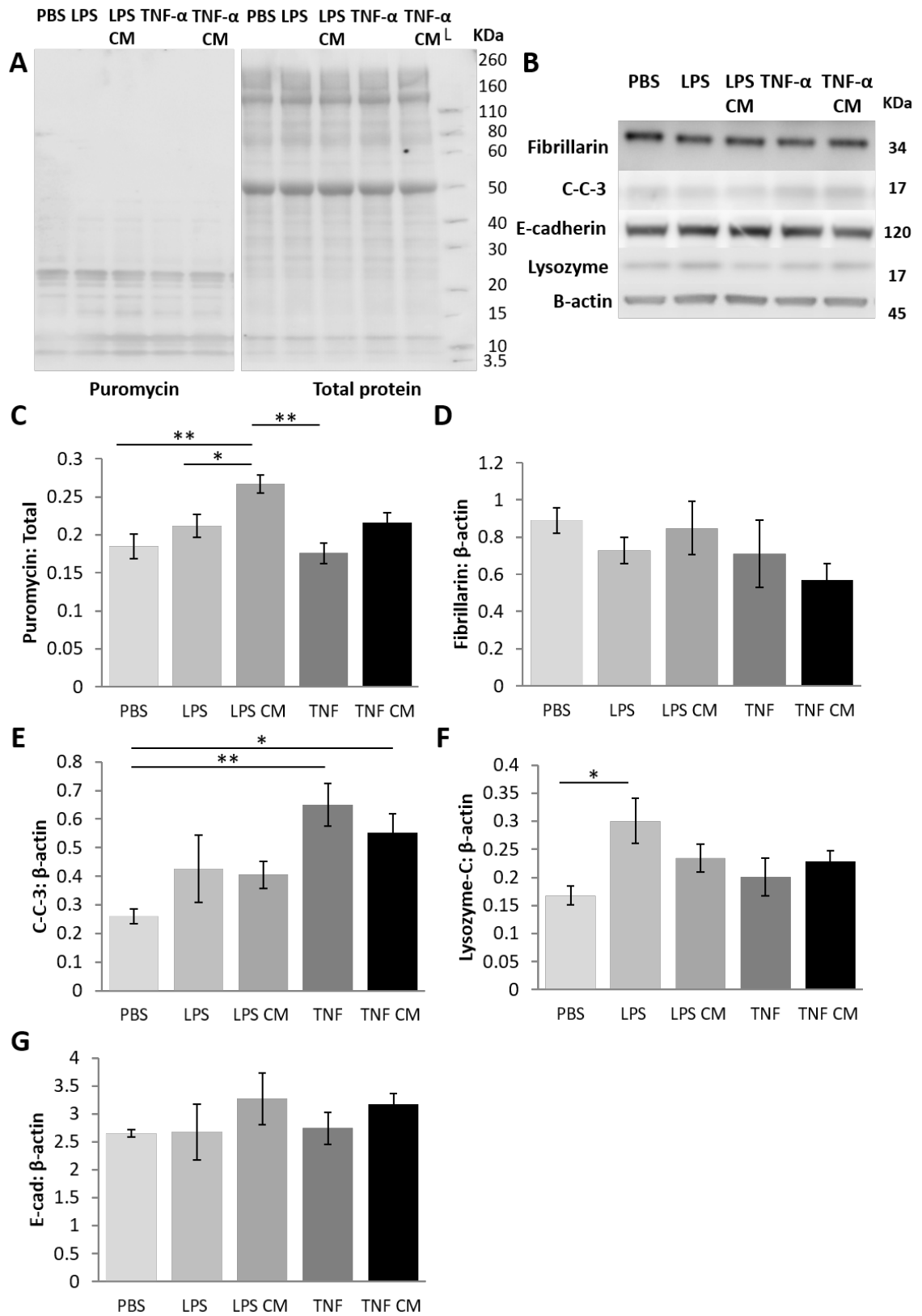


Figure 6.15

Figure 6.15: Protein expression of organoids stimulated with either 50µg/ml E.coli LPS or 10ng/ml TNF-α for 72 hours and treated with AF-CM. (A) Western blots of puromycin incorporated proteins and ponceau staining for total protein following 15 minutes of organoids being incubated in puromycin before lysis. **(B)** Western blots of proteins analysed. Analysis of **(C)** puromycin incorporated proteins normalised to total protein. **(D)** Protein expression of Fibrillarlin. **(E)** Protein expression of cleaved Caspase-3 (CC3), **(F)** Lysozyme and **(G)** E-cadherin. Values are expressed as means ± SEM (n=4). p < 0.05 (*), p < 0.01 (**) or p < 0.001 (***).

Autophagy Signalling in 72 hour Long Stimulated Organoids

Finally, further Western blots were carried out on the organoids stimulated with LPS and TNF- α for key autophagy related proteins (Figure 6.16.A-F). Levels of p62, CHOP or calculated LC3BII/ LC3BI ratios did not significantly differ between any groups of treated organoids. LPS stimulation alone did not alter levels of BIP, however upon treatment with AF-CM levels significantly increased by 51.2% from the unstimulated control (n=4, p<0.05). Levels following the AF-CM were also significantly higher than that of the TNF- α stimulated organoids treated with AF-CM by 67.4% (n=4, p<0.01). Regarding LC3B-I, only stimulation with TNF- α alone increased levels significantly from the control by 88.1%, but also those stimulated with LPS by at least 73.8% and those stimulated with TNF- α not treated with AF-CM by 52.9% (n=4, p<0.001, <0.01 and <0.05). TNF- α stimulation alone also significantly increased LC3B-II levels from the control and those stimulated with LPS but not the TNF- α stimulated AF-CM treated organoids (n=4, p<0.05). Following TNF- α stimulation alone, levels of LC3B-II were 90.4% higher than the control and at least 79.7% higher than those stimulated with LPS.

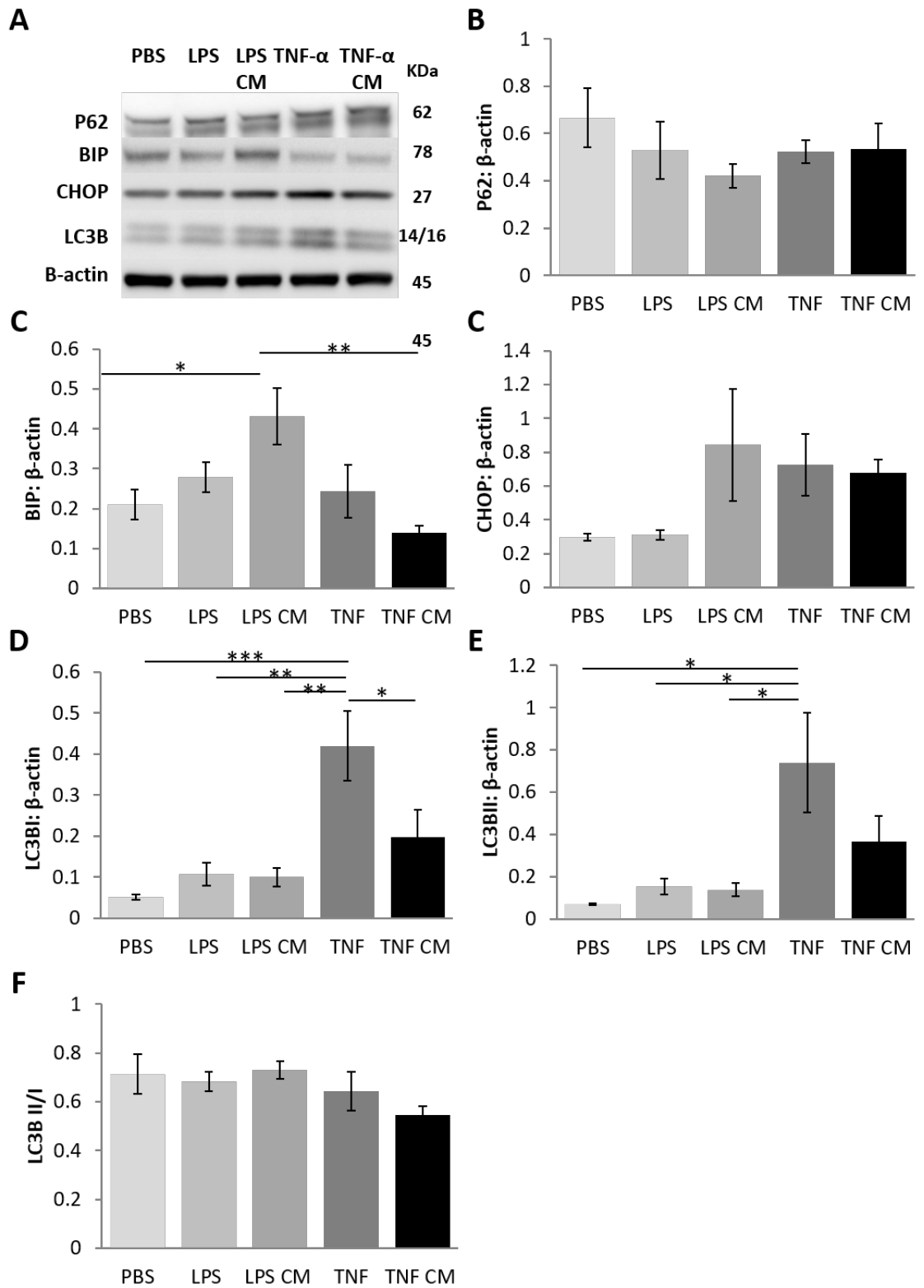


Figure 6.16

Figure 6.16: Expression of autophagy signalling proteins in organoids stimulated with either 50µg/ml E. coli LPS or 10ng/ml TNF-α for 72 hours and treated with AF-CM. (A) Western blots of proteins analysed. Protein expression of (B) p62, (C) BIP, (D) CHOP, (E) LC3BI, (F) LC3BII and (G) calculated ratios of LC3BII/ LC3BI. Values are expressed as means ± SEM (n=4). p < 0.05 (*), p < 0.01 () or p < 0.001 (***)**.

To summarise the results a variety of 3D intestinal organoid based model were developed, which included stimulating organoids with either E. coli LPS or TNF- α at different concentrations for different lengths of time. From these models an inflammatory related gene expression was shown to alter as well as the apoptotic protein marker CC3 and protein markers associated with cell types found within the intestine. Expression of selected genes did not significantly alter with AF-CM treatment compared to their positive controls at shorter time points such as 30 minute and 1 hour exposures to stimuli. However, on a protein level AF-CM was shown to inhibit certain changes from the control following stimulation alone after just 2 hours. Furthermore, after 24 hours TNF- α or LPS stimulation changes to specific genes tested were seen to alter, some of which were reversed by AF-CM treatment. This result was further corroborated by changes to protein levels measured after extending the time for which organoids were stimulated with TNF- α or LPS. Some of the changes that occurred were of proteins associated with protein synthesis and autophagy.

Time point	Summary
2 hours	<ul style="list-style-type: none"> • Lower concentrations of LPS decrease apoptosis and increase proliferation • Alterations in signalling indicative of an initial pro-inflammatory response to LPS
24 hours	<ul style="list-style-type: none"> • TNF-α induced a large pro-inflammatory response in organoid gene expression. • TNF-α caused a reduction in Lysozyme and Mucin gene expression
48 hours	<ul style="list-style-type: none"> • LPS did not induce an increase in apoptosis • TNF-α increased the levels of apoptosis • LPS with AF-CM, TNF-α and TNF-α with AF-CM led to reduced levels of unfolded protein response proteins
72 hours	<ul style="list-style-type: none"> • AF-CM improved stem cell proliferation from the reduction following TNF-α stimulation. • Changes to barrier function unclear

Table 6.1: A summary of the results seen in organoids stimulated with LPS or TNF- α for 2, 24, 48 or 72 hours with and without AF-Cm treatment.

Discussion

Intestinal organoids have been previously used to model NEC and it was therefore an aim to replicate these conditions so that the AF-CM could be tested on them (Neal et al., 2012, Hackam et al., 2013). Cultured organoids presented with the lumen, crypts and villous domains found in a normal intestine *in-vivo*. Stimulation of organoids with either *E. coli* LPS or TNF- α for varying amounts of time and at different concentration produced reactions that were revealing of an inflammatory response but also healthy homeostasis. Furthermore, the use of AF-CM as a treatment in a bid to inhibit the effects of TNF- α or LPS stimulation for 2 hours or less was seen to affect organoids on a post-translational level and was shown to reduce the level of apoptosis. Western blot results did not conclusively identify changes in protein synthesis or autophagy; however, changes to individual proteins within each of the pathways were seen. AF-CM was shown to not only bring some of these changes back to a level seen in the unstimulated control but also accentuated the response following stimulation.

LPS and TNF- α Induced Cell Death and Inflammation in Organoids

Organoids were stimulated with previously tested concentrations of *E. coli* LPS at 10 μ g/ml along with 10ng/ml TNF- α for time points ranging from 30 minutes to 2 hours. Gene expression of TNF- α was increased with the TNF- α stimulation after 1 hour, decreased with LPS after 2 hours. The pattern of expression following TNF- α stimulation could be explained through the cyclical patterns of NF- κ B signalling found previously *in-vitro* (Zeuner et al., 2016). As discussed, NF- κ B signalling stimulated by TNF- α and TNFR interactions lead to NF- κ B translocating into the nucleus thus acting as a transcription factor and promoting the expression of genes such as *TNF- α* . An increase in *TNF- α* expression and subsequent TNF- α release would further potentiate the signalling pathway. On the other hand LPS reduced *TNF- α* gene expression. It has been previously suggested that short term stimulation by LPS leading to increased TNF- α production is not controlled on the transcriptional level but instead post-transcriptionally (Gao et al., 2001). If true, increases in TNF- α due to post-transcriptional regulation may in fact activate negative feedback mechanisms to inhibit *TNF- α* gene

expression. Inhibition of *TNF- α* gene expression has been previously postulated in murine macrophage cell lines as being due to TNF- α -inhibiting factor (TIF) repression of the *TNF- α* promoter (Baer et al., 1998). The repressive activity of TIF was also suggested as being activated by selective induction of the NF- κ B p50 subunit following LPS stimulation.

Mucin-2 gene expression at 30 minutes was increased prior to decreasing to the norm after 2 hours. This has been previously shown to increase in p14 and p28 mice ileum samples following TNF- α injections 8h before resection (McElroy et al., 2011). The reduced expression is suggested as being due to TNFR-2 dependent signalling as opposed to TNFR-1 dependent, which would otherwise cause apoptosis of mucin laden Goblet cells instead. Negative feedback mechanisms or even saturation of TNFR-2 by TNF- α would explain the fall towards the basal level seen in unstimulated organoids after 30 minutes.

Interestingly the use of 10 μ g/ml LPS, previously shown to induce apoptosis and cell death, did not increase levels of CC3, a marker suggestive of apoptosis (Neal et al., 2012). On the other hand, the higher concentrations of 50 μ g/ml and 100 μ g/ml LPS did increase CC3. The cells of the intestine within the villi and also the crypts are known to synergistically interact with the body's microbiota (Rakoff-Nahoum et al., 2004, Shirkey et al., 2006, Vaishnava et al., 2008). This interplay is key to maintaining the normal homeostasis of cells in the intestine and the way they function such as their proliferation and secretion of substances into the lumen including Mucins and Lysozymes. This normal interaction inevitably leads to LPS contact and this bacterial polysaccharide has been suggested as being key to some of the functions such as proliferation and cell secretion (Vaishnava et al., 2008, Kuo et al., 2015, Shirkey et al., 2006, Rakoff-Nahoum et al., 2004). A low level of LPS exposure to the organoids, which have already been previously exposed to LPS naturally, would not significantly alter LPS related signalling. Which is why a higher level than what is usually used in other cell types that are not naturally associated with LPS must be used to induce a response in organoids. On the other hand, the exact mechanism by which LPS had been introduced to the organoids previously has not been documented and it is therefore presumed, and as carried out here, that LPS

was dosed in the culture media. Dosing of the Matrigel, as opposed to relying on diffusion of LPS from the media may have a more potent outcome on signalling and gene expression and in this case activation of apoptotic pathways leading to cleavage of caspase-3.

A 10µg/ml LPS exposure unlike the other concentrations of LPS increased Ki-67 co-localisation (Figure 6.2.A-E). This increase may be postulated to occur as a pathological response of the Lgr5⁺ or Bmi1⁺ stem cell population following inflammation as previously noted to occur for other stem cell populations such as skeletal muscle satellite cells previously discussed (Zhu et al., 2013, Tian et al., 2011, Yan et al., 2012). On the other hand, due to a lack of an increase in the level of apoptosis at this concentration the 10µg/ml stimulation of organoids could be hypothesised as promoting a healthy environment and thus normal proliferation as opposed to inducing stress (Rakoff-Nahoum et al., 2004). The lack of alteration in E-cadherin levels may also reflect a lack of pathology and stress (Figure 6.2.A-F). However, much of the research looking at changes to barrier function has tended to look at this measure after longer exposure periods to LPS (Rentea et al., 2017, Guo et al., 2013, Khailova et al., 2009). The 2 hour time point may therefore be too early to identify changes to E-cadherin on a protein level.

Additionally, after 48h of exposure to the same concentration of LPS, gene expression of *Mucin-2*, *Lysozyme* and *Lgr5* was increased (figure 6.3.A-E). It is interesting to see that at this later time point the *Mucin-2* expression is increased on a transcriptional level not seen previously at the lower time points tested. This extended exposure could have come about from a natural pathogenic or inflammatory response (Ahn et al., 2005). In this hypothesis, the intestine would benefit from increases in antibacterial *Mucin-2* and *Lysozyme-1*. *Lysozyme-1* is known to directly kill bacteria through hydrolysis of bacterial wall components (Tanabe et al., 2005). The upregulation of *Lgr5* is indicative of an increase in stem cell proliferation because of its role, although not well understood, in facilitating R-spondin induced Wnt signalling (Sato et al., 2009, Sato et al., 2011). This also, as discussed, would be beneficial to the intestine if an infection took place to counter an increase in cell loss. Furthermore, *Lgr5* expression increase was seen after TNF-α stimulation, which can also be

explained as a consequence of the stem cell inflammatory response via the NF- κ B pathway shared by LPS.

AF-CM and AF-EV Organoids Treatment Acts Post-Transcriptionally

Due to TNF- α inducing an inflammatory response in organoids treated for 1 hour as before indicated by TNF- α expression, organoids were stimulated with TNF- α for 1 hour and 30 minutes as a comparison with or without AF-CM treatment (Figure 6.4.A-D). However, the AF-CM treatment did not alter the increase in TNF- α level seen after 1 hour. The lack of response suggests that AF-CM was not acting on a transcriptional level and was therefore hypothesised to be more likely acting on a post-transcriptional level. Any gene expression changes subsequent to this would be likely detectable at later time points, hence the 24 hour time point used later. The lack of changes in the positive controls to other gene expression levels may reflect variability in the model at this lower time point. The fact that AF-CM, AD-CM and AF-EV treatments over the 1 hour stimulation interval with TNF- α did not alter the expression of genes tested from the positive control also reflects the potential mechanism of action of the AF-CM on the post-transcriptional level (Figure 6.5.A-B). Evidence for this is first highlighted with the immunofluorescent staining of NF- κ B-p65 and analysis of its intensity within the nucleus insightful of nuclear translocation (Figure 6.5.C-D). All CM treatments reduced nuclear intensity from the positive control thus providing evidence, along with the previous data, that AF-CM was indeed acting on a post-transcriptional level and in particular through repression of the NF- κ B pathway. However, AF-CM treatment did not differ from AD-CM suggesting a similar ability to reduce NF- κ B nuclear translocation in organoids. Similarly, AF-CM did not differ from its resultant AF-EV fraction suggesting that much of the ability of AF-CM to reduce NF- κ B signalling is facilitated by its EV fraction.

AF-CM Modulates Lysozyme Levels via NF- κ B Signalling Pathways

Although variability between assays utilising LPS for shorter exposure times was seen, in assays the AF-CM can be seen further to affect protein levels compared to a positive control (Figure 6.6.A-D). Western blot analysis of CC3 revealed significant reductions in CC3 from those stimulated with

100µg/ml LPS. Lysozyme levels were significantly increased with the 50µg/ml LPS control and reversed with AF-CM back to a level similar to that of the control. This result along with the previous results is indicative of an increase in the inflammatory response instigated through LPS signalling. However it has been previously suggested that changes to the level of Lysozyme due to LPS stimulation is independent of TLR-4 signalling (Tanabe et al., 2005). The LPS used in this study is ultra-pure and therefore believed to be unable to stimulate other pathways other than through TLR-4. On the other hand, it may also be beneficial for the model to use standard LPS, which may potentiate more signalling pathways and exacerbated changes to Lysozyme levels. However, it is also likely that the effects of LPS on other cell types within the model lead to paracrine signalling which activates the increase in Lysozyme within Paneth cells indirectly. The drop in apoptosis at the 50µg/ml concentration would also match the increase in proliferation of the resident stem cells. Looking at the previous p65 staining it is therefore proposed that this reversal in lysozyme level is modulated with AF-CM via repression of NF-κB signalling.

Longer Exposures to LPS or TNF-α in Organoids Mimic NEC

Comparison between CC3 levels seen after this 2 hour time point and that seen at 48 hour (Figure 10B) and 72 hour (Figure 6.15.D) showed further variation with those stimulated with 50µg/ml LPS. Although not all results were significant, CC3 levels at 2 hour and 48 hours were lower than the control. On the other hand, exposure for 72 hours showed an increase (not significant). The results further suggested that 50µg/ml LPS stimulation of organoids over a short period of time up to at least 48 hours is beneficial for the organoids, potentially having a role in homeostatic regulation. However, increases in stimulation time leads to increases in apoptosis. This increase suggests that the extended exposure to the LPS may become disadvantageous and thus increases apoptosis. In order to take advantage of this outcome, organoids in future could be stimulated for longer time-points in an attempt to induce further and significant increases apoptosis. A limiting factor that led to the original choice of time points included the need to passage the organoids after 6 days post passaging. Organoids become extremely large with detrimental intraluminal deposits of dead cells

and debris. Passaging and mechanically breaking up the organoids during an exposure time point would allow LPS to access the intraluminal side of the organoids, which could potentiate a differing effect. On the other hand, exposure of organoids intra-luminally to LPS and also TNF- α may be more representative of the gut being over-run by pathogenic bacteria. However, previous research suggests that introduction of Gram-negative derived LPS within the organoid lumen mimics normal intestinal colonisation, whereas introduction of this LPS basally promotes an outcome similar to 'life-threatening septicaemia' (Karve et al., 2017). It must however be noted that the source of the LPS used was not specified in previous studies and the variation in responses to LPS derived from different species of bacterium can lead to differing responses with respect to NF- κ B signalling as discussed previously.

An increase in exposure to TNF- α for 24 and 48 hours can be thought of as promoting an inflammatory response as suggested by *TNF- α* gene expression levels. This data along with the increased *TGF- β* mimics what is seen in the gut of human inflammatory bowel disease (IBD) (Ihara et al., 2017). However, it has also been hypothesised that elevated levels of TGF- β in a variety of inflammatory gut conditions is simply part of a response by the epithelium and the stromal tissue to reduce inflammation (Ihara et al., 2017). It is therefore suggested that the significant further increase in *TGF- β* with AF-CM treatment following LPS stimulation is anti-inflammatory and beneficial longer term, although TNF- α gene expression levels with AF-CM treatment had not changed yet from the positive control. Interestingly, the TNF- α and LPS reduced *Lysozyme-1* and *Mucin-2* gene expression. This reduction is also believed to be representative of what is seen in inflammatory bowel disease. Following the initial increases in Mucin expression as inflammatory response through NF- κ B signalling, TNF- α has also been shown to induce JNK signalling (Ahn et al., 2005). The activation of JNK is thought to act as a negative feedback response and therefore provides an explanation for reduced *Mucin-2* levels following extended stimulation, which would reduce the level of protection from pathogenic bacteria in the gut. Reversal of this reduction was not seen with AF-CM treatment suggesting that the AF-CM could not directly inhibit the JNK signalling. Use of AF-CM may therefore be questionable if it still represses NF- κ B signalling, which could potentiate further a reduction in

Mucin-2 expression. This may also help to explain why there was a significant decrease in E-cadherin from the LPS control, which did not differ from the unstimulated control, when AF-CM was used as treatment. This decrease is a concern because it may have a detrimental effect on barrier function and therefore increased permeability to further LPS or bacterial aggravation. It would therefore be of interest to look at the level of CD14 in the organoids. CD14 co-localises with TLR-4 to mediate some of the LPS effects in particular tight junction permeability (Guo et al., 2013). However, the level of CD14 expression also relies on the LPS and TLR-4 interactions and downstream signalling via NF- κ B. The lack of reduced E-cadherin following LPS stimulation alone could stem from LPS stimulation not being for long enough to increase levels of CD14 at the membrane of cells, which is suggested to be a key driver in reducing barrier integrity (Guo et al., 2013). Although the study looking at the effects of LPS on intestinal tight junctions were carried out in mainly Caco-2 cells, TLR-4 was also only shown to increase at the membrane following 4 days of LPS stimulation (Guo et al., 2013).

AF-CM did not Conclusively Alter Autophagy Signalling

Reduced Fibrillarin and pFOXO-3a/ FOXO-3a protein levels with AF-CM treatment following LPS stimulation for 48 hours would suggest that the AF-CM has reduced the level of mRNA translation. A bypass in the protein synthesis signalling pathway due to introduction of miRNA may explain the lack of change seen with AKT, EIF2 α , 4EBP1 and their respective phosphorylated levels. This result along with the increase in the key autophagy regulator p-62 and decrease in BIP and CHOP, suggesting a lack of autophagy, questions whether mRNA is being deleted prior to translation. miRNA found in MSC-CM, as has been recorded in various studies, would reduce mRNA levels and translation (Mead and Tomarev, 2017, Mellows et al., 2017, Thomou et al., 2017). It has already been shown that rRNA levels and effects of miRNA are linked through chromatin binding of Argonaute-2 along with DICER interactions (Atwood et al., 2016). Reduced mRNA would decrease the need for translational machinery and therefore rRNA, potentially leading to reduced rRNA production and as a result a smaller nucleolus, as represented here by the level of Fibrillarin. Interestingly, the AF-CM treatment of organoids stimulated for 72 hours with LPS led to an increase in protein translation as shown by

puromycin incorporation. However, puromycin incorporated bands of protein are all of low molecular weight. A longer puromycin incubation period for the organoids may lead to larger proteins incorporating puromycin. Furthermore, the results suggest puromycin incorporation levels are not correlated to the Fibrillarin because levels of Fibrillarin do not significantly differ. Intriguingly, the pattern portrayed by p62 and CHOP levels and those significantly seen to change with BIP suggest that the AF-CM treatment of LPS stimulated organoids have higher levels of autophagy or unfolded protein response signalling. Although this does not translate into changes between the ratio of LC3BII/ LC3BI, the autophagic signalling through BIP, CHOP and p62 along with simultaneous increases in protein synthesis (puromycin data) can be explained through the recycling of unwanted proteins through autophagy thus providing amino acids for protein synthesis. This has also been shown previously by others who showed a transient increase in protein translation along with autophagy whilst the proteolysis as a whole remained high in skeletal muscle of spinal cord injury patients (S. et al.).

AF-CM Decreased the Levels of Lysozyme per Paneth Cell

Immuno-histological analysis 72 hour stimulated organoids showed that there was less lysozyme/Paneth cell in TNF- α stimulated organoids treated with AF-CM. This is interesting because there was actually no decrease in the total lysozyme following western blot analysis. On the other hand, organoids stimulated with TNF- α were also shown to contain more CC3, presumably showing increased apoptosis. It is therefore suggested that the TNF- α is causing an inflammatory response and therefore cell death. The AF-CM may be as discussed modulating NF- κ B signalling thus leading to reduced lysozyme. Yet with an increase in cellular apoptosis, a reduced number of Paneth cells and total lysozyme level would be expected. The reduced proliferation as demarked by the reduced Ki-67 staining in TNF- α stimulated organoids may suggest a reduced stem cell population and a capability of organoids to produce Paneth cells or any other cell for that matter. Although AF-CM had not altered total lysozyme levels it had inhibited the reduction of E-Cadherin intensity following TNF- α stimulation following histological analysis. However, western blot analysis showed E-cadherin levels

did not change with any treatment. This variation in results probably stems from the number of organoids being analysed within each analysis. Measuring E-cadherin intensity is not carried out on every one of the hundreds of organoids present within the Matrigel. On the other hand, western blot analysis is carried out on all organoids in each well tested and could be perceived as being more reliable due to the higher power of the study.

To conclude, further studies need to be carried out on the organoids using different LPS and or TNF- α stimulation parameters. The use of LPS and TNF- α had caused organoids to alter expression of key genes and proteins thought to be involved in the stress of NEC, however further experimentation would be required to establish a reliable and predictable model. On the other hand, AF-CM also altered levels following stimulation and was thought to be due to post-transcriptional modification of signalling pathways at least partly related to NF- κ B.

7. General Discussion

The general aim of this project was to create and characterise an AFSC derived CM that could be translated into a clinically compliant therapeutic for NEC. Currently, treatment of NEC concentrates on managing the symptoms through the use of antibiotics, reduced enteral feeding and in more severe cases surgery to remove affected portions of the bowel (Sharma and Hudak, 2013, Zani and Pierro, 2015). However, much of this treatment either leads to long term intestinal problems such as short bowel syndrome or does not directly aid recovery through the enticement of regeneration. It had been previously shown that treatment of NEC rodent models with AFSCs had extended lifespan and activated regenerative programmes (Zani et al., 2014). However, many of these positive outcomes were evident in the absence of AFSC engraftment, as had also been shown in other studies using different MSCs for a multitude of pathologies (Zani et al., 2014, Gneccchi et al., 2006, Gneccchi et al., 2005, Gneccchi et al., 2016). It was therefore hypothesised that the regenerative effects seen following MSC therapy were in fact largely due to paracrine secretions.

In order to translate the AFSC paracrine factors into a clinically compliant therapy, AF-CM was collected so that it was free of exogenous molecules. AFSCs surface expression was characterised to ensure that AF-CM was collected from AFSCs that expressed generally accepted MSC markers. Furthermore, their differentiation potential was tested. AF-CM was then investigated to understand if it contained EVs, and if so their sizes to understand what type of EV existed in the AF-CM. Additionally an extensive characterisation of the protein and RNA content in the AF-EV and soluble fraction was carried out. To test whether AF-CM could influence the activity of non-autologous cells, various cell types were treated with AF-CM to test their effect on proliferation and migration, the ability of AF-CM to protect from senescence and finally its ability to dampen inflammatory signalling. Once the AF-CM had been shown to alter cellular properties *in-vitro*, its ability to increase regeneration in an established model of acute damage was tested. Finally, to understand whether any regenerative traits could be translated into treatment of NEC, an attempt to create an intestinal organoid model of NEC was carried out. The model was used to test the efficacy of AF-CM to attenuate disease associated features.

The data presented provides evidence that the AFSCs used to create AF-CM expressed MSC surface markers but was also capable of differentiating into chondrogenic, osteogenic and angiogenic cell types thus proving them to be MSCs. Investigation of the AF-CM revealed that it contained small EVs typical in size to exosomes (They et al., 2002b, They et al., 2006, Lötvald et al., 2014). Characterisation of the AF-CM cargo showed a diverse assortment of proteins both in the soluble fraction and the AF-EV. Of particular interest was the fact that RNA within the AF-EV fraction was made up almost entirely of miRNA, contrary to previous reports stating the presence of mRNA also within MSC derived EVs (Valadi et al., 2007, Eirin et al., 2014). Not only did AF-CM support proliferation and migration capacity of non-autologous stem cells, it protected IMR90 cells from H₂O₂ induced senescence. In addition, AF-CM was shown to reduce NF-κB activity and nuclear translocation which may also explain its ability to reduce the levels of the pro-inflammatory marker (CD80) on THP-1 macrophages. Thereafter we showed that AF-CM could accelerate the regeneration of skeletal muscle *in vivo* following acute damage to skeletal muscle induced by CTX. Comparison of AF-CM and its derivative fractions, AF-EV and soluble fraction, revealed that although much of the activity was shown to derive from the AF-EV, it was believed that in general the use of a whole AF-CM with both fractions present would be more beneficial to producing a regenerative response. Finally, we attempted to replicate an NEC mimicking intestinal organoid model, as previously carried out by others. However we were unable to reproduce published findings. Nevertheless we found that the AF-CM was capable of altering organoid signalling post-transcriptionally.

AF-CM Molecular Content Modulates Cellular Activity Beneficial to Regeneration *in Vitro*

In vitro results showed that AF-CM increased the capacity of non-autologous stem cell proliferation and migration. With mass spectrometry analysis and miRNA arrays it was possible to speculate how the AF-CM was able to potentiate these effects. Proteins such as the heat shock family of proteins (HSPs) and HMGB1 known to have 'alarmin' functionality is proposed to be at least partly responsible for these attributes. Alarmins have been discussed as providing a forewarning like signal to the cell of interest (Bianchi, 2007). Although these proteins have been recorded as having inflammatory

functions, their presence prior to stress caused by pathology initiates a minor stress response in cells to brace them for more extreme stressors (Mollica et al., 2007, Bianchi, 2007, Beninson et al., 2014). Low levels of inflammatory stimuli are known to increase cellular proliferation and migration (Prisco et al., 2016, Barreca et al., 2017, Widera et al., 2006). Regarding the HSPs they are believed to mediate their effects by binding to two main types of receptor, TLRs and scavenger receptors, in particular TLR4, TLR2 and CD91 have been identified (Barreca et al., 2017). It has further been found that downstream of this binding, signalling pathways including PI3K/ AKT and NF- κ B were activated leading to upregulation of MMPs such as MMP9, in this example from T cell EVs (Barreca et al., 2017). The upregulation of these signalling pathways was shown to increase in mesangioblast migration (Barreca et al., 2017).

In addition to HSPs, HMGB1 was also found in the AF-CM, which has been previously shown to increase both migration and proliferation (Palumbo et al., 2004, Limana et al., 2005). The increase in proliferation, as well as inhibition of apoptosis, was proposed to be facilitated by HMGB1 binding to RAGE/TLR4 as opposed to RAGE on its own (X. et al., 2014). Once again, the effects of this binding were found to be PI3K/ AKT mediated (X. et al., 2014). Although we have not specifically looked at PI3K/ AKT activity following AF-CM treatment within these *in vitro* assays, it can be speculated that AF-CM alters PI3K/ AKT signalling to bring about increased proliferation and migration following HMGB1 and HSP binding to receptors such as TLR4 and RAGE. Along with the evidence that AF-CM reduces NF- κ B activity in cells stimulated with pro-inflammatory molecules such as TNF- α and LPS, and the knowledge that these alarmins also increase NF- κ B activity, it can also be hypothesised that AF-CM treatment may initiate this signalling as well as the PI3K/ AKT pathway to upregulate the proliferation and migration seen.

Additionally, insignificant NF- κ B signalling stimulating negative feedback responses and preparing the cell for further more extreme insult may explain the protection afforded by AF-CM to the IMR-90 cells stressed with H₂O₂ thus preventing senescence. It would however be of interest to understand whether the AF-CM is protecting cells from senescence via an alarmin like system. T72 AF-CM was

shown to increase NF- κ B activity on its own without inflammatory stimulation, whereas the T24 AF-CM did not. On the other hand, T72 AF-CM afforded greater protection from senescence. The T24 AF-CM is therefore hypothesised as having the optimum level of alarmin molecules without causing a net pro-inflammatory response in target cells. Levels are believed to cause an anti-inflammatory response whilst also increasing migration and proliferation capacity and affording protection from senescence. A senescent state is often taken on by a cell as opposed to apoptosis, so it could be possible that AF-CM is instead pushing cells towards an apoptotic fate instead. Future work could involve analysing with a flow cytometer to not only establish the level of p53 and p21, as markers of senescence, but also perform a cell count to establish if cell death is increased compared to that of stressed cell without AF-CM treatment.

With regard to AF-EV miRNA content, some of the top 50 compiled miRNAs found to be present have been previously shown to be pro-survival, pro-migratory and capable of increasing proliferation. Examples included miR3196, miR125b-5p, miR1273-3p, miR762, miR3960, miR24-3p and miR382 (Liu et al., 2016, Yu et al., 2017, Xu et al., 2016, Xia et al., 2015, Seok et al., 2014, Niu et al., 2016). Induction of pro-survival signalling from a regenerative context would often be depicted as being a positive feature of miRNA. However, as discussed causing cells to survive instead of undergoing apoptosis may instead drive them into senescence. A senescent state is counterintuitive for regeneration because of the increased basal levels of inflammatory factors produced in such cells as well as them being unable to divide and replace lost tissue. It can therefore be speculated that if AF-CM is indeed preventing senescence it could be due to its protein content as opposed to miRNA content. The *in vitro* results also show no significant differences between the use of AF-CM and AF-EV. miRNA will only survive within the protective environment of the EVs without the need of the RISC proteins (not found in the soluble fraction). If the miRNA afforded protection from senescence it would be expected that the AF-EV would protect cells from senescence more so than the whole AF-CM either due to miRNA alone or synergistic effects of protein and miRNA. This is not the case and so the transfer of protein within the soluble fraction with AF-EV or AF-EV alone is believed to support the anti-senescent effect.

Interestingly, AF-CM reduced NF- κ B activity and nuclear translocation in addition to reducing the level of CD80 in M1 macrophages. AF-EV contained Let7b, a miRNA known to target mRNA of proteins involved in the inflammatory response (Teng et al., 2013, Ti et al., 2015). In particular, let7b has been shown to target and reduce the level of TLR4 (Teng et al., 2013). TLR4 is upregulated following reception of an inflammatory stimulus such as LPS (Wan et al., 2016). Targeting of TLR4 by let7b would reduce the level of surface TLR4 capable of binding LPS and therefore reduce downstream Nf- κ B signalling, as also hypothesised by others to occur following MSC-EV treatment (Ti et al., 2015). Let7b within AF-CM is therefore believed to be at least partly responsible for the reduced inflammatory state of THP-1 macrophages and reduced NF- κ B activity seen in the U251 cells. The data here also presents a possible role for AFSCs within the AF. It is believed that the level of NF- κ B activity regulates the switch to induce labor in the pregnant mother (Lee et al., 2012b, Lim et al., 2012, Kim et al., 2015) . It is therefore suggested that AFSCs play a role in stifling the level of NF- κ B activity in order to inhibit pre-term labor as well as reducing harmful pro-inflammatory cytokines for the foetus. Stress during the pregnancy would be hypothesised to induce AFSCs into secreting anti-inflammatory factors such as those characterised in the AF-CM.

The ability of the different cells used to take up AF-EVs was postulated to be mainly through active endocytic processes. From results showing the size of AF-EVs as well as the proteins present, it was suggested that the majority of AF-EVs were exosomes. Macro-pinocytosis has been suggested as being the most efficient mechanism of exosome uptake (Nakase et al., 2015). Efficiency of this uptake was found to be enhanced with stimulation of EGF receptors (Nakase et al., 2015). It may be beneficial to test if AF-CM treatment with EGF increases AF-EV uptake by cells and enables lower concentrations of AF-CM to be used both for research and clinically. A more efficient uptake of AF-EV with AF-CM treatment would reduce the volume required for therapy and lower costs for both the manufacturer and potentially the subsequent consumer.

Whole AF-CM provides a More Effective Regenerative Therapy *in Vivo* than AF-EV Alone

Similarly to results seen *in vitro*, the effects of AF-EV were seen to vary in comparison to the use of whole AF-CM *in vivo*. *In vitro* results showed no difference between AF-CM and AF-EV in reducing the level of senescence. However, AF-EV was shown to be more effective at reducing NF- κ B nuclear translocation although levels of expression, as judged by luciferase levels, were found to be reduced similarly by AF-CM. On the other hand, due to the AF-EV not effecting the regeneration of damaged muscle equally between the deep and superficial regions it was concluded that the use of AF-CM and not AF-EV alone was more beneficial. It is believed that although the majority of AF-CM actions are potentiated by AF-EV cargo, the secretome within the soluble fraction is also important and could act synergistically or control cellular events that the AF-EV could not. One aspect of the accelerated regeneration, as indicated by the larger fibre CSA in AF-CM treated mice, was the increased level of active resident stem cells. As discussed, activation of stem cells is often preceded by inflammatory stimulation. Some of the proteins as well as miRNA within the AF-CM, including the HSPs, HMGB1, miR3960 and miR24-3p (discussed previously) could potentiate this effect and activate satellite cells. Furthermore, the increases in proliferation and migration could be afforded to these cells by the AF-CM via mechanisms discussed previously. This would therefore increase the number of satellite cells capable of fusing, leading to larger fibres but also increase the speed in which they migrate to the area of damage, further accelerating regeneration. Although some of these proteins are present within the AF-EV only, it is also important to note that some were present in both, whilst others only in the soluble fraction. Although the exact mechanism of action of all proteins present in the AF-CM are not known, it can be speculated that at least some in each fraction are important for this increased satellite cell activity leading to increased fibre size in both the superficial and deep regions of muscle.

Another aspect of regeneration measured was the blood vessel density of damaged muscles. miRNA within the AF-EV, such as miR382 and let7b, has been suggested to be pro-angiogenic (Seok et al., 2014). It is therefore suggested that miRNA such as these are at least partly responsible for the increased angiogenesis *in vivo*. However, varying effects were seen with AF-EV treatment on vessel

density, whilst treatment with the whole AF-CM consistently led to increases in blood vessel per fibre. Other cargo within the AF-CM is therefore believed to increase angiogenesis within the muscle, including the proteins. However the ability of AF-CM to modulate NF- κ B activity *in vitro* is believed to provide a means to bringing about normal homeostatic regulation of NF- κ B levels so that signalling persists to enhance proangiogenic events such as the increased endothelial proliferation and migration, but not excessively which would have otherwise led to higher levels of pro-inflammation.

Although not a great deal of change was seen with regard to F4/80⁺ cell levels within the muscle sections, thought to be indicative of macrophages, the data recorded *in vitro* suggests that their inflammatory activity could have been altered by the AF-CM. Although the level of F4/80⁺ cells increased with AF-CM treatment, the levels following AF-EV treatment did not. This contrasts the *in vitro* data suggesting that the AF-EV contained the majority of anti-inflammatory molecules and once again highlights the importance of using both the soluble and AF-EV fraction together to harness the effects of both miRNA and protein. However, the *in vitro* data does provide more evidence, along with the time in which muscles were collected, that the increase in F4/80⁺ cells seen is likely due to increases in anti-inflammatory M2 macrophages. The *in vitro* data also suggests that although AF-CM was not enough to bring CD-80 levels in THP-1 cells down to a level seen in M2 macrophages and therefore prevent or reverse M1 polarisation, it may be enough to ease the transition of the M1 phase in the muscle towards the M2 phase. Further experiments are required as discussed later to establish this *in vivo*.

Effect of AF-CM on LPS and TNF- α Stimulated Intestinal Organoids

Although the intestinal organoid model used in this work did not provide predictable outputs for analysis, a number of hypotheses can be proposed regarding the ability of AF-CM to alter organoid signalling and therefore potentially in NEC patients. From our findings it was recognised that AF-CM post-transcriptionally regulates cells including that of the organoids. Furthermore, the post-transcriptional regulation was comparatively similar to what was seen in previous *in vitro* studies

where NF- κ B activity was modified. In addition, the ability of AF-CM to reduce NF- κ B activity along with reduced apoptosis can be explained by some of the identified AF-CM cargo.

Arguably the most important finding into the study of AF-CM effects on the organoids was the ability of AF-CM to reduce NF- κ B nuclear translocation. This was similar to that found within the *in vitro* U251 cell assays. Comparison between the preliminary *in vitro* assays and those conducted in organoids would suggest that the same mechanisms of action exist following AF-CM treatment. These mechanisms of action as discussed may include the transfer of miRNA such as let7b thus leading to reduced levels of TLR4 but also Nf- κ B signalling. It was previously shown in rat models of NEC that AFSCs increased the level of COX-2 within the intestine thus bringing about enhanced survival and repair (Zani et al., 2014). The increase in COX-2 might explain the reduction in NF- κ B signalling seen here in these results because contrary to its classical pro-inflammatory activity COX-2 also negatively regulates NF- κ B expression, which was shown to be decreased in the U251 cells, as indicated by luciferase activity (Poligone and Baldwin, 2001). Activity of COX-2 is also known to be controlled by prostaglandins, in particular cyclopentenone prostaglandins such as PGJ₂ (Poligone and Baldwin, 2001). Therefore it may be of interest to identify whether AF-CM contains lipid based signalling molecules, such as PGJ₂ that could affect COX-2 signalling and subsequent NF- κ B activity. Furthermore, the ability of AF-CM to reduce the level of CD-80 in M1 THP-1 cells suggests that AF-CM could reduce the activity of M1 macrophages within an *in vivo* NEC setting. If proved capable of doing so, a reduced M1 pro-inflammatory response would help bring the overactive inflammatory state of these macrophages towards that seen normally. A reduced pro-inflammatory state would be suggested to reduce the level of cytokine induced necrosis but also stabilise the homeostasis of cell turn over.

Interestingly although NF- κ B activity was altered, the level of stem cell proliferation within the organoids did not mirror that seen in previous *in vitro* assays. No change in E-cadherin levels were seen, even though components within the AF-CM such as let7b and miR125b, known to reduce tight junction permeability and increase intestinal barrier function were present (Liu et al., 2018, Martinez

et al., 2017). The previous research showed that let7b prevented intestinal barrier dysfunction by targeting p38 MAPK leading to reduced PTEN expression and therefore increased AKT and occludin levels within NCM460 cells (Liu et al., 2018). Occludin has been shown to regulate the flux of macromolecules across the intestinal epithelial barrier (Al-Sadi et al., 2011). Additionally, miR125b-5p has been shown to regulate the expression of the tight junction related gene cingulin (Martinez et al., 2017). An increase in cingulin expression was found in IBS-D samples. Increases in cingulin corresponded with decreases in miR125b-5b and may reflect the body's response to try and increase cingulin levels to aid barrier function (Martinez et al., 2017). It could therefore be speculated that AF-CM, containing miR125b, in this instance would hinder this response and potentially reduce tight junction functionality. On the other hand, the levels of cingulin may reflect hyperactivity and dysregulation of homeostasis due to the disease. Introduction of miR125 with the AF-CM would be hypothesised to bring about a reduction in cingulin and normalise its homeostatic levels. Contrary to the lack of activity seen, reduced apoptosis following AF-CM treatment of organoids stimulated with high concentrations of LPS suggest that its cargo has a protective effect. This data is evidenced by the protection it afforded from senescence *in vitro* in IMR90 cells but also the cargo it was found to contain discussed previously. Further investigation towards making the organoid model more representative of NEC is required. It is clear that LPS and TNF- α activity from these results does not mirror that seen by others and may derive from variable diffusion rates of stimulants but also AF-CM cargo through the Matrigel (Neal et al., 2012).

On the other hand, *in vitro* results as well as those seen within the acute damage *in vivo* model suggest that the AF-CM possess molecules beneficial to NEC intestinal regeneration such as increased proliferation, protection from stressors and anti-inflammatory actions. The increased *in vivo* angiogenesis seen in our results suggest that AF-CM could produce similar results within an *in vivo* NEC setting. Increased vasculature would improve the all-important oxygen supply to the tissues and coupled with the NF- κ B modulating activity of AF-CM reduce inflammation and cell death. The AF-CM created here has been proven to improve the activity of cells in favour of regeneration. Under the conditions it was created, it provides a clinically relevant source of paracrine factors that could be

used in the future therapeutically. With regard to NEC, the AF-CM here has the potential to be used as a therapeutic because of its ability to also improve regeneration in an acute damage setting *in vivo*.

Main Study Limitations

In summary, although the work carried out showed that AF-CM reduced the amount of NF- κ B signalling, protected from senescence and increased migration and proliferation capacity, the exact mechanism by which it did so was not conclusive and only speculated surrounding the known functions of some of the cargo identified within the AF-CM and AF-EV. However, due to the vast array of protein and miRNA species identified, which all had both varying but also shared functions, not any single molecule can be identified as being the only effector within the AF-CM. Furthermore, comparison to an AF-CM created from adherent cells as opposed to the stressful conditions used here should be carried out. Additionally, the anti-inflammatory effects, suggested in the U251 and THP-1 macrophages, were established only *in vitro*. Studies on how the AF-CM effects macrophage polarisation and activity should be further investigated *in vivo*. Arguably the main limitation of the study was the ability to recreate a reproducible model of NEC within intestinal organoids. It is therefore of interest to study how experimental variation affects the organoid model in order to better mimic NEC and therefore obtain an experimentally viable model to test the regenerative ability of AF-CM against NEC.

Future Work

Establishing the Anti-inflammatory Properties of AF-CM Further

In order to understand how AF-CM affects macrophage activity *in vivo*, the macrophages first need to be isolated from the tissue of interest for characterisation. In contrast, the tissue containing the macrophage population could be processed for protein or gene expression analysis. Isolation of macrophages from the tissue can be then be analysed for M1 and M2 markers. Flow cytometry can be carried out to measure levels of Ly6C, CD80 (or CD86) as well as Arginase and CD206 for M1 and M2 marker levels respectively. Furthermore, ELISA assays should be carried out for known pro-inflammatory (TNF- α and IL-6) and anti-inflammatory cytokines (IL-10 and CCL2/MCP-1) in the CM produced from either differentiated and polarised THP-1 cells or primary cell cultures of isolated macrophages. However isolation of macrophages from tissue can prove problematic because of the

time it takes to breakdown surrounding tissue thus affecting macrophage viability but also the tendency of isolation reagents to activate damage signalling within tissues. For example, collagenase is often used to dissociate muscle fibres enabling satellite cells to be studied (Otto et al., 2011). However, activation of satellite cells on the muscle fibres enabling migration studies would also lead to chemokine responses from fibres and satellite cell alike and potentially affect the polarisation of macrophages. A simpler but less targeted way of studying the macrophage activity within the diseased tissue would be to dissociate the tissue as a whole and perform qPCR on genes known to be involved in inflammation (TNF- α , IL-6, IL-10 and IL-1 β) to get a profile of the inflammatory state throughout the whole tissue.

Establishing the Active molecules within AF-CM

To establish whether the miRNA species or protein species are more important for the AF-CM effect on proliferation, migration, senescence and NF- κ B activity either of them should be deleted from the CM prior to treatment. Removing miRNA can be carried out by first solubilising the miRNA with detergent thus disrupting AF-EV membranes. Secondly RNase added to the AF-CM would destroy all miRNA within the AF-CM. Alternatively, the AF-CM can be heated to 80°C for at least 5 minutes to irreversibly denature the protein present but without significantly damaging the miRNA integrity (Matsuura et al., 2015, Jung et al., 2010). If the effects of AF-CM are inhibited completely by the heat treatment it is likely that the protein is the more significant effector and vice versa. Although it is likely that a mixture of the AF-CM components have pivotal roles for promoting the effects seen *in vitro*, selective miRNAs can be knocked down in the AF-CM. By treating the AFSCs during AF-CM collection with siRNA species selective to let7b for example would reduce the level of let7b being packaged into the AF-EV. Reduced activity following treatment with the let7b deprived AF-CM would suggest that let7b is responsible for the improved activity seen previously without the knockdown. However, siRNAs are known to have issues with bio-stability, delivery and specificity leading to off target effects particularly *in vivo* (Elmén et al., 2005). It has been shown that providing the siRNA with a phosphorothioate backbone dramatically increases its targeting efficiency and improves

stability within serum thus creating a locked nucleic acid modified oligonucleotide (LNA) (Elmén et al., 2005, Elmén et al., 2008). LNA mediated silencing of miR122 has also been shown *in vivo*, also presenting the first report of antagonism in primates (Elmén et al., 2008). This technology could therefore also be used to silence specific miRNA being packaged within the AF-CM but also to knockdown its systemic effects *in vivo*, for example within the CTX model. Similarly, a new specific targeting method for protein knockdown within a cell has been developed, without the need of modifying the genome and miRNA, called Trim-Away (Clift et al., 2017). Trim-Away utilises the body's natural antibody bound bacterial targeting system, which specifically uses the protein Trim21 (Clift et al., 2017). Trim-21 auto-ubiquitinates upon binding to the bound antibody and targets it for proteasomal degradation (Clift et al., 2017). By introducing an antibody specific to the protein of interest along with exogenous Trim protein, the protein of interest is rapidly targeted and destroyed even in non-dividing cells (Clift et al., 2017). This technique could therefore be used to knockdown proteins such as HMGB1 within the AFSCs thus reducing transfer into the AF-CM or used directly in recipient target cells.

Comparison of AF-CM to AF-CM Collected from Non-Stressed Adherent AFSCs

AF-CM created in a similar fashion to that produced and used previously as a therapeutic in a rat model of NEC should be compared in its make-up to the AF-CM used throughout this project (Zani et al., 2014). AF-CM created under non-stressful conditions should be collected as previously carried out over 30 hours in α -mem from adherent AFSCs. The resulting adherent AF-CM (A-AF-CM) should be characterised for the number of EVs contained within it because as discussed it is thought that stress induces stem cells to secrete higher concentrations of exosomes. Furthermore, the protein and RNA content of the A-AF-CM should be characterised and compared to the AF-CM as carried out here in this project. Additionally, investigation into the A-AF-CM regenerative potential both *in vitro* and *in vivo*, as completed here in this project, could be carried out alongside the AF-CM for comparison.

Increasing the Reproducibility of the Organoid NEC Model

A number of potential faults in the way organoids were treated in order to mimic NEC were identified. Investigations into whether these necessary modifications better mimic and create a reproducible model are therefore required. The first step to take would be to stimulate organoids with LPS or TNF- α that has been mixed within the Matrigel itself. This would have to be done either during a mechanical passage or simply dissolving the current Matrigel that organoids reside in and re-suspending them in the new treated Matrigel. However, it must be noted that introducing the stimulants to Matrigel after mechanical passaging will allow them to interact directly with the intraluminal side of the organoid. Secondly, investigation into the differences in effect between ultra-pure LPS (TLR4 specific) used here and the standard LPS (capable of binding TLR4/2) should be carried out. The dual stimulation of TLR4 and TLR2 may potentiate a more pathogenic response compared to TLR4 alone. Another variable that could be tested is the use of LPS and TNF- α stimulation simultaneously as opposed to their individual use throughout this study. The combined action of LPS and TNF- α through their separate receptors may lead to significantly more pro-inflammatory signalling and reliable cell death. Additionally, LPS and TNF- α are not the only factors that contribute to NEC. The culture of organoids under hypoxic conditions (1% or 5% O₂) as opposed to normoxia (20% O₂, 5% CO₂) would be expected to increase further damage to the organoids and mimic the cellular environment of intestinal cells in NEC (Jun et al., 2014). This can be carried out in combination with LPS or TNF- α stimulation or independently to understand its effects on cell death. Cell death analysis can be carried out as done previously via western blotting and densitometric analysis of CC3 stained protein bands.

Testing the Ability of AF-CM as a Therapeutic for NEC *in Vivo*

To truly test the ability of AF-CM as a potential therapeutic for NEC it must be tested in an *in vivo* NEC model. As discussed, a number of model variations exist that use mainly either mouse or rat models (Zani et al., 2016, Zani et al., 2014). The ability to replicate these experimental models as carried out by others would also enable the investigation into the surrounding tissues of the intestinal epithelium such as the mesenteric nervous system but also the innate immune systems

response to determine if the damage here can also be alleviated (Zani et al., 2014, Zani et al., 2016). Once the efficacy of the AF-CM has been established *in vivo*, its safety and toxicology should also be assessed prior to any use in humans. Control animals treated with AF-CM alone will also provide data suggesting whether the AF-CM can be classed as safe at this stage and understand if it has no adverse effects such as an unwanted inflammatory reaction. Data on how the AF-CM is metabolised and its safe to toxic levels must be established to understand the safest and most optimum dosing regimen. Clinical research using AF-CM must ensure that the AF-CM is created using good manufacturing practice (GMP) guidelines such as its manufacture in a GMP approved lab. Potentially, its use in healthy human volunteers would be carried out with the scaled-up dosing regimens to establish further AF-CM safety and dosage. Finally, a phase 1/2 clinical trial surrounding the use of AF-CM as a therapeutic for NEC in patients would help show whether AF-CM actually increases survival rate of patients with NEC and arguably more importantly, if it increases the quality of life following survival due to increased regeneration of the gut therefore reducing the need for surgery. Further phase 3 and 4 clinical trials would test the use of AF-CM in hundreds to thousands of patients over a number of years to further establish the long-term outcome of the treatment, adverse effects and safety.

8. Appendix I

Primary antibodies:

Antibody	Working Dilution	Source	Supplier	Catalogue Number
4EBP1	1:1000	Rabbit	Cell signalling	9452
Akt	1:1000	Rabbit	Cell signalling	9272
BiP (C50B12)	1:1000	Rabbit	Cell signalling	3177
CD-31	1:200	Rat	BioRad	MCA2388
CHOP	1:1000	Rabbit	Cell signalling	5554
Cleaved Caspase-3 (D175)	1:1000	Rabbit	Cell signalling	9664
E-cadherin	1:200	Mouse	BD Transduction	610182
eIF2 α	1:1000	Rabbit	Cell signalling	9722
Embryonic MHC3	1:200	Mouse	Santa Cruz	SC-53091
F4/80	1:200	Rat	BioRad	MCA497R
Fibrillarin	1:2000	Rabbit	Abcam	Ab5821
FoxO3a (D19A7)	1:1000	Rabbit	Cell signalling	12829
GAPDH	1:1000	Mouse	Millipore	MAB374
Ki-67	1:400	Rabbit	Cell signalling	9129
LC3B	1:1000	Rabbit	Cell signalling	2775
Lysozyme-C	1:200	Goat	Santa Cruz	Sc-27958
Mannose	1:200	Rabbit	Abcam	Ab64693
Mucin-2 (H-300)	1:200	Rabbit	Santa Cruz	Sc-15334
MyoD	1:200	Rabbit	Santa Cruz	Sc-760
p-4EBP1 (Thr37/46)(236B4)	1:1000	Rabbit	Cell signalling	2855
P62/ SQSTM1	1:1000	Rabbit	Sigma	P0067
p-Akt (ser473)	1:1000	Rabbit	Cell signalling	4060
Pax-7	1:1	Goat	DSHB	
p-eIF2 α	1:1000	Rabbit	Abcam	Ab32157
p-FoxO3a (ser253)	1:1000	Rabbit	Cell signalling	13129
Puromycin	1:1000	Mouse	Millipore	MABE343
α -Tubulin	1:1000	Mouse	Cell signalling	3873
β -actin	1:1000	Rabbit	Cell signalling	4970

Table 8.1: Primary antibodies

Secondary antibodies:

Antibody	Working Dilution	Source	Supplier	Catalogue Number
Alexa fluor 488 anti-goat	1:200	Donkey	Molecular probes	A11055
Alexa fluor 488 anti-mouse	1:200	Goat	Invitrogen	A11029
Alexa fluor 488 anti-mouse	1:200	Goat	Invitrogen	A11032
Alexa fluor 488 anti-rabbit	1:200	Goat	Invitrogen	A11034
Alexa fluor 488 anti-Rat	1:200	Goat	Molecular Probes	A21212
Alexa fluor 594 anti-rabbit	1:200	Goat	Invitrogen	A11037
HRP conjugated ant- Mouse	1:10000	Rabbit	Dako	P0260
HRP conjugated ant- Rat	1:5000	Goat	R and D Systems	HAF 005
HRP conjugated ant-goat	1:5000	Rabbit	Dako	P0160
HRP conjugated ant-Rabbit	1:5000	Goat	Invitrogen	65-6120

Table 8.2: Secondary antibodies**Microbeads**

Antibody	Working Dilution	Source	Supplier	Catalogue Number
CD117 Microbead Kit - Human	100 μ L/ 10^8 cells	clone AC126	Miltenyi Biotec	130-091-332

Table 8.3: Microbeads**Flow cytometry antibodies**

Antibody	Working Dilution	Source	Supplier	Catalogue Number
CD-105	1:200	Mouse	Millipore	CS208
CD-117/APC	1:200	Mouse	R&D Biosystems	FAB332A-025
CD34/FITC	1:200	Mouse	Millipore	CBL555F
CD-44/Alexa fluor 647	1:200	Mouse	Millipore	CS208200
CD-45/FITC	1:200	Mouse	Biolegend	304105
CD-73/ PE	1:200	Mouse	Biolegend	344004
CD-80	1:200	Mouse	Biolegend	305207
CD-90/ PE	1:200	Mouse	Biolegend	328107

Table 8.4: Flow cytometry antibodies

9. Appendix II

RT-qPCR Primers

Primer	Forward 3'	Reverse 5'
m LGR5	ATT CGG TGC ATT TAG CTT GG	CGA ACA CCT GCG TGA ATA TG
m Mucin-2	CCG ACT TCA ACC CAA GTG AT	GAG CAA GGG ACT CTG GTC TG
m Lysozyme-1	GTC ACA CTT CCT CGC TTT CC	TGG CTT TGC TGA CTG ACA AG
m Chromogranin-A	AAG GTG ATG AAG TGC GTC CT	GGT GTC GCA GGA TAG AGA GG
m TNF α	CAG GCG GTG CCT ATG TCT C	CGA TCA CCC CGA AGT TCA GTA G
m TGF β	CTT CAA TAC GTC AGA CAT TCG GG	GTA ACG CCA GGA ATT GTT GCT A

Table 9.1: RT-qPCR primers

10. Appendix III

Solutions

1X PBS

One PBS (Oxoid) tablet was dissolved in Ultrapure H₂O (80ml) and pH adjusted to 7.4 with HCl (1M) prior to making up to 100ml with ultrapure H₂O and autoclaving.

Permeabilisation buffer

Sucrose (20.54g), HEPES (0.952g), NaCl (0.584g), MgCl₂ (0.260g), sodium azide (0.1g) and Triton-X-100 (1ml) were made up to 200ml with dH₂O.

Wash Buffer

Foetal bovine serum (FBS – 25ml), sodium azide (200mg) and Triton X-100 (250µl) were dissolved in 1X PBS and made up to a final volume of 500ml.

DAPI fluorescent stain

DAPI (7.5µl) were mixed in Dako Fluorescent mounting medium (15ml).

4% Paraformaldehyde (PFA) in PBS

PFA powder (20g) was dissolved in 1X PBS (480ml) by heating to 65°C and made up to 500ml with 1X PBS.

Lysis Buffer

EDTA (1mM), EGTA (5mM), Triton-X 100 (0.5%), Tris-HCl (50mM, pH 7), 2-mercaptoethanol (2%), 4% SDS, Urea (4M) made up in ultrapure water.

1x Running Buffer

Ultrapure dH₂O (950ml) and of 20X NuPAGE running buffer (Novex, Life Technologies - 50ml) were mixed. Antioxidant (0.5ml) was added to 200ml of 1X running buffer mix.

Transfer Buffer

Methanol (30ml), 20X NuPAGE transfer buffer (Novex, Life Technologies - 15ml) and antioxidant (0.3ml), were mixed and made up to 300ml with Ultrapure H₂O.

PBS-T

Tween-20 (250µl, 0.05%) was dissolved in 1X PBS (500ml).

Blocking buffer

Microbiological grade bovine serum albumin (2.5g, 5%) was mixed in PBS-T (30ml) and made up to a final volume of 50ml.

Reducing sample treatment buffer (6X RSTB)

Sodium dodecyl sulfate (SDS – 12g) was dissolved in a mix of β-mercaptoethanol (30ml), Glycerol (30ml), Tris-HCl (0.5M, pH 6.8) and ultrapure H₂O (10ml).

Freezing Media stock

FBS and DMSO solution were mixed 90/10 % by volume.

Alizarin Red S working solution

Alizarin Red S (1mg/ml) was made up in ultrapure H₂O and adjusted to pH 5.5 using ammonium hydroxide.

Oil Red O stock and working solution

For stock Oil Red O (3mg/ml) was dissolved in 99% isopropanol. For a working solution, Oil Red O stock was mixed with ultrapure H₂O: 60/40 % by volume and allowed to sit for 10 minutes before filtering through a 0.2µm filter. Stable for up to 2 hours.

Alcian Blue working solution

Alcian blue (0.1mg/ml) was made up in ethanol (98-100%) and acetic acid (98-100%) mixed 60/40% by volume. Stable for up to a year. De-staining solution was the same without the addition of Alcian blue.

Acid phosphatase staining solution

Sodium acetate (0.2M): anhydrous sodium acetate (1.64g, MW82) or sodium acetate trihydrate (mw136, 2.72g) was made up to 100ml with dH₂O.

Acetic Acid: glacial acetic acid (1.2ml) was made up to 100ml with dH₂O.

Acetate buffer: sodium acetate (35.2ml) and acetic acid (14.8ml) was made up to 100ml with dH₂O.

Solution A: Pararsaniline Hydrochloride (40mg) was dissolved in HCl (1ml, 2M).

Solution B: Sodium nitrite (40mg) was dissolved in dH₂O (1ml).

Solutions A and B were mixed 50/50 % by volume and left for 1-2 minutes until a pale straw colour formed.

Naphthol AS-BI phosphate solution: of Naphthol AS-BI phosphate (25mg) was dissolved in DMSO (10 drops).

Working stain: All the Naphthol AS-BI phosphate solution, dH₂O (30ml), Acetate buffer (12.5ml, 0.1M, pH 5.0) and HPR (2ml) were mixed and pH adjusted to 5.0 using NaOH (1M).

Senescence Fixative (0.2% Glutaraldehyde, 2% PFA/PBS)

Glutaraldehyde stock solution (25%), PFA/PBS (4%) and dH₂O were mixed at 0.8/50/49.2 % by volume.

Senescence staining solution

Sodium Phosphate pH 6.0; Potassium Ferricyanide Stock (3.29g/100ml, 100 μ M); Potassium Ferrocyanide Stock (4.22g/100ml, 100 μ M); NaCl stock (14.6g/100ml, 2.5M); MgCl₂ stock (20.3g/100ml, 1M); X-gal (50mg/ml); dH₂O

For Sodium Phosphate two solutions were made up: NaH₂PO₄ (1.370g/100ml, 0.1M) and Na₂HPO₄ (1.779g/100ml, 0.1M). Na₂HPO₄ added to NaH₂PO₄ (80ml) until the pH=6 before making up to 100ml with dH₂O.

For 20ml of stain:

Sodium phosphate (pH6, 4ml), Potassium Ferricyanide (1ml), Potassium Ferrocyanide (1ml), NaCl (2.4ml, 2.5M), MgCl₂ (40μl, 1M), dH₂O (10.56ml) and X-gal (1ml) were mixed.

Citrate Buffer (0.01M)

Citrate Buffer 0.01M: 9ml solution A, 41ml Solution B and 450ml H₂O)

- Solution A (21.01g/L Citric acid 0.1M in H₂O)
- Solution B (29.41g/L Sodium citrate 0.1M in H₂O)

Chemicals

Substance	Supplier	Catalogue number
2-mercaptoethanol	Sigma-Aldrich	63689
Alcian Blue	Sigma-Aldrich	A-3157
Alizarin Red	Sigma-Aldrich	A5533
Ammonium hydroxide	Sigma-Aldrich	221228-M
Anhydrous sodium acetate	Sigma-Aldrich	W302406
BSA	Fisher scientific	BP9700-100
Citric acid	Sigma-Aldrich	C0759
DMSO	AnalaR	103234L
EDTA	Fisher scientific	10618973
EGTA	Tocris	28071G
Glacial acetic acid	Fisher scientific	10050000
Glutaraldehyde	Millipore MERCK	1.04239.0250
Glycerol	Sigma-Aldrich	G6279
HCL	Sigma-Aldrich	W530574
HEPES powder	Fisher scientific	BP410-500
Isopentane	Acros organics	126470010
Isopropanol	Fisher Scientific	BP2618-212
Methanol	Fisher Scientific	M/4056/17
MgCl ₂	Sigma-Aldrich	M2670-500
N-acetylcysteine	Enzo Lifesciences	ALX-105-005-G005
NaCl	Sigma-Aldrich	71382
Naphthol AS Biphosphate	Acros organics	1919-91-1
Oil Red O	Sigma-Aldrich	O0625
Pararsaniline HCl	Acros organics	270100050
PBS tablets	Oxoid	BR0014G
PFA	Fisher Scientific	P/0840/53
Potassium ferricyanide	Acros organics	223111000
Potassium ferrocyanide	Acros organics	424130025
SDS	Fisher Scientific	S/5200/53
Sodium Azide	Acros organics	190381000
Sodium citrate	BDH	30128
Sodium nitrite	Fisher Chemical	S/5640/62
Sodium phosphate	Fisher scientific	BP330-500
Sucrose	Fisher Chemical	S/8560/53
Trypan blue	Gibco	11538886
Urea	AnalaR	102908D
Valproic acid	Sigma-Aldrich	P4543-25G
X-gal	VWR	0428-16
Xylene	Fisher Scientific	X/0250/17

Table 10.1: Chemicals

Materials and reagents:

Substance	Supplier	Catalogue number
1x Passive lysis buffer	Promega	E153A
AdDMEM F12	Invitrogen	12634010
Agarose	Sigma-Aldrich	A4679
Amersham ECL Prime Western Blotting Detection Reagent	GE Healthcare	RPN2232
B27 supplement	Invitrogen	17504-044
Cell recovery solution	Corning	354253
Cell Titer 96 Non-radioactive Cell Proliferation Assay	Sarsted	G4002
Chang B/C	Irvine scientific	T101-019
CT99021	Selleckchem	S2924
DAPI	Molecular probes	D-1306
DC BioRad protein assay	BioRad	5000112
DMEM 4.5g/l glucose	Gibco	10741574
DPX mounting media	Fisher Scientific	D/5319/05
E.coli LPS	Invivogen	Tlrl-eklps
Eosin	Sigma-Aldrich	318906-500ml
FBS	Gibco	10270-106
FcR Blocking reagent	Miltenyi Biotec	130-059-901
Glutamax	Gibco	11574466
Growth factor reduced, Phenol red free Matrigel	Corning	356231
h-rR-spondin	PeproTech	120-38
Hydro mounting media	Agar scientific	R1356
L-glutamine	Gibco	11539876
LPS-SM Ultrapure	InvivoGen	Tlrl-smlps
Luciferase Assay System	Promega	E1500
MACS Multistand	Miltenyi Biotec	130-042-303
Mayers Haematoxylin	Sigma-Aldrich	MHS16-500ml
Mesenpro RSTM	Gibco	10212293
MiniMACS Separator	Miltenyi Biotec	130-042-102
m-rEGF	R&D systems	2028-EG-200
m-rNoggin	PeproTech	250-38
MS MACS Column	Miltenyi Biotec	130-042-201
N2 supplement	Invitrogen	17502-048
Naja pallida CTX	Latoxan	L8102
Penicillin/streptomycin	Gibco	11568876
PKH26	Sigma	P9691
Protease Inhibitor Cocktail Set 1	Calbiochem	539131
Recombinant Human TNF- α	PeproTech	300 01A
SilverXpress silver staining kit	Invitrogen	LC6100
Solubilization Solution/Stop Mix	Promega	G401A
Stem XVivo Adipogenic supplement	R&D systems	13472505
Stem XVivo chondrogenic supplement	R&D systems	13462505
Stem XVivo osteogenic supplement	R&D systems	13482505

Stem osteogenic/adipogenic media	XVivo base	R&D systems	13412515
Triton X-100		Fisher scientific	T/3751/08
TrpLE Select		Gibco	12093745
Ultra-pure E.coli LPS		Invivogen	Tlrl-peklps
α -MEM		Gibco	12509069
Phorbol-12-myristate-13-acetate		Sigma	P8139-1MG
Gibco RPMI 1640 Medium (ATCC modification)		Gibco	11504566
Recombinant Human IFN- γ		Biologend	713906
Recombinant Human IL-4		Biologend	714904
Recombinat Human IL-13		Biologend	571102
Recombinant Human TNF- α		Peprotech	300-01A

Table 10.2: Materials and reagents

11. References

- ABRAMI, L., FIVAZ, M., DECROLY, E., SEIDAH, N. G., JEAN, F., THOMAS, G., LEPPLA, S. H., BUCKLEY, J. T. & VAN DER GOOT, F. G. 1998. The pore-forming toxin proaerolysin is activated by furin. *J Biol Chem*, 273, 32656-61.
- ADMYRE, C., JOHANSSON, S. M., PAULIE, S. & GABRIELSSON, S. 2006. Direct exosome stimulation of peripheral human T cells detected by ELISPOT. *Eur J Immunol*, 36, 1772-81.
- ADUTLER-LIEBER, S., BEN-MORDECHAI, T., NAFTALI-SHANI, N., ASHER, E., LOBERMAN, D., RAANANI, E. & LEOR, J. 2013. Human macrophage regulation via interaction with cardiac adipose tissue-derived mesenchymal stromal cells. *J Cardiovasc Pharmacol Ther*, 18, 78-86.
- AHN, D. H., CRAWLEY, S. C., HOKARI, R., KATO, S., YANG, S. C., LI, J. D. & KIM, Y. S. 2005. TNF-alpha activates MUC2 transcription via NF-kappaB but inhibits via JNK activation. *Cell Physiol Biochem*, 15, 29-40.
- AKAGAWA, K. S. 2002. Functional heterogeneity of colony-stimulating factor-induced human monocyte-derived macrophages. *Int J Hematol*, 76, 27-34.
- AL-SADI, R., KHATIB, K., GUO, S., YE, D., YOUSSEF, M. & MA, T. 2011. Occludin regulates macromolecule flux across the intestinal epithelial tight junction barrier. *Am J Physiol Gastrointest Liver Physiol*, 300, G1054-64.
- ALCAZAR, O., HAWKRIDGE, A. M., COLLIER, T. S., COUSINS, S. W., BHATTACHARYA, S. K., MUDDIMAN, D. C. & MARIN-CASTANO, M. E. 2009. Proteomics characterization of cell membrane blebs in human retinal pigment epithelium cells. *Mol Cell Proteomics*, 8, 2201-11.
- ALVAREZ-GARCIA, I. & MISKA, E. A. 2005. MicroRNA functions in animal development and human disease. *Development*, 132, 4653-62.
- ALVAREZ, M. L., KHOSROHEIDARI, M., KANCHI RAVI, R. & DISTEFANO, J. K. 2012. Comparison of protein, microRNA, and mRNA yields using different methods of urinary exosome isolation for the discovery of kidney disease biomarkers. *Kidney Int*, 82, 1024-1032.
- ANDERSON, D. J., GAGE, F. H. & WEISSMAN, I. L. 2001. Can stem cells cross lineage boundaries? *Nat Med*, 7, 393-395.
- ANDERSON, P., CARRILLO-GÁLVEZ, A. B., GARCÍA-PÉREZ, A., COBO, M. & MARTÍN, F. 2013. CD105 (Endoglin)-Negative Murine Mesenchymal Stromal Cells Define a New Multipotent Subpopulation with Distinct Differentiation and Immunomodulatory Capacities. *PLOS ONE*, 8, e76979.
- ANDREAKOS, E., SACRE, S. M., SMITH, C., LUNDBERG, A., KIRIAKIDIS, S., STONEHOUSE, T., MONACO, C., FELDMANN, M. & FOXWELL, B. M. 2004. Distinct pathways of LPS-induced NF-kappa B activation and cytokine production in human myeloid and nonmyeloid cells defined by selective utilization of MyD88 and Mal/TIRAP. *Blood*, 103, 2229-37.
- ANG, Y. S., TSAI, S. Y., LEE, D. F., MONK, J., SU, J., RATNAKUMAR, K., DING, J., GE, Y., DARR, H., CHANG, B., WANG, J., RENDL, M., BERNSTEIN, E., SCHANIEL, C. & LEMISCHKA, I. R. 2011. Wdr5 mediates self-renewal and reprogramming via the embryonic stem cell core transcriptional network. *Cell*, 145, 183-97.
- ARNOLD, L., HENRY, A., PORON, F., BABA-AMER, Y., VAN ROOIJEN, N., PLONQUET, A., GHERARDI, R. K. & CHAZAUD, B. 2007. Inflammatory monocytes recruited after skeletal muscle injury switch into antiinflammatory macrophages to support myogenesis. *The Journal of Experimental Medicine*, 204, 1057-1069.
- ASAKURA, A., KOMAKI, M. & RUDNICKI, M. 2001. Muscle satellite cells are multipotential stem cells that exhibit myogenic, osteogenic, and adipogenic differentiation. *Differentiation*, 68, 245-53.
- ASEA, A., JEAN-PIERRE, C., KAUR, P., RAO, P., LINHARES, I. M., SKUPSKI, D. & WITKIN, S. S. 2008. Heat shock protein-containing exosomes in mid-trimester amniotic fluids. *Journal of Reproductive Immunology*, 79, 12-17.

- ATWOOD, B. L., WOOLNOUGH, J. L., LEFEVRE, G. M., SAINT JUST RIBEIRO, M., FELSENFELD, G. & GILES, K. E. 2016. Human Argonaute 2 Is Tethered to Ribosomal RNA through MicroRNA Interactions. *The Journal of Biological Chemistry*, 291, 17919-17928.
- BABST, M. 2005. A protein's final ESCRT. *Traffic*, 6, 2-9.
- BAER, M., DILLNER, A., SCHWARTZ, R. C., SEDON, C., NEDOSPASOV, S. & JOHNSON, P. F. 1998. Tumor Necrosis Factor Alpha Transcription in Macrophages Is Attenuated by an Autocrine Factor That Preferentially Induces NF- κ B p50. *Molecular and Cellular Biology*, 18, 5678-5689.
- BAILO, M., SONCINI, M., VERTUA, E., SIGNORONI, P. B., SANZONE, S., LOMBARDI, G., ARIENTI, D., CALAMANI, F., ZATTI, D., PAUL, P., ALBERTINI, A., ZORZI, F., CAVAGNINI, A., CANDOTTI, F., WENGLER, G. S. & PAROLINI, O. 2004. Engraftment potential of human amnion and chorion cells derived from term placenta. *Transplantation*, 78, 1439-48.
- BALBI, C., PICCOLI, M., BARILE, L., PAPAIT, A., ARMIROTTI, A., PRINCIPI, E., REVERBERI, D., PASCUCCI, L., BECHERINI, P., VARESIO, L., MOGNI, M., COVIELLO, D., BANDIERA, T., POZZOBON, M., CANCEDDA, R. & BOLLINI, S. First Characterization of Human Amniotic Fluid Stem Cell Extracellular Vesicles as a Powerful Paracrine Tool Endowed with Regenerative Potential. *STEM CELLS Translational Medicine*, n/a-n/a.
- BANGEN, J. M., SCHADE, F. U. & FLOHÉ, S. B. 2007. Diverse regulatory activity of human heat shock proteins 60 and 70 on endotoxin-induced inflammation. *Biochemical and Biophysical Research Communications*, 359, 709-715.
- BAO, M.-H., FENG, X., ZHANG, Y.-W., LOU, X.-Y., CHENG, Y. & ZHOU, H.-H. 2013. Let-7 in Cardiovascular Diseases, Heart Development and Cardiovascular Differentiation from Stem Cells. *International Journal of Molecular Sciences*, 14, 23086-23102.
- BARBARA, N. P., WRANA, J. L. & LETARTE, M. 1999. Endoglin is an accessory protein that interacts with the signaling receptor complex of multiple members of the transforming growth factor-beta superfamily. *J Biol Chem*, 274, 584-94.
- BARKER, T. H. & HAGOOD, J. S. 2009. Getting a grip on Thy-1 signaling. *Biochim Biophys Acta*, 1793, 921-3.
- BARRECA, M. M., SPINELLO, W., CAVALIERI, V., TURTURICI, G., SCONZO, G., KAUR, P., TINNIRELLO, R., ASEA, A. A. & GERACI, F. 2017. Extracellular Hsp70 Enhances Mesoangioblast Migration via an Autocrine Signaling Pathway. *J Cell Physiol*, 232, 1845-1861.
- BEALL, M. H., VAN DEN WIJNGAARD, J. P. H. M., VAN GEMERT, M. J. C. & ROSS, M. G. 2007. Amniotic Fluid Water Dynamics. *Placenta*, 28, 816-823.
- BECKER, A. J., MC, C. E. & TILL, J. E. 1963. Cytological demonstration of the clonal nature of spleen colonies derived from transplanted mouse marrow cells. *Nature*, 197, 452-4.
- BENINSON, L. A., BROWN, P. N., LOUGHRIDGE, A. B., SALUDES, J. P., MASLANIK, T., HILLS, A. K., WOODWORTH, T., CRAIG, W., YIN, H. & FLESHNER, M. 2014. Acute Stressor Exposure Modifies Plasma Exosome-Associated Heat Shock Protein 72 (Hsp72) and microRNA (miR-142-5p and miR-203). *PLoS ONE*, 9, e108748.
- BERGERS, G. & SONG, S. 2005. The role of pericytes in blood-vessel formation and maintenance. *Neuro-Oncology*, 7, 452-464.
- BHASIN, A., SRIVASTAVA, M. V., KUMARAN, S. S., MOHANTY, S., BHATIA, R., BOSE, S., GAIKWAD, S., GARG, A. & AIRAN, B. 2011. Autologous mesenchymal stem cells in chronic stroke. *Cerebrovasc Dis Extra*, 1, 93-104.
- BIANCHI, M. E. 2007. DAMPs, PAMPs and alarmins: all we need to know about danger. *J Leukoc Biol*, 81, 1-5.
- BIANCO, P. & GEHRON ROBEY, P. 2000. Marrow stromal stem cells. *The Journal of Clinical Investigation*, 105, 1663-1668.
- BISBAL, C., MARTINAND, C., SILHOL, M., LEBLEU, B. & SALEHZADA, T. 1995. Cloning and characterization of a RNase L inhibitor. A new component of the interferon-regulated 2-5A pathway. *J Biol Chem*, 270, 13308-17.
- BJORNSON, C. R., CHEUNG, T. H., LIU, L., TRIPATHI, P. V., STEEPER, K. M. & RANDO, T. A. 2012. Notch signaling is necessary to maintain quiescence in adult muscle stem cells. *Stem Cells*, 30, 232-42.

- BLANPAIN, C., HORSLEY, V. & FUCHS, E. Epithelial Stem Cells: Turning over New Leaves. *Cell*, 128, 445-458.
- BOHÓRQUEZ, D. V., SHAHID, R. A., ERDMANN, A., KREGER, A. M., WANG, Y., CALAKOS, N., WANG, F. & LIDDLE, R. A. 2015. Neuroepithelial circuit formed by innervation of sensory enteroendocrine cells. *The Journal of Clinical Investigation*, 125, 782-786.
- BRACE, R. A., WLODEK, M. E., COCK, M. L. & HARDING, R. 1994. Swallowing of lung liquid and amniotic fluid by the ovine fetus under normoxic and hypoxic conditions. *American Journal of Obstetrics and Gynecology*, 171, 764-770.
- BROWN, S. L., RIEHL, T. E., WALKER, M. R., GESKE, M. J., DOHERTY, J. M., STENSON, W. F. & STAPPENBECK, T. S. 2007. Myd88-dependent positioning of Ptg2-expressing stromal cells maintains colonic epithelial proliferation during injury. *J Clin Invest*, 117, 258-69.
- BURGOS, K., MALENICA, I., METPALLY, R., COURTRIGHT, A., RAKELA, B., BEACH, T., SHILL, H., ADLER, C., SABBAGH, M., VILLA, S., TEMBE, W., CRAIG, D. & VAN KEUREN-JENSEN, K. 2014. Profiles of extracellular miRNA in cerebrospinal fluid and serum from patients with Alzheimer's and Parkinson's diseases correlate with disease status and features of pathology. *PLoS One*, 9, e94839.
- BUSSOLATI, B., MOGGIO, A., COLLINO, F., AGHEMO, G., D'ARMENTO, G., GRANGE, C. & CAMUSSI, G. 2012. Hypoxia modulates the undifferentiated phenotype of human renal inner medullary CD133+ progenitors through Oct4/miR-145 balance. *American Journal of Physiology - Renal Physiology*, 302, F116-F128.
- CAHAN, P. & DALEY, G. Q. 2013. Origins and implications of pluripotent stem cell variability and heterogeneity. *Nat Rev Mol Cell Biol*, 14, 357-68.
- CALZAROSSA, C., BOSSOLASCO, P., BESANA, A., MANCA, M. P., DE GRADA, L., DE COPPI, P., GIARDINO, D., SILANI, V. & COVA, L. 2013. Neurorescue effects and stem properties of chorionic villi and amniotic progenitor cells. *Neuroscience*, 234, 158-72.
- CAMPISI, J. & D'ADDA DI FAGAGNA, F. 2007. Cellular senescence: when bad things happen to good cells. *Nat Rev Mol Cell Biol*, 8, 729-740.
- CAMUSSI, G., DEREGIBUS, M. C., BRUNO, S., CANTALUPPI, V. & BIANCONE, L. 2010. Exosomes/microvesicles as a mechanism of cell-to-cell communication. *Kidney Int*, 78, 838-848.
- CAPLAN, A. I. 1991. Mesenchymal stem cells. *J Orthop Res*, 9, 641-50.
- CARMEN, J., BURGER, S. R., MCCAMAN, M. & ROWLEY, J. A. 2012. Developing assays to address identity, potency, purity and safety: cell characterization in cell therapy process development. *Regen Med*, 7, 85-100.
- CARRARO, G., PERIN, L., SEDRAKYAN, S., GIULIANI, S., TIOZZO, C., LEE, J., TURCATEL, G., DE LANGHE, S. P., DRISCOLL, B., BELLUSCI, S., MINOO, P., ATALA, A., DE FILIPPO, R. E. & WARBURTON, D. 2008. Human amniotic fluid stem cells can integrate and differentiate into epithelial lung lineages. *Stem Cells*, 26, 2902-11.
- CASTELLANI, C., VESCOVO, G., RAVARA, B., FRANZIN, C., POZZOBON, M., TAVANO, R., GORZA, L., PAPINI, E., VETTOR, R., DE COPPI, P., THIENE, G. & ANGELINI, A. 2013. The contribution of stem cell therapy to skeletal muscle remodeling in heart failure. *Int J Cardiol*, 168, 2014-21.
- CERADINI, D. J., KULKARNI, A. R., CALLAGHAN, M. J., TEPPER, O. M., BASTIDAS, N., KLEINMAN, M. E., CAPLA, J. M., GALIANO, R. D., LEVINE, J. P. & GURTNER, G. C. 2004. Progenitor cell trafficking is regulated by hypoxic gradients through HIF-1 induction of SDF-1. *Nat Med*, 10, 858-64.
- CHAINEDAU, M., DANGLLOT, L. & GALLI, T. 2009. Multiple roles of the vesicular-SNARE TI-VAMP in post-Golgi and endosomal trafficking. *FEBS Lett*, 583, 3817-26.
- CHAN, K. L., HO, J. C., CHAN, K. W. & TAM, P. K. 2002. A study of gut immunity to enteral endotoxin in rats of different ages: a possible cause for necrotizing enterocolitis. *J Pediatr Surg*, 37, 1435-40.
- CHANPUT, W., MES, J. J., SAVALKOUL, H. F. J. & WICHERS, H. J. 2013. Characterization of polarized THP-1 macrophages and polarizing ability of LPS and food compounds. *Food & Function*, 4, 266-276.

- CHEN, C.-L., YU, X., JAMES, I. O. A., ZHANG, H.-Y., YANG, J., RADULESCU, A., ZHOU, Y. & BESNER, G. E. 2012. Heparin-binding EGF-like growth factor protects intestinal stem cells from injury in a rat model of necrotizing enterocolitis. *Laboratory Investigation; a Journal of Technical Methods and Pathology*, 92, 331-344.
- CHEN, G. & GOEDDEL, D. V. 2002. TNF-R1 Signaling: A Beautiful Pathway. *Science*, 296, 1634-1635.
- CHEN, H., YANG, J., LOW, P. S. & CHENG, J. X. 2008. Cholesterol level regulates endosome motility via Rab proteins. *Biophys J*, 94, 1508-20.
- CHEN, Y., KOIKE, Y., MIYAKE, H., LI, B., LEE, C., HOCK, A., ZANI, A. & PIERRO, A. 2016. Formula feeding and systemic hypoxia synergistically induce intestinal hypoxia in experimental necrotizing enterocolitis. *Pediatr Surg Int*, 32, 1115-1119.
- CHENG, H. & LEBLOND, C. P. 1974. Origin, differentiation and renewal of the four main epithelial cell types in the mouse small intestine. V. Unitarian Theory of the origin of the four epithelial cell types. *Am J Anat*, 141, 537-61.
- CHI, S. W., ZANG, J. B., MELE, A. & DARNELL, R. B. 2009. Argonaute HITS-CLIP decodes microRNA-mRNA interaction maps. *Nature*, 460, 479-86.
- CHIAVEGATO, A., BOLLINI, S., POZZOBON, M., CALLEGARI, A., GASPAROTTO, L., TAIANI, J., PICCOLI, M., LENZINI, E., GEROSA, G., VENDRAMIN, I., COZZI, E., ANGELINI, A., IOP, L., ZANON, G. F., ATALA, A., DE COPPI, P. & SARTORE, S. 2007. Human amniotic fluid-derived stem cells are rejected after transplantation in the myocardium of normal, ischemic, immuno-suppressed or immuno-deficient rat. *J Mol Cell Cardiol*, 42, 746-59.
- CHO, D.-I., KIM, M. R., JEONG, H.-Y., JEONG, H. C., JEONG, M. H., YOON, S. H., KIM, Y. S. & AHN, Y. 2014. Mesenchymal stem cells reciprocally regulate the M1/M2 balance in mouse bone marrow-derived macrophages. *Experimental & Molecular Medicine*, 46, e70.
- CLAYTON, A., COURT, J., NAVABI, H., ADAMS, M., MASON, M. D., HOBOT, J. A., NEWMAN, G. R. & JASANI, B. 2001. Analysis of antigen presenting cell derived exosomes, based on immunomagnetic isolation and flow cytometry. *J Immunol Methods*, 247, 163-74.
- CLIFT, D., MCEWAN, W. A., LABZIN, L. I., KONIECZNY, V., MOGESSIE, B., JAMES, L. C. & SCHUH, M. 2017. A Method for the Acute and Rapid Degradation of Endogenous Proteins. *Cell*, 171, 1692-1706.e18.
- COCUCCI, E., RACCHETTI, G. & MELDOLESI, J. 2009. Shedding microvesicles: artefacts no more. *Trends in Cell Biology*, 19, 43-51.
- COLLINO, F., DEREGIBUS, M. C., BRUNO, S., STERPONE, L., AGHEMO, G., VILTONO, L., TETTA, C. & CAMUSSI, G. 2010. Microvesicles derived from adult human bone marrow and tissue specific mesenchymal stem cells shuttle selected pattern of miRNAs. *PLoS One*, 5.
- COLLINS, C. A., OLSEN, I., ZAMMIT, P. S., HESLOP, L., PETRIE, A., PARTRIDGE, T. A. & MORGAN, J. E. 2005. Stem cell function, self-renewal, and behavioral heterogeneity of cells from the adult muscle satellite cell niche. *Cell*, 122, 289-301.
- CORNELISON, D. D., OLWIN, B. B., RUDNICKI, M. A. & WOLD, B. J. 2000. MyoD(-/-) satellite cells in single-fiber culture are differentiation defective and MRF4 deficient. *Dev Biol*, 224, 122-37.
- CORNELISON, D. D. & WOLD, B. J. 1997. Single-cell analysis of regulatory gene expression in quiescent and activated mouse skeletal muscle satellite cells. *Dev Biol*, 191, 270-83.
- CUMMINS, E. P., BERRA, E., COMERFORD, K. M., GINOUVES, A., FITZGERALD, K. T., SEEBALLUCK, F., GODSON, C., NIELSEN, J. E., MOYNAGH, P., POUYSSEGUR, J. & TAYLOR, C. T. 2006. Prolyl hydroxylase-1 negatively regulates I κ B kinase-beta, giving insight into hypoxia-induced NF κ B activity. *Proc Natl Acad Sci U S A*, 103, 18154-9.
- D'ALBIS, A., COUTEAUX, R., JANMOT, C., ROULET, A. & MIRA, J. C. 1988. Regeneration after cardiotoxin injury of innervated and denervated slow and fast muscles of mammals. Myosin isoform analysis. *Eur J Biochem*, 174, 103-10.
- D'AMICO, M. A., GHINASSI, B., IZZICUPO, P., MANZOLI, L. & DI BALDASSARRE, A. 2014. Biological function and clinical relevance of chromogranin A and derived peptides. *Endocrine Connections*, 3, R45-R54.

- DAIGNEAULT, M., PRESTON, J. A., MARRIOTT, H. M., WHYTE, M. K. B. & DOCKRELL, D. H. 2010. The Identification of Markers of Macrophage Differentiation in PMA-Stimulated THP-1 Cells and Monocyte-Derived Macrophages. *PLoS ONE*, 5, e8668.
- DANZER, K. M., RUF, W. P., PUTCHA, P., JOYNER, D., HASHIMOTO, T., GLABE, C., HYMAN, B. T. & MCLEAN, P. J. 2011. Heat-shock protein 70 modulates toxic extracellular α -synuclein oligomers and rescues trans-synaptic toxicity. *The FASEB Journal*, 25, 326-336.
- DATE, S. & SATO, T. 2015. Mini-Gut Organoids: Reconstitution of the Stem Cell Niche. *Annual Review of Cell and Developmental Biology*, 31, 269-289.
- DE COPPI, P., BARTSCH, G., SIDDIQUI, M. M., XU, T., SANTOS, C. C., PERIN, L., MOSTOSLAVSKY, G., SERRE, A. C., SNYDER, E. Y., YOO, J. J., FURTH, M. E., SOKER, S. & ATALA, A. 2007. Isolation of amniotic stem cell lines with potential for therapy. *Nature Biotechnology*, 25, 100-106.
- DE GASSART, A., GEMINARD, C., FEVRIER, B., RAPOSO, G. & VIDAL, M. 2003. Lipid raft-associated protein sorting in exosomes. *Blood*, 102, 4336-44.
- DEBACQ-CHAINIAUX, F., ERUSALIMSKY, J. D., CAMPISI, J. & TOUSSAINT, O. 2009. Protocols to detect senescence-associated beta-galactosidase (SA-beta-gal) activity, a biomarker of senescent cells in culture and in vivo. *Nat Protoc*, 4, 1798-806.
- DEL CONDE, I., SHRIMPTON, C. N., THIAGARAJAN, P. & LOPEZ, J. A. 2005. Tissue-factor-bearing microvesicles arise from lipid rafts and fuse with activated platelets to initiate coagulation. *Blood*, 106, 1604-11.
- DEREGIBUS, M. C., CANTALUPPI, V., CALOGERO, R., LO IACONO, M., TETTA, C., BIANCONE, L., BRUNO, S., BUSSOLATI, B. & CAMUSSI, G. 2007. Endothelial progenitor cell derived microvesicles activate an angiogenic program in endothelial cells by a horizontal transfer of mRNA. *Blood*, 110, 2440-2448.
- DI TRAPANI, M., BASSI, G., FONTANA, E., GIACOMELLO, L., POZZOBON, M., GUILLOT, P. V., DE COPPI, P. & KRAMPERA, M. 2015. Immune regulatory properties of CD117(pos) amniotic fluid stem cells vary according to gestational age. *Stem Cells Dev*, 24, 132-43.
- DITADI, A., DE COPPI, P., PICONE, O., GAUTREAU, L., SMATI, R., SIX, E., BONHOMME, D., EZINE, S., FRYDMAN, R., CAVAZZANA-CALVO, M. & ANDRE-SCHMUTZ, I. 2009. Human and murine amniotic fluid c-Kit+Lin- cells display hematopoietic activity. *Blood*, 113, 3953-60.
- DOMINICI, M., LE BLANC, K., MUELLER, I., SLAPER-CORTENBACH, I., MARINI, F., KRAUSE, D., DEANS, R., KEATING, A., PROCKOP, D. & HORWITZ, E. 2006. Minimal criteria for defining multipotent mesenchymal stromal cells. The International Society for Cellular Therapy position statement. *Cytotherapy*, 8, 315-7.
- DONOVAN, P. J. & GEARHART, J. 2001. The end of the beginning for pluripotent stem cells. *Nature*, 414, 92-97.
- EA, C. K., DENG, L., XIA, Z. P., PINEDA, G. & CHEN, Z. J. 2006. Activation of IKK by TNFalpha requires site-specific ubiquitination of RIP1 and polyubiquitin binding by NEMO. *Mol Cell*, 22, 245-57.
- EBBEN, J. D., ZORNIK, M., CLARK, P. A. & KUO, J. S. 2011. Introduction to induced pluripotent stem cells: advancing the potential for personalized medicine. *World Neurosurg*, 76, 270-5.
- EGAN, C. E., SODHI, C. P., GOOD, M., LIN, J., JIA, H., YAMAGUCHI, Y., LU, P., MA, C., BRANCA, M. F., WEYANDT, S., FULTON, W. B., NIÑO, D. F., PRINDLE, T., JR., OZOLEK, J. A. & HACKAM, D. J. 2015. Toll-like receptor 4-mediated lymphocyte influx induces neonatal necrotizing enterocolitis. *The Journal of Clinical Investigation*, 126, 495-508.
- EIRIN, A., RIESTER, S. M., ZHU, X.-Y., TANG, H., EVANS, J. M., O'BRIEN, D., VAN WIJNEN, A. J. & LERMAN, L. O. 2014. MicroRNA and mRNA cargo of extracellular vesicles from porcine adipose tissue-derived mesenchymal stem cells. *Gene*, 551, 55-64.
- EISSA, N., HUSSEIN, H., HENDY, G. N., BERNSTEIN, C. N. & GHIA, J.-E. 2018. Chromogranin-A and its derived peptides and their pharmacological effects during intestinal inflammation. *Biochemical Pharmacology*, 152, 315-326.
- ELMÉN, J., LINDOW, M., SCHÜTZ, S., LAWRENCE, M., PETRI, A., OBAD, S., LINDHOLM, M., HEDTJÄRN, M., HANSEN, H. F., BERGER, U., GULLANS, S., KEARNEY, P., SARNOW, P., STRAARUP, E. M. & KAUPPINEN, S. 2008. LNA-mediated microRNA silencing in non-human primates. *Nature*, 452, 896.

- ELMÉN, J., THONBERG, H., LJUNGBERG, K., FRIEDEN, M., WESTERGAARD, M., XU, Y., WAHREN, B., LIANG, Z., ØRUM, H., KOCH, T. & WAHLESTEDT, C. 2005. Locked nucleic acid (LNA) mediated improvements in siRNA stability and functionality. *Nucleic Acids Research*, 33, 439-447.
- EMAMI, C. N., PETROSYAN, M., GIULIANI, S., WILLIAMS, M., HUNTER, C., PRASADARAO, N. V. & FORD, H. R. 2009. Role of the Host Defense System and Intestinal Microbial Flora in the Pathogenesis of Necrotizing Enterocolitis. *Surgical Infections*, 10, 407-417.
- ENGLER, A. J., SEN, S., SWEENEY, H. L. & DISCHER, D. E. 2006. Matrix Elasticity Directs Stem Cell Lineage Specification. *Cell*, 126, 677-689.
- FENG, D., ZHAO, W. L., YE, Y. Y., BAI, X. C., LIU, R. Q., CHANG, L. F., ZHOU, Q. & SUI, S. F. 2010. Cellular internalization of exosomes occurs through phagocytosis. *Traffic*, 11, 675-87.
- FITZGERALD, K. A., ROWE, D. C., BARNES, B. J., CAFFREY, D. R., VISINTIN, A., LATZ, E., MONKS, B., PITHA, P. M. & GOLENBOCK, D. T. 2003. LPS-TLR4 signaling to IRF-3/7 and NF-kappaB involves the toll adapters TRAM and TRIF. *J Exp Med*, 198, 1043-55.
- FOLMES, C. D., NELSON, T. J., MARTINEZ-FERNANDEZ, A., ARRELL, D. K., LINDOR, J. Z., DZEJA, P. P., IKEDA, Y., PEREZ-TERZIC, C. & TERZIC, A. 2011. Somatic oxidative bioenergetics transitions into pluripotency-dependent glycolysis to facilitate nuclear reprogramming. *Cell Metab*, 14, 264-71.
- FRY, C. S., LEE, J. D., JACKSON, J. R., KIRBY, T. J., STASKO, S. A., LIU, H., DUPONT-VERSTEEGDEN, E. E., MCCARTHY, J. J. & PETERSON, C. A. 2014. Regulation of the muscle fiber microenvironment by activated satellite cells during hypertrophy. *Faseb j*, 28, 1654-65.
- FU, X., XIAO, J., WEI, Y., LI, S., LIU, Y., YIN, J., SUN, K., SUN, H., WANG, H., ZHANG, Z., ZHANG, B. T., SHENG, C., WANG, H. & HU, P. 2015. Combination of inflammation-related cytokines promotes long-term muscle stem cell expansion. *Cell Res*, 25, 655-73.
- FUSUNYAN, R. D., NANTHAKUMAR, N. N., BALDEON, M. E. & WALKER, W. A. 2001. Evidence for an innate immune response in the immature human intestine: toll-like receptors on fetal enterocytes. *Pediatr Res*, 49, 589-93.
- GAO, J. J., XUE, Q., PAPASIAN, C. J. & MORRISON, D. C. 2001. Bacterial DNA and Lipopolysaccharide Induce Synergistic Production of TNF- α Through a Post-Transcriptional Mechanism. *The Journal of Immunology*, 166, 6855-6860.
- GAO, S., MAO, F., ZHANG, B., ZHANG, L., ZHANG, X., WANG, M., YAN, Y., YANG, T., ZHANG, J., ZHU, W., QIAN, H. & XU, W. 2014. Mouse bone marrow-derived mesenchymal stem cells induce macrophage M2 polarization through the nuclear factor-kappaB and signal transducer and activator of transcription 3 pathways. *Exp Biol Med (Maywood)*, 239, 366-75.
- GARCIA-PRAT, L., MARTINEZ-VICENTE, M., PERDIGUERO, E., ORTET, L., RODRIGUEZ-UBREVA, J., REBOLLO, E., RUIZ-BONILLA, V., GUTARRA, S., BALLESTAR, E., SERRANO, A. L., SANDRI, M. & MUNOZ-CANOVES, P. 2016. Autophagy maintains stemness by preventing senescence. *Nature*, 529, 37-42.
- GARY, R. K. & KINDELL, S. M. 2005. Quantitative assay of senescence-associated β -galactosidase activity in mammalian cell extracts. *Analytical Biochemistry*, 343, 329-334.
- GEKAS, J., WALTHER, G., SKUK, D., BUJOLD, E., HARVEY, I. & BERTRAND, O. F. 2010. In vitro and in vivo study of human amniotic fluid-derived stem cell differentiation into myogenic lineage. *Clin Exp Med*, 10, 1-6.
- GENIN, M., CLEMENT, F., FATTACCIOLI, A., RAES, M. & MICHIELS, C. 2015. M1 and M2 macrophages derived from THP-1 cells differentially modulate the response of cancer cells to etoposide. *BMC Cancer*, 15, 577.
- GHOSH, S. & DASS, J. F. 2016. Study of pathway cross-talk interactions with NF-kappaB leading to its activation via ubiquitination or phosphorylation: A brief review. *Gene*, 584, 97-109.
- GNECCHI, M., DANIELI, P., MALPASSO, G. & CIUFFREDA, M. C. 2016. Paracrine Mechanisms of Mesenchymal Stem Cells in Tissue Repair. *Methods Mol Biol*, 1416, 123-46.
- GNECCHI, M., HE, H., LIANG, O. D., MELO, L. G., MORELLO, F., MU, H., NOISEUX, N., ZHANG, L., PRATT, R. E., INGWALL, J. S. & DZAU, V. J. 2005. Paracrine action accounts for marked protection of ischemic heart by Akt-modified mesenchymal stem cells. *Nat Med*, 11, 367-8.

- GNECCHI, M., HE, H., NOISEUX, N., LIANG, O. D., ZHANG, L., MORELLO, F., MU, H., MELO, L. G., PRATT, R. E., INGWALL, J. S. & DZAU, V. J. 2006. Evidence supporting paracrine hypothesis for Akt-modified mesenchymal stem cell-mediated cardiac protection and functional improvement. *Faseb j*, 20, 661-9.
- GOSDEN, C. M. 1983. Amniotic fluid cell types and culture. *British Medical Bulletin*, 39, 348-354.
- GROSS, J. C., CHAUDHARY, V., BARTSCHERER, K. & BOUTROS, M. 2012. Active Wnt proteins are secreted on exosomes. *Nat Cell Biol*, 14, 1036-45.
- GUAN, X., DELO, D. M., ATALA, A. & SOKER, S. 2011. In vitro cardiomyogenic potential of human amniotic fluid stem cells. *J Tissue Eng Regen Med*, 5, 220-8.
- GUESCINI, M., GUIDOLIN, D., VALLORANI, L., CASADEI, L., GIOACCHINI, A. M., TIBOLLO, P., BATTISTELLI, M., FALCIERI, E., BATTISTIN, L., AGNATI, L. F. & STOCCHI, V. 2010. C2C12 myoblasts release micro-vesicles containing mtDNA and proteins involved in signal transduction. *Experimental Cell Research*, 316, 1977-1984.
- GUO, J., SANG, Y., YIN, T., WANG, B., YANG, W., LI, X., LI, H. & KANG, Y. 2016. miR-1273g-3p participates in acute glucose fluctuation-induced autophagy, dysfunction, and proliferation attenuation in human umbilical vein endothelial cells. *Am J Physiol Endocrinol Metab*, 310, E734-43.
- GUO, S., AL-SADI, R., SAID, H. M. & MA, T. Y. 2013. Lipopolysaccharide Causes an Increase in Intestinal Tight Junction Permeability in Vitro and in Vivo by Inducing Enterocyte Membrane Expression and Localization of TLR-4 and CD14. *The American Journal of Pathology*, 182, 375-387.
- HABERMAN, Y., TICKLE, T. L., DEXHEIMER, P. J., KIM, M. O., TANG, D., KARNS, R., BALDASSANO, R. N., NOE, J. D., ROSH, J., MARKOWITZ, J., HEYMAN, M. B., GRIFFITHS, A. M., CRANDALL, W. V., MACK, D. R., BAKER, S. S., HUTTENHOWER, C., KELJO, D. J., HYAMS, J. S., KUGATHASAN, S., WALTERS, T. D., ARONOW, B., XAVIER, R. J., GEVERS, D. & DENSON, L. A. 2014. Pediatric Crohn disease patients exhibit specific ileal transcriptome and microbiome signature. *J Clin Invest*, 124, 3617-33.
- HACKAM, D. J., AFRAZI, A., GOOD, M. & SODHI, C. P. 2013. Innate Immune Signaling in the Pathogenesis of Necrotizing Enterocolitis. *Journal of Immunology Research*, 2013.
- HAKULINEN, J., JUNNIKALA, S., SORSA, T. & MERI, S. 2004. Complement inhibitor membrane cofactor protein (MCP; CD46) is constitutively shed from cancer cell membranes in vesicles and converted by a metalloproteinase to a functionally active soluble form. *Eur J Immunol*, 34, 2620-9.
- HALME, D. G. & KESSLER, D. A. 2006. FDA regulation of stem-cell-based therapies. *N Engl J Med*, 355, 1730-5.
- HARRIS, J. B. 2003. Myotoxic phospholipases A2 and the regeneration of skeletal muscles. *Toxicol*, 42, 933-945.
- HARVEY, J., HARDY, S. C. & ASHFORD, M. L. J. 1999. Dual actions of the metabolic inhibitor, sodium azide on KATP channel currents in the rat CRI-G1 insulinoma cell line. *British Journal of Pharmacology*, 126, 51-60.
- HATA, T., MURAKAMI, K., NAKATANI, H., YAMAMOTO, Y., MATSUDA, T. & AOKI, N. 2010. Isolation of bovine milk-derived microvesicles carrying mRNAs and microRNAs. *Biochemical and Biophysical Research Communications*, 396, 528-533.
- HATTERMANN, K., GEBHARDT, H., KROSSA, S., LUDWIG, A., LUCIUS, R., HELD-FEINDT, J. & MENTLEIN, R. 2016. Transmembrane chemokines act as receptors in a novel mechanism termed inverse signaling. *eLife*, 5, e10820.
- HAUSER, P. V., DE FAZIO, R., BRUNO, S., SDEI, S., GRANGE, C., BUSSOLATI, B., BENEDETTO, C. & CAMUSSI, G. 2010. Stem cells derived from human amniotic fluid contribute to acute kidney injury recovery. *Am J Pathol*, 177, 2011-21.
- HESLOP, L., MORGAN, J. E. & PARTRIDGE, T. A. 2000. Evidence for a myogenic stem cell that is exhausted in dystrophic muscle. *J Cell Sci*, 113 (Pt 12), 2299-308.
- HOEHN, H., BRYANT, E. M., FANTEL, A. G. & MARTIN, G. M. 1975. Cultivated cells from diagnostic amniocentesis in second trimester pregnancies. *Humangenetik*, 29, 285-290.

- HOLDEN, C. & VOGEL, G. 2002. Plasticity: Time for a Reappraisal? *Science*, 296, 2126-2129.
- HONMOU, O., HOUKIN, K., MATSUNAGA, T., NIITSU, Y., ISHIAI, S., ONODERA, R., WAXMAN, S. G. & KOCSIS, J. D. 2011. Intravenous administration of auto serum-expanded autologous mesenchymal stem cells in stroke. *Brain*, 134, 1790-807.
- HSU, C., MOROHASHI, Y., YOSHIMURA, S.-I., MANRIQUE-HOYOS, N., JUNG, S., LAUTERBACH, M. A., BAKHTI, M., GRØNBORG, M., MÖBIUS, W., RHEE, J., BARR, F. A. & SIMONS, M. 2010. Regulation of exosome secretion by Rab35 and its GTPase-activating proteins TBC1D10A-C. *The Journal of Cell Biology*, 189, 223-232.
- HSU, H., HUANG, J., SHU, H. B., BAICHWAL, V. & GOEDEL, D. V. 1996a. TNF-dependent recruitment of the protein kinase RIP to the TNF receptor-1 signaling complex. *Immunity*, 4, 387-96.
- HSU, H., SHU, H. B., PAN, M. G. & GOEDEL, D. V. 1996b. TRADD-TRAF2 and TRADD-FADD interactions define two distinct TNF receptor 1 signal transduction pathways. *Cell*, 84, 299-308.
- HU, X., YU, S. P., FRASER, J. L., LU, Z., OGLE, M. E., WANG, J. A. & WEI, L. 2008. Transplantation of hypoxia-preconditioned mesenchymal stem cells improves infarcted heart function via enhanced survival of implanted cells and angiogenesis. *J Thorac Cardiovasc Surg*, 135, 799-808.
- HUNSUCKER, S. A., MITCHELL, B. S. & SPYCHALA, J. 2005. The 5'-nucleotidases as regulators of nucleotide and drug metabolism. *Pharmacol Ther*, 107, 1-30.
- HURLEY, J. H. 2008. ESCRT complexes and the biogenesis of multivesicular bodies. *Current Opinion in Cell Biology*, 20, 4-11.
- HUTVAGNER, G. & SIMARD, M. J. 2008. Argonaute proteins: key players in RNA silencing. *Nat Rev Mol Cell Biol*, 9, 22-32.
- IHARA, S., HIRATA, Y. & KOIKE, K. 2017. TGF- β in inflammatory bowel disease: a key regulator of immune cells, epithelium, and the intestinal microbiota. *Journal of Gastroenterology*, 52, 777-787.
- IKEGAME, Y., YAMASHITA, K., NAKASHIMA, S., NOMURA, Y., YONEZAWA, S., ASANO, Y., SHINODA, J., HARA, H. & IWAMA, T. 2014. Fate of graft cells: what should be clarified for development of mesenchymal stem cell therapy for ischemic stroke? *Front Cell Neurosci*, 8, 322.
- IN 'T ANKER, P. S., SCHERJON, S. A., KLEIJBURG-VAN DER KEUR, C., NOORT, W. A., CLAAS, F. H., WILLEMZE, R., FIBBE, W. E. & KANHAI, H. H. 2003. Amniotic fluid as a novel source of mesenchymal stem cells for therapeutic transplantation. *Blood*, 102, 1548-9.
- JALILI, R. B., FOROUZANDEH, F., BAHAR, M. A. & GHAHARY, A. 2007. The immunoregulatory function of indoleamine 2, 3 dioxygenase and its application in allotransplantation. *Iran J Allergy Asthma Immunol*, 6, 167-79.
- JILLING, T., SIMON, D., LU, J., MENG, F. J., LI, D., SCHY, R., THOMSON, R. B., SOLIMAN, A., ARDITI, M. & CAPLAN, M. S. 2006. The Roles of Bacteria and TLR4 in Rat and Murine Models of Necrotizing Enterocolitis. *Journal of immunology (Baltimore, Md. : 1950)*, 177, 3273-3282.
- JONES, N. C., TYNER, K. J., NIBARGER, L., STANLEY, H. M., CORNELISON, D. D. W., FEDOROV, Y. V. & OLWIN, B. B. 2005. The p38 α / β MAPK functions as a molecular switch to activate the quiescent satellite cell. *The Journal of Cell Biology*, 169, 105-116.
- JUN, E. K., ZHANG, Q., YOON, B. S., MOON, J. H., LEE, G., PARK, G., KANG, P. J., LEE, J. H., KIM, A. & YOU, S. 2014. Hypoxic conditioned medium from human amniotic fluid-derived mesenchymal stem cells accelerates skin wound healing through TGF-beta/SMAD2 and PI3K/Akt pathways. *Int J Mol Sci*, 15, 605-28.
- JUNG, M., SCHAEFER, A., STEINER, I., KEMPKENSTEFFEN, C., STEPHAN, C., ERBERSDOBLER, A. & JUNG, K. 2010. Robust microRNA stability in degraded RNA preparations from human tissue and cell samples. *Clin Chem*, 56, 998-1006.
- JUNG, S. A., LEE, H. K., YOON, J. S., KIM, S. J., KIM, C. Y., SONG, H., HWANG, K. C., LEE, J. B. & LEE, J. H. 2007. Upregulation of TGF-beta-induced tissue transglutaminase expression by PI3K-Akt pathway activation in human subconjunctival fibroblasts. *Invest Ophthalmol Vis Sci*, 48, 1952-8.

- KAFIAN, S., MOBARREZ, F., WALLEN, H. & SAMAD, B. 2014. Association between platelet reactivity and circulating platelet-derived microvesicles in patients with acute coronary syndrome. *Platelets*, 1-7.
- KAIDI, A., QUALTROUGH, D., WILLIAMS, A. C. & PARASKEVA, C. 2006. Direct transcriptional up-regulation of cyclooxygenase-2 by hypoxia-inducible factor (HIF)-1 promotes colorectal tumor cell survival and enhances HIF-1 transcriptional activity during hypoxia. *Cancer Res*, 66, 6683-91.
- KAJI, K., NORRBY, K., PACA, A., MILEIKOVSKY, M., MOHSENI, P. & WOLTJEN, K. 2009. Virus-free induction of pluripotency and subsequent excision of reprogramming factors. *Nature*, 458, 771-5.
- KALTSCHMIDT, B., KALTSCHMIDT, C., HEHNER, S. P., DROGE, W. & SCHMITZ, M. L. 1999. Repression of NF-kappaB impairs HeLa cell proliferation by functional interference with cell cycle checkpoint regulators. *Oncogene*, 18, 3213-25.
- KARALAKI, M., FILI, S., PHILIPPOU, A. & KOUTSILIERIS, M. 2009. Muscle regeneration: cellular and molecular events. *In Vivo*, 23, 779-96.
- KARPOWICZ, P. & PERRIMON, N. 2010. All for one, and one for all: the clonality of the intestinal stem cell niche. *F1000 Biol Rep*, 2, 73.
- KARVE, S. S., PRADHAN, S., WARD, D. V. & WEISS, A. A. 2017. Intestinal organoids model human responses to infection by commensal and Shiga toxin producing Escherichia coli. *PLOS ONE*, 12, e0178966.
- KAWAI, T., ADACHI, O., OGAWA, T., TAKEDA, K. & AKIRA, S. 1999. Unresponsiveness of MyD88-deficient mice to endotoxin. *Immunity*, 11, 115-22.
- KAWAI, T. & AKIRA, S. 2007. Signaling to NF-kappaB by Toll-like receptors. *Trends Mol Med*, 13, 460-9.
- KELLER, S., RUPP, C., STOECK, A., RUNZ, S., FOGEL, M., LUGERT, S., HAGER, H. D., ABDEL-BAKKY, M. S., GUTWEIN, P. & ALTEVOGT, P. 2007. CD24 is a marker of exosomes secreted into urine and amniotic fluid. *Kidney International*, 72, 1095-1102.
- KHAILOVA, L., DVORAK, K., ARGANBRIGHT, K. M., HALPERN, M. D., KINOUCI, T., YAJIMA, M. & DVORAK, B. 2009. *Bifidobacterium bifidum* improves intestinal integrity in a rat model of necrotizing enterocolitis.
- KHAILOVA, L., MOUNT PATRICK, S. K., ARGANBRIGHT, K. M., HALPERN, M. D., KINOUCI, T. & DVORAK, B. 2010. *Bifidobacterium bifidum* reduces apoptosis in the intestinal epithelium in necrotizing enterocolitis. *American Journal of Physiology. Gastrointestinal and Liver Physiology*, 299, G1118-1127.
- KIM, J., LEE, Y., KIM, H., HWANG, K. J., KWON, H. C., KIM, S. K., CHO, D. J., KANG, S. G. & YOU, J. 2007. Human amniotic fluid-derived stem cells have characteristics of multipotent stem cells. *Cell Proliferation*, 40, 75-90.
- KIM, S. H., MACINTYRE, D. A., FIRMINO DA SILVA, M., BLANKS, A. M., LEE, Y. S., THORNTON, S., BENNETT, P. R. & TERZIDOU, V. 2015. Oxytocin activates NF-kappaB-mediated inflammatory pathways in human gestational tissues. *Mol Cell Endocrinol*, 403, 64-77.
- KLAMMT, S., WOJAK, H. J., MITZNER, A., KOBALL, S., RYCHLY, J., REISINGER, E. C. & MITZNER, S. 2012. Albumin-binding capacity (ABiC) is reduced in patients with chronic kidney disease along with an accumulation of protein-bound uraemic toxins. *Nephrol Dial Transplant*, 27, 2377-83.
- KOIKE, Y., LI, B., LEE, C., CHENG, S., MIYAKE, H., WELSH, C., HOCK, A., BELIK, J., ZANI, A. & PIERRO, A. 2017. Gastric emptying is reduced in experimental NEC and correlates with the severity of intestinal damage. *Journal of Pediatric Surgery*, 52, 744-748.
- KONSTANTINOV, I. E. 2000. In search of Alexander A. Maximow: the man behind the unitarian theory of hematopoiesis. *Perspect Biol Med*, 43, 269-76.
- KOOPMAN, R., LY, C. H. & RYALL, J. G. 2014. A metabolic link to skeletal muscle wasting and regeneration. *Frontiers in Physiology*, 5, 32.
- KOZAR, S., MORRISSEY, E., NICHOLSON, A. M., VAN DER HEIJDEN, M., ZECCHINI, H. I., KEMP, R., TAVARE, S., VERMEULEN, L. & WINTON, D. J. 2013. Continuous clonal labeling reveals small

- numbers of functional stem cells in intestinal crypts and adenomas. *Cell Stem Cell*, 13, 626-33.
- KUANG, S., GILLESPIE, M. A. & RUDNICKI, M. A. 2008. Niche regulation of muscle satellite cell self-renewal and differentiation. *Cell Stem Cell*, 2, 22-31.
- KUNDU, A. K. & PUTNAM, A. J. 2006. Vitronectin and collagen I differentially regulate osteogenesis in mesenchymal stem cells. *Biochemical and Biophysical Research Communications*, 347, 347-357.
- KUO, W. T., LEE, T. C., YANG, H. Y., CHEN, C. Y., AU, Y. C., LU, Y. Z., WU, L. L., WEI, S. C., NI, Y. H., LIN, B. R., CHEN, Y., TSAI, Y. H., KUNG, J. T., SHEU, F., LIN, L. W. & YU, L. C. H. 2015. LPS receptor subunits have antagonistic roles in epithelial apoptosis and colonic carcinogenesis. *Cell Death and Differentiation*, 22, 1590-1604.
- LAKKARAJU, A. & RODRIGUEZ-BOULAN, E. 2008. Itinerant exosomes: emerging roles in cell and tissue polarity. *Trends in Cell Biology*, 18, 199-209.
- LANDSKRONER-EIGER, S., MONEKE, I. & SESSA, W. C. 2013. miRNAs as Modulators of Angiogenesis. *Cold Spring Harbor Perspectives in Medicine*, 3, a006643.
- LEBRAND, C., CORTI, M., GOODSON, H., COSSON, P., CAVALLI, V., MAYRAN, N., FAURE, J. & GRUENBERG, J. 2002. Late endosome motility depends on lipids via the small GTPase Rab7. *Embo j*, 21, 1289-300.
- LEE, C., MITSIALIS, S. A., ASLAM, M., VITALI, S. H., VERGADI, E., KONSTANTINOPOULOS, G., SDRIMAS, K., FERNANDEZ-GONZALEZ, A. & KOUREMBANAS, S. 2012a. Exosomes Mediate the Cytoprotective Action of Mesenchymal Stromal Cells on Hypoxia-Induced Pulmonary Hypertension. *Circulation*, 126, 2601-2611.
- LEE, E. Y., XIA, Y., KIM, W. S., KIM, M. H., KIM, T. H., KIM, K. J., PARK, B. S. & SUNG, J. H. 2009. Hypoxia-enhanced wound-healing function of adipose-derived stem cells: increase in stem cell proliferation and up-regulation of VEGF and bFGF. *Wound Repair Regen*, 17, 540-7.
- LEE, R. C., FEINBAUM, R. L. & AMBROS, V. 1993. The *C. elegans* heterochronic gene *lin-4* encodes small RNAs with antisense complementarity to *lin-14*. *Cell*, 75, 843-54.
- LEE, T. T., GREEN, B. A., DIETRICH, W. D. & YEZERSKI, R. P. 1999. Neuroprotective effects of basic fibroblast growth factor following spinal cord contusion injury in the rat. *J Neurotrauma*, 16, 347-56.
- LEE, Y., SOORANNA, S. R., TERZIDOU, V., CHRISTIAN, M., BROSENS, J., HUHTINEN, K., POUTANEN, M., BARTON, G., JOHNSON, M. R. & BENNETT, P. R. 2012b. Interactions between inflammatory signals and the progesterone receptor in regulating gene expression in pregnant human uterine myocytes. *Journal of Cellular and Molecular Medicine*, 16, 2487-2503.
- LEFAUCHEUR, J. P. & SEBILLE, A. 1995. Muscle regeneration following injury can be modified in vivo by immune neutralization of basic fibroblast growth factor, transforming growth factor beta 1 or insulin-like growth factor I. *J Neuroimmunol*, 57, 85-91.
- LEPPER, C., CONWAY, S. J. & FAN, C. M. 2009. Adult satellite cells and embryonic muscle progenitors have distinct genetic requirements. *Nature*, 460, 627-31.
- LEPPER, C. & FAN, C. M. 2010. Inducible lineage tracing of Pax7-descendant cells reveals embryonic origin of adult satellite cells. *Genesis*, 48, 424-36.
- LESPAGNOL, A., DUFLAUT, D., BEEKMAN, C., BLANC, L., FIUCCI, G., MARINE, J. C., VIDAL, M., AMSON, R. & TELERMAN, A. 2008. Exosome secretion, including the DNA damage-induced p53-dependent secretory pathway, is severely compromised in TSAP6//Steap3-null mice. *Cell Death Differ*, 15, 1723-1733.
- LI, B., ZANI, A., LEE, C., ZANI-RUTTENSTOCK, E., ZHANG, Z., LI, X., IP, W., GONSKA, T. & PIERRO, A. 2016. Endoplasmic reticulum stress is involved in the colonic epithelium damage induced by maternal separation. *Journal of Pediatric Surgery*, 51, 1001-1004.
- LI, Z. B., KOLLIAS, H. D. & WAGNER, K. R. 2008. Myostatin Directly Regulates Skeletal Muscle Fibrosis. *The Journal of Biological Chemistry*, 283, 19371-19378.
- LIANG, H., GUAN, D., GAO, A., YIN, Y., JING, M., YANG, L., MA, W., HU, E. & ZHANG, X. 2014. Human amniotic epithelial stem cells inhibit microglia activation through downregulation of tumor

- necrosis factor-alpha, interleukin-1beta and matrix metalloproteinase-12 in vitro and in a rat model of intracerebral hemorrhage. *Cytotherapy*, 16, 523-34.
- LIM, S., MACINTYRE, D. A., LEE, Y. S., KHANJANI, S., TERZIDOU, V., TEOH, T. G. & BENNETT, P. R. 2012. Nuclear factor kappa B activation occurs in the amnion prior to labour onset and modulates the expression of numerous labour associated genes. *PLoS One*, 7, e34707.
- LIMANA, F., GERMANI, A., ZACHEO, A., KAJSTURA, J., DI CARLO, A., BORSELLINO, G., LEONI, O., PALUMBO, R., BATTISTINI, L., RASTALDO, R., MÜLLER, S., POMPILIO, G., ANVERSA, P., BIANCHI, M. E. & CAPOGROSSI, M. C. 2005. Exogenous High-Mobility Group Box 1 Protein Induces Myocardial Regeneration After Infarction via Enhanced Cardiac C-Kit⁺ Cell Proliferation and Differentiation. *Circulation Research*, 97, e73-e83.
- LIN, H. H., FAUNCE, D. E., STACEY, M., TERAJEWICZ, A., NAKAMURA, T., ZHANG-HOOVER, J., KERLEY, M., MUCENSKI, M. L., GORDON, S. & STEIN-STREILEIN, J. 2005. The macrophage F4/80 receptor is required for the induction of antigen-specific efferent regulatory T cells in peripheral tolerance. *J Exp Med*, 201, 1615-25.
- LIU, Y., ZHANG, R., YAN, K., CHEN, F., HUANG, W., LV, B., SUN, C., XU, L., LI, F. & JIANG, X. 2014. Mesenchymal stem cells inhibit lipopolysaccharide-induced inflammatory responses of BV2 microglial cells through TSG-6. *Journal of Neuroinflammation*, 11, 135-135.
- LIU, Z., CHEN, X., WU, Q., SONG, J., WANG, L. & LI, G. 2016. miR-125b inhibits goblet cell differentiation in allergic airway inflammation by targeting SPDEF. *Eur J Pharmacol*, 782, 14-20.
- LIU, Z., TIAN, Y., JIANG, Y., CHEN, S., LIU, T., MOYER, M. P., QIN, H. & ZHOU, X. 2018. Protective Effects of Let-7b on the Expression of Occludin by Targeting P38 MAPK in Preventing Intestinal Barrier Dysfunction. *Cell Physiol Biochem*, 45, 343-355.
- LO SICCO, C., REVERBERI, D., BALBI, C., ULIVI, V., PRINCIPI, E., PASCUCCI, L., BECHERINI, P., BOSCO, M. C., VAREGIO, L., FRANZIN, C., POZZOBON, M., CANCEDDA, R. & TASSO, R. 2017. Mesenchymal Stem Cell-Derived Extracellular Vesicles as Mediators of Anti-Inflammatory Effects: Endorsement of Macrophage Polarization. *STEM CELLS Translational Medicine*, n/a-n/a.
- LÖTVALL, J., HILL, A. F., HOCHBERG, F., BUZÁS, E. I., DI VIZIO, D., GARDINER, C., GHO, Y. S., KUROCHKIN, I. V., MATHIVANAN, S., QUESENBERRY, P., SAHOO, S., TAHARA, H., WAUBEN, M. H., WITWER, K. W. & THÉRY, C. 2014. Minimal experimental requirements for definition of extracellular vesicles and their functions: a position statement from the International Society for Extracellular Vesicles. *Journal of Extracellular Vesicles*, 3, 10.3402/jev.v3.26913.
- LOTVALL, J. & VALADI, H. 2007. Cell to cell signalling via exosomes through esRNA. *Cell Adhesion & Migration*, 1, 156-158.
- LUDWIG, A., SCHULTE, A., SCHNACK, C., HUNDHAUSEN, C., REISS, K., BRODWAY, N., HELD-FEINDT, J. & MENTLEIN, R. 2005. Enhanced expression and shedding of the transmembrane chemokine CXCL16 by reactive astrocytes and glioma cells. *J Neurochem*, 93, 1293-303.
- LV, F. J., TUAN, R. S., CHEUNG, K. M. & LEUNG, V. Y. 2014. Concise review: the surface markers and identity of human mesenchymal stem cells. *Stem Cells*, 32, 1408-19.
- MA, C., SONG, H., YU, L., GUAN, K., HU, P., LI, Y., XIA, X., LI, J., JIANG, S. & LI, F. 2016. miR-762 promotes porcine immature Sertoli cell growth via the ring finger protein 4 (RNF4) gene. *Sci Rep*, 6, 32783.
- MA, X., ZHANG, S., ZHOU, J., CHEN, B., SHANG, Y., GAO, T., WANG, X., XIE, H. & CHEN, F. 2012. Clone-derived human AF-amniotic fluid stem cells are capable of skeletal myogenic differentiation in vitro and in vivo. *J Tissue Eng Regen Med*, 6, 598-613.
- MACDONALD, B. T., TAMAI, K. & HE, X. 2009. Wnt/ β -catenin signaling: components, mechanisms, and diseases. *Developmental cell*, 17, 9-26.
- MADRIGAL, M., RAO, K. S. & RIORDAN, N. H. 2014. A review of therapeutic effects of mesenchymal stem cell secretions and induction of secretory modification by different culture methods. *J Transl Med*, 12, 260.
- MAGUIRE, C. T., DEMAREST, B. L., HILL, J. T., PALMER, J. D., BROTHMAN, A. R., YOST, H. J. & CONDIC, M. L. 2013. Genome-wide analysis reveals the unique stem cell identity of human amniocytes. *PLoS One*, 8, e53372.

- MANTOVANI, A., SICA, A., SOZZANI, S., ALLAVENA, P., VECCHI, A. & LOCATI, M. 2004. The chemokine system in diverse forms of macrophage activation and polarization. *Trends in Immunology*, 25, 677-686.
- MARALDI, T., RICCIO, M., RESCA, E., PISCIOTTA, A., LA SALA, G. B., FERRARI, A., BRUZZESI, G., MOTTA, A., MIGLIARESI, C., MARZONA, L. & DE POL, A. 2011. Human amniotic fluid stem cells seeded in fibroin scaffold produce in vivo mineralized matrix. *Tissue Eng Part A*, 17, 2833-43.
- MARK, P., KLEINSORGE, M., GAEBEL, R., LUX, C. A., TOELK, A., PITTERMANN, E., DAVID, R., STEINHOFF, G. & MA, N. 2013. Human Mesenchymal Stem Cells Display Reduced Expression of CD105 after Culture in Serum-Free Medium. *Stem Cells Int*, 2013, 698076.
- MARTINEZ, C., RODINO-JANEIRO, B. K., LOBO, B., STANIFER, M. L., KLAUS, B., GRANZOW, M., GONZALEZ-CASTRO, A. M., SALVO-ROMERO, E., ALONSO-COTONER, C., PIGRAU, M., ROETH, R., RAPPOLD, G., HUBER, W., GONZALEZ-SILOS, R., LORENZO, J., DE TORRES, I., AZPIROZ, F., BOULANT, S., VICARIO, M., NIESLER, B. & SANTOS, J. 2017. miR-16 and miR-125b are involved in barrier function dysregulation through the modulation of claudin-2 and cingulin expression in the jejunum in IBS with diarrhoea. *Gut*, 66, 1537-1538.
- MATHIVANAN, S., JI, H. & SIMPSON, R. J. 2010. Exosomes: extracellular organelles important in intercellular communication. *J Proteomics*, 73, 1907-20.
- MATHIVANAN, S. & SIMPSON, R. J. 2009. ExoCarta: A compendium of exosomal proteins and RNA. *Proteomics*, 9, 4997-5000.
- MATSUURA, Y., TAKEHIRA, M., JOTI, Y., OGASAHARA, K., TANAKA, T., ONO, N., KUNISHIMA, N. & YUTANI, K. 2015. Thermodynamics of protein denaturation at temperatures over 100 °C: CutA1 mutant proteins substituted with hydrophobic and charged residues. *Scientific Reports*, 5, 15545.
- MCCONNELL, R. E., HIGGINBOTHAM, J. N., SHIFRIN, D. A., JR., TABB, D. L., COFFEY, R. J. & TYSKA, M. J. 2009. The enterocyte microvillus is a vesicle-generating organelle. *J Cell Biol*, 185, 1285-98.
- MCELROY, S. J., PRINCE, L. S., WEITKAMP, J.-H., REESE, J., SLAUGHTER, J. C. & POLK, D. B. 2011. Tumor necrosis factor receptor 1-dependent depletion of mucus in immature small intestine: a potential role in neonatal necrotizing enterocolitis. *American Journal of Physiology - Gastrointestinal and Liver Physiology*, 301, G656-G666.
- MEAD, B. & TOMAREV, S. 2017. Bone Marrow-Derived Mesenchymal Stem Cells-Derived Exosomes Promote Survival of Retinal Ganglion Cells Through miRNA-Dependent Mechanisms. *STEM CELLS Translational Medicine*, n/a-n/a.
- MELLOWS, B., MITCHELL, R., ANTONIOLI, M., KRETZ, O., CHAMBERS, D., ZEUNER, M. T., DENECKE, B., MUSANTE, L., RAMACHANDRA, D. L., DEBACQ-CHAINIAUX, F., HOLTHOFER, H., JOCH, B., RAY, S., WIDERA, D., DAVID, A. L., HUBER, T. B., DENGJEL, J., DE COPPI, P. & PATEL, K. 2017. Protein and Molecular Characterization of a Clinically Compliant Amniotic Fluid Stem Cell-Derived Extracellular Vesicle Fraction Capable of Accelerating Muscle Regeneration Through Enhancement of Angiogenesis. *Stem Cells Dev*, 26, 1316-1333.
- MENDELL, J. T. & OLSON, E. N. 2012. MicroRNAs in stress signaling and human disease. *Cell*, 148, 1172-1187.
- MITTELBRUNN, M., GUTIÉRREZ-VÁZQUEZ, C., VILLARROYA-BELTRI, C., GONZÁLEZ, S., SÁNCHEZ-CABO, F., GONZÁLEZ, M. Á., BERNAD, A. & SÁNCHEZ-MADRID, F. 2011. Unidirectional transfer of microRNA-loaded exosomes from T cells to antigen-presenting cells. *Nature Communications*, 2.
- MIZRAHI, A., BARLOW, O., BERDON, W., BLANC, W. A. & SILVERMAN, W. A. 1965. NECROTIZING ENTEROCOLITIS IN PREMATURE INFANTS. *J Pediatr*, 66, 697-705.
- MOLKENTIN, J. D., BLACK, B. L., MARTIN, J. F. & OLSON, E. N. 1995. Cooperative activation of muscle gene expression by MEF2 and myogenic bHLH proteins. *Cell*, 83, 1125-36.
- MOLLICA, L., DE MARCHIS, F., SPITALERI, A., DALLACOSTA, C., PENNACCHINI, D., ZAMAI, M., AGRESTI, A., TRISCIUOGGIO, L., MUSCO, G. & BIANCHI, M. E. 2007. Glycyrrhizin Binds to High-Mobility Group Box 1 Protein and Inhibits Its Cytokine Activities. *Chemistry & Biology*, 14, 431-441.
- MONTECALVO, A., LARREGINA, A. T., SHUFESKY, W. J., STOLZ, D. B., SULLIVAN, M. L. G., KARLSSON, J. M., BATY, C. J., GIBSON, G. A., ERDOS, G., WANG, Z., MILOSEVIC, J., TKACHEVA, O. A., DIVITO,

- S. J., JORDAN, R., LYONS-WEILER, J., WATKINS, S. C. & MORELLI, A. E. 2012. Mechanism of transfer of functional microRNAs between mouse dendritic cells via exosomes. *Blood*, 119, 756-766.
- MOOREFIELD, E. C., MCKEE, E. E., SOLCHAGA, L., ORLANDO, G., YOO, J. J., WALKER, S., FURTH, M. E. & BISHOP, C. E. 2011a. Cloned, CD117 selected human amniotic fluid stem cells are capable of modulating the immune response. *PLoS One*, 6.
- MOOREFIELD, E. C., MCKEE, E. E., SOLCHAGA, L., ORLANDO, G., YOO, J. J., WALKER, S., FURTH, M. E. & BISHOP, C. E. 2011b. Cloned, CD117 Selected Human Amniotic Fluid Stem Cells Are Capable of Modulating the Immune Response. *PLoS ONE*, 6, e26535.
- MORAES, D. A., SIBOV, T. T., PAVON, L. F., ALVIM, P. Q., BONADIO, R. S., DA SILVA, J. R., PIC-TAYLOR, A., TOLEDO, O. A., MARTI, L. C., AZEVEDO, R. B. & OLIVEIRA, D. M. 2016. A reduction in CD90 (THY-1) expression results in increased differentiation of mesenchymal stromal cells. *Stem Cell Research & Therapy*, 7, 97.
- MORAN, G. W., LESLIE, F. C., LEVISON, S. E. & MCLAUGHLIN, J. T. 2008. Review: Enteroendocrine cells: Neglected players in gastrointestinal disorders? *Therapeutic Advances in Gastroenterology*, 1, 51-60.
- MOSCHIDOU, D., MUKHERJEE, S., BLUNDELL, M. P., DREWS, K., JONES, G. N., ABDULRAZZAK, H., NOWAKOWSKA, B., PHOOLCHUND, A., LAY, K., RAMASAMY, T. S., CANANZI, M., NETTERSHEIM, D., SULLIVAN, M., FROST, J., MOORE, G., VERMEESCH, J. R., FISK, N. M., THRASHER, A. J., ATALA, A., ADJAYE, J., SCHORLE, H., DE COPPI, P. & GUILLOT, P. V. 2012. Valproic acid confers functional pluripotency to human amniotic fluid stem cells in a transgene-free approach. *Mol Ther*, 20, 1953-67.
- MOSSER, D. M. 2003. The many faces of macrophage activation. *Journal of Leukocyte Biology*, 73, 209-212.
- MOTOHASHI, N. & ASAKURA, A. 2014. Muscle Satellite Cell Heterogeneity and Self-Renewal. *Frontiers in Cell and Developmental Biology*, 2.
- MOURIKIS, P., SAMBASIVAN, R., CASTEL, D., ROCHETEAU, P., BIZZARRO, V. & TAJBAKSH, S. 2012. A critical requirement for notch signaling in maintenance of the quiescent skeletal muscle stem cell state. *Stem Cells*, 30, 243-52.
- MULCAHY, L. A., PINK, R. C. & CARTER, D. R. 2014. Routes and mechanisms of extracellular vesicle uptake. *J Extracell Vesicles*, 3.
- MURAKAMI, T., OAKES, M., OGURA, M., TOVAR, V., YAMAMOTO, C. & MITSUHASHI, M. 2014. Development of glomerulus-, tubule-, and collecting duct-specific mRNA assay in human urinary exosomes and microvesicles. *PLoS One*, 9, e109074.
- MURALIDHARAN-CHARI, V., CLANCY, J., PLOU, C., ROMAO, M., CHAVRIER, P., RAPOSO, G. & D'SOUZA-SCHOREY, C. 2009. ARF6-regulated shedding of tumor cell-derived plasma membrane microvesicles. *Curr Biol*, 19, 1875-85.
- MURPHY, M. B., MONCIVAIS, K. & CAPLAN, A. I. 2013. Mesenchymal stem cells: environmentally responsive therapeutics for regenerative medicine. *Exp Mol Med*, 45, e54.
- MURPHY, M. M., LAWSON, J. A., MATHEW, S. J., HUTCHESON, D. A. & KARDON, G. 2011. Satellite cells, connective tissue fibroblasts and their interactions are crucial for muscle regeneration. *Development*, 138, 3625-37.
- NAKAMURA, Y., MIYAKI, S., ISHITOBI, H., MATSUYAMA, S., NAKASA, T., KAMEI, N., AKIMOTO, T., HIGASHI, Y. & OCHI, M. 2015. Mesenchymal-stem-cell-derived exosomes accelerate skeletal muscle regeneration. *FEBS Letters*, 589, 1257-1265.
- NAKASE, I., KOBAYASHI, N. B., TAKATANI-NAKASE, T. & YOSHIDA, T. 2015. Active macropinocytosis induction by stimulation of epidermal growth factor receptor and oncogenic Ras expression potentiates cellular uptake efficacy of exosomes. *Scientific Reports*, 5, 10300.
- NEAL, M. D., SODHI, C. P., JIA, H., DYER, M., EGAN, C. E., YAZJI, I., GOOD, M., AFRAZI, A., MARINO, R., SLAGLE, D., MA, C., BRANCA, M. F., PRINDLE, T., GRANT, Z., OZOLEK, J. & HACKAM, D. J. 2012. Toll-like Receptor 4 Is Expressed on Intestinal Stem Cells and Regulates Their Proliferation and Apoptosis via the p53 Up-regulated Modulator of Apoptosis. *The Journal of Biological Chemistry*, 287, 37296-37308.

- NICHENKO, A. S., SOUTHERN, W. M., ATUAN, M., LUAN, J., PEISSIG, K. B., FOLTZ, S. J., BEEDLE, A. M., WARREN, G. L. & CALL, J. A. 2016. Mitochondrial maintenance via autophagy contributes to functional skeletal muscle regeneration and remodeling. *American Journal of Physiology-Cell Physiology*, 311, C190-C200.
- NIU, X., FU, N., DU, J., WANG, R., WANG, Y., ZHAO, S., DU, H., WANG, B., ZHANG, Y., SUN, D. & NAN, Y. 2016. miR-1273g-3p modulates activation and apoptosis of hepatic stellate cells by directly targeting PTEN in HCV-related liver fibrosis. *FEBS Lett*, 590, 2709-24.
- NIWA, H., MIYAZAKI, J. & SMITH, A. G. 2000. Quantitative expression of Oct-3/4 defines differentiation, dedifferentiation or self-renewal of ES cells. *Nat Genet*, 24, 372-6.
- NOLTE-T HOEN, E. N., BUSCHOW, S. I., ANDERTON, S. M., STOOORVOGEL, W. & WAUBEN, M. H. 2009. Activated T cells recruit exosomes secreted by dendritic cells via LFA-1. *Blood*, 113, 1977-81.
- NOVAK, M. L., BRYER, S. C., CHENG, M., NGUYEN, M. H., CONLEY, K. L., CUNNINGHAM, A. K., XUE, B., SISSON, T. H., YOU, J. S., HORNBERGER, T. A. & KOH, T. J. 2011. Macrophage-specific expression of urokinase-type plasminogen activator promotes skeletal muscle regeneration. *J Immunol*, 187, 1448-57.
- OHNUKI, M. & TAKAHASHI, K. 2015. Present and future challenges of induced pluripotent stem cells. *Philos Trans R Soc Lond B Biol Sci*, 370, 20140367.
- OLIVER, K. M., TAYLOR, C. T. & CUMMINS, E. P. 2009. Hypoxia. Regulation of NFkappaB signalling during inflammation: the role of hydroxylases. *Arthritis Res Ther*, 11, 215.
- OMAIRI, S., HAU, K.-L., COLLIN-HOOPER, H., MONTANARO, F., GOYENVALLE, A., GARCIA, L. & PATEL, K. 2017. Link between MHC Fiber Type and Restoration of Dystrophin Expression and Key Components of the DAPC by Tricyclo-DNA-Mediated Exon Skipping. *Molecular Therapy - Nucleic Acids*, 9, 409-418.
- ONO, Y., CALHABEU, F., MORGAN, J. E., KATAGIRI, T., AMTHOR, H. & ZAMMIT, P. S. 2011. BMP signalling permits population expansion by preventing premature myogenic differentiation in muscle satellite cells. *Cell Death Differ*, 18, 222-234.
- ORKIN, S. H. & ZON, L. I. 2002. Hematopoiesis and stem cells: plasticity versus developmental heterogeneity. *Nat Immunol*, 3, 323-328.
- OSTROWSKI, M., CARMO, N. B., KRUMEICH, S., FANGET, I., RAPOSO, G., SAVINA, A., MOITA, C. F., SCHAUER, K., HUME, A. N., FREITAS, R. P., GOUD, B., BENARROCH, P., HACOEN, N., FUKUDA, M., DESNOS, C., SEABRA, M. C., DARCHEN, F., AMIGORENA, S., MOITA, L. F. & THERY, C. 2010. Rab27a and Rab27b control different steps of the exosome secretion pathway. *Nature Cell Biology*, 12, 19-30; sup pp 1-13.
- OTTO, A., COLLINS-HOOPER, H., PATEL, A., DASH, P. R. & PATEL, K. 2011. Adult skeletal muscle stem cell migration is mediated by a blebbing/amoeboid mechanism. *Rejuvenation Res*, 14, 249-60.
- OUSTANINA, S., HAUSE, G. & BRAUN, T. 2004. Pax7 directs postnatal renewal and propagation of myogenic satellite cells but not their specification. *Embo j*, 23, 3430-9.
- P, M., S, H., R, M., M, G. & W, S. K. 2011. Adult mesenchymal stem cells and cell surface characterization - a systematic review of the literature. *Open Orthop J*, 5, 253-60.
- PALUMBO, R., SAMPAOLESI, M., DE MARCHIS, F., TONLORENZI, R., COLOMBETTI, S., MONDINO, A., COSSU, G. & BIANCHI, M. E. 2004. Extracellular HMGB1, a signal of tissue damage, induces mesoangioblast migration and proliferation. *The Journal of Cell Biology*, 164, 441-449.
- PANARITI, A., MISEROCCHI, G. & RIVOLTA, I. 2012. The effect of nanoparticle uptake on cellular behavior: disrupting or enabling functions? *Nanotechnology, Science and Applications*, 5, 87-100.
- PARK, H. B., GOLUBOVSKAYA, V., XU, L., YANG, X., LEE, J. W., SCULLY, S., 2ND, CRAVEN, R. J. & CANCE, W. G. 2004. Activated Src increases adhesion, survival and alpha2-integrin expression in human breast cancer cells. *Biochem J*, 378, 559-67.
- PAROLINI, I., FEDERICI, C., RAGGI, C., LUGINI, L., PALLESCHI, S., DE MILITO, A., COSCIA, C., IESSI, E., LOGOZZI, M., MOLINARI, A., COLONE, M., TATTI, M., SARGIACOMO, M. & FAIS, S. 2009. Microenvironmental pH is a key factor for exosome traffic in tumor cells. *J Biol Chem*, 284, 34211-22.

- PEACH, R. J., BAJORATH, J., NAEMURA, J., LEYTZE, G., GREENE, J., ARUFFO, A. & LINSLEY, P. S. 1995. Both extracellular immunoglobulin-like domains of CD80 contain residues critical for binding T cell surface receptors CTLA-4 and CD28. *J Biol Chem*, 270, 21181-7.
- PEISTER, A., WOODRUFF, M. A., PRINCE, J. J., GRAY, D. P., HUTMACHER, D. W. & GULDBERG, R. E. 2011. Cell sourcing for bone tissue engineering: amniotic fluid stem cells have a delayed, robust differentiation compared to mesenchymal stem cells. *Stem Cell Res*, 7, 17-27.
- PERDIGUERO, E., KHARRAZ, Y., SERRANO, A. L. & MUÑOZ-CÁNOVES, P. 2012. MKP-1 coordinates ordered macrophage-phenotype transitions essential for stem cell-dependent tissue repair. *Cell Cycle*, 11, 877-886.
- PERDIGUERO, E., SOUSA-VICTOR, P., RUIZ-BONILLA, V., JARDÍ, M., CAELLES, C., SERRANO, A. L. & MUÑOZ-CÁNOVES, P. 2011. p38/MKP-1-regulated AKT coordinates macrophage transitions and resolution of inflammation during tissue repair. *The Journal of Cell Biology*, 195, 307-322.
- PERIN, L., SEDRAKYAN, S., GIULIANI, S., DA SACCO, S., CARRARO, G., SHIRI, L., LEMLEY, K. V., ROSOL, M., WU, S., ATALA, A., WARBURTON, D. & DE FILIPPO, R. E. 2010. Protective effect of human amniotic fluid stem cells in an immunodeficient mouse model of acute tubular necrosis. *PLoS One*, 5, e9357.
- PICCOLI, M., FRANZIN, C., BERTIN, E., URBANI, L., BLAAUW, B., REPELE, A., TASCHIN, E., CENEDESE, A., ZANON, G. F., ANDRÉ-SCHMUTZ, I., ROSATO, A., MELKI, J., CAVAZZANA-CALVO, M., POZZOBON, M. & DE COPPI, P. 2012. Amniotic Fluid Stem Cells Restore the Muscle Cell Niche in a HSA-Cre, SmnF7/F7 Mouse Model. *STEM CELLS*, 30, 1675-1684.
- PIPER, R. C. & KATZMANN, D. J. 2007. Biogenesis and Function of Multivesicular Bodies. *Annual review of cell and developmental biology*, 23, 519-547.
- PISCAGLIA, A. C., RUTELLA, S., LATERZA, L., CESARIO, V., CAMPANALE, M., CAZZATO, I. A., IANIRO, G., BARBARO, F., DI MAURIZIO, L., BONANNO, G., CENCI, T., CAMMAROTA, G., LAROCCA, L. M. & GASBARRINI, A. 2015. Circulating hematopoietic stem cells and putative intestinal stem cells in coeliac disease. *Journal of Translational Medicine*, 13, 220.
- POLIGONE, B. & BALDWIN, A. S. 2001. Positive and negative regulation of NF-kappaB by COX-2: roles of different prostaglandins. *J Biol Chem*, 276, 38658-64.
- POZZOBON, M., PICCOLI, M. & DE COPPI, P. 2014. Stem cells from fetal membranes and amniotic fluid: markers for cell isolation and therapy. *Cell Tissue Bank*, 15, 199-211.
- POZZOBON, M., PICCOLI, M., SCHIAVO, A. A., ATALA, A. & DE COPPI, P. 2013. Isolation of c-Kit+ human amniotic fluid stem cells from second trimester. *Methods Mol Biol*, 1035, 191-8.
- PRISCO, A. R., HOFFMANN, B. R., KACZOROWSKI, C. C., MCDERMOTT-ROE, C., STODOLA, T. J., EXNER, E. C. & GREENE, A. S. 2016. TNF α Regulates Endothelial Progenitor Cell Migration via CADM1 and NF-kB. *Stem cells (Dayton, Ohio)*, 34, 1922-1933.
- PROSKURYAKOV, S. Y. A., KONOPLYANNIKOV, A. G. & GABAI, V. L. 2003. Necrosis: a specific form of programmed cell death? *Experimental Cell Research*, 283, 1-16.
- PRUSA, A.-R. & HENGSTSCHLAGER, M. 2002. Amniotic fluid cells and human stem cell research: a new connection. *Medical Science Monitor: International Medical Journal of Experimental and Clinical Research*, 8, RA253-257.
- PRUSA, A. R., MARTON, E., ROSNER, M., BERNASCHEK, G. & HENGSTSCHLAGER, M. 2003. Oct-4-expressing cells in human amniotic fluid: a new source for stem cell research? *Hum Reprod*, 18, 1489-93.
- QIANG, L., ZHAO, B., MING, M., WANG, N., HE, T.-C., HWANG, S., THORBURN, A. & HE, Y.-Y. 2014. Regulation of cell proliferation and migration by p62 through stabilization of Twist1. *Proceedings of the National Academy of Sciences of the United States of America*, 111, 9241-9246.
- QIN, Y. & ZHANG, C. 2017. The Regulatory Role of IFN-gamma on the Proliferation and Differentiation of Hematopoietic Stem and Progenitor Cells. *Stem Cell Rev*, 13, 705-712.
- RABINOWITZ, R., PETERS, M. T., VYAS, S., CAMPBELL, S. & NICOLAIDES, K. H. 1989. Measurement of fetal urine production in normal pregnancy by real-time ultrasonography. *American Journal of Obstetrics and Gynecology*, 161, 1264-1266.

- RAHBARGHAZI, R., NASSIRI, S. M., KHAZRAINI, P., KAJBAFZADEH, A. M., AHMADI, S. H., MOHAMMADI, E., MOLAZEM, M. & ZAMANI-AHMADMAHMUDI, M. 2013. Juxtacrine and paracrine interactions of rat marrow-derived mesenchymal stem cells, muscle-derived satellite cells, and neonatal cardiomyocytes with endothelial cells in angiogenesis dynamics. *Stem Cells Dev*, 22, 855-65.
- RAKOFF-NAHOUM, S., PAGLINO, J., ESLAMI-VARZANEH, F., EDBERG, S. & MEDZHITOV, R. 2004. Recognition of commensal microflora by toll-like receptors is required for intestinal homeostasis. *Cell*, 118, 229-41.
- RAMACHANDRA, D. L., SHAW, S. S. W., SHANGARIS, P., LOUKOGEORGAKIS, S., GUILLOT, P. V., COPPI, P. D. & DAVID, A. L. 2014. In utero therapy for congenital disorders using amniotic fluid stem cells. *Frontiers in Pharmacology*, 5, 270.
- RAMADASAN-NAIR, R., GAYATHRI, N., MISHRA, S., SUNITHA, B., MYTHRI, R. B., NALINI, A., SUBBANNAYYA, Y., HARSHA, H. C., KOLTHUR-SEETHARAM, U. & BHARATH, M. M. S. 2014. Mitochondrial Alterations and Oxidative Stress in an Acute Transient Mouse Model of Muscle Degeneration: IMPLICATIONS FOR MUSCULAR DYSTROPHY AND RELATED MUSCLE PATHOLOGIES. *The Journal of Biological Chemistry*, 289, 485-509.
- RATAJCZAK, J., MIEKUS, K., KUCIA, M., ZHANG, J., RECA, R., DVORAK, P. & RATAJCZAK, M. Z. 2006. Embryonic stem cell-derived microvesicles reprogram hematopoietic progenitors: evidence for horizontal transfer of mRNA and protein delivery. *Leukemia*, 20, 847-856.
- REES, C. M., EATON, S. & PIERRO, A. 2008. Trends in infant mortality from necrotising enterocolitis in England and Wales and the USA. *Archives of Disease in Childhood - Fetal and Neonatal Edition*, 93, F395.
- RENTEA, R. M., GUO, Y., ZHU, X., MUSCH, M. W., CHANG, E. B., GOURLAY, D. M. & LIEDEL, J. L. 2017. Role of intestinal Hsp70 in barrier maintenance: contribution of milk to the induction of Hsp70.2. *Pediatric Surgery International*.
- RHOADS, R. P., JOHNSON, R. M., RATHBONE, C. R., LIU, X., TEMM-GROVE, C., SHEEHAN, S. M., HOYING, J. B. & ALLEN, R. E. 2009. Satellite cell-mediated angiogenesis in vitro coincides with a functional hypoxia-inducible factor pathway. *Am J Physiol Cell Physiol*, 296, C1321-8.
- RICCIO, M., MARALDI, T., PISCIOTTA, A., LA SALA, G. B., FERRARI, A., BRUZZESI, G., MOTTA, A., MIGLIARESI, C. & DE POL, A. 2012. Fibroin scaffold repairs critical-size bone defects in vivo supported by human amniotic fluid and dental pulp stem cells. *Tissue Eng Part A*, 18, 1006-13.
- ROBINSON, A. M., SAKKAL, S., PARK, A., JOVANOVSKA, V., PAYNE, N., CARBONE, S. E., MILLER, S., BORNSTEIN, J. C., BERNARD, C., BOYD, R. & NURGALI, K. 2014. Mesenchymal stem cells and conditioned medium avert enteric neuropathy and colon dysfunction in guinea pig TNBS-induced colitis. *Am J Physiol Gastrointest Liver Physiol*, 307, G1115-29.
- RODRIGUES, C. E., CAPCHA, J. M., DE BRAGANCA, A. C., SANCHES, T. R., GOUVEIA, P. Q., DE OLIVEIRA, P. A., MALHEIROS, D. M., VOLPINI, R. A., SANTINHO, M. A., SANTANA, B. A., CALADO, R. D., NORONHA, I. L. & ANDRADE, L. 2017. Human umbilical cord-derived mesenchymal stromal cells protect against premature renal senescence resulting from oxidative stress in rats with acute kidney injury. *Stem Cell Res Ther*, 8, 19.
- ROEMELING-VAN RHIJN, M., MENSCH, F. K. F., KOREVAAR, S. S., LEIJS, M. J., VAN OSCH, G. J. V. M., IJZERMANS, J. N. M., BETJES, M. G. H., BAAN, C. C., WEIMAR, W. & HOOGDIJN, M. J. 2013. Effects of Hypoxia on the Immunomodulatory Properties of Adipose Tissue-Derived Mesenchymal Stem cells. *Frontiers in Immunology*, 4, 203.
- ROLF, H. J., NIEBERT, S., NIEBERT, M., GAUS, L., SCHLIEPHAKE, H. & WIESE, K. G. 2012. Intercellular Transport of Oct4 in Mammalian Cells: A Basic Principle to Expand a Stem Cell Niche? *PLoS ONE*, 7.
- ROMAN, W. & GOMES, E. R. 2017. Nuclear positioning in skeletal muscle. *Seminars in Cell & Developmental Biology*.
- ROMANI, R., PIRISINU, I., CALVITTI, M., PALLOTTA, M. T., GARGARO, M., BISTONI, G., VACCA, C., DI MICHELE, A., ORABONA, C., ROSATI, J., PIRRO, M., GIOVAGNOLI, S., MATINO, D., PRONTERA, P., ROSI, G., GROHMANN, U., TALES, V. N., DONTI, E., PUCETTI, P. & FALLARINO, F. 2015.

- Stem cells from human amniotic fluid exert immunoregulatory function via secreted indoleamine 2,3-dioxygenase¹. *Journal of Cellular and Molecular Medicine*, 19, 1593-1605.
- RONQUIST, K. G., SANCHEZ, C., DUBOIS, L., CHIOUREAS, D., FONSECA, P., LARSSON, A., ULLÉN, A., YACHNIN, J., RONQUIST, G. & PANARETAKIS, T. 2016. Energy-requiring uptake of prostasomes and PC3 cell-derived exosomes into non-malignant and malignant cells. *Journal of Extracellular Vesicles*, 5, 10.3402/jev.v5.29877.
- ROTA, C., IMBERTI, B., POZZOBON, M., PICCOLI, M., DE COPPI, P., ATALA, A., GAGLIARDINI, E., XINARIS, C., BENEDETTI, V., FABRICIO, A. S., SQUARCINA, E., ABBATE, M., BENIGNI, A., REMUZZI, G. & MORIGI, M. 2012. Human amniotic fluid stem cell preconditioning improves their regenerative potential. *Stem Cells Dev*, 21, 1911-23.
- ROZENFELD, R. A., LIU, X., DEPLAEN, I. & HSUEH, W. 2001. Role of gut flora on intestinal group II phospholipase A2 activity and intestinal injury in shock. *Am J Physiol Gastrointest Liver Physiol*, 281, G957-63.
- RUMIO, C., DUSIO, G. F., COLOMBO, B., GASPARRI, A., CARDANI, D., MARCUCCI, F. & CORTI, A. 2012. The N-terminal fragment of chromogranin A, vasostatin-1 protects mice from acute or chronic colitis upon oral administration. *Dig Dis Sci*, 57, 1227-37.
- S., L. L., M., S., E., K., O., I. P., R., Z. J., A., K., V., C. A. & U., W. Protein translation, proteolysis and autophagy in human skeletal muscle atrophy after spinal cord injury. *Acta Physiologica*, 0, e13051.
- SALDEEN, J. 2000. Cytokines induce both necrosis and apoptosis via a common Bcl-2-inhibitable pathway in rat insulin-producing cells. *Endocrinology*, 141, 2003-10.
- SALMINEN, A., HUUSKONEN, J., OJALA, J., KAUPPINEN, A., KAARNIRANTA, K. & SUURONEN, T. 2008. Activation of innate immunity system during aging: NF- κ B signaling is the molecular culprit of inflamm-aging. *Ageing Res Rev*, 7, 83-105.
- SALOMON, C., RYAN, J., SOBREVIA, L., KOBAYASHI, M., ASHMAN, K., MITCHELL, M. & RICE, G. E. 2013. Exosomal Signaling during Hypoxia Mediates Microvascular Endothelial Cell Migration and Vasculogenesis. *PLoS ONE*, 8, e68451.
- SATO, T., VAN ES, J. H., SNIPPERT, H. J., STANGE, D. E., VRIES, R. G., VAN DEN BORN, M., BARKER, N., SHROYER, N. F., VAN DE WETERING, M. & CLEVERS, H. 2011. Paneth cells constitute the niche for Lgr5 stem cells in intestinal crypts. *Nature*, 469, 415-418.
- SATO, T., VRIES, R. G., SNIPPERT, H. J., VAN DE WETERING, M., BARKER, N., STANGE, D. E., VAN ES, J. H., ABO, A., KUJALA, P., PETERS, P. J. & CLEVERS, H. 2009. Single Lgr5 stem cells build crypt-villus structures in vitro without a mesenchymal niche. *Nature*, 459, 262-5.
- SAVICKIENE, J., TREIGYTE, G., BARONAITE, S., VALIULIENE, G., KAUPINIS, A., VALIUS, M., ARLAUSKIENE, A. & NAVAKAUSKIENE, R. 2015. Human Amniotic Fluid Mesenchymal Stem Cells from Second- and Third-Trimester Amniocentesis: Differentiation Potential, Molecular Signature, and Proteome Analysis. *Stem Cells Int*, 2015, 319238.
- SAVINA, A., FURLÁN, M., VIDAL, M. & COLOMBO, M. I. 2003. Exosome release is regulated by a calcium-dependent mechanism in K562 cells. *The Journal of Biological Chemistry*, 278, 20083-20090.
- SCHIAFFINO, S., ROSSI, A. C., SMERDU, V., LEINWAND, L. A. & REGGIANI, C. 2015. Developmental myosins: expression patterns and functional significance. *Skelet Muscle*, 5, 22.
- SCHMIDT, E. K., CLAVARINO, G., CEPPI, M. & PIERRE, P. 2009. SUnSET, a nonradioactive method to monitor protein synthesis. *Nat Methods*, 6, 275-7.
- SCHOFIELD, C. J. & RATCLIFFE, P. J. 2004. Oxygen sensing by HIF hydroxylases. *Nat Rev Mol Cell Biol*, 5, 343-54.
- SCHOREY, J. S. & BHATNAGAR, S. 2008. Exosome function: from tumor immunology to pathogen biology. *Traffic (Copenhagen, Denmark)*, 9, 871-881.
- SCHULZE-LUEHRMANN, J. & GHOSH, S. 2006. Antigen-Receptor Signaling to Nuclear Factor κ B. *Immunity*, 25, 701-715.
- SCHWOEBEL, E. D., HO, T. H. & MOORE, M. S. 2002. The mechanism of inhibition of Ran-dependent nuclear transport by cellular ATP depletion. *The Journal of Cell Biology*, 157, 963-974.

- SEALE, P., SABOURIN, L. A., GIRGIS-GABARDO, A., MANSOURI, A., GRUSS, P. & RUDNICKI, M. A. 2000. Pax7 is required for the specification of myogenic satellite cells. *Cell*, 102, 777-86.
- SEOK, J.-K., LEE, S. H., KIM, M. J. & LEE, Y.-M. 2014. MicroRNA-382 induced by HIF-1 α is an angiogenic miR targeting the tumor suppressor phosphatase and tensin homolog. *Nucleic Acids Research*, 42, 8062-8072.
- SHABBIR, A., ZISA, D., LIN, H., MASTRI, M., ROLOFF, G., SUZUKI, G. & LEE, T. 2010. Activation of host tissue trophic factors through JAK-STAT3 signaling: a mechanism of mesenchymal stem cell-mediated cardiac repair. *American Journal of Physiology. Heart and Circulatory Physiology*, 299, H1428-1438.
- SHABBIR, A., ZISA, D., SUZUKI, G. & LEE, T. 2009. Heart failure therapy mediated by the trophic activities of bone marrow mesenchymal stem cells: a noninvasive therapeutic regimen. *Am J Physiol Heart Circ Physiol*, 296, H1888-97.
- SHARMA, R. & HUDAK, M. L. 2013. A Clinical Perspective of Necrotizing Enterocolitis: Past, Present, and Future. *Clinics in perinatology*, 40, 27-51.
- SHEN, B., WU, N., YANG, J. M. & GOULD, S. J. 2011. Protein targeting to exosomes/microvesicles by plasma membrane anchors. *J Biol Chem*, 286, 14383-95.
- SHI, L., WANG, J. S., LIU, X. M., HU, X. Y. & FANG, Q. 2007. Upregulated functional expression of Toll like receptor 4 in mesenchymal stem cells induced by lipopolysaccharide. *Chin Med J (Engl)*, 120, 1685-8.
- SHIBUYA, M. 2011. Vascular Endothelial Growth Factor (VEGF) and Its Receptor (VEGFR) Signaling in Angiogenesis: A Crucial Target for Anti- and Pro-Angiogenic Therapies. *Genes & Cancer*, 2, 1097-1105.
- SHIRKEY, T. W., SIGGERS, R. H., GOLDADE, B. G., MARSHALL, J. K., DREW, M. D., LAARVELD, B. & VAN KESSEL, A. G. 2006. Effects of commensal bacteria on intestinal morphology and expression of proinflammatory cytokines in the gnotobiotic pig. *Exp Biol Med (Maywood)*, 231, 1333-45.
- SHIVDASANI, R. A. 2014. Radiation redux: reserve intestinal stem cells miss the call to duty. *Cell Stem Cell*, 14, 135-6.
- SIEBENLIST, U., FRANZOSO, G. & BROWN, K. 1994. Structure, regulation and function of NF-kappa B. *Annu Rev Cell Biol*, 10, 405-55.
- SIMINOVITCH, L., MCCULLOCH, E. A. & TILL, J. E. 1963. THE DISTRIBUTION OF COLONY-FORMING CELLS AMONG SPLEEN COLONIES. *J Cell Physiol*, 62, 327-36.
- SINGH, S. R., BILLINGTON, C. K., SAYERS, I. & HALL, I. P. 2014. Clonally expanded human airway smooth muscle cells exhibit morphological and functional heterogeneity. *Respiratory Research*, 15, 57-57.
- SKOG, J., WÜRDINGER, T., VAN RIJN, S., MEIJER, D. H., GAINCHE, L., SENA-ESTEVEZ, M., CURRY, W. T., CARTER, B. S., KRICHEVSKY, A. M. & BREAKEFIELD, X. O. 2008. Glioblastoma microvesicles transport RNA and proteins that promote tumour growth and provide diagnostic biomarkers. *Nature Cell Biology*, 10, 1470-1476.
- SPENCE, J. R., MAYHEW, C. N., RANKIN, S. A., KUCHAR, M. F., VALLANCE, J. E., TOLLE, K., HOSKINS, E. E., KALINICHENKO, V. V., WELLS, S. I., ZORN, A. M., SHROYER, N. F. & WELLS, J. M. 2010. Directed differentiation of human pluripotent stem cells into intestinal tissue in vitro. *Nature*, 470, 105.
- STOECK, A., KELLER, S., RIEDLE, S., SANDERSON, M. P., RUNZ, S., LE NAOUR, F., GUTWEIN, P., LUDWIG, A., RUBINSTEIN, E. & ALTEVOGT, P. 2006. A role for exosomes in the constitutive and stimulus-induced ectodomain cleavage of L1 and CD44. *Biochem J*, 393, 609-18.
- SÜDHOF, T. C. & ROTHMAN, J. E. 2009. Membrane fusion: grappling with SNARE and SM proteins. *Science (New York, N.Y.)*, 323, 474-477.
- SZADE, A., GROCHOT-PRZECZEK, A., FLORCZYK, U., JOZKOWICZ, A. & DULAK, J. 2015. Cellular and molecular mechanisms of inflammation-induced angiogenesis. *IUBMB Life*, 67, 145-59.
- TAKAHASHI, K. & YAMANAKA, S. 2006. Induction of Pluripotent Stem Cells from Mouse Embryonic and Adult Fibroblast Cultures by Defined Factors. *Cell*, 126, 663-676.

- TAKAHASHI, T., UENO, H. & SHIBUYA, M. 1999. VEGF activates protein kinase C-dependent, but Ras-independent Raf-MEK-MAP kinase pathway for DNA synthesis in primary endothelial cells. *Oncogene*, 18, 2221-30.
- TAKAHASHI, T., YAMAGUCHI, S., CHIDA, K. & SHIBUYA, M. 2001. A single autophosphorylation site on KDR/Flk-1 is essential for VEGF-A-dependent activation of PLC-gamma and DNA synthesis in vascular endothelial cells. *Embo j*, 20, 2768-78.
- TANABE, H., AYABE, T., BAINBRIDGE, B., GUINA, T., ERNST, R. K., DARVEAU, R. P., MILLER, S. I. & OUELLETTE, A. J. 2005. Mouse Paneth Cell Secretory Responses to Cell Surface Glycolipids of Virulent and Attenuated Pathogenic Bacteria. *Infection and Immunity*, 73, 2312-2320.
- TARASSISHIN, L., BAUMAN, A., SUH, H. S. & LEE, S. C. 2013. Anti-viral and anti-inflammatory mechanisms of the innate immune transcription factor interferon regulatory factor 3: relevance to human CNS diseases. *J Neuroimmune Pharmacol*, 8, 132-44.
- TATSUMI, R., HATTORI, A., IKEUCHI, Y., ANDERSON, J. E. & ALLEN, R. E. 2002. Release of hepatocyte growth factor from mechanically stretched skeletal muscle satellite cells and role of pH and nitric oxide. *Mol Biol Cell*, 13, 2909-18.
- TAYLOR, D. D. & GERCEL-TAYLOR, C. 2008. MicroRNA signatures of tumor-derived exosomes as diagnostic biomarkers of ovarian cancer. *Gynecologic Oncology*, 110, 13-21.
- TENG, G.-G., WANG, W.-H., DAI, Y., WANG, S.-J., CHU, Y.-X. & LI, J. 2013. Let-7b Is Involved in the Inflammation and Immune Responses Associated with Helicobacter pylori Infection by Targeting Toll-Like Receptor 4. *PLOS ONE*, 8, e56709.
- TENG, Y. D., MOCCHETTI, I., TAVEIRA-DASILVA, A. M., GILLIS, R. A. & WRATHALL, J. R. 1999. Basic fibroblast growth factor increases long-term survival of spinal motor neurons and improves respiratory function after experimental spinal cord injury. *J Neurosci*, 19, 7037-47.
- THERY, C., AMIGORENA, S., RAPOSO, G. & CLAYTON, A. 2006. Isolation and characterization of exosomes from cell culture supernatants and biological fluids. *Curr Protoc Cell Biol*, Chapter 3, Unit 3.22.
- THERY, C., BOUSSAC, M., VERON, P., RICCIARDI-CASTAGNOLI, P., RAPOSO, G., GARIN, J. & AMIGORENA, S. 2001. Proteomic analysis of dendritic cell-derived exosomes: a secreted subcellular compartment distinct from apoptotic vesicles. *J Immunol*, 166, 7309-18.
- THERY, C., DUBAN, L., SEGURA, E., VERON, P., LANTZ, O. & AMIGORENA, S. 2002a. Indirect activation of naive CD4+ T cells by dendritic cell-derived exosomes. *Nat Immunol*, 3, 1156-62.
- THERY, C., OSTROWSKI, M. & SEGURA, E. 2009. Membrane vesicles as conveyors of immune responses. *Nat Rev Immunol*, 9, 581-93.
- THERY, C., ZITVOGEL, L. & AMIGORENA, S. 2002b. Exosomes: composition, biogenesis and function. *Nat Rev Immunol*, 2, 569-79.
- THOMAS, E. D., LOCHTE, H. L., LU, W. C. & FERREBEE, J. W. 1957. Intravenous Infusion of Bone Marrow in Patients Receiving Radiation and Chemotherapy. *New England Journal of Medicine*, 257, 491-496.
- THOMOU, T., MORI, M. A., DREYFUSS, J. M., KONISHI, M., SAKAGUCHI, M., WOLFRUM, C., RAO, T. N., WINNAY, J. N., GARCIA-MARTIN, R., GRINSPOON, S. K., GORDEN, P. & KAHN, C. R. 2017. Adipose-derived circulating miRNAs regulate gene expression in other tissues. *Nature*, advance online publication.
- TI, D., HAO, H., TONG, C., LIU, J., DONG, L., ZHENG, J., ZHAO, Y., LIU, H., FU, X. & HAN, W. 2015. LPS-preconditioned mesenchymal stromal cells modify macrophage polarization for resolution of chronic inflammation via exosome-shuttled let-7b. *Journal of Translational Medicine*, 13, 308.
- TIAN, H., BIEHS, B., WARMING, S., LEONG, K. G., RANGELL, L., KLEIN, O. D. & DE SAUVAGE, F. J. 2011. A reserve stem cell population in small intestine renders Lgr5-positive cells dispensable. *Nature*, 478, 255-9.
- TREMBLAY, É., THIBAUT, M.-P., FERRETTI, E., BABAKISSA, C., BERTELLE, V., BETTOLLI, M., BURGHARDT, K. M., COLOMBANI, J.-F., GRYNSPAN, D., LEVY, E., LU, P., MAYER, S., MÉNARD, D., MOUTERDE, O., RENES, I. B., SEIDMAN, E. G. & BEAULIEU, J.-F. 2016. Gene expression

- profiling in necrotizing enterocolitis reveals pathways common to those reported in Crohn's disease. *BMC Medical Genomics*, 9, 6.
- TSAI, C. C., CHEN, Y. J., YEW, T. L., CHEN, L. L., WANG, J. Y., CHIU, C. H. & HUNG, S. C. 2011. Hypoxia inhibits senescence and maintains mesenchymal stem cell properties through down-regulation of E2A-p21 by HIF-TWIST. *Blood*, 117, 459-69.
- TSAI, M.-S., HWANG, S.-M., TSAI, Y.-L., CHENG, F.-C., LEE, J.-L. & CHANG, Y.-J. 2006. Clonal amniotic fluid-derived stem cells express characteristics of both mesenchymal and neural stem cells. *Biology of Reproduction*, 74, 545-551.
- TUGAL, D., LIAO, X. & JAIN, M. K. 2013. Transcriptional Control of Macrophage Polarization. *Arteriosclerosis, Thrombosis, and Vascular Biology*, 33, 1135-1144.
- URBANELLI, L., MAGINI, A., BURATTA, S., BROZZI, A., SAGINI, K., POLCHI, A., TANCINI, B. & EMILIANI, C. 2013. Signaling pathways in exosomes biogenesis, secretion and fate. *Genes*, 4, 152-170.
- VAISHNAVA, S., BEHRENDT, C. L., ISMAIL, A. S., ECKMANN, L. & HOOPER, L. V. 2008. Paneth cells directly sense gut commensals and maintain homeostasis at the intestinal host-microbial interface. *Proceedings of the National Academy of Sciences of the United States of America*, 105, 20858-20863.
- VALADI, H., EKSTRÖM, K., BOSSIOS, A., SJÖSTRAND, M., LEE, J. J. & LÖTVALL, J. O. 2007. Exosome-mediated transfer of mRNAs and microRNAs is a novel mechanism of genetic exchange between cells. *Nature Cell Biology*, 9, 654-659.
- VALLI, A., ROSNER, M., FUCHS, C., SIEGEL, N., BISHOP, C. E., DOLZNIG, H., MADEL, U., FEICHTINGER, W., ATALA, A. & HENGSTSCHLAGER, M. 2010. Embryoid body formation of human amniotic fluid stem cells depends on mTOR. *Oncogene*, 29, 966-77.
- VAN DE WETERING, M., SANCHO, E., VERWEIJ, C., DE LAU, W., OVING, I., HURLSTONE, A., VAN DER HORN, K., BATLLE, E., COUDREUSE, D., HARAMIS, A. P., TJON-PON-FONG, M., MOERER, P., VAN DEN BORN, M., SOETE, G., PALS, S., EILERS, M., MEDEMA, R. & CLEVERS, H. 2002. The beta-catenin/TCF-4 complex imposes a crypt progenitor phenotype on colorectal cancer cells. *Cell*, 111, 241-50.
- VAN ROOIJ, E., SUTHERLAND, L. B., QI, X., RICHARDSON, J. A., HILL, J. & OLSON, E. N. 2007. Control of stress-dependent cardiac growth and gene expression by a microRNA. *Science*, 316, 575-9.
- VATER, R., CULLEN, M. J. & HARRIS, J. B. 1994. The expression of vimentin in satellite cells of regenerating skeletal muscle in vivo. *The Histochemical Journal*, 26, 916-928.
- VERRECK, F. A. W., DE BOER, T., LANGENBERG, D. M. L., VAN DER ZANDEN, L. & OTTENHOFF, T. H. M. 2006. Phenotypic and functional profiling of human proinflammatory type-1 and anti-inflammatory type-2 macrophages in response to microbial antigens and IFN- γ - and CD40L-mediated costimulation. *Journal of Leukocyte Biology*, 79, 285-293.
- VILLALTA, S. A., NGUYEN, H. X., DENG, B., GOTOH, T. & TIDBALL, J. G. 2009. Shifts in macrophage phenotypes and macrophage competition for arginine metabolism affect the severity of muscle pathology in muscular dystrophy. *Hum Mol Genet*, 18, 482-96.
- VILLARROYA-BELTRI, C., GUTIERREZ-VAZQUEZ, C., SANCHEZ-CABO, F., PEREZ-HERNANDEZ, D., VAZQUEZ, J., MARTIN-COFRECES, N., MARTINEZ-HERRERA, D. J., PASCUAL-MONTANO, A., MITTELBRUNN, M. & SANCHEZ-MADRID, F. 2013. Sumoylated hnRNP A2B1 controls the sorting of miRNAs into exosomes through binding to specific motifs. *Nat Commun*, 4, 2980.
- VISIONGAIN 2012. Stem Cell Technologies: World Market Outlook 2012–2022.
- WAN, J., SHAN, Y., FAN, Y., FAN, C., CHEN, S., SUN, J., ZHU, L., QIN, L., YU, M. & LIN, Z. 2016. NF- κ B inhibition attenuates LPS-induced TLR4 activation in monocyte cells. *Molecular Medicine Reports*, 14, 4505-4510.
- WANG, C. H. & WU, W. G. 2005. Amphiphilic beta-sheet cobra cardiotoxin targets mitochondria and disrupts its network. *FEBS Lett*, 579, 3169-74.
- WANG, H.-X., LAU, S.-Y., HUANG, S.-J., KWAN, C.-Y. & WONG, T.-M. 1997. Cobra Venom Cardiotoxin Induces Perturbations of Cytosolic Calcium Homeostasis and Hypercontracture in Adult Rat Ventricular Myocytes. *Journal of Molecular and Cellular Cardiology*, 29, 2759-2770.
- WARREN, L., MANOS, P. D., AHFELDT, T., LOH, Y. H., LI, H., LAU, F., EBINA, W., MANDAL, P. K., SMITH, Z. D., MEISSNER, A., DALEY, G. Q., BRACK, A. S., COLLINS, J. J., COWAN, C., SCHLAEGER, T. M.

- & ROSSI, D. J. 2010. Highly efficient reprogramming to pluripotency and directed differentiation of human cells with synthetic modified mRNA. *Cell Stem Cell*, 7, 618-30.
- WASZAK, P., ALPHONSE, R., VADIVEL, A., IONESCU, L., EATON, F. & THÉBAUD, B. 2012. Preconditioning enhances the paracrine effect of mesenchymal stem cells in preventing oxygen-induced neonatal lung injury in rats. *Stem Cells and Development*, 21, 2789-2797.
- WATANABE, K., UENO, M., KAMIYA, D., NISHIYAMA, A., MATSUMURA, M., WATAYA, T., TAKAHASHI, J. B., NISHIKAWA, S., NISHIKAWA, S., MUGURUMA, K. & SASAI, Y. 2007. A ROCK inhibitor permits survival of dissociated human embryonic stem cells. *Nat Biotechnol*, 25, 681-6.
- WATERMAN, R. S., TOMCHUCK, S. L., HENKLE, S. L. & BETANCOURT, A. M. 2010. A New Mesenchymal Stem Cell (MSC) Paradigm: Polarization into a Pro-Inflammatory MSC1 or an Immunosuppressive MSC2 Phenotype. *PLoS ONE*, 5, e10088.
- WEISSMAN, I. L. 2000. Stem Cells: Units of Development, Units of Regeneration, and Units in Evolution. *Cell*, 100, 157-168.
- WEISSMAN, I. L., ANDERSON, D. J. & GAGE, F. 2001. STEM AND PROGENITOR CELLS: Origins, Phenotypes, Lineage Commitments, and Transdifferentiations. *Annual Review of Cell and Developmental Biology*, 17, 387-403.
- WESTHOFF, M. A., SERRELS, B., FINCHAM, V. J., FRAME, M. C. & CARRAGHER, N. O. 2004. Src-Mediated Phosphorylation of Focal Adhesion Kinase Couples Actin and Adhesion Dynamics to Survival Signaling. *Molecular and Cellular Biology*, 24, 8113-8133.
- WIDERA, D., MIKENBERG, I., ELVERS, M., KALTSCHMIDT, C. & KALTSCHMIDT, B. 2006. Tumor necrosis factor alpha triggers proliferation of adult neural stem cells via IKK/NF-kappaB signaling. *BMC Neurosci*, 7, 64.
- WIESMANN, A., BÜHRING, H.-J., MENTRUP, C. & WIESMANN, H.-P. 2006. Decreased CD90 expression in human mesenchymal stem cells by applying mechanical stimulation. *Head & Face Medicine*, 2, 8-8.
- WIGHTMAN, B., HA, I. & RUVKUN, G. 1993. Posttranscriptional regulation of the heterochronic gene *lin-14* by *lin-4* mediates temporal pattern formation in *C. elegans*. *Cell*, 75, 855-62.
- WIKLANDER, O. P., NORDIN, J. Z., O'LOUGHLIN, A., GUSTAFSSON, Y., CORSO, G., MAGER, I., VADER, P., LEE, Y., SORK, H., SEOW, Y., HELDRING, N., ALVAREZ-ERVITI, L., SMITH, C. E., LE BLANC, K., MACCHIARINI, P., JUNGEBLUTH, P., WOOD, M. J. & ANDALOUSSI, S. E. 2015. Extracellular vesicle in vivo biodistribution is determined by cell source, route of administration and targeting. *J Extracell Vesicles*, 4, 26316.
- WILLIAMS, R. L. & URBE, S. 2007. The emerging shape of the ESCRT machinery. *Nat Rev Mol Cell Biol*, 8, 355-68.
- WILLMS, E., JOHANSSON, H. J., MÄGER, I., LEE, Y., BLOMBERG, K. E. M., SADIK, M., ALAARG, A., SMITH, C. I. E., LEHTIÖ, J., EL ANDALOUSSI, S., WOOD, M. J. A. & VADER, P. 2016. Cells release subpopulations of exosomes with distinct molecular and biological properties. *Scientific Reports*, 6, 22519.
- WOLFRUM, K., WANG, Y., PRIGIONE, A., SPERLING, K., LEHRACH, H. & ADJAYE, J. 2010. The LARGE principle of cellular reprogramming: lost, acquired and retained gene expression in foreskin and amniotic fluid-derived human iPS cells. *PLoS One*, 5, e13703.
- X., X., H., Z., T., W., Y., S., P., N., Y., L., S., T., P., A. B., H., S., W., X., H., X. & Z., S. 2014. Exogenous High-Mobility Group Box 1 Inhibits Apoptosis and Promotes the Proliferation of Lewis Cells via RAGE/TLR4-Dependent Signal Pathways. *Scandinavian Journal of Immunology*, 79, 386-394.
- XIA, Z. Y., HU, Y., XIE, P. L., TANG, S. Y., LUO, X. H., LIAO, E. Y., CHEN, F. & XIE, H. 2015. Runx2/miR-3960/miR-2861 Positive Feedback Loop Is Responsible for Osteogenic Transdifferentiation of Vascular Smooth Muscle Cells. *Biomed Res Int*, 2015, 624037.
- XIAO, H. & WONG, D. T. 2012. Proteomic analysis of microvesicles in human saliva by gel electrophoresis with liquid chromatography-mass spectrometry. *Anal Chim Acta*, 723, 61-7.
- XU, C., ZHANG, L., DUAN, L. & LU, C. 2016. MicroRNA-3196 is inhibited by H2AX phosphorylation and attenuates lung cancer cell apoptosis by downregulating PUMA. *Oncotarget*, 7, 77764-77776.

- YAN, K. S., CHIA, L. A., LI, X., OOTANI, A., SU, J., LEE, J. Y., SU, N., LUO, Y., HEILSHORN, S. C., AMIEVA, M. R., SANGIORGI, E., CAPECCHI, M. R. & KUO, C. J. 2012. The intestinal stem cell markers *Bmi1* and *Lgr5* identify two functionally distinct populations. *Proc Natl Acad Sci U S A*, 109, 466-71.
- YANG, C. C., SHIH, Y. H., KO, M. H., HSU, S. Y., CHENG, H. & FU, Y. S. 2008. Transplantation of human umbilical mesenchymal stem cells from Wharton's jelly after complete transection of the rat spinal cord. *PLoS One*, 3, e3336.
- YANG, D., YUAN, Q., BALAKRISHNAN, A., BANTEL, H., KLUSMANN, J.-H., MANNS, M. P., OTT, M., CANTZ, T. & SHARMA, A. D. 2016. MicroRNA-125b-5p mimic inhibits acute liver failure. *Nature Communications*, 7, 11916.
- YANG, D. Y., SHEU, M. L., SU, H. L., CHENG, F. C., CHEN, Y. J., CHEN, C. J., CHIU, W. T., YIIN, J. J., SHEEHAN, J. & PAN, H. C. 2012. Dual regeneration of muscle and nerve by intravenous administration of human amniotic fluid-derived mesenchymal stem cells regulated by stromal cell-derived factor-1alpha in a sciatic nerve injury model. *J Neurosurg*, 116, 1357-67.
- YAO, H., YANG, S. R., EDIRISINGHE, I., RAJENDRASOZHAN, S., CAITO, S., ADENUGA, D., O'REILLY, M. A. & RAHMAN, I. 2008. Disruption of p21 attenuates lung inflammation induced by cigarette smoke, LPS, and fMLP in mice. *Am J Respir Cell Mol Biol*, 39, 7-18.
- YEO, S. C. L., XU, L., REN, J., BOULTON, V. J., WAGLE, M. D., LIU, C., REN, G., WONG, P., ZAHN, R., SASAJALA, P., YANG, H., PIPER, R. C. & MUNN, A. L. 2003. Vps20p and Vta1p interact with Vps4p and function in multivesicular body sorting and endosomal transport in *Saccharomyces cerevisiae*. *Journal of Cell Science*, 116, 3957-3970.
- YEUNG, A. W., TERENCE, A. C., KING, N. J. & THOMAS, S. R. 2015. Role of indoleamine 2,3-dioxygenase in health and disease. *Clin Sci (Lond)*, 129, 601-72.
- YU, B., ZHANG, X. & LI, X. 2014. Exosomes derived from mesenchymal stem cells. *International Journal of Molecular Sciences*, 15, 4142-4157.
- YU, G., JIA, Z. & DOU, Z. 2017. miR-24-3p regulates bladder cancer cell proliferation, migration, invasion and autophagy by targeting DEDD. *Oncol Rep*, 37, 1123-1131.
- YU, X., HARRIS, S. L. & LEVINE, A. J. 2006. The Regulation of Exosome Secretion: a Novel Function of the p53 Protein. *Cancer Research*, 66, 4795-4801.
- YUE, F., BI, P., WANG, C., LI, J., LIU, X. & KUANG, S. 2016. Conditional Loss of Pten in Myogenic Progenitors Leads to Postnatal Skeletal Muscle Hypertrophy but Age-Dependent Exhaustion of Satellite Cells. *Cell Rep*, 17, 2340-2353.
- ZAMMIT, P. S., GOLDING, J. P., NAGATA, Y., HUDON, V., PARTRIDGE, T. A. & BEAUCHAMP, J. R. 2004. Muscle satellite cells adopt divergent fates: a mechanism for self-renewal? *J Cell Biol*, 166, 347-57.
- ZANI, A., CANANZI, M., FASCETTI-LEON, F., LAURITI, G., SMITH, V. V., BOLLINI, S., GHIONZOLI, M., D'ARRIGO, A., POZZOBON, M., PICCOLI, M., HICKS, A., WELLS, J., SIOW, B., SEBIRE, N. J., BISHOP, C., LEON, A., ATALA, A., LYTHGOE, M. F., PIERRO, A., EATON, S. & DE COPPI, P. 2014. Amniotic fluid stem cells improve survival and enhance repair of damaged intestine in necrotising enterocolitis via a COX-2 dependent mechanism. *Gut*, 63, 300-9.
- ZANI, A. & PIERRO, A. 2015. Necrotizing enterocolitis: controversies and challenges. *F1000Research*, 4, F1000 Faculty Rev-1373.
- ZANI, A., ZANI-RUTTENSTOCK, E., PEYVANDI, F., LEE, C., LI, B. & PIERRO, A. 2016. A spectrum of intestinal injury models in neonatal mice. *Pediatr Surg Int*, 32, 65-70.
- ZEUNER, M.-T., KRÜGER, C. L., VOLK, K., BIEBACK, K., COTTRELL, G. S., HEILEMANN, M. & WIDERA, D. 2016. Biased signalling is an essential feature of TLR4 in glioma cells. *Biochimica et Biophysica Acta (BBA) - Molecular Cell Research*, 1863, 3084-3095.
- ZEUNER, M.-T., VALLANCE, T., VAIYAPURI, S., COTTRELL, G. S. & WIDERA, D. 2017. Development and Characterisation of a Novel NF-κB Reporter Cell Line for Investigation of Neuroinflammation. *Mediators of Inflammation*, 2017, 6209865.
- ZHANG, H., FREITAS, D., KIM, H. S., FABIJANIC, K., LI, Z., CHEN, H., MARK, M. T., MOLINA, H., MARTIN, A. B., BOJMAR, L., FANG, J., RAMPERSAUD, S., HOSHINO, A., MATEI, I., KENIFIC, C. M., NAKAJIMA, M., MUTVEI, A. P., SANSONE, P., BUEHRING, W., WANG, H., JIMENEZ, J. P.,

- COHEN-GOULD, L., PAKNEJAD, N., BRENDEL, M., MANOVA-TODOROVA, K., MAGALHAES, A., FERREIRA, J. A., OSORIO, H., SILVA, A. M., MASSEY, A., CUBILLOS-RUIZ, J. R., GALLETI, G., GIANNAKAKOU, P., CUERVO, A. M., BLENIS, J., SCHWARTZ, R., BRADY, M. S., PEINADO, H., BROMBERG, J., MATSUI, H., REIS, C. A. & LYDEN, D. 2018. Identification of distinct nanoparticles and subsets of extracellular vesicles by asymmetric flow field-flow fractionation. *Nat Cell Biol*, 20, 332-343.
- ZHANG, J., KHVOROSTOV, I., HONG, J. S., OKTAY, Y., VERGNES, L., NUEBEL, E., WAHJUDI, P. N., SETOGUCHI, K., WANG, G., DO, A., JUNG, H. J., MCCAFFERY, J. M., KURLAND, I. J., REUE, K., LEE, W. N., KOEHLER, C. M. & TEITELL, M. A. 2011. UCP2 regulates energy metabolism and differentiation potential of human pluripotent stem cells. *Embo j*, 30, 4860-73.
- ZHANG, J., LOU, X., JIN, L., ZHOU, R., LIU, S., XU, N. & LIAO, D. J. 2014. Necrosis, and then stress induced necrosis-like cell death, but not apoptosis, should be the preferred cell death mode for chemotherapy: clearance of a few misconceptions. *Oncoscience*, 1, 407-422.
- ZHANG, J., NUEBEL, E., DALEY, G. Q., KOEHLER, C. M. & TEITELL, M. A. 2012. Metabolic regulation in pluripotent stem cells during reprogramming and self-renewal. *Cell Stem Cell*, 11, 589-95.
- ZHANG, R., LIU, Y., YAN, K., CHEN, L., CHEN, X. R., LI, P., CHEN, F. F. & JIANG, X. D. 2013. Anti-inflammatory and immunomodulatory mechanisms of mesenchymal stem cell transplantation in experimental traumatic brain injury. *J Neuroinflammation*, 10, 106.
- ZHAO, Y., SAMAL, E. & SRIVASTAVA, D. 2005. Serum response factor regulates a muscle-specific microRNA that targets Hand2 during cardiogenesis. *Nature*, 436, 214-20.
- ZHAO, Z., LU, P., ZHANG, H., XU, H., GAO, N., LI, M. & LIU, C. 2014. Nestin positively regulates the Wnt/ β -catenin pathway and the proliferation, survival and invasiveness of breast cancer stem cells. *Breast Cancer Research : BCR*, 16, 408-408.
- ZHU, Y., HUANG, Y. F., KEK, C. & BULAVIN, D. V. 2013. Apoptosis differently affects lineage tracing of Lgr5 and Bmi1 intestinal stem cell populations. *Cell Stem Cell*, 12, 298-303.
- ZÖLLER, M. 2015. CD44, Hyaluronan, the Hematopoietic Stem Cell, and Leukemia-Initiating Cells. *Frontiers in Immunology*, 6, 235.
- ZWAAL, R. F. & SCHROIT, A. J. 1997. Pathophysiologic implications of membrane phospholipid asymmetry in blood cells. *Blood*, 89, 1121-32.

12. Bibliography

MELLOWS, B., MITCHELL, R., ANTONIOLI, M., KRETZ, O., CHAMBERS, D., ZEUNER, M. T., DENECKE, B., MUSANTE, L., RAMACHANDRA, D. L., DEBACQ-CHAINIAUX, F., HOLTHOFER, H., JOCH, B., RAY, S., WIDERA, D., DAVID, A. L., HUBER, T. B., DENGJEL, J., DE COPPI, P. & PATEL, K. 2017. Protein and Molecular Characterization of a Clinically Compliant Amniotic Fluid Stem Cell-Derived Extracellular Vesicle Fraction Capable of Accelerating Muscle Regeneration Through Enhancement of Angiogenesis. *Stem Cells Dev*, 26, 1316-1333.

